ISSN 0021-9673

VOL. 623 NO. 2 OCTOBER 16, 1992

THIS ISSUE COMPLETES VOL. 623

JOURNAL OF CHROMATOGRAPHY

INCLUDING ELECTROPHORESIS AND OTHER SEPARATION METHODS

ELSEVIER

JOURNAL OF CHROMATOGRAPHY

INCLUDING ELECTROPHORESIS AND OTHER SEPARATION METHODS

Scope. The *Journal of Chromatography* publishes papers on all aspects of **chromatography, electrophoresis** and related methods. Contributions consist mainly of research papers dealing with chromatographic theory, instrumental developments and their applications. The section *Biomedical Applications*, which is under separate editorship, deals with the following aspects: developments in and applications of chromatographic and electrophoretic techniques related to clinical diagnosis or alterations during medical treatment; screening and profiling of body fluids or tissues related to the analysis of active substances and to metabolic disorders; drug level monitoring and pharmacokinetic studies; clinical toxicology; forensic medicine; veterinary medicine; occupational medicine; results from basic medical research with direct consequences in clinical practice. In *Symposium volumes*, which are under separate editorship, proceedings of symposia on chromatography, electrophoresis and related methods are published.

Submission of Papers. The preferred medium of submission is on disk with accompanying manuscript (see *Electronic manuscripts* in the Instructions to Authors, which can be obtained from the publisher, Elsevier Science Publishers B.V., P.O. Box 330, 1000 AH Amsterdam, Netherlands). Manuscripts (in English; *four* copies are required) should be submitted to: Editorial Office of *Journal of Chromatography*, P.O. Box 681, 1000 AR Amsterdam, Netherlands, Telefax (+31-20) 5862 304, or to: The Editor of *Journal of Chromatography, Biomedical Applications*, P.O. Box 681, 1000 AR Amsterdam, Netherlands. Review articles are invited or proposed in writing to the Editors who welcome suggestions for subjects. An outline of the proposed review should first be forwarded to the Editors for preliminary discussion prior to preparation. Submission of an article is understood to imply that the article is original and unpublished and is not being considered for publication elsewhere. For copyright regulations, see below.

Publication. The *Journal of Chromatography* (incl. *Biomedical Applications*) has 40 volumes in 1993. The subscription prices for 1993 are:

J. Chromatogr. (incl. *Cum. Indexes, Vols. 601–650*) + *Biomed. Appl.* (Vols. 612–651):
Dfl. 8520.00 plus Dfl. 1320.00 (p.p.h.) (total *ca.* US$ 5927.75)

J. Chromatogr. (incl. *Cum. Indexes, Vols. 601–650*) only (Vols. 623–651):
Dfl. 7047.00 plus Dfl. 957.00 (p.p.h.) (total *ca.* US$ 4821.75)

Biomed. Appl. only (Vols. 612–622):
Dfl. 2783.00 plus Dfl. 363.00 (p.p.h.) (total *ca.* US$ 1895.25).

Subscription Orders. The Dutch guilder price is definitive. The US$ price is subject to exchange-rate fluctuations and is given as a guide. Subscriptions are accepted on a prepaid basis only, unless different terms have been previously agreed upon. Subscriptions orders can be entered only by calender year (Jan.–Dec.) and should be sent to Elsevier Science Publishers, Journal Department, P.O. Box 211, 1000 AE Amsterdam, Netherlands, Tel. (+31-20) 5803 642, Telefax (+31-20) 5803 598, or to your usual subscription agent. Postage and handling charges include surface delivery except to the following countries where air delivery via SAL (Surface Air Lift) mail is ensured: Argentina, Australia, Brazil, Canada, China, Hong Kong, India, Israel, Japan*, Malaysia, Mexico, New Zealand, Pakistan, Singapore, South Africa, South Korea, Taiwan, Thailand, USA. *For Japan air delivery (SAL) requires 25% additional charge of the normal postage and handling charge. For all other countries airmail rates are available upon request. Claims for missing issues must be made within three months of our publication (mailing) date, otherwise such claims cannot be honoured free of charge. Back volumes of the *Journal of Chromatography* (Vols. 1–611) are available at Dfl. 217.00 (plus postage). Customers in the USA and Canada wishing information on this and other Elsevier journals, please contact Journal Information Center, Elsevier Science Publishing Co. Inc., 655 Avenue of the Americas, New York, NY 10010, USA, Tel. (+1-212) 633 3750, Telefax (+1-212) 633 3764.

Abstracts/Contents Lists published in Analytical Abstracts, Biochemical Abstracts, Biological Abstracts, Chemical Abstracts, Chemical Titles, Chromatography Abstracts, Clinical Chemistry Lookout, Current Awareness in Biological Sciences (CABS), Current Contents/Life Sciences, Current Contents/Physical, Chemical & Earth Sciences, Deep-Sea Research/Part B: Oceanographic Literature Review, Excerpta Medica, Index Medicus, Mass Spectrometry Bulletin, PASCAL-CNRS, Pharmaceutical Abstracts, Referativnyi Zhurnal, Research Alert, Science Citation Index and Trends in Biotechnology.

US Mailing Notice. *Journal of Chromatography* (main section ISSN 0021-9673, *Biomedical Applications* section ISSN 0378-4347) is published (78 issues/year) by Elsevier Science Publishers (Sara Burgerhartstraat 25, P.O. Box 211, 1000 AE Amsterdam, Netherlands). Annual subscription price in the USA US$ 5927.75 (subject to change), including air speed delivery. Application to mail at second class postage rate is pending at Jamaica, NY 11431. **USA POSTMASTERS:** Send address changes to *Journal of Chromatography*, Publications Expediting, Inc., 200 Meacham Avenue, Elmont, NY 11003. Airfreight and mailing in the USA by Publication Expediting.

See inside back cover for Publication Schedule, Information for Authors and information on Advertisements.

0021-9673/92/$05.00

CONTENTS

(Abstracts/Contents Lists published in Analytical Abstracts, Biochemical Abstracts, Biological Abstracts, Chemical Abstracts, Chemical Titles, Chromatography Abstracts, Current Awareness In Biological Sciences (CABS), Current Contents/Life Sciences, Current Contents/Physical, Chemical & Earth Sciences, Deep-Sea Research/Part B: Oceanographic Literature Review, Excerpta Medica, Index Medicus, Mass Spectrometry Bulletin, PASCAL-CNRS, Referativnyi Zhurnal, Research Alert and Science Citation Index)

REGULAR PAPERS

Column Liquid Chromatography

Gas Chromatography

Supercritical Fluid Chromatography

(Continued overleaf)

Journal of Chromatography, 623 (1992) 207–220
Elsevier Science Publishers B.V., Amsterdam

CHROM. 24 453

Comparison of high-performance liquid chromatographic methods for the analysis of basic drugs

R. J. M. Vervoort, F. A. Maris and H. Hindriks

Department of Analytical Chemistry, Organon International BV, AKZO Pharma Group, P.O. Box 20, 5340 BH Oss (Netherlands)

(First received September 19th, 1991; revised manuscript received June 25th, 1992)

ABSTRACT

Problems that are often encountered in the high-performance liquid chromatographic analysis of basic compounds are severe peak asymmetry and low separation efficiency. In attempting to solve these problems, one can become confused by the variety of suggestions given by the specialists and by the numerous stationary phases available. In this work, the analysis of basic drugs was studied from two directions. In both approaches a set of 32 basic drugs was used, differing in basicity, polarity and number and type of nitrogen atoms. In the first approach the effect of mobile phase additives and buffers on the performance of a single column was determined. It was found that tertiary and quaternary amines can be applied successfully as silanol blockers. The latter proved to be aggressive towards silica-based stationary phases. Addition of triethylamine showed a remarkable improvement in peak shape in different columns. Other aspects, such as pK_a, retention and amount injected, were systematically studied. In the second approach, eight different columns, specially recommended for the chromatography of basic drugs, were evaluated. The chromatographic results showed great variability. As far as peak shape as a function of pH is concerned, an electrostatically shielded stationary phase was most promising for the analysis of basic compounds. This column can even be used without buffers, which can be an advantage in liquid chromatography–mass spectrometry coupling. Because some results were inconsistent with published results, a third approach was to study three columns in more detail.

INTRODUCTION

Peak asymmetry, which is often observed in the chromatography of basic drugs, is an important performance characteristic for a given stationary phase. In routine analysis, system suitability criteria are set for the maximum allowable asymmetry, expressed as asymmetry factor. For quantitative analysis an asymmetry factor of less than 1.5 is preferred. It is generally accepted that the severe peak asymmetry of basic drugs in reversed-phase chromatography is caused by ionic interaction of the charged solutes with free silanol groups of the packing. Despite these negative effects, reversed-phase high-performance liquid chromatography (RP-HPLC) is still the most widely used method because of the fast equilibration time, the selectivity characteristics and the retention reproducibility. As can be seen in Fig. 1, we are in fact in a bad situation. The

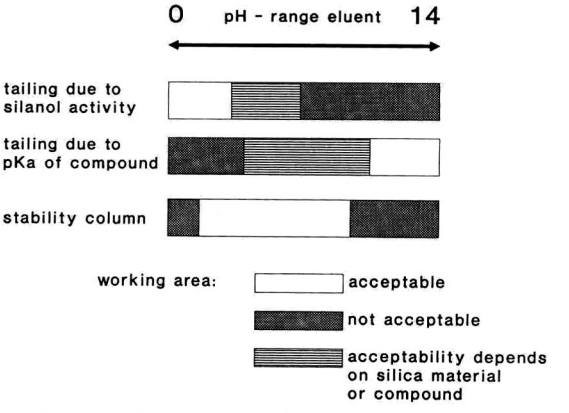

Fig. 1. Qualitative illustration of the working area for the analysis of basic compounds on silica-based reversed-phase materials.

Correspondence to: Dr. H. Hindriks, Department of Analytical Chemistry, Organon International BV, AKZO Pharma Group, P.O. Box 20, 5340 BH Øss, Netherlands.

0021-9673/92/$05.00

requirements for a good chromatographic performance with strongly basic compounds conflict with the demands for high stability of the column. Good performance requires a high pH to avoid ionization of the basic solute or a low pH to suppress the formation of free silanol groups.

Over the years, numerous suggestions have been put forward to improve this situation. Special attention has been given (i) to reducing the number of free silanols (end-capping), (ii) to diminishing the effect of free silanols by choosing the correct mobile phase pH and reducing the acidity of the silica and (iii) to eliminating silanol effects by adding inorganic and organic salts. The use of blocking agents such as tertiary and quaternary amines proved to be a useful approach [1,2].

Alternative solutions have been proposed by workers who used bare silica, dynamically modified silica or alumina [3,4]. These methods, however, did not gain widespread application. In RP-HPLC, the most obvious solution is the choice of a suitable column. Stadalius *et al.* [1] pointed to the existence of "acidic" and "basic" columns. The latter clearly are the best for this particular task. Over more than a decade our approach has been to improve the mobile phase composition and to test new stationary phases. As a result of this, μBondapak C_{18} and Nova-Pak C_{18} columns have been used more or less as a standard for the analysis of basic drugs. However, research on LC packings is continuing and recently resulted in the introduction of new columns specially designed for the chromatography of basic drugs [5].

In this paper, we present data on the influence of the mobile phase composition (pH, buffers, additives) on peak performance and on the stability of μBondapak C_{18}. We also compared the chromatographic performance of special column materials. For both, a set of 32 basic drugs was used. These drugs differ widely in pK_a, polarity and number and structural type of the nitrogen atoms.

EXPERIMENTAL

Chemicals

All basic drugs were obtained from Organon International (Oss, Netherlands). Methanol was freshly distilled and water was obtained from a Milli-Q quality purification system (Millipore). Tetramethylammonium hydroxide (TMAH) was obtained from Southwestern Analytical Chemicals (Austin, TX, USA). Disodium hydrogenphosphate (Na_2HPO_4), sodium dihydrogenphosphate (NaH_2PO_4) and 25% ammonia solution were supplied by J. T. Baker (Deventer, Netherlands), acetonitrile (CH_3CN) and concentrated phosphoric acid (H_3PO_4) by Merck (Darmstadt, Germany), sodium 1-hexanesulphonate by Eastman Kodak (Rochester, NY, USA) and triethylamine (TEA, Sequanal grade) by Pierce (Rockford, IL, USA).

The pK_a values of the basic drugs were determined in 60% methanol at 37°C because of the low solubility in water. As a rule these pK_a values are *ca.* 0.5–1 unit lower than in water.

Apparatus

The experiments were carried out on an HP 1090M liquid chromatograph equipped with an HP 1040M diode-array detector. Data were collected on an HP 79994A HPLC workstation (Hewlett-Packard, Amstelveen, Netherlands).

Experimental set-up

The experiments can be divided into three parts. In the first part of the study we used a μBondapak C_{18} column and chromatographed a set of 32 basic drugs with different mobile phases, as explained in Fig. 2A. The influence of the mobile phase parameters on the asymmetry factor was studied quantitatively, and more qualitatively on plate number. We also checked their influence on the stability of the stationary phase.

In the second part, recent developments in column technology were explored. For this we used different stationary phases, specially recommended by the manufacturers for the chromatography of basic drugs. With a constant mobile phase composition we studied the chromatographic performance of these columns with our set of basic drugs. In Fig. 2B an overview is shown of these experiments. The results will be described in a qualitative way.

In order to show column effects and differences between columns as well as possible, we performed comparative experiments under critical conditions. Therefore, we chose pH values of 3.5 and 7.4 and plain buffer without additives, as the addition of silanol blockers can mask differences.

For this study a set of 32 basic drugs was selected

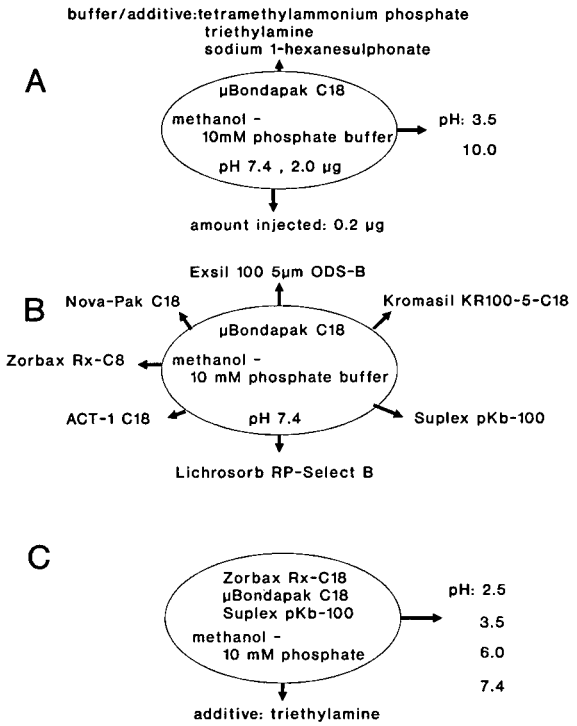

Fig. 2. Overview of the experiments in this study.

and a representative group of them is shown in Table I. The selection of 32 compounds was based on the following characteristics: basicity, with pK_a values ranging from 3 to 9, polarity, with retention indices [6] between 400 and 1600, number of nitrogen atoms, from 1 to 5, and different structural type of nitrogen atom.

In the third part the effects of pH and the addition of triethylamine were studied for seven "difficult" compounds on three selected columns (see Fig. 2C).

Chromatographic conditions

All bonded-phase materials were obtained from the manufacturers as prepacked columns. An overview of the stationary phases is given in Table II. The mobile phases used in this study are shown in Table III.

The pH of the buffers was measured before mixing with the organic modifier. They were prepared by dissolving 3.58 g (10 m*M*) of disodium hydrogenphosphate or 9.05 g (50 m*M*) of tetramethylammonium hydroxide in 1 l of water. Occasionally 2 ml (15 m*M*) of triethylamine was added to the phosphate solution. Concentrated phosphoric acid or 0.5 *M* sodium hydroxide was finally added until the desired pH was reached.

The amount of basic drug injected was 2.0 μl of a 1 mg/ml solution in methanol, *i.e.*, 2 μg injected, unless indicated otherwise. After 10–20 injections of the basic drugs, a test solution was injected to check the column performance for changes in silanol activity, hydrophobicity and metal activity. The test solution consisted of a mixture of acetylacetone, aniline, phenol, benzene and anthracene. Methanol–water (60:40, v/v) was used as mobile phase for the test solution. The column temperature was 40°C and UV detection was carried out at 210 nm. Triethylamine should be of a high-purity grade to prevent a high UV offset. For basic drugs the flow-rate was set at 1.0 ml/min and for the test solution at 1.5 ml/min.

Calculations

The asymmetry factors were calculated at 10% of the peak height using the ratio of the width of the rear and front sides of the peak [7]. Because most peaks do not have an ideal Gaussian shape, we used the second moment of the peak for the calculation of the plate numbers [8].

RESULTS AND DISCUSSION

Varying the mobile phase composition using a μBondapak C_{18} column

The aim of this study was to find the best mobile phase conditions for the analysis of basic compounds. In the first set of experiments we chromatographed all basic drugs on a μBondapak column, using the starting conditions given in Fig. 2A [methanol–10 m*M* phosphate (pH 7.4), 2 μg injected]. Clearly, as can be seen in Fig. 3, there is a strong correlation between the pK_a value of the compound and the asymmetry factor. Generally, peak tailing increases with increasing pK_a values. These results have been confirmed by others [1]. Peak tailing is also a function of the capacity factor, as illustrated in Fig. 4 for a number of basic drugs. Therefore, the data given in Fig. 3 were normalized for a k' value of 5.

TABLE I

COMPOUNDS USED WITH THEIR pK_a VALUES AND RETENTION INDICES (I)

Asymmetry factors (A_s) were obtained under the conditions described in Fig. 3.

No.	Structure	pK_a	I	A_s
1	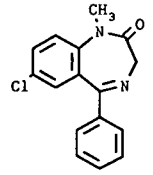	<3	790	1.0
2	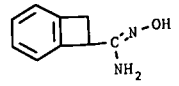	5.0	460	1.7
3	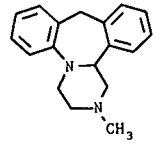	6.5	1120	2.6
4	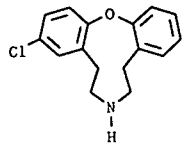	8.2	1380	5.2
5	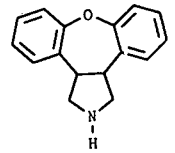	8.3	1160	3.6
6	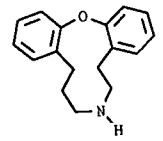	8.7	1550	9.1
7	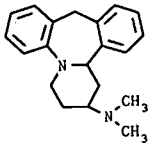	7.9	1360	4.8
8	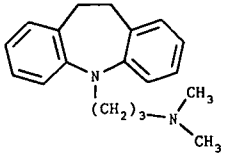	8.0	1310	4.0
9	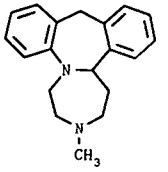	7.7	1310	5.7
10	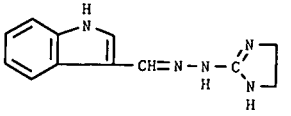	8.7	690	5.6
11	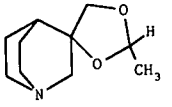	7.7 (not included in the test set)		

TABLE II

STATIONARY PHASES USED

No.	Column	Manufacturer	Dimensions [length × I.D. (mm)]	Particle size (μm)
1	μBondapak C_{18}	Waters–Millipore	300 × 3.9	10
2	Novapak C_{18}	Waters–Millipore	300 × 3.9	4
3	Zorbax Rx-C_8	Rockland Technologies	250 × 4.6	5
4	Zorbax Rx-C_{18}	Rockland Technologies	250 × 4.6	5
5	LiChrosorb RP-Select B	Merck	250 × 4.0	5
6	Exsil 100 5 μm ODS-B	Exmere	250 × 4.6	5
7	Kromasil KR100-5-C_{18}	Eka Nobel	250 × 4.6	5
8	Suplex pKb-100	Supelco	250 × 4.6	5
9	ACT-1 C_{18}	Interaction	150 × 4.6	10

For compounds having $pK_a < 6$ we did not observe any problems. Peaks were symmetric with asymmetry factors <1.5 and plate numbers were about 4000–6000. Asymmetric peaks were obtained for compounds with $pK_a > 6$. These compounds are partly protonated and hence more strongly bound to the acidic silanol groups:

$$XH^+ + SiO^-Na^+ \rightleftharpoons SiO^-XH^+ + Na^+ \quad (1)$$

There are indications that the pK_a value is not the only parameter that influences peak tailing. It is thought that structural factors also play a role. For example, substances having comparable pK_a values show widely differing asymmetry factors. Generally it is observed that the flexibility of the protonated N atom and hence the possibility of interacting with silanol sites plays a predominant role. For instance, when we compare substances **6**, **4** and **5** (see Table I) the decrease in the flexibility in this order of the (protonated) N atom is significant. The asymmetry factor decreased likewise. Data on the flexibility of protonated and unprotonated N atoms were taken from NMR measurements.

TABLE III

MOBILE PHASES USED WITH THE VARIOUS COLUMNS

Mobile phase	Columns used
CH_3OH–50 m*M* TMAH, pH 7.4	1
CH_3OH–10 m*M* NaH_2PO_4, pH 2.5	1,4,8
CH_3OH–10 m*M* NaH_2PO_4, pH 3.5	1,4,8
CH_3OH–10 m*M* Na_2HPO_4, pH 6.0	1,4,8
CH_3OH–10 m*M* Na_2HPO_4, pH 7.4	1,2,3,4,5,6,7,8
CH_3OH–10 m*M* Na_2HPO_4, pH 10.0	1
CH_3OH–10 m*M* NaH_2PO_4 + 15 m*M* TEA, pH 2.5	1,4,8
CH_3OH–10 m*M* NaH_2PO_4 + 15 m*M* TEA, pH 3.5	1,4,8
CH_3OH–10 m*M* Na_2HPO_4 + 15 m*M* TEA, pH 6.0	1,4,8
CH_3OH–10 m*M* Na_2HPO_4 + 4 m*M* TEA, pH 7.4	1
CH_3OH–10 m*M* Na_2HPO_4 + 15 m*M* TEA, pH 7.4	1,4,8
CH_3OH–10 m*M* Na_2HPO_4 + 10 m*M* IPR, pH 3.5	1
CH_3OH–H_2O	6,8
CH_3CN–1% NH_3, pH 11.2	9

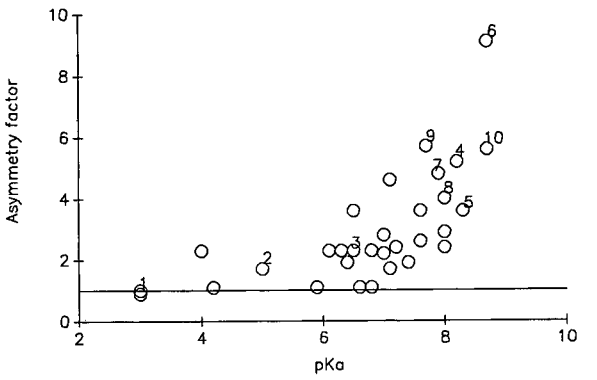

Fig. 3. Scatter plot of pK_a *versus* peak asymmetry, normalized for $k' = 5$. The numbers in the plot correspond to compounds in Table I. For HPLC conditions, see starting conditions in Fig. 2A.

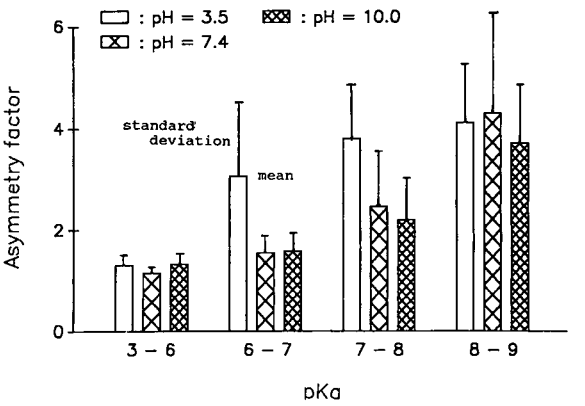

Fig. 5. Influence of the buffer pH on peak asymmetry. Methanol was used as modifier and 2.0 μg were injected. For HPLC conditions, see Fig. 2A. The bars represent the mean and standard deviation (as shown).

Influence of the pH of the buffer

The influence of the pH of the buffer was tested with 10 m*M* sodium phosphate at different pH values in the range 3.5–10. Lowering the pH to 3.5 will result in less dissociation of the silanol groups, whereas at pH 10.0 none of the compounds is protonated. In the literature a pH of less than 3.5 is often recommended to suppress silanol activity as effectively as possible. On purpose we chose a pH of 3.5, which in our view was sufficiently critical to show differences between columns. The effects of lower pH will be discussed later.

As is shown in Fig. 5, the overall results on a μBondapak column were in favour of the higher pH values, especially for substances with pK_a = 6–8. The effects on peak asymmetry are probably not statistically different for compounds with pK_a 3–6 and 8–9. At pH 7.4 most of the test compounds are not protonated and the effect of dissociated silanols is therefore small. Strongly basic compounds (pK_a > 8) will be retained by the mechanism shown in eqn. 1. An effect that is often overlooked is that the pH of a methanol–buffer mixture differs significantly from that of the starting buffer. For instance, 10 m*M* phosphate buffer (pH 7.4) shows a virtual pH of 8.6 in a 1:1 mixture with methanol. These results conflict with the general opinion that a low pH is the best condition for the chromatography of basic compounds. In order to support our conclusions, we present additional data on this pH effect for three different columns in the last section of this paper.

The use of a buffer of pH 10.0 led to a small improvement only for very basic substances. This high pH is in fact unrealistic and was only incorporated to see whether unexpected effects would arise. Summarizing, we recommend a pH of *ca.* 7.

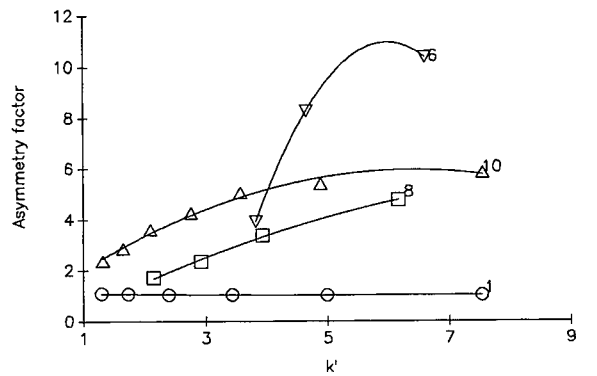

Fig. 4. Relationship between asymmetry factor and k' for substances covering the pK_a range <3–8.7.

Influence of the type of buffer

To determine the influence of the type of buffer, we compared 50 m*M* tetramethylammonium phosphate and 10 m*M* sodium phosphate buffers. A low concentration of sodium phosphate was necessary because of the low solubility in eluents with a high methanol concentration. In our laboratory tetra-

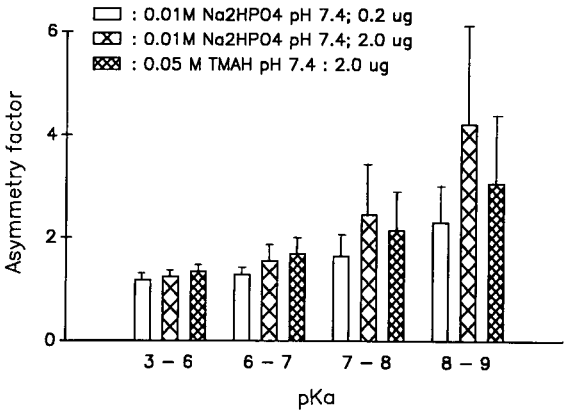

Fig. 6. Influence of the type of buffer and the amount injected on peak asymmetry. Methanol was used as modifier. For HPLC conditions, see Fig. 2A, using tetramethylammonium phosphate (TMAH) buffer.

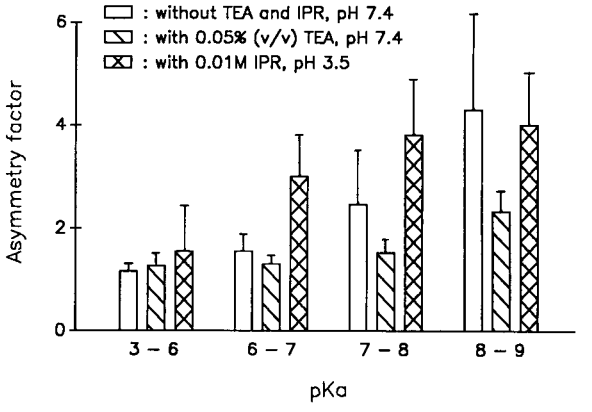

Fig. 7. Influence of triethylamine (TEA) and sodium 1-hexanesulphonate (IPR) on peak asymmetry. Methanol was used as modifier and 2.0 μg were injected. For HPLC conditions, see Fig. 2A.

methylammonium phosphate buffer is being used as a standard for the HPLC of basic drugs. The results obtained with the two buffers are summarized in Fig. 6. For compounds with $pK_a < 8$ almost no difference in peak shape was noticed. As far as plate numbers are concerned the use of sodium phosphate resulted in a slight increase. For compounds with $pK_a > 8$ tetramethylammonium phosphate showed better results (although not statistically significant), but the asymmetry factors were still > 2. Overall it can be concluded that tetramethylammonium phosphate can be used successfully to improve peak shapes by effectively blocking silanol activity. It should be added, however, that the tetramethylammonium ion is aggressive.

Influence of the type of additive

To determine the influence of a silanol blocking agent, triethylamine was used with 10 m*M* sodium phosphate buffer (pH 7.4). The results were compared with those without triethylamine and are shown in Fig. 7 and Table V. Triethylamine (TEA) is a very basic compound ($pK_a \approx 11$) which will also interact with silanol groups and so compete with the basic drugs. Dimethyloctylamine (DMOA) has been successfully used by others [1] for the same purpose. A comparison between TEA and DMOA is now under study. As can be seen in Fig. 7, the addition of triethylamine resulted in a clear improvement in peak shape. Particularly for compounds with $pK_a > 6$ the tailing clearly decreased, resulting in plate numbers of 3000–6000 with acceptable symmetry. However, several basic drugs still have unacceptable peak shapes. Comparing Figs. 6 and 7 it can be concluded that the effect of TEA is better than that of tetramethylammonium. Whether the addition of TEA is to be preferred at high (*ca.* 7) or low (*ca.* 3) pH will be discussed later.

Sodium 1-hexanesulphonate was also tested as an ion-pair reagent (IPR). For this the basic drugs have to be protonated and 10 m*M* sodium phosphate (pH 3.5) was used as a buffer. Comparing these results with those obtained with 10 m*M* sodium phosphate buffer (pH 3.5), the addition of IPR did not result in a clear improvement of peak symmetry. Compared with sodium phosphate (pH 7.4), the peak symmetry is even worse, except for compounds with $pK_a = 8$–9, where addition of IPR seems to result in less tailing.

Influence of the amount injected

For the determination of the influence of the amount of basic drug injected on to the column, several experiments were compared. Amounts of 0.2 and 2.0 μg were injected and 50 m*M* tetramethylammonium phosphate (pH 7.4) and 10 m*M* sodium phosphate (pH 3.5 and 7.4) were used.

Decreasing the amount injected can dramatically improve the peak symmetry (Fig. 6). Although Fig. 6 shows only data at pH 7.4, the effect is also seen at

pH 3.5, for both sodium phosphate and tetramethylammonium phosphate. Most asymmetry factors were < 2 when 0.2 μg was injected. For very tailing compounds the asymmetry factor was even reduced by a factor of 2 for small amounts injected. Especially for substances with low UV absorbance (see compound **11**, Table I) the large amounts injected are the main reason for peak tailing. When the amount of sample is reduced, the saturation of the acidic sites of the residual silanol groups will be avoided.

Influence of mobile phase composition on column stability

The analysis of basic compounds with RP-HPLC is often used in quality control and stability studies. This means that many samples have to be analysed and that mobile phase volumes of the order of 1000 ml and more are pumped over the column. Therefore, it is important to use a mobile phase–stationary phase combination that is not destructive.

During the experiments, as shown in Fig. 2A, the μBondapak column was tested for changes in silanol activity, hydrophobicity and metal activity. To check the silanol activity a mixture of aniline and phenol was injected. For well deactivated stationary phases aniline elutes before phenol [9,10]. To check the hydrophobicity a mixture of anthracene and benzene was injected. A change in the ratio of the retention times indicates a change in hydrophobicity [9]. Acetylacetone was used to determine the metal activity [9]. It can form a complex with metal ions, resulting in a broad and tailing peak that is retained. In Fig. 8 a chromatogram of the test solution is shown.

When tetramethylammonium phosphate and sodium phosphate (pH 7.4) were compared it was seen that the former is more aggressive and strips off the stationary phase. As shown in Figs. 9 and 10, the change in silanol activity and hydrophobicity is less pronounced with sodium phosphate. These conclusions were confirmed by Wherli *et al.* [11], who also found that quaternary ammonium compounds are aggressive towards silica-based stationary phases. Adding triethylamine or sodium 1-hexanesulphonate to the mobile phase did not clearly influence the stability of the column.

As far as the metal activity is concerned, when tetramethylammonium phosphate was used the peak shape of acetylacetone was sharp and eluted after $k' = 1$ at the beginning of the experiment. The tailing steadily increased and the retention decreased to $k' = 0.1$ after 1000 ml mobile phase had been pumped over the column. Subsequently the peak symmetry and retention time remained stable. An increase in tailing indicates an increase in metal

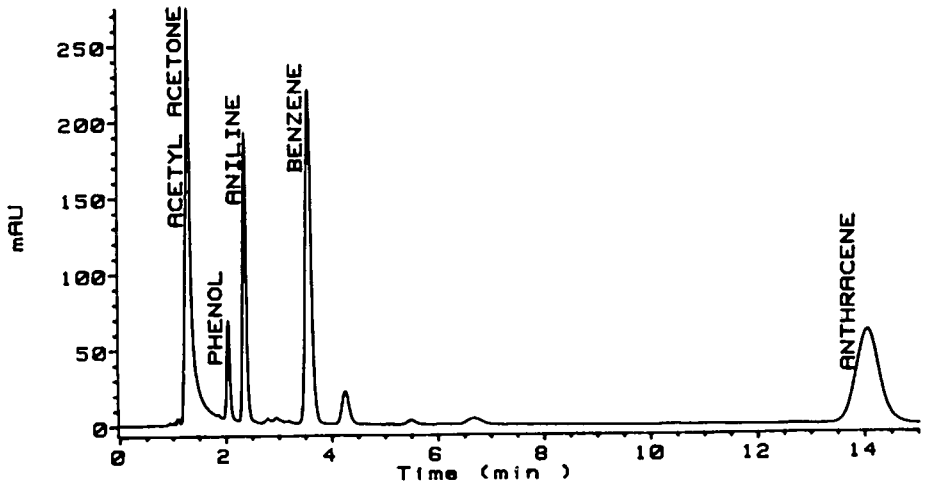

Fig. 8. Chromatogram of the test compounds on a μBondapak C_{18} column (300 × 3.9 mm I.D.). Methanol–water (60:40, v/v) was used as eluent.

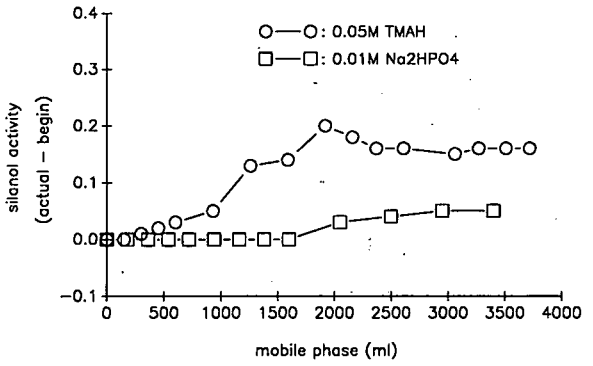

Fig. 9. Influence of the type of buffer and the volume pumped over the column on silanol activity (expressed as the difference between the actual and the starting values). For HPLC conditions, see Figs. 2A and 5.

activity. The decrease in retention indicated a decrease in metal activity or could be a result of reduced reversed phase activity due to a loss of bonded phase. When phosphate was used the peak shape was asymmetric but stable. The retention time decreased from $k' = 0.4$ to 0.1 after 3400 ml of mobile phase had been pumped over the column.

Another parameter that can influence the stability of the column is the pH of the mobile phase. In Fig. 11 the influence of the pH on silanol activity is shown. It was found that the use of high pH resulted in a rapid increase in silanol activity and a decrease in hydrophobicity. This high pH will strip off the stationary phase. The use of pH 3.5 showed no change in silanol activity and hydrophobicity, whereas for pH 7.4 a slight change after about 1500 ml was noticed.

Varying the stationary phase

Stationary phases specially developed for the analysis of basic compounds were investigated and the results were compared with those with the μBondapak column, using methanol–10 m*M* sodium phosphate buffer (pH of 7.4) as the mobile phase. In order to ensure a fair appraisal, the columns were compared in the same k' range. The results are described in a qualitative way.

Nova-Pak C_{18}. The Nova-Pak C_{18} column showed more tailing for most compounds with a $pK_a > 7$. For compounds with $pK_a < 7$ there is less difference. Most compounds have asymmetry factors of $\leqslant 2$. Owing to the smaller particle size of the Nova-Pak phase, for symmetrical peaks it gives about twice as many plates as μBondpak C_{18} under comparable conditions.

Zorbax Rx-C_8, Kromasil KR-5-C_{18} and LiChrosorb RP-Select B. These three columns are offered as stationary phases specially deactivated for basic compounds. They did not show a clear improvement in peak symmetry compared with a μBondapak C_{18} column. For nine compounds with $pK_a >$ 7 the Kromasil column even showed asymmetry factors of $\geqslant 3$. However, for symmetrical peaks the plate number was over 10 000.

Exsil 100 5 μm ODS-B. The Exsil phase is also specially deactivated for basic compounds and, ac-

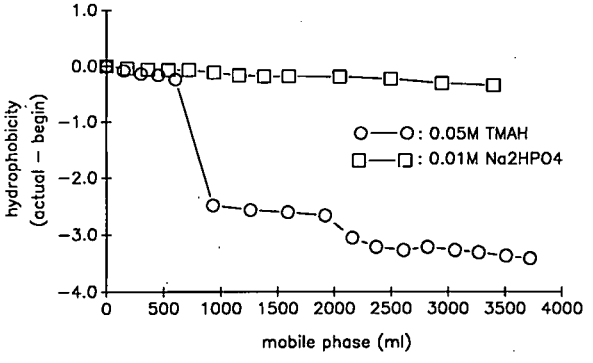

Fig. 10. Influence of the type of buffer and the volume pumped over the column on hydrophobicity (expressed as the difference between the actual and the starting values). For HPLC conditions, see Figs. 2A and 5.

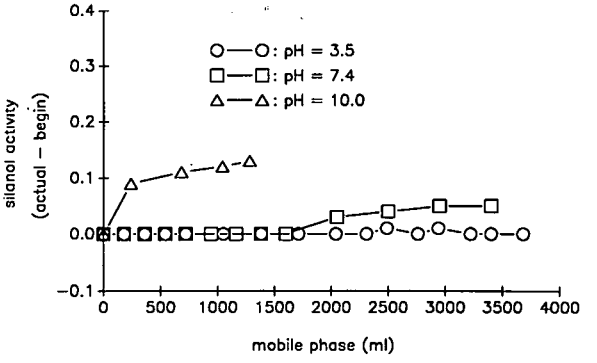

Fig. 11. Influence of the pH of sodium phosphate buffer and volume pumped over the column on silanol activity (expressed as the difference between the actual and the starting values). For HPLC conditions, see Figs. 2A and 6.

cording to the manufacturer, basic compounds can be eluted even without buffer. For the compounds in our test series this was correct. All compounds, however, had extremely asymmetric peaks with asymmetry factors of $\geqslant 6$. The use of 10 m*M* sodium phosphate (pH 7.4) instead of water did not reduce the peak asymmetry significantly.

Suplex pKb-100. The Suplex column is a silica-based C_{18} stationary phase in which residual silanols are electrostatically shielded. First this column was tested with methanol–10 m*M* sodium phosphate (pH 7.4) as eluent. As can be seen in Fig. 12, good peak shapes were obtained. Only six compounds had an asymmetry factor larger than 2 and plate numbers were in the range 3000–11 000. Compared with μBondapak, this stationary phase is more suitable for the analysis of basic compounds.

The column was also tested without buffer using a methanol–water mobile phase, which can be advantageous when the system is coupled to a mass spectrometer. In that event the column should be "conditioned" by washing with 10 m*M* buffer. Under these conditions good peak shapes were also obtained. Only one compound showed an asymmetry factor > 2. Plate numbers were also in the range 3000–11 000. However, five compounds with $pK_a > 8$ showed fronting peaks. This phenomenon

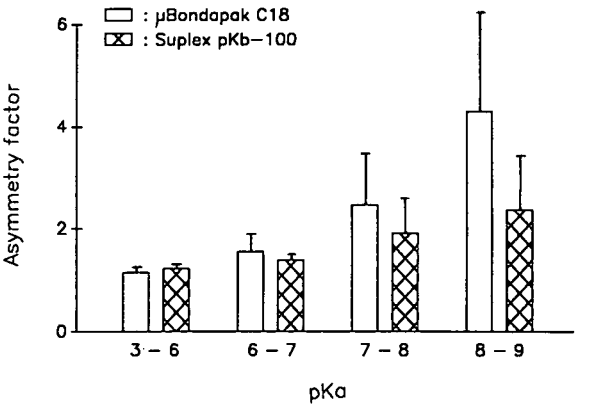

Fig. 12. Comparison between μBondapak C_{18} and Suplex pKb-100. Methanol–10 m*M* sodium phosphate (pH 7.4) was used as eluent and 2.0 μg were injected.

was not observed using a phosphate buffer. Of course, for a rugged method involving ionic and ionizable compounds, the mobile phase should always be carefully buffered. In Fig. 13 chromatograms of a compound with $pK_a = 8.7$ with and without buffer are shown.

In our experience, it was found that for this column the equilibration time is longer than usual. Reproducibility proved to be good in comparison with

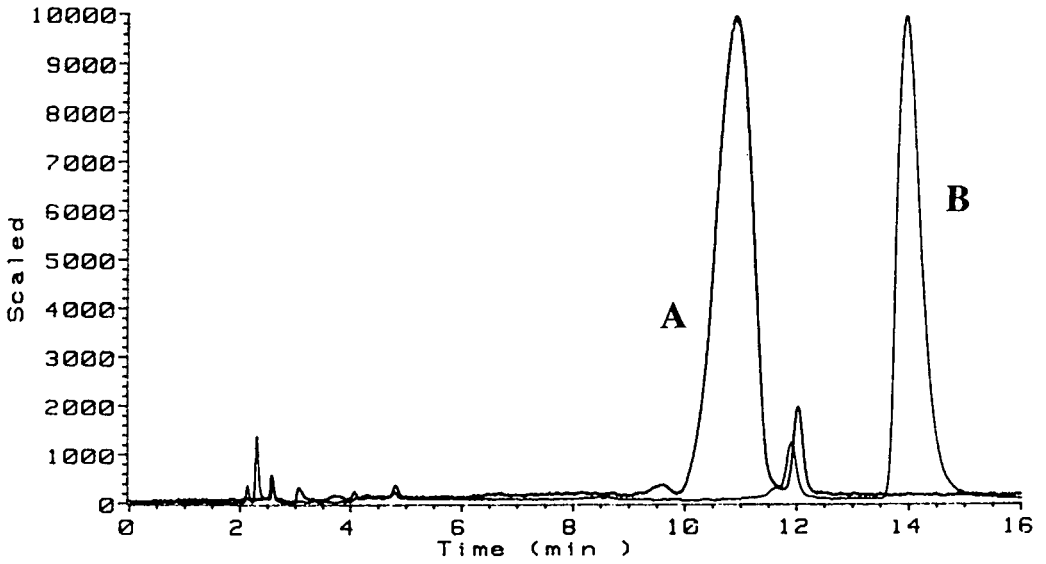

Fig. 13. Chromatograms of a basic compound ($pK_a = 8.7$) (A) without and (B) with 10 m*M* sodium phosphate (pH 7.4) on the Suplex pKb-100 column.

TABLE IV

COMPARISON OF THE STATIONARY PHASES

Column	Peak shape[a]	Plate number[a]	Stability[a]	Remarks
μBondapak C_{18}	0	0	0	
Nova-Pak C_{18}	−	+	0	
Kromasil KR100-5-C_{18}	0	+	0	
Zorbax Rx-C_8	0	+	0	
Lichrosorb RP-Select B	0	+	0	
Exsil 100 5 μm ODS-B	− −	−	0	Can be used without buffer
Suplex pKb-100	+	+	0	Can be used without buffer
ACT-1 C_{18}	0	− −	+	Very pH stable

[a] − −, very bad; −, bad; 0, acceptable; +, good.

conventional columns. For better stability acetonitrile should be used instead of methanol.

ACT-1 C_{18}. This column is based on a C_{18}-polymer stationary phase. The advantage over silica-based columns is that there are no ionic or ionizable species present. Further, these columns are very stable and a pH range of 0–14 can be used. Our results with this column show acceptable tailing, of the order of 1.5–3. However, a great disadvantage is the low plate numbers obtained. They are of the order of 50–250, which is less than 10% of the plate numbers obtained with a μBondapak C_{18} column.

The results obtained with the different stationary phases are summarized in Table IV, with the advantages and/or disadvantages of each column.

Comparison of μBondapak C_{18}, Zorbax Rx-C_{18} and Suplex pKb-100

The experiments in the first section under Results and Discussion strongly suggest that at pH 3.5, where the compounds are protonated, the dissociated silanols are still fully active. Even at pH 2.5, a pH recommended by most manufacturers, the peak shape improved only marginally (see Table V). Plain buffers are therefore unable to mask effectively silanol effects.

A further illustration, also using a Zorbax Rx-C_{18} column, is given in Fig. 14. At a buffer pH of 7.4 the substances are not protonated and a high portion of methanol is needed to elute them from the column. With a buffer of pH 6.0 the compounds

TABLE V

COMPARISON OF THREE COLUMNS TESTED UNDER LOW pH CONDITIONS

Column	Eluent[a]	Compound	pK_a	pH 3.5		pH 2.5		pH 2.5 + 15 m*M* TEA	
				k'	A_s	k'	A_s	k'	A_s
Zorbax Rx-C_{18}	A	**7**	7.9	3.2	5.1	3.1	4.3	3.1	2.1
		6	8.7	2.1	4.1	1.7	4.3	1.8	2.5
		9	7.7	2.6	4.5	2.1	4.0	2.2	2.0
		8	8.0	4.4	5.1	4.1	4.5	4.3	2.2
μBondapak C_{18}	A	**7**	7.9	3.3	8.6	3.3	7.3	3.2	1.7
		6	8.7	2.2	7.4	2.3	5.6	2.2	2.1
		9	7.7	2.4	7.7	2.5	5.8	2.4	1.6
		8	8.0	4.6	9.7	4.6	7.6	4.5	1.7
Suplex pKb-100	B	**7**	7.9	4.5	1.9	4.8	1.9	4.1	1.7
		6	8.7	1.9	1.6	2.0	1.5	1.8	1.7
		9	7.7	2.9	1.7	2.9	1.6	2.7	1.5
		8	8.0	6.2	2.0	6.4	1.9	5.4	1.7

[a] A = methanol–10 m*M* sodium dihydrogenphosphate (50:50); B = methanol–10 m*M* sodium dihydrogenphosphate (25:75).

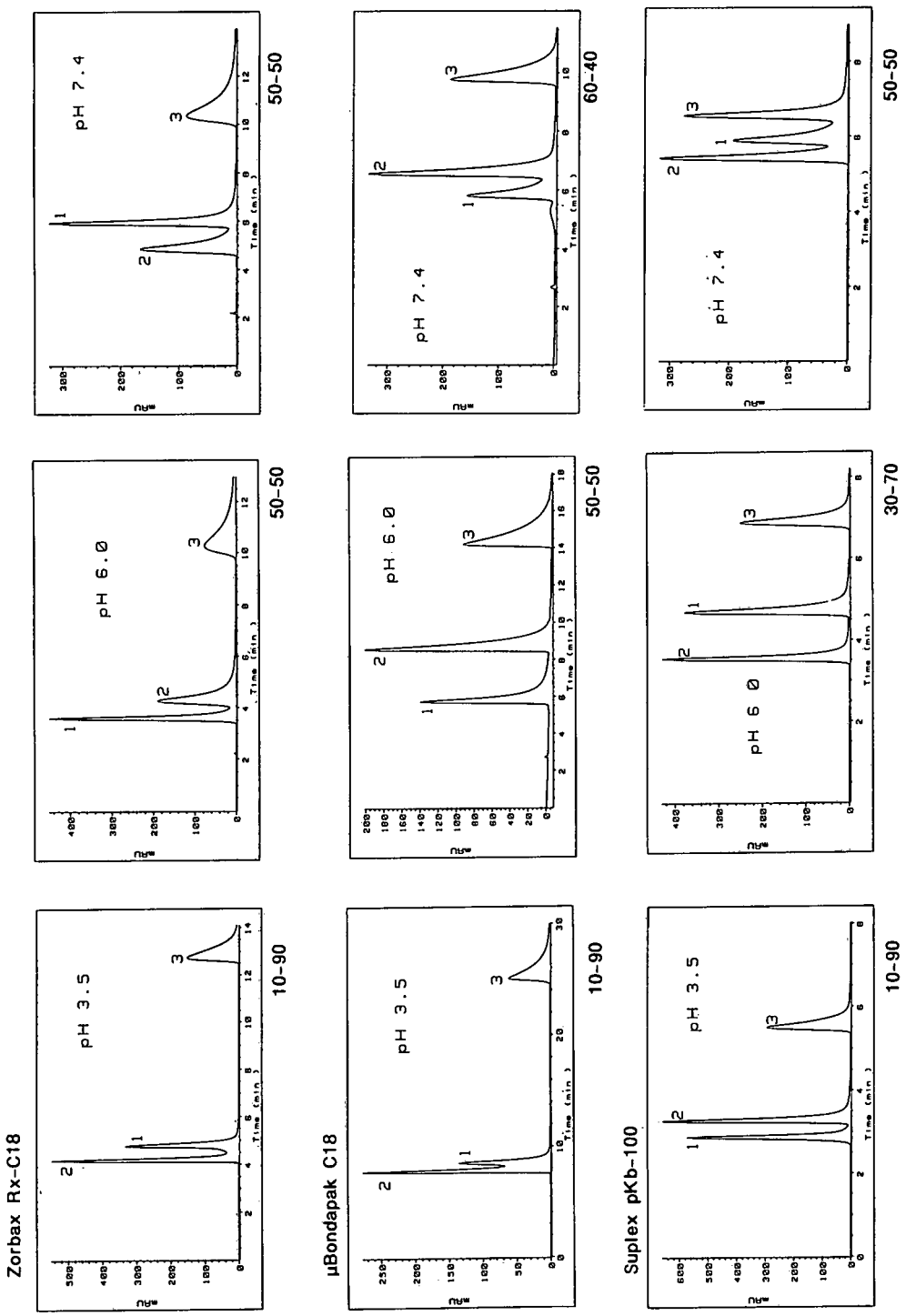

Fig. 14. Comparison of Zorbax Rx-C_{18}, µBondapak C_{18} and Supex pKb-100 at pH 7.4, 6.0 and 3.5. Solutes: 1 = oxymorphone, pK_a = 7.65; 2 = morphine, pK_a = 7.08; 3 = codeine, pK_a = 7.00. The methanol–10 m*M* phosphate compositions are given beneath the plots.

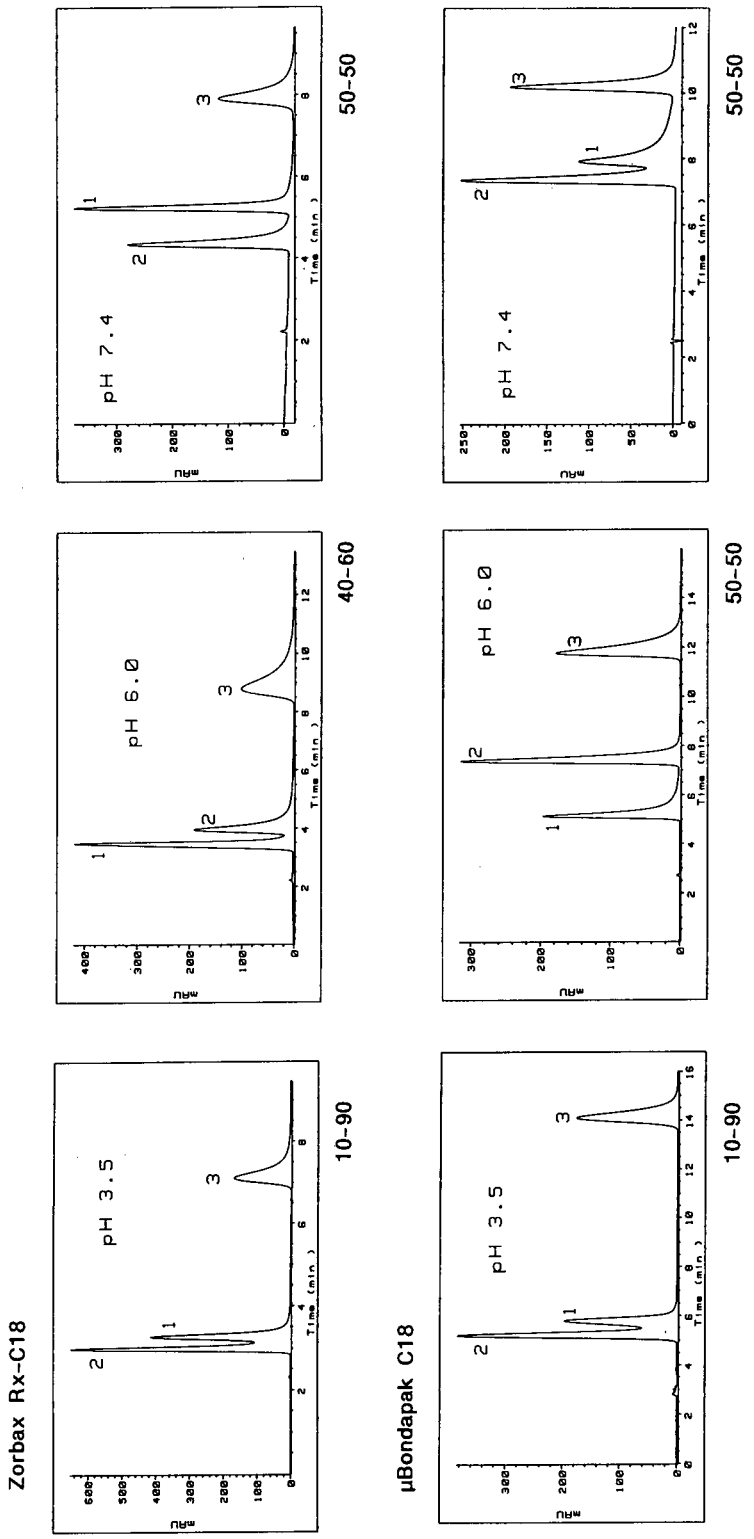

Fig. 15. Chromatograms of the separation of three morphines at pH 7.4, 6.0 and 3.5 after addition of 15 m*M* triethylamine to the mobile phase. The methanol–10 m*M* phosphate compositions are given beneath the plots.

are partly protonated (more polar, less methanol needed), which, especially for codeine, leads to increased tailing. At a pH of 3.5 the peaks are sharpened and silanol effects are suppressed. A remarkable effect is the inversion of morphine and oxymorphone as a result of the pH change.

For a set of four "difficult" compounds we also studied the effect of the addition of TEA at pH 2.5. As shown in Table V for μBondapak C_{18} and Zorbax Rx C_{18} dramatic improvements were obtained. We conclude from this critical evaluation that despite a low eluent pH and column deactivation, many active sites still exist that can only be masked by adding TEA.

A major conclusion for the chromatographer is that a low pH in the presence of TEA represents the best condition for the chromatography of basic compounds on conventional reversed-phase columns. This recommendation is again illustrated in Fig. 15. The morphines already shown in Fig. 14 were now eluted under the same conditions except for the addition of 15 m*M* TEA. Here also the results are significant.

For the Suplex column a different result was obtained. The special character of this stationary phase can also be deduced from the data in Table V. Clearly, the shielding is so effective that addition of TEA is no longer necessary. As a further illustration we refer to Fig. 14 for the separation of morphine, oxymorphone and codeine. The best condition proved to be pH 3.5, but without TEA.

CONCLUSIONS

The optimization of the peak shapes of basic compounds is difficult and many parameters can be varied. It was found that the peak tailing depends on the pK_a value and structural parameters of a compound. When tailing occurs the addition of silanol blocking reagents, such as triethylamine, was most effective in suppressing this effect. The addition of ion-pair reagents, however, did not improve the symmetry.

As far as the stationary phases are concerned, the use of an electrostatically shielded phase improved the peak shapes. This type of column showed acceptable tailing, even without the addition of additives that suppress silanol activity. With a polymer-based stationary phase reasonable peak shapes were obtained. However, owing to the low plate number, this column has a poor separation efficiency.

REFERENCES

1 M. Stadalius, J. Berus and L. Snyder, *LC · GC*, 6 (1988) 494.
2 J. Kiel, S. Morgan and R. Abramson, *J. Chromatogr.*, 320 (1985) 313.
3 S. Hansen, P. Helboe and M. Thomsen, *Trends Anal. Chem.*, 7 (1988) 389.
4 H. Lingeman and W. Underberg, *Trends Anal. Chem.*, 7 (1988) 346.
5 T. Ascah and B. Feibush, *J. Chromatogr.*, 506 (1990) 357.
6 J. Baker and C. Ma, *J. Chromatogr.*, 26 (1979) 107.
7 L. R. Snyder and J. J. Kirkland, *Introduction to Modern Liquid Chromatography*, Wiley, New York, 2nd ed., 1979, p. 222.
8 J. Foley and J. Dorsey, *Anal. Chem.*, 55 (1983) 730.
9 L. Sander, *J. Chromatogr. Sci.*, 26 (1988) 380.
10 H. Engelhardt and M. Jungheim, *Chromatographia*, 29 (1990) 59.
11 A. Wherli, J. Hildenbrand, H. Keller, R. Stampfli and R. Frei, *J. Chromatogr.*, 149 (1978) 199.

Journal of Chromatography, 623 (1992) 221–228
Elsevier Science Publishers B.V., Amsterdam

CHROM. 24 480

Development of a flavoprotein column for chiral separation by high-performance liquid chromatography

Nariyasu Mano, Yoshiya Oda, Naoki Asakawa, Yutaka Yoshida and Tadashi Sato

Department of Physical and Analytical Chemistry, Tsukuba Research Laboratories, Eisai Co., Ltd., 5-1-3 Tokodai, Tsukuba, Ibaraki 300-26 (Japan)

Toshinobu Miwa

Department of Pharmaceutical Research Laboratory, Eisai Co., Ltd., 2-1 Takehaya-machi, Kawashima-cho, Hashima-gun, Gifu 483 (Japan)

(First received March 26th, 1992; revised manuscript received June 25th, 1992)

ABSTRACT

A new chiral stationary phase using flavoprotein, a glycoprotein present in chicken egg-white, was developed for high-performance liquid chromatography. This column could achieve baseline separations of acidic (ketoprofen), weakly acidic (warfarin) and neutral (benzoin) compounds. In the flavoprotein-conjugated silica gel column, the capacity factor and enantioselectivity for several model drugs were greatly influenced by the pH and the concentration of organic solvents and salts in the mobile phase, and the optimum conditions for chiral separation varied from compound to compound. However, this column shows good stability to pH variation and to organic solvents, and it should be applicable for the chiral separation of many compounds in the reversed-phase mode. This column can directly separate optical isomers with an aqueous mobile phase, so it should be very useful in the fields of pharmacokinetics and clinical chemistry.

INTRODUCTION

Many pharmaceutical drugs have asymmetric centres, but most of them are used clinically in racemic form. However, drug enantiomers can have qualitatively or even quantitatively different physiological actions, so chiral resolution has become an important subject in the development and use of pharmaceutical drugs. Some direct chiral separations have been achieved by high-performance liquid chromatography (HPLC) in the normal-phase mode, but laborious pretreatments were required in the application of these methods to biological samples for pharmacokinetic and pharmacological research. Further, many of the direct chiral separation columns have very high selectivity and cannot be used with a wide range of compounds. Therefore, there is an urgent requirement for direct chiral separation columns with a wide selectivity in the reversed-phase mode, for rapid and simple determination of enantiomers of clinically relevant drugs. Such columns would be very useful for research in the fields of pharmacokinetics and pharmacology.

Recently, various chiral stationary phases that can be used under reversed-phase conditions have been developed, such as protein-conjugated columns, cyclodextrin-conjugated columns [1,2], and a triacetylcellulose column [3]. Protein-conjugated columns have been proved useful by Allenmark *et al.*, who developed a bovine serum albumin (BSA)-conjugated column [4], and by Hermansson, who developed an α_1-acid glycoprotein (α_1-AGP)-con-

Correspondence to: Dr. N. Mano, Department of Physical and Analytical Chemistry, Eisai Co., Ltd., 5-1-3 Tokoda, Tsukuba, Ibaraki 300-26, Japan.

0021-9673/92/$05.00

jugated column [5]. A BSA-conjugated column has been used to resolve enantiomers of acidic compounds [4], and an α_1-AGP-conjugated column to resolve racemic amines [5,6]. On the other hand, Miwa *et al.* have developed a highly effective column for chiral recognition by using ovomucoid, an acidic glycoprotein found in chicken egg-white [7]. An ovomucoid column, which is now commercially available, can resolve acidic and basic enantiomers [8,9], and is relatively stable to variation of pH, to heat, and to organic solvents [7,10]. Kirkland *et al.* have reported that an ovomucoid column has a higher stability and better chiral resolution than an α_1-AGP-conjugated column [11]. Oda *et al.* have recently performed on-line simultaneous determination and resolution of enantiomers of verapamil and its metabolites in plasma with an ovomucoid column and a column-switching technique [12].

As mentioned above, protein-conjugated columns, such as the ovomucoid column, can be useful for pharmacokinetic studies because of their applicability to a reasonably wide range of drug enantiomers in the reversed-phase mode. However, there are still many enantiomers that cannot be resolved by commercially available protein-conjugated columns. Therefore, we still require new materials with a high chiral recognition ability and a wider range of selectivity when used in the reversed-phase mode.

In this study, we used flavoprotein, which is present in chicken egg-white, as a ligand for chiral separation by means of reversed-phase HPLC. Flavoprotein is a glycoprotein which has 14% carbohydrate, consisting of mannose, galactose, and glucosamide. Its p*I* value is *ca.* 3.9–4.1 [13], which is similar to that of ovomucoid (3.9–4.3), and its molecular mass is 32 000–36 000. Interestingly, it also has the ability to bind to riboflavin [14]. This paper describes a new stationary phase for chiral resolution, flavoprotein-conjugated silica gel, which allows the separation of many drug enantiomers by means of reversed-phase HPLC.

EXPERIMENTAL

Apparatus

A Tosoh CCPM pump (Tosoh, Tokyo, Japan) equipped with a UVIDEC100-VI variable-wavelength UV spectrophotometer (Japan Spectroscopic, Tokyo, Japan) was used. A stainless-steel column (150 mm × 4.6 mm I.D.) was packed with flavoprotein-conjugated silica gel. The samples were injected with a WISP 712 Autosampler (Waters Assoc., Milford, MA, USA). The pH was measured with a TDA HM-60S pH meter (Toa Electronics, Tokyo).

Preparation of flavoprotein column

Flavoprotein-conjugated silica gel was prepared as follows: Nucleosil 5NH_2 (2 g) and N,N-disuccinimidyl carbonate (3 g) reacted for 12 h in acetonitrile (50 ml) at room temperature in a rotary evaporator. The activated silica gel was collected by filtration and washed with acetonitrile and then with the coupling buffer (50 m*M* potassium phosphate buffer, pH 7.5). Flavoprotein (2 g) was dissolved in 50 ml of coupling buffer and then the activated silica gel was added. The mixture was allowed to react for 2 h at room temperature in a rotary evaporator, then the flavoprotein-conjugated silica gel was collected by filtration and washed with water and 2-propanol–water (1:2). This gel was packed into a stainless-steel column (150 mm × 4.6 mm I.D.) by a conventional high-pressure slurry-packing procedure.

Reagents and materials

Flavoprotein was purified from chicken egg-white [14]. Ketoprofen (KE), ibuprofen (IB), flurbiprofen (FL), and warfarin (WA) were purchased from Sigma (St. Louis, MO, USA). α,ε-Dibenzoyllysine (DB) and benzoin (BE) were from Tokyo Kasei Company (Tokyo). N,N-Disuccinimidyl carbonate was purchased from Wako (Osaka, Japan). Nucleosil 5NH_2 was purchased from Macherey-Nagel (Düren, Germany). Organic solvents and water were of HPLC-grade, and other chemicals were of high purity.

Sample preparation

Known amounts of drug enantiomers were dissolved in methanol, and each solution was diluted with water or water–methanol (1:1) to a concentration of 20 ng/ml, and 10 μl were injected into the HPLC column.

RESULTS AND DISCUSSION

Protein-conjugated columns generally show higher chiral recognition ability than other HPLC col-

umns used under reversed-phase conditions. However, there are many drug enantiomers that cannot be resolved on the currently available protein-conjugated columns. Flavoprotein is a chicken egg-white glycoprotein with the capacity to bind riboflavin in a ratio of 1:1 [15] at pH 4.0 or above [14]. This protein plays an important role in the transfer of riboflavin from blood to egg-white [15]. It is very stable to heat, retaining its riboflavin-binding capacity after heating at 100°C and pH 7.0 for 15 min [14]. So we expected that flavoprotein would be a stable ligand for chiral recognition, and we chose this protein to develop a new chiral stationary phase for HPLC with an aqueous mobile phase.

Ketoprofen (KE), ibuprofen (IB), and flurbiprofen (FL) are antiinflammatory drugs used extensively in clinical medicine (Fig. 1). Fig. 2A–C shows the chromatographic resolution of these acidic profen enantiomers on the new column. KE was baseline-resolved with 50 m*M* KH_2PO_4 (pH 4.6) containing 10% ethanol for elution, as shown in Fig. 2A. But IB (Fig. 2B) and FL (Fig. 2C) were not appreciably resolved under the same conditions in spite of their similar structures.

α,ε-Dibenzoyllysine (DB), another carboxyl group-containing compound (Fig. 1), gave almost the same chromatogram as IB (Fig. 2D). Warfarin (WA), an anticoagulant, is a weakly acidic compound (Fig. 1). With WA, we obtained the dramatic result that the retention time of the second-eluted enantiomer was twice that of the first-eluted enantiomer (Fig. 2E). However, benzoin (BE), which is a neutral compound (Fig. 1), was not well resolved under the same conditions (Fig. 2F): its retention time was far shorter than those of the other compounds.

Next we examined the character of the flavoprotein column in more detail by using KE, DB, WA, and BE as model compounds. First we examined the effect of the concentration of organic

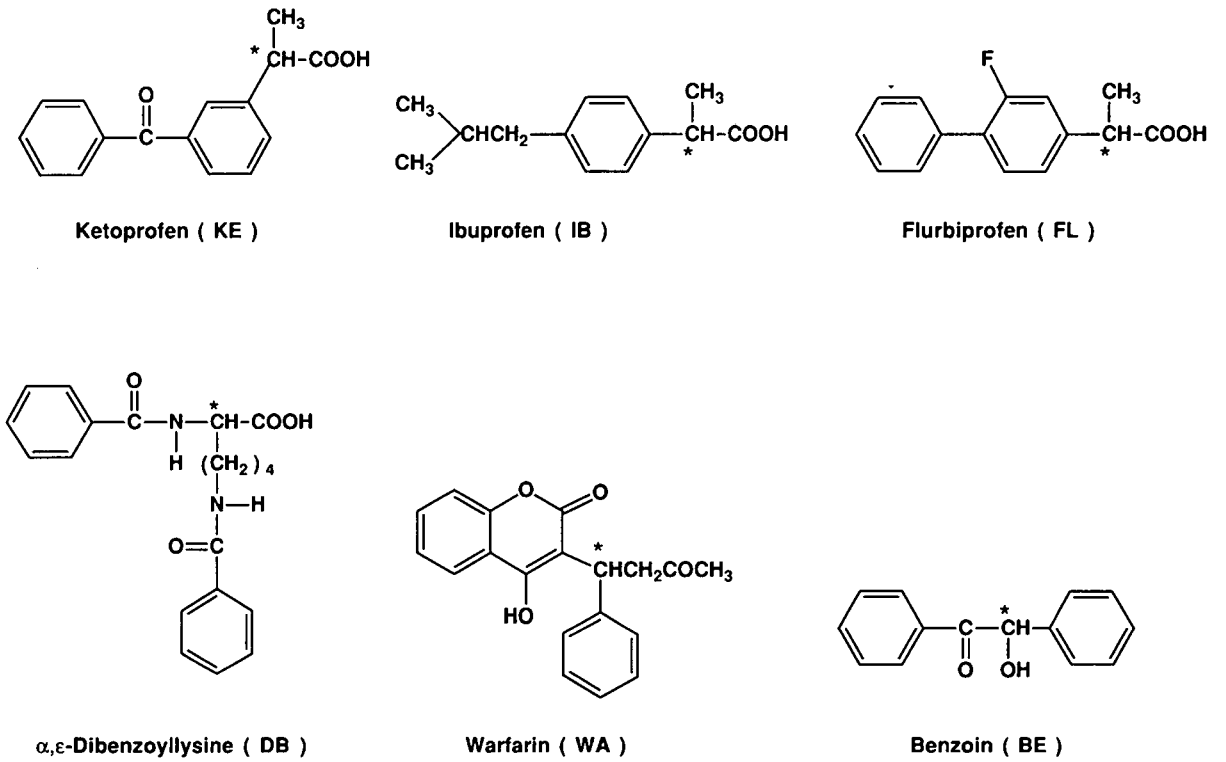

Fig. 1. Molecular structures of compounds resolved by HPLC on a flavoprotein-conjugated column. The chiral centres are indicated by asterisks.

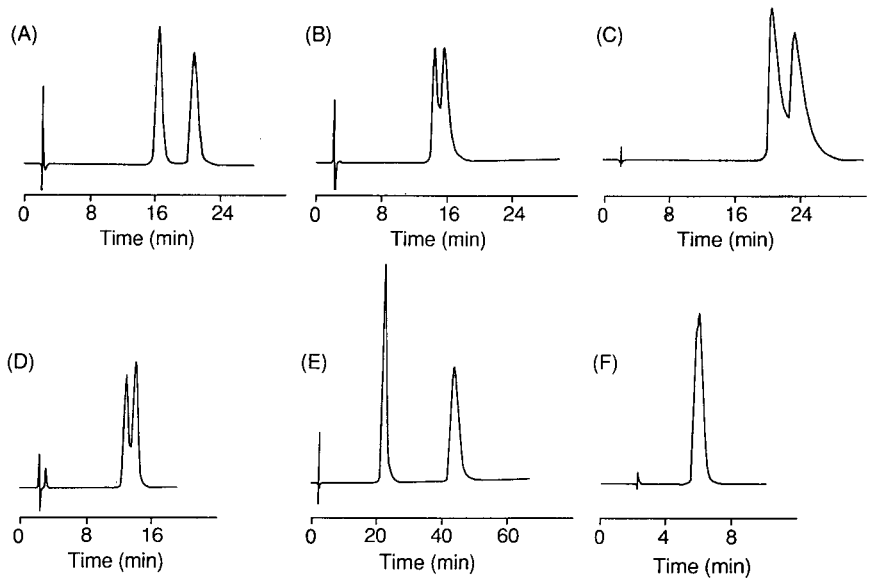

Fig. 2. Chromatograms of each compound on a flavoprotein-conjugated column: (A) KE; (B) IB; (C) FL; (D) DB; (E) WA; (F) BE. Chromatographic conditions: mobile phase, 50 m*M* KH_2PO_4 containing 10% ethanol; UV detection wavelength 230 nm; flow-rate, 1.0 ml/min; column temperature, room temperature.

solvent in the mobile phase on the capacity factor (k') and enantioselectivity. The column operation was apparently reversed-phase, as shown in Table I, because all the drugs showed longer retention times with a reduction in the concentration of organic solvent in the mobile phase. DB and BE, which could not be well resolved by elution with 50 m*M* KH_2PO_4 (pH 4.6) containing 10% ethanol, as mentioned above, showed increased separation factors (α value) and resolution (R_s value) with decreasing concentration of ethanol; this stronger retention of DB and BE led to better chiral separation, as described later. On the other hand, KE and WA did not show a regular variation of α values and R_s values, and the best resolution was obtained at 6% ethanol. However, these compounds were retained too strongly at 6% ethanol, and the peaks were considerably broadened. So the optimum concentration for chiral separation of KE and WA appears to be *ca.* 10% ethanol.

The performance of this column was greatly affected by the pH of the mobile phase. We examined the effect of the pH of the eluent containing 10% ethanol on the chiral separation. Fig. 3A shows the effect of pH on the retention of KE and DB. The *pK* value of a carboxylic acid is generally *ca.* 4 or 5, so KE and DB carry a negative charge above pH 4.0. The k' values of KE and DB decreased with increasing pH from pH 4.0. As noted in the Introduction, the p*I* value of flavoprotein is 3.9–4.1, so its charge is negative over pH 4.0 and positive below pH 4.0. Therefore, these results may reflect electrostatic repulsion between the ionized carboxylic acid (KE or DB) and the negative charge of the flavoprotein. On the other hand, the flavoprotein column most strongly retained KE and DB at pH 4.0. This is reasonable because this solid phase shows its maximum hydrophobicity at pH *ca.* 4.0.

The best pH for the chiral separation of KE was 4.6, and its R_s value was 3.04 (Table II), though the retention of KE was the strongest at pH 4.0 in this pH range. That is to say, the pH that gave the best chiral separation was different from the pH that gave rise to the strongest retention. This seems to show that the separating ability of the chiral recognition site is independent of the total charge of the protein molecule. On the other hand, DB gave the best resolution (R_s 1.53) at pH 4.0, at which value the retention was also strongest, and DB could not be resolved at pH values above 5.0. It was clear that the

TABLE I

EFFECT OF CONCENTRATION OF ORGANIC SOLVENT IN THE MOBILE PHASE ON CAPACITY FACTOR AND ENANTIOSELECTIVITY

k'_1, first-eluted enantiomer; k'_2, second-eluted enantiomer. Chromatographic conditions: mobile phase, 50 m*M* KH_2PO_4 containing ethanol at the concentration shown; other conditions were the same as in Fig. 2.

Ethanol conc. (%)	k'_1	k'_2	α	R_s
Ketoprofen (KE)				
4	23.94	30.95	1.29	2.09
6	10.94	15.00	1.37	5.23
8	8.60	11.08	1.29	4.09
10	6.84	8.38	1.23	2.97
12	5.82	6.81	1.17	2.08
Dibenzoyllysine (DB)				
4	13.13	15.00	1.14	1.94
6	9.13	10.22	1.12	1.25
8	6.90	7.56	1.10	1.05
10	5.46	5.83	1.07	0.76
12	4.45	4.65	1.04	0.55
Warfarin (WA)				
4	44.64	101.27	2.27	4.99
6	16.41	35.43	2.16	8.13
8	12.00	26.27	2.19	7.07
10	9.01	17.38	1.93	5.68
12	7.01	13.02	1.86	6.77
Benzoin (BE)				
4	5.69	6.50	1.14	1.02
6	3.21	3.49	1.09	0.71
8	2.84	3.03	1.07	0.64
10	2.51	2.60	1.04	0.40
12	2.32	2.32	1.00	0

optimum conditions for chiral separation differ from compound to compound.

Fig. 3B shows the effect of the pH of the mobile phase on the k' values for WA and BE, which each have only one hydroxyl group as an ionic functional group. The k' value of the first-eluted enantiomer of WA did not change much between pH 4.0 and 4.6, but that of the second was considerably affected. WA (p*K* 5.03–5.06 [16]) was best resolved (R_s 6.99) at pH 4.6, a similar value to that for KE. As shown in Table II, KE and WA gave the best results in terms of the R_s and α values at pH 4.6. That is to say, the chiral recognition ability of this column for KE and WA is clearly highest at pH 4.6.

TABLE II

EFFECT OF pH OF THE MOBILE PHASE ON ENANTIOSELECTIVITY

Chromatographic conditions: mobile phase, 50 m*M* potassium phosphate buffer (pH as shown) containing 10% ethanol; other conditions were the same as in Fig. 2.

pH	α	R_s	pH	α	R_s
Ketoprofen (KE)			*Warfarin (WA)*		
3.8	1.17	1.46	3.8	1.55	2.94
4.0	1.23	2.09	4.0	1.73	4.48
4.2	1.26	2.33	4.2	1.84	4.97
4.6	1.27	3.04	4.6	1.98	6.99
4.8	1.23	2.08	4.8	1.97	5.43
5.0	1.19	1.72	5.0	1.91	5.03
5.6	1.09	0.84	5.6	1.66	4.10
Dibenzoyllysine (DB)			*Benzoin (BE)*		
3.8	1.11	1.16	3.8	1.00	0
4.0	1.13	1.53	4.0	1.00	0
4.2	1.13	1.31	4.2	1.00	0
4.6	1.09	1.01	4.6	1.00	0
4.8	1.06	0.64	4.8	1.05	0.48
5.0	1.00	0	5.0	1.07	0.57
5.6	1.00	0	5.6	1.10	0.68

Another compound which has a hydroxyl group, BE, could be resolved at pH values above 4.8, but its retention did not change much in the pH range 3.8–5.6. Interestingly, its R_s and k' values were increasingly enhanced with a rise of the pH of the mobile phase. So in the case of BE, the chiral recognition ability became higher with increasing pH, independent of retention.

The retention for each compound on this column was also greatly affected by the ionic strength of the mobile phase. Fig. 4 shows the effect of the salt concentration in the mobile phase for the retention of each enantiomer. The retention of acidic compounds, which carry a negative charge at the pH values examined, decreased with increasing salt concentration. This tendency was not observed with BE. On the other hand, the α values of these compounds were not greatly influenced in the salt concentration range 10–250 m*M*, except for DB at 250 m*M* (data not shown). Thus the ionic interactions between the drugs and the protein may be a minor factor in the chiral separation. The retention of these compounds is affected by electrostatic

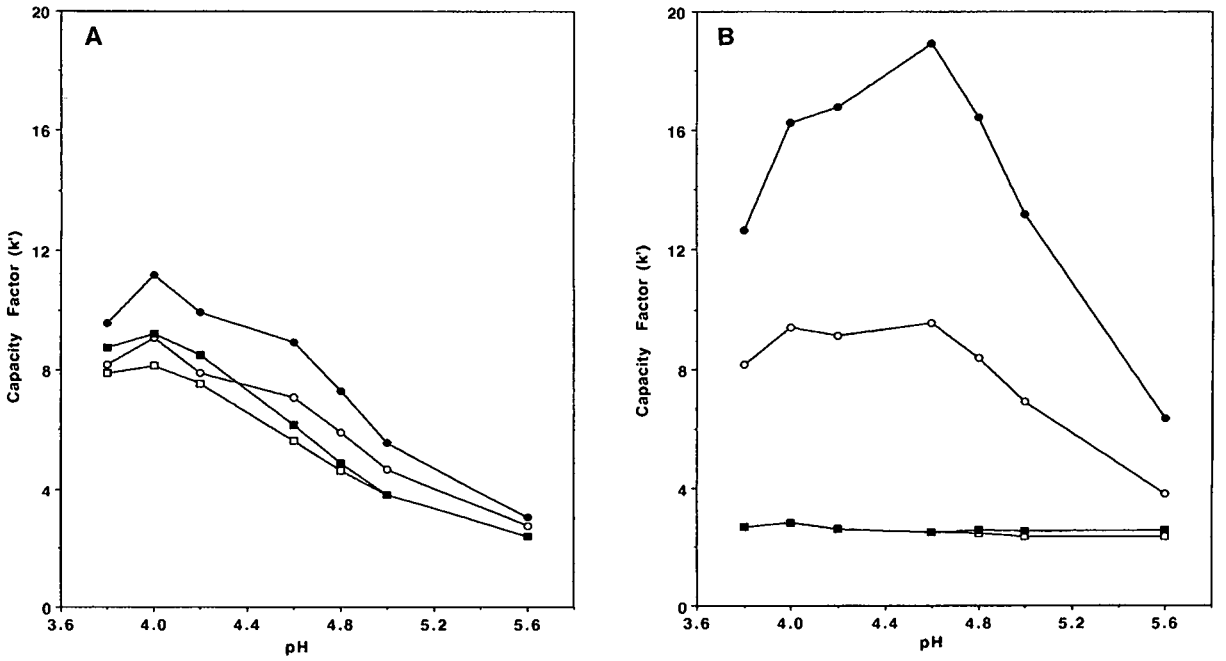

Fig. 3. Effect of pH of the mobile phase on capacity factors. (A) KE and DB: (○) first-eluted enantiomer of KE; (●) second-eluted enantiomer of KE; (□) first-eluted enantiomer of DB; (■) second-eluted enantiomer of DB. (B) WA and BE. (○) first-eluted enantiomer of WA; (●) second-eluted enantiomer of WA; (□) first-eluted enantiomer of BE; (■) second-eluted enantiomer of BE. Chromatographic conditions: pH of the mobile phase was as shown in the figure and other conditions were the same as in Fig. 2.

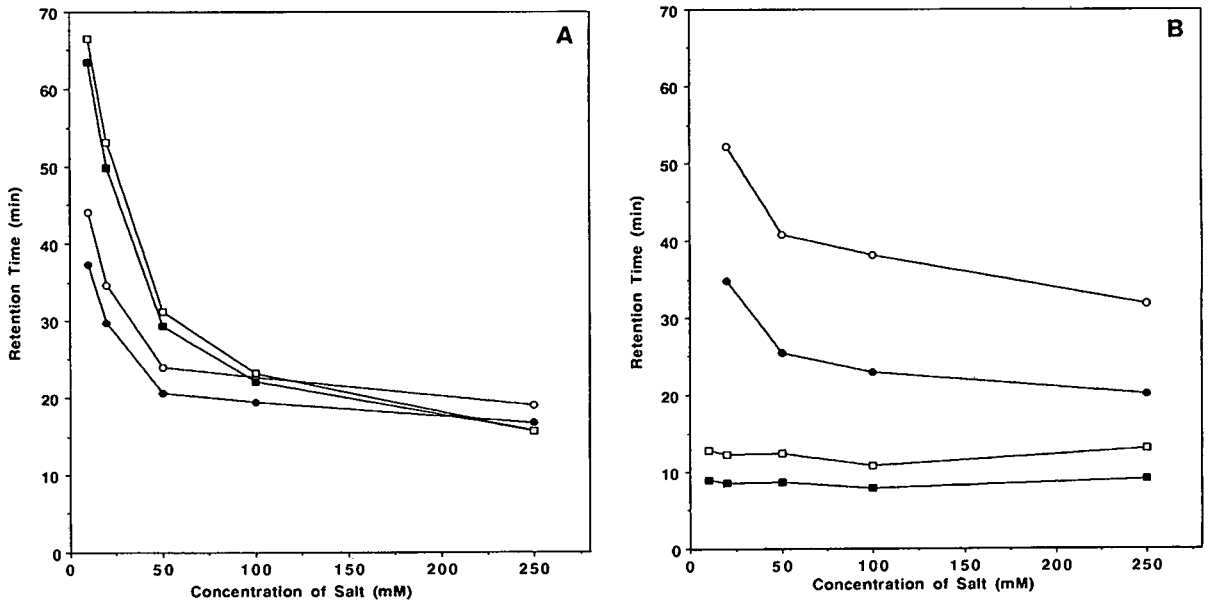

Fig. 4. Effect of salt concentration in the mobile phase on retention. (A) KE and DB: (●) first-eluted enantiomer of KE; (○) second-eluted enantiomer of KE; (■) first-eluted enantiomer of DB; (□) second-eluted enantiomer of DB. (B) WA and BE: (●) first-eluted enantiomer of WA; (○) second-eluted enantiomer of WA; (■) first-eluted enantiomer of BE; (□) second-eluted enantiomer of BE. Chromatographic conditions: salt concentration in the mobile phase was as shown in the figure, and ethanol concentrations were 10% (KE), WA), 6% (DB), and 4% (BE); other conditions were the same as in Fig. 2.

TABLE III

EFFECT OF ORGANIC MODIFIERS IN THE MOBILE PHASE ON CAPACITY FACTOR AND ENANTIOSELECTIVITY

k'_1, first-eluted enantiomer; k'_2, second-eluted enantiomer; n = plate number of first-eluted enantiomer. Chromatographic conditions: mobile phase buffer concentration 50 mM; pH 4.0 (DB), 4.6 (KE, WA), and 5.6 (BE), concentration of organic solvents, 4% (BE), 6% (DB), and 10% (KE, WA), other conditions were the same as in Fig. 2.

Compound	Solvent	k'_1	k'_2	α	R_s	n
KE	Methanol	12.35	15.42	1.25	2.01	1576
	Ethanol	9.25	10.69	1.16	1.39	1669
	1-Propanol	5.50	5.50	1.00	0	695
	1-Butanol[a]	–	–	–	–	–
	2-Propanol	7.00	7.82	1.12	0.87	1158
	tert.-Butanol	8.24	9.67	1.17	1.03	903
	Acetonitrile	5.82	6.35	1.09	0.79	1705
DB	Methanol	18.15	20.92	1.15	1.16	1176
	Ethanol	12.28	13.03	1.06	0.65	2383
	1-Propanol	6.95	6.95	1.00	0	1493
	1-Butanol	5.92	5.92	1.00	0	1921
	2-Propanol	9.17	9.60	1.05	0.55	2486
	tert.-Butanol	10.43	10.86	1.04	0.48	3574
	Acetonitrile	9.40	9.40	1.00	0	1105
WA	Methanol	16.39	32.60	1.99	5.61	851
	Ethanol	11.43	18.25	1.60	4.79	1409
	1-Propanol	6.23	6.49	1.04	0.40	2487
	1-Butanol[a]	–	–	–	–	–
	2-Propanol	8.33	10.78	1.29	1.92	795
	tert.-Butanol	10.04	13.53	1.35	2.21	661
	Acetonitrile	7.33	9.57	1.31	2.13	1053
BE	Methanol	4.11	6.00	1.46	3.01	1185
	Ethanol	3.71	5.36	1.44	2.81	869
	1-Propanol	2.53	3.06	1.21	1.76	1445
	1-Butanol	2.13	2.24	1.05	0.55	2208
	2-Propanol	3.06	4.24	1.39	2.54	1215
	tert.-Butanol	3.46	5.22	1.51	3.12	1258
	Acetonitrile	3.57	4.29	1.20	1.25	576

[a] 50 mM KH_2PO_4 (pH 4.6) containing 10% 1-butanol could not used because it was not mixed.

interactions, such as ion exchange and salting-out effects of the protein.

The effect of organic modifiers in the mobile phase on the retention and the enantioselectivity was examined (Table III). These results show that the k' values of all of the compounds examined decreased with increasing carbon number of the primary alcohol, and this agrees well with the data in Table I. In the case of primary alcohol solvents, the less hydrophobic solvents, methanol and ethanol, gave better R_s values than the more hydrophobic solvents, such as 1-propanol and 1-butanol. But in the case of branched-chain alcohol solvents, such as 2-propanol and *tert.*-butanol, this rule did not necessarily hold. This result was the same as that obtained with the ovomucoid column [10] and the conalbumin column [17]. These facts mean that the chiral separation of protein columns depends strongly on the kind of organic solvent used.

As described earlier, DB and BE did not give good resolution with 50 mM KH_2PO_4 (pH 4.6) containing 10% ethanol, as shown in Fig. 2D and F. Based on the above results, we considered that DB and BE might be effectively resolved by changing the pH and using a lower concentration of organic solvent. Indeed, we found that the enantiomers of DB were

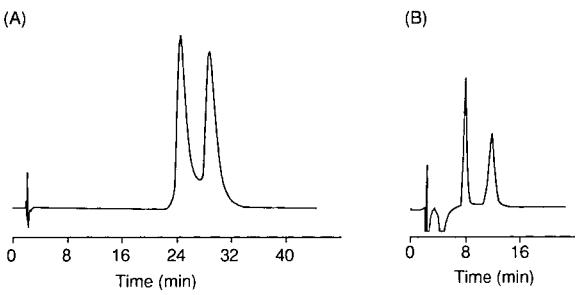

Fig. 5. Chromatograms of (A) DB and (B) BE on a flavoprotein-conjugated column. Chromatographic conditions: mobile phase, (A) 50 m*M* potassium phosphate buffer (pH 4.0) containing 6% ethanol, (B) 50 m*M* potassium phosphate buffer (pH 5.6) containing 4% *tert.*-butanol; other conditions were the same as in Fig. 2.

almost baseline-resolved by elution with 50 m*M* potassium phosphate buffer (pH 4.0) containing 6% ethanol, and its R_s value was 1.78, as shown in Fig. 5A. On the other hand, the retention of BE was very much weaker than those of the other compounds. Further, the best resolution of BE was obtained at pH 5.6 in the range pH 3.8–5.6. Finally, elution with 50 m*M* potassium phosphate buffer (pH 5.6) containing 4% *tert.*-butanol was found to be the best for chiral separation; the R_s value was 3.12, as shown in Fig. 5B.

CONCLUSION

In this study, we prepared a new chiral stationary phase using a flavoprotein for reversed-phase HPLC, and examined the performance of this material. The results indicate that the retention and enantioselectivity are affected by various mobile phase conditions. The retention may be reflect the hydrophobic and coulombic interactions between the solutes and the solid phase. However, these interactions may not have much effect on the chiral separation. On the other hand, each compound requires characteristic conditions for chiral separation, so this may occur at distinctive chiral recognition sites that are different from the retention regions.

During this investigation, direct chiral separation of several acidic and neutral compounds was achieved by reversed-phase HPLC, though the resolution and optimum conditions for separation varied from compound to compound. Nevertheless, this material appears to have great potential for chiral separation, and further studies are planned to extend its range of applicability to other clinically used drugs.

ACKNOWLEDGEMENT

We are grateful to Mr. Hiroshi Inoue, Kawashima Factory, Eisai Co., Ltd., for the purification and supply of flavoprotein.

REFERENCES

1 W. L. Hinze, T. E. Riehl, D. W. Armstrong, W. DeMond, A. Alak and T. Ward, *Anal. Chem.*, 57 (1985) 237.
2 J. I. Seeman, H. V. Secor, D. W. Armstrong, K. D. Timmons and T. J. Ward, *Anal. Chem.*, 60 (1988) 2120.
3 R. Isaksson, P. Erlandsson, L. Hansson, A. Holmberg and S. Berner, *J. Chromatogr.*, 498 (1990) 257.
4 S. Allenmark, B. Bomgren and H. Boren, *J. Chromatogr.*, 264 (1983) 63.
5 J. Hermansson, *J. Chromatogr.*, 269 (1983) 71.
6 G. Schill, I. W. Wainer and S. A. Barkan, *J. Liq. Chromatogr.*, 9 (1986) 641.
7 T. Miwa, M. Ichikawa, M. Tsuno, T. Hattori, T. Miyakawa, M. Kayano and Y. Miyake, *Chem. Pharm. Bull.*, 35 (1987) 682.
8 T. Miwa, T. Miyakawa, M. Kayano and Y. Miyake, *J. Chromatogr.*, 408 (1987) 316.
9 T. Miwa, H. Kuroda, S. Sakashita, N. Asakawa and Y. Miyake, *J. Chromatogr.*, 511 (1990) 89.
10 J. Iredale, A. F. Aubry and I. Wainer, *Chromatographia*, 31 (1991) 329.
11 K. M. Kirkland, K. L. Neilson and D. A. McCombs, *J. Chromatogr.*, 545 (1991) 43.
12 Y. Oda, N. Asakawa, T. Kajima, Y. Yoshida and T. Sato, *Pharmaceutical Res.*, 8 (1991) 997.
13 Y. Sato and K. Watanabe, *Proteins, nucleic acids and enzymes*, 23 (1978) 54.
14 M. B. Rhodes, N. Bennett and R. E. Feeney, *J. Biol. Chem.*, 234 (1959) 2054.
15 W. P. Winter, E. G. Buss, C. O. Clagett and R. V. Boucher, *Comp. Biochem. Physiol.*, 22 (1967) 897.
16 V. J. Stella, K. G. Mooney and J. D. Pipkin, *J. Pharm. Sci.*, 73 (1984) 946.
17 N. Mano, Y. Oda, T. Miwa, N. Asakawa, Y. Yoshida and T. Sato, *J. Chromatogr.*, 603 (1992) 105.

Journal of Chromatography, 623 (1992) 229–235
Elsevier Science Publishers B.V., Amsterdam

CHROM. 24 458

High-performance liquid chromatography procedure for the determination of purity of di-N-*n*-propylamine

Sean D. McCrossen, Robert G. Giles, Paul W. Oxley and James V. McArdle

Analytical Sciences, SmithKline Beecham Pharmaceuticals, Tonbridge, Kent TN11 9AN (UK)

(First received April 15th, 1992; revised manuscript received June 26th, 1992)

ABSTRACT

Di-N-*n*-propylamine (DNP) is used in the final step of the synthesis of ropinirole (SK&F 101468-A). Trace impurities in DNP give rise to significant impurities in the raw drug substances. A high-performance liquid chromatographic (HPLC) method for the trace analysis of the impurities in DNP was developed and validated. The trace enrichment method uses a simple derivatisation reaction with oxindole analogous to the final step of the ropinirole synthesis. DNP samples of varying purity were reacted with oxindole and were used in the preparation of ropinirole. The products were then assayed by the HPLC method. A specific impurity in ropinirole was shown to correlate well with the product of the reaction with oxindole. From the correlation data a calibration curve was constructed which enabled a specification for DNP to be determined based on the reaction with oxindole. Thus, the HPLC method could be used to assess the acceptability of DNP for use in the ropinirole synthesis.

INTRODUCTION

Ropinirole, 4-[2-(dipropylamino)ethyl]-1,3,dihydro-(2H)-indol-2-one monohydrochloride, SK&F 101468-A **I**, is a dopamine agonist used in the treatment of Parkinson's disease. Di-N-*n*-propylamine (DNP) is used in 10-fold excess in the last step of the synthesis of ropinirole [1] as shown in the reaction below (1).

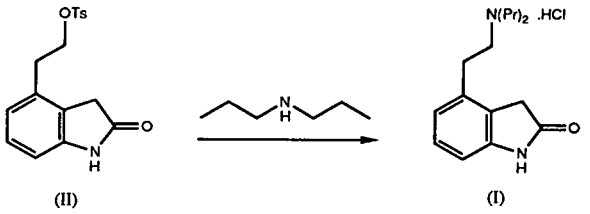

(1)

We developed a sensitive gas chromatography–mass spectrometry (GC–MS) procedure to determine the impurity profile of DNP (Fig. 1). However, trace amounts of unknown impurities in the DNP can lead to detectable levels of impurities in the final product. The trace impurities in the reagent become significant because of the 10-fold excess used. Different reaction kinetics may also contribute to the importance of trace impurities. References concerning the determination of impurities in or purity of DNP are not apparent in the literature. Using GC and GC–MS techniques, we have not yet been able to correlate any single impurity in DNP with impurities that appear in **I**. Further, we have shown by GC-MS that propionaldehyde, a suspected impurity, was absent from a batch of DNP used in the manufacture of impure **I**. We would normally perform a "use-test" on a reagent to judge its acceptability. A use-test is a small scale reaction that mimics the reaction performed in the manufacturing plant. If the use-test gives product that meets specification then the reagents may be considered acceptable. Use-tests on DNP are impractical for

Correspondence to: S. D. McCrossen, Analytical Sciences, SmithKline Beecham Pharmaceuticals, Tonbridge, Kent TN11 9AN, UK.

0021-9673/92/$05.00

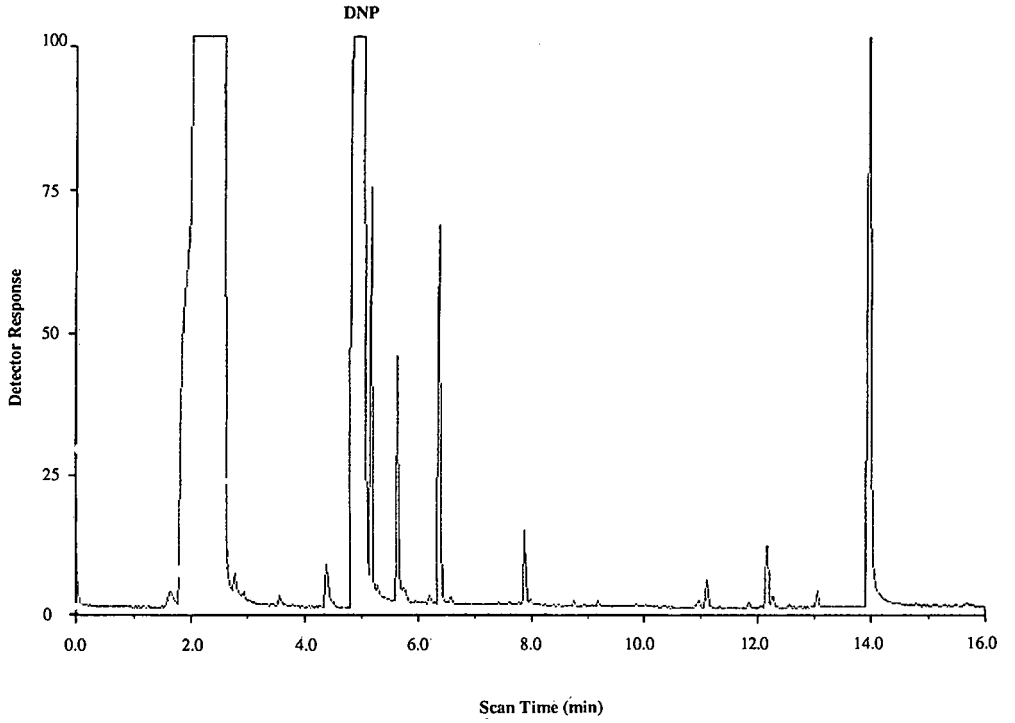

Fig. 1. Gas chromatograhic separation of impurities in DNP using electron impact (EI)-MS detection. Column: DB-5, 5% phenyl methylsilicone 30 m × 0.25 mm. Program: 30°C hold 1 min then ramp to 250°C at 10°C/min. Injection: 1 μl splitless at 200°C. Flow-rate: helium at 1.0 ml/min. Solvent: dichloromethane.

the following reasons: (1) A number of side reactions with the tosylate precursor **II** are possible. (2) Testing a large number of batches by this method is time consuming. (3) The use-test involves a two-phase reaction under reflux at 80–85°C and maintenance of an oxygen-free atmosphere throughout the reaction. DNP is sensitive to oxygen and degrades upon exposure to air. Oxindole **III** reacts with the unknown impurities in DNP to give the derivatisation products **IV** and **V**.

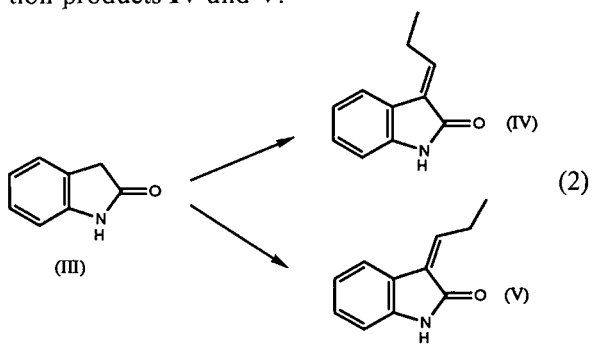

(2)

The major product is **IV**, (*E*)-3-propylidene-1,3-dihydro-(2H)-indol-2-one. The amount of **IV** formed from the reaction with oxindole is determined by high-performance liquid chromatography (HPLC) using an external standard. One of the impurities that arises in the final step of the ropinirole synthesis is 4-[2-(dipropylamino)ethyl]-3-propylidene-1,3-dihydro-(2H)-indol-2-one monohydrochloride, **VI**. A single batch of DNP may be used in reaction **1** and in reaction **2**. In this report we show that the amount of **VI** produced in reaction **1** correlates well with the amount of **IV** produced in reaction **2**. Conditions for reaction **2** were optimised and the HPLC

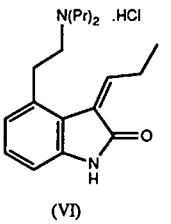

method used to quantitate **IV** was validated. Thus, the model reaction of DNP with oxindole may be used to assess the quality of DNP for use in the synthesis of ropinirole.

EXPERIMENTAL

Apparatus

A Grant Model W6 thermostatic bath circulator (Cambridge, UK) was used to thermostat the reactions and samples. HPLC separations were performed on a Beckman System Gold HPLC apparatus (High Wycombe, UK) with either a Model 166 variable wavelength detector or a Model 168 diode array detector, a Model 126 pump and either a Model 506 or 507 autosampler. A Jones Chromatography Model 7961 column oven (Hengoed, UK) was used to thermostat the column. Data collection and reduction were performed with the Perkin-Elmer Class 2000 system (Beaconsfield, UK). The chromatographic separations were performed on a Kromasil C_8 25 cm × 4.6 mm I.D. stainless steel column with 5-μm packing (Technicol, Stockport, UK).

Reagents

HPLC-grade solvents (Romil Chemicals, Loughborough, UK) were used throughout the investigations. Purified water was obtained from a Milli-Q water purification system (Millipore, Watford, UK). DNP was obtained from BASF (Cheadle, UK). Oxindole was obtained from Merck (Lutterworth, UK). Phosphoric acid (AR) was obtained from Aldrich Chemicals (Gillingham, Dorset, UK). Ammonium acetate (HPLC grade) was obtained from Fisons (Loughborough, UK). Standard compound **IV** and **V** were prepared using the method of Tacconi [2] by reacting oxindole with propionaldehyde. The *E* and *Z* isomers were separated and purified by flash column chromatography. The stereochemical structures were established using ^{13}C NMR spectroscopy. The coupling constant for $^3J_{CH}$ was found to be 12.8 ± 1 Hz for the *Z* and 5.5 ± 1 Hz for the *E* isomer. Standard compound **VI** was prepared and purified using an in-house method based on the reaction of oxindole with propionaldehyde [3]. The stereochemical structure was established using single crystal X-ray crystallography (SmithKline Beecham Pharmaceuticals, Upper Merion, PA, USA).

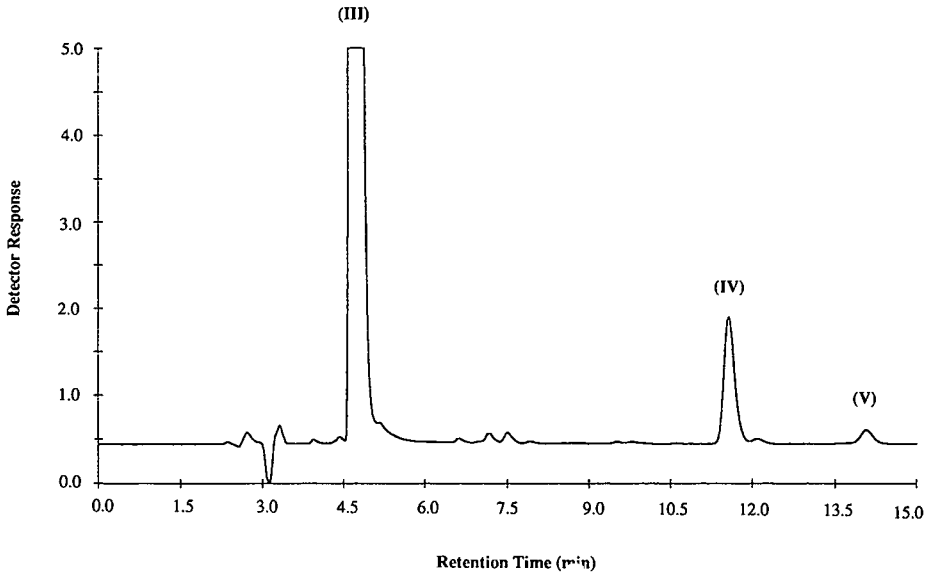

Fig. 2. Chromatograhic separation of **IV** in the oxindole reaction mixture with degraded DNP. Column: 5-μm Kromasil C_8 (25 cm × 4.6 mm I.D.). Mobile phase: 0.05 *M* ammonium acetate (pH 2.5)–[methanol–acetonitrile (30:70)], (55:45). Detection: 250 nm. Flow-rate: 1.0 ml/min.

Methods

Reaction of DNP with oxindole. Oxindole (0.5 g) was dissolved in 50% aqueous methanol (30 ml) to give an oxindole stock solution. DNP (200 μl) was reacted with oxindole stock solution (200 μl) in 50% aqueous methanol (total volume 25 ml). Reaction time and reaction temperature were varied to obtain a rapid reaction and good stability of the product.

Chromatographic determination of ***IV.*** Solvent A was prepared by dissolving ammonium acetate (3.85 g) in water (1000 ml) and adjusting the pH to 2.5 with phosphoric acid. Solvent B was prepared by mixing acetonitrile (700 ml) with methanol (300 ml). The solvents were filtered and degassed before use. An isocratic program (45% solvent B) was performed for 15 min using a 1.0 ml/min flow-rate and UV detection at 250 nm. Oxindole reaction solution (10 μl) was injected on to the pre-equilibrated column at 40°C in duplicate. A typical chromatogram is shown in Fig. 2. A standard solution of **IV** was prepared by dissolving 500 μg in 100 ml of 50% aqueous methanol and chromatographed.

The weight in μg of **IV** formed per g of DNP was determined using the equation:

$$\mu\text{g of IV per g DNP} = \frac{APV_s}{RVD}$$

where:

A = average area under the peak of compound **IV** in the sample chromatogram
P = purity of reference standard of compound **IV** expressed as a decimal fraction
= 0.982 for the current standard
V_s = volume of reaction solution (25 ml)
R = average response factor of compound **IV** from the chromatograms of standard solution [area/concentration (μg/ml)]
D = density of DNP (0.74 g/ml)
V = volume of DNP used in the reaction (0.2 ml)

Preparation of DNP of varying purity. DNP was rendered impure by refluxing in air for 18 h. DNP was purified by refluxing with oxindole in the absence of air then distilling. DNP mixtures of pure and impure samples were prepared volumetrically to give reagent with varying purity. The samples were mixed in volume ratios pure:impure of 100:0, 75:25, 50:50, 25:75 and 0:100.

Reaction of DNP with ***II.*** DNP of varying purity (10.5 ml, prepared as described above) was mixed with **II** (2.5 g) and water (18 ml). The mixture was thoroughly degassed with nitrogen, then heated at reflux for two hours. The mixture was then acidified with concentrated HCl to pH 1 and cooled under nitrogen to give ropinirole in solution. The whole was then diluted quantitatively to 100 ml with acetonitrile–water (70:30). A solution for analysis was prepared by diluting a 5-ml aliquot to 100 ml with 16% solvent B in water.

Chromatographic determination of ***VI*** *in* ***I.*** The same column and conditions as for the chromatographic determination of **IV** were used. An isocratic elution by 16% solvent B for 16 min was followed by a linear gradient to 80% solvent B over 20 min. Ten μl of the solution for analysis prepared as described above were injected in duplicate. The chromatogram obtained from one solution is shown in Fig. 3. The concentration of **VI** is expressed as a peak area ratio relative to the peak area for **I**. This method has been fully validated in terms of linearity, precision, peak homogeneity, and ruggedness. The limit of detection of **VI** in **I** is 0.01 area %.

RESULTS

Kinetics of reaction between DNP and oxindole

The course of the reaction was followed by sampling a reaction mixture at regular intervals and determining the content of **IV** by HPLC.

The reaction proceeds at room temperature but is unacceptably slow. The effect of varying the temperature on the kinetic profile is shown in Fig. 4. At 30°C the reaction was not complete until about 8 h. At 40°C significant decomposition of the product was detected by a reduction in peak area at 6 h. At 35°C the reaction is complete after 5 h with some decomposition detected after about 6 h. Thus reaction for 5 h at 35°C was chosen as optimal.

Reaction mixtures were chromatographed within 30 min of completion of reaction. The stability of the reference standard **IV** was tested in aqueous methanol at room temperature by monitoring the UV absorbance at 250 nm over a 16-h period. The results showed that **IV** in 50% aqueous methanol was unstable and that standard solutions need to be used within 6 h of preparation.

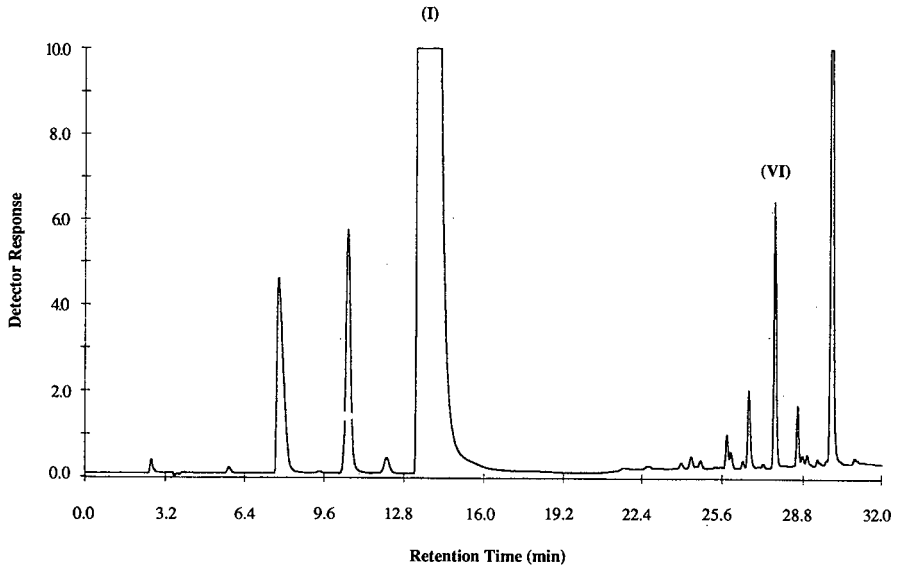

Fig. 3. Chromatograhic separation of impurities in **I** prepared by reaction with degraded DNP. Column: 5-μm Kromasil C_8 (25 cm × 4.6 mm I.D.). Mobile phase A: 0.05 *M* ammonium acetate, pH 2.5. Mobile phase B: methanol–acetonitrile (30:70). Gradient program: 16% B (16 min) then 16% B to 80% B (20 min). Detection: 250 nm. Flow-rate: 1.0 ml/min.

Linearity of response

The linearity of response of **IV** was determined. A stock solution of the reference standard of **IV** (approximately 500 μg per ml) was prepared and serially diluted to give five solutions with a concentration range between 0.5 and 5.0 μg/ml. The solutions were chromatographed according to the method. A plot of area *versus* concentration of **IV** gave a straight line. The least squares fit of the data gave the equation

$$\text{area} = (3.784 \pm 0.009) \cdot 10^4 \cdot \text{concentration } (\mu\text{g/ml}) + (31 \pm 260)$$

The correlation coefficient is 1.000. The intercept is not significant.

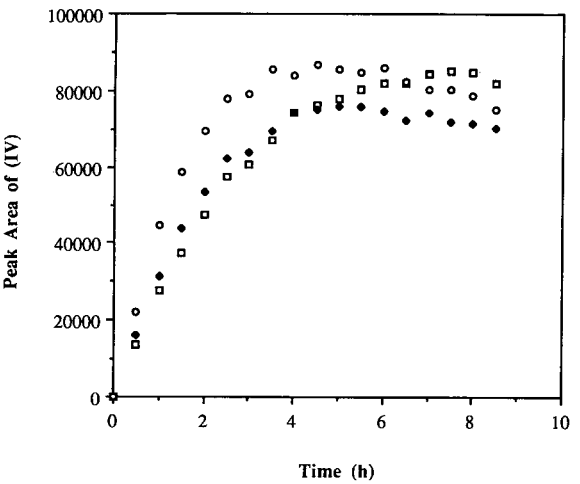

Fig. 4. Kinetic profile of oxindole reaction at 30 (□), 35 (◆) and 40°C. (○).

Peak homogeneity

The purity of the chromatographic peak of **IV** was determined by diode array spectroscopy. A sample of DNP was reacted and chromatographed according to the method. The UV spectrum of the eluent from the chromatographic run was recorded. Analysis of the chromatographic peak of **IV** showed it to be pure with respect to other components with different ultraviolet spectra.

Limit of detection

The limit of detection for the method was determined from a chromatogram of a standard **IV** solution. The limit of detection defined as the concentration of analyte that gives a peak height equal to three times the baseline noise was determined as 0.02 μg/ml.

Precision

The reproducibility of the procedure was tested by performing five determinations over two separate days on the same DNP sample. For each determination the reaction with oxindole was performed and the amount of **IV** produced was determined. The results for day one in units of μg **IV** produced/g DNP were 144.4, 152.0, 153.7, 152.1, and 154.4; for day two, they were 142.2, 153.1, 149.0, 145.8, and 149.9. The mean for day one was 151.3 with a standard deviation of 4.0; the mean for day two is 148.0 with a standard deviation of 4.1. There is no significant difference between the means of the two days ($p = 0.05$).

Correlation data

The five samples of DNP of varying quality were reacted with oxindole. The same samples of DNP were reacted with **II** at the same time. The products were analysed according to the methods described here. The amount of **IV** formed in the reaction with oxindole was directly proportional to the purity of the DNP. A plot of the data is shown in Fig. 5. The equation of the least squares fit of the data is

$$\mu g\ \mathbf{IV}\ \text{formed/g DNP} = (7.55 \pm 0.34) \cdot \text{purity} + (57 \pm 21)$$

where purity is expressed as % impure DNP in reagent. The correlation coefficient is 0.994. The amount of **VI** formed in the reaction with **II** also

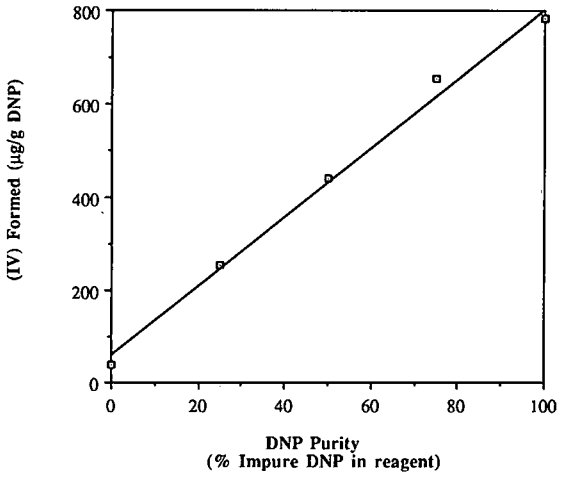

Fig. 5. Plot of **IV** formed from the reaction of oxindole with DNP of varying purity.

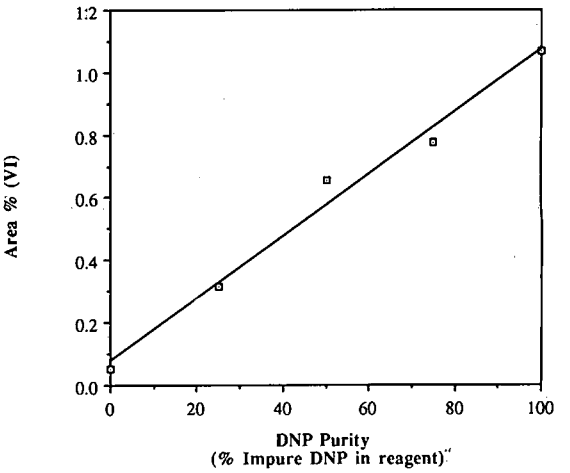

Fig. 6. Plot of **VI** formed from the reaction of **II** with DNP of varying purity. The concentration of **VI** is expressed as a peak area ratio relative to the peak area for **I**.

was directly proportional to the purity of the DNP. A plot of the data is shown in Fig. 6. The equation of the least squares fit of the data is

$$\text{area \% } \mathbf{VI} = (9.94 \pm 0.72) \cdot 10^{-3} \cdot \text{purity} + (0.076 \pm 0.044)$$

where purity is expressed as % impure DNP in reagent. The correlation coefficient is 0.985. Since the two sets of data were generated from the same five DNP samples, one set of data may be plotted against the other. Fig. 7 shows area % of **VI** plotted

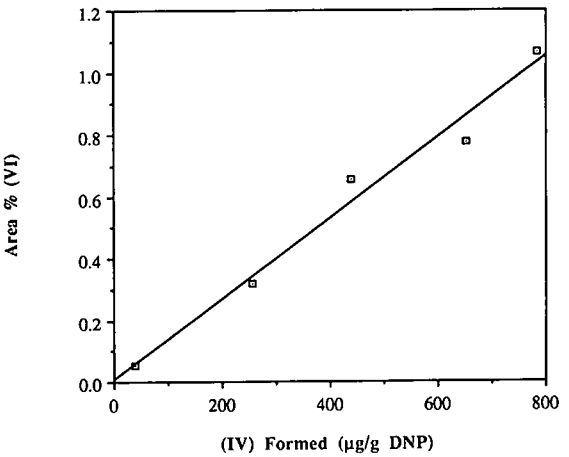

Fig. 7. Correlation of compounds **IV** formed to area % **VI** for reaction with DNP of varying purity.

as a function of μg **IV** formed/g DNP. The least squares fit of the data is

area % of **VI** = (1.31 ± 0.12) · 10^{-3} · μg **IV** formed/g DNP + (0.006 ± 0.060)

The correlation coefficient is 0.976.

A specification for DNP, in terms of **IV** formed from the oxindole reaction, was established using Fig. 7. DNP not satisfying the specification could thus be rejected for use in the synthesis of ropinirole. DNP should be used as soon as practicable after testing, since DNP will degrade upon exposure to air.

CONCLUSION

An unknown trace impurity or impurities in DNP lead to the formation of an unwanted impurity in the drug substance ropinirole. A simple model reaction of oxindole with impurities in DNP was shown to produce a product analogous to the impurity in ropinirole and the kinetics of the model reaction were optimised. An HPLC procedure to quantitate the products of the model reaction was developed and validated. The method was shown to be linear over the concentration range of interest, specific and sensitive. The amount of product in the model reaction was shown to correlate with the impurity in ropinirole to levels below 0.1% when the same batch of DNP was used in both reactions. Therefore, the model reaction and the corresponding HPLC procedure can be used to determine the acceptability of DNP for use in the ropinirole synthesis.

ACKNOWLEDGEMENTS

The authors wish to thank J. J. Richards for providing the NMR spectroscopy data, B.M. Stockton for the GC–MS data and D.S. Eggleston for the single crystal X-ray crystallography data.

REFERENCES

1 R. G. Giles and T. C. Walsgrove, *UK Pat. Appl., 9008605.9 (1990)*.
2 G. Tacconi, *J. Chem. Soc., Perkin Trans 2*, (1976) 150.
3 A. Wahl and P. Bagard, *Bull. Soc. Chim. Fr.*, 5 (1909) 1033.

Journal of Chromatography, 623 (1992) 237–245
Elsevier Science Publishers B.V., Amsterdam

CHROM. 24 451

Enantioseparation of amino compounds by derivatization with *o*-phthalaldehyde and D-3-mercapto-2-methylpropionic acid

A. L. L. Duchateau, H. Knuts, J. M. M. Boesten and J. J. Guns

DSM Research, P.O. Box 18, 6160 MD Geleen (Netherlands)

(First received April 9th, 1992; revised manuscript received June 11th, 1992)

ABSTRACT

o-Phthalaldehyde in combination with D-3-mercapto-2-methylpropionic acid is described as a chiral reagent for the enantioseparation of amino compounds. The reagent was applied to the optical resolution of α-amino acids, α-alkyl-α-amino acids, α-amino acid amides, α-alkyl-α-amino acid amides, β-amino alcohols and β-alkyl-β-amino alcohols. Separation of the diastereomers was carried out by reversed-phase chromatography and the derivatives were detected fluorimetrically. The diastereoselectivity obtained was compared with that of other commercially available chiral thiols. The rate of the reaction of various amino compounds with *o*-phthalaldehyde–D-3-mercapto-2-methylpropionic acid was studied, together with the stability of the derivatives obtained. Application of the method to the enantioseparation of chiral monofunctional amines was demonstrated by using α-methylbenzylamine as a model compound. The method described offers good enantioselectivity combined with high sensitivity for various chiral amino compounds derived from chemo-enzymatic processes.

INTRODUCTION

o-Phthalaldehyde (OPA) in combination with a thiol compound is a widely used reagent for high-performance liquid chromatographic (HPLC) analysis of amino compounds. By using an optically active thiol compound, *e.g.*, N-acetyl-L-cysteine (NAC), in the OPA reaction, it was shown that this reaction is applicable to the enantiomeric analysis of amino compounds [1]. Since then, several chiral thiols have been employed in the OPA reaction, *e.g.*, N-acylated cysteines [2–7], thiosugars [8–10], neomenthylthiol [11] and captopril [7]. In addition to use with protein α-H-α-amino acids, the applicability of the OPA–chiral thiol approach has been demonstrated for a large number of amino compounds, *e.g.*, α-alkyl-α-amino acids [12–15], α-amino acid amides [12,14], α-amino carboxylic esters [12], β-amino alcohols [4,10,16], α-hydroxymethyl-α-amino acids [17] and non-protein α-H-α-amino acids [6,12,18–20]. Most of the separations have been performed by reversed-phase chromatography, but in some studies the diastereomeric adducts were separated by means of ligand-exchange chromatography [14,16,21,22].

An important aspect when employing the OPA–chiral thiol reaction for enantiomeric amines is how the chemical structure of the thiol influences the diastereoselectivity observed for the isoindole adducts. For OPA–N-acylcysteine derivatives, intramolecular interactions between the carboxylic group of the cysteine part and the isoindole nitrogen may give rise to the diastereoselectivity obtained [23]. However, this mechanism cannot be applied for, *e.g.*, neomenthylthiol.

Employing chiral thiols with different chemical structures in the OPA reaction may therefore lead to a better understanding of the structure requirements for the isoindole adducts to improve the dia-

Correspondence to: Dr. A. L. L. Duchateau, DSM Research, Department FA, P.O. Box 18, 6160 MD Geleen, Netherlands.

0021-9673/92/$05.00

stereoselectivity. The aim of this study was to evaluate the use of D-3-mercapto-2-methylpropionic acid (MMPA) in the OPA reaction for the enantioseparation of chiral amines and to compare the diastereoselectivity obtained with that of other commercially available chiral thiols.

The OPA–MMPA reaction was applied to the enantioseparation of various amino compounds from chemo-enzymatic processes, *i.e.*, α-amino acids (AAs), α-alkyl-α-amino acids (α-alkyl-α-AAs), α-amino acid amides (AAs-NH_2), α-alkyl-α-amino acid amides (α-alkyl-α-AAs-NH_2), β-amino alcohols and β-alkyl-β-amino alcohols.

EXPERIMENTAL

Materials

AAs, N-acetyl-D-penicillamine (NAP) and 2,3,4,6-tetra-O-acetyl-1-thio-β-glucopyranoside (TATG) were obtained from Sigma (St. Louis, MO, USA). AAs-NH_2, α-alkyl-α-AAs, α-alkyl-α-AAs-NH_2, β-amino alcohols and β-alkyl-β-amino alcohols were synthesized in our laboratory [24]. For each amino compound, both the racemic form and at least one optically pure enantiomer were available. N-*tert*.-Butyloxycarbonyl-L-cysteine (Boc-Cys), N-isobutyryl-L-cysteine (*i*-But-Cys) and D-S-acetyl-3-mercapto-2-methylpropionic acid (supplier's name: D-S-acetyl-β-mercaptoisobutyric acid) were purchased from Novabiochem (Läufelfingen, Switzerland). N-Acetyl-L-cysteine (NAC) and α-methylbenzylamine were obtained from Janssen (Beerse, Belgium). OPA and HPLC-grade methanol and acetonitrile were supplied by Merck (Darmstadt, Germany). Water was purified with a Milli-Q system (Millipore). All other chemicals were of analytical-reagent grade.

Instrumentation

The chromatographic system consisted of a Hewlett-Packard (Palo Alto, CA, USA) Model 1090 liquid chromatograph and a Gilson Model 231-401 autosampling injector for derivatization and injection. The injection loop had a 20-μl capacity. The columns used were Nucleosil-120-C_{18} (250 × 4.0 mm I.D., 5 μm, for isocratic elution, and 250 × 4.0 mm I.D., 3 μm, for gradient elution). The flow-rate was 1 ml/min and and the column temperature was kept at 40°C.

The derivatives were monitored with a Waters (Milford, MA, USA) Model 420 fluorescence detector. For excitation a 338-nm band-pass filter was used, and for emission a 415-nm long-pass filter was chosen. Quantification was performed with a Hewlett-Packard Model 3350 laboratory automation system.

^{1}H NMR analysis was performed with a Bruker (Karlsruhe, Germany) AM 400 instrument. Spectra were recorded at 400 MHz and samples were diluted with ^2H_2O. For LC–mass spectrometry (MS), a Finnigan MAT TSQ-70 triple quadrupole mass spectrometer equipped with a thermospray interface (Finnigan MAT, San José, CA, USA) was used. MS analysis was performed using chemical ionization with gaseous ammonia [25].

A Waters Model 481 UV detector was used for detection at 210 nm.

Eluent, reagent and derivatization procedure

The mobile phase consisted of 50 m*M* sodium acetate buffer, titrated to pH 6.0 with acetic acid. For isocratic runs, the concentration of methanol in the mobile phase was as indicated in the Tables.

The OPA reagent was prepared by dissolving 60 mg of OPA in 3 ml of methanol and 15 ml of 0.4 *M* sodium borate buffer (pH 9.4). The MMPA reagent was prepared by dissolving 6.5 mg of D-S-acetyl-3-mercapto-2-methylpropionic acid per ml of 1 *M* sodium hydroxide solution. The solution was stirred for 10 min at room temperature. The MMPA solution thus obtained was titrated to pH 7.0 with phosphoric acid solution. For the other thiols used in this study, 25 m*M* solutions were prepared in water–methanol (1:1, v/v) except TATG, which was dissolved in methanol. The amino compounds studied were dissolved in water.

Derivatization was performed automatically with a Gilson Model 231-401 system. The following volumes were mixed: 75 μl of sample solution, 300 μl of OPA reagent and 30 μl of thiol reagent. After at least 2 min (30 min for α-alkyl compounds) at room temperature, an aliquot of the reaction mixture was injected into the chromatographic system.

For LC–thermospray MS, the eluent consisted of a 10 m*M* solution of formic acid and acetonitrile. Analysis was performed using a gradient from 0 to 60% acetonitrile in 30 min.

RESULTS AND DISCUSSION

Chemical and optical purity of MMPA reagent

The chemical purity of the MMPA reagent was studied by HPLC–UV detection, LC–thermospray MS and ^{1}H NMR. HPLC–UV analysis of the MMPA solution, prepared by base-catalysed hydrolysis of the S-acetyl precursor, showed the absence of the precursor and the presence of acetate, a large peak at retention time (t_R) = 14 min and a minor peak at t_R = 22 min. Using the same elution conditions, the MMPA solution was studied by LC–thermospray MS. The mass spectrum of the compound at t_R = 14 min showed several characteristic mass peaks for MMPA : $[M + NH_4]^+$ (m/z = 138), $[M + NH_4 + CH_3CN]^+$ (m/z = 179) and $[nM + NH_4]^+$ (m/z = 258, 378, 498 for n = 2, 3 and 4, respectively). The latter type of ions probably result from intermolecular associations of MMPA molecules in the MS source. MS analysis of the compound at t_R = 22 min showed typical mass peaks of MMPA disulphide : $[MH]^+$ (m/z = 239), $[M + NH_4]^+$ (m/z = 256) and $[MH - H_2O]^+$ (m/z = 221).

^{1}H NMR analysis of the MMPA solution showed characteristic resonances for MMPA and its disulphide form: δ 2.55 (m, 2H), 2.40 (m, 1H) and 1.06 (d, 3H) for the main product, *i.e.*, MMPA, and δ 2.77 (m, 2H) and 1.09 (d, 3H) for the secondary compound, *i.e.*, MMPA disulphide (the CH was obscured by other resonances).

From the ^{1}H NMR data the concentration of MMPA and its disulphide form were calculated. The concentration of the MMPA disulphide was 10% of that of MMPA. As the disulphide form does not react with OPA, the presence of this compound in the MMPA reagent will not influence the analysis. The concentration of MMPA was 21 m*M*.

With respect to the initial concentration of D-S-acetyl-3-mercapto-2-methylpropionic acid, a conversion of 85% was found. The stability of the MMPA reagent at pH 7 was evaluated and a decrease of < 10% was found after 34 h. According to the supplier, the optical purity of D-S-acetyl-3-mercapto-2-methylpropionic acid was ⩾98%. After hydrolysis, the optical purity of the resulting MMPA was measured using the "reverse" OPA reaction with L-Val (optical purity 99.9%) as chiral selector. The value found for MMPA was 98.7%.

Comparison of MMPA with other chiral thiols

The spectroscopic and chromatographic properties of MMPA were compared with those of five other commercially available thiols. For this investigation, Val was used as the test compound. The data obtained are given in Table I. The excitation spectra of the derivatives showed two maxima: one below 300 nm and the other, given in Table I, above 300 nm. The excitation wavelengths obtained for the six thiol derivatives were nearly identical. The emission spectra of the OPA derivatives of MMPA, *i*-But-Cys, Boc-Cys and NAC showed maxima in the 443–454-nm region, whereas the derivatives of NAP and TATG showed maximum fluorescence at 412 and 414 nm, respectively. With respect to the chromatographic properties of the chiral thiols, *i*-But-Cys gave the highest α-value among the N-acylcysteines tested. A comparable value was found for TATG. MMPA, however, gave the highest α-value for the whole series.

The detection limit for the first eluting valine enantiomer, based on a signal-to-noise ratio of 3, was compared for four thiols at λ_{exc} = 338 nm and λ_{em} > 415 nm. The values found for MMPA, *i*-But-Cys, Boc-Cys and NAC were 2.0, 2.8, 3.7 and 2.3 pmol, respectively.

Enantioselective analysis

The reaction of OPA and MMPA with AAs, AAs-NH_2, β-amino alcohols and the corresponding alkylated compounds yielded highly fluorescent de-

TABLE I

SPECTROSCOPIC AND CHROMATOGRAPHIC PROPERTIES OF OPA DERIVATIVES OF VALINE WITH VARIOUS CHIRAL THIOLS

For conditions, see Experimental.

Chiral thiol	Excitation maximum (nm)	Emission maximum (nm)	k'^a	α
MMPA	331	454	1.82	2.10
i-But-Cys	333	445	1.41	1.62
TATG	329	414	15.45	1.60
Boc-Cys	332	444	4.01	1.50
NAP	330	412	1.42	1.09
NAC	332	443	0.72	1.30

[a] Capacity factor of the first-eluted diastereomer; concentration of methanol in the mobile phase is 45% (v/v).

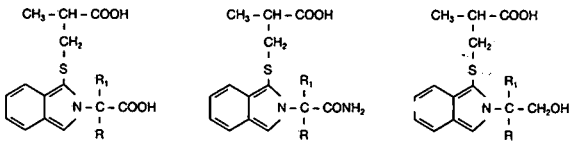

I II III

Fig. 1. Proposed structures for the diastereoisomeric adducts formed in the reaction of OPA–MMPA with (I) AAs, (II) AAs-NH_2 and (III) β-amino alcohols. R_1 = H or alkyl; R = residue of the amino compound.

rivatives, which are assumed to be analogous to the adducts from the OPA–mercaptoethanol reaction [26] (Fig. 1).

In our investigation of the OPA–MMPA reaction for amino compounds, the corresponding OPA–NAC derivatives were used for comparison. In Table II the data for the OPA–MMPA derivatives of several AAs and α-alkyl-α-AAs are presented. Using MMPA as chiral selector, enantioseparation could be obtained for all the protein AAs listed. The highest α-values were obtained for the aliphatic AAs, *i.e.*, Leu, Ile and Val. Compared with NAC, the use of MMPA resulted in higher α-values for all the AAs tested, except Trp, where equal performance was obtained. To illustrate the resolution obtained with MMPA, the enantioseparation of a standard mixture, composed of the non-chiral Gly and seventeen DL pairs of protein AAs, is shown in Fig. 2. Under the conditions employed, all the enantiomeric pairs and Gly could be separated in a single gradient run (D-Ile and L-Val are eluted together). In contrast with NAC, the elution order of the OPA–MMPA derivatives of the AAs was D before L in all instances. The OPA–MMPA deriva-

TABLE II

CAPACITY FACTORS (k') AND SELECTIVITIES (α) OF OPA–L-NAC AND OPA–D-MMPA DERIVATIVES OF AA COMPOUNDS

For chromatographic conditions, see Experimental.

AA	Reagent					
	OPA–L-NAC			OPA–D-MMPA		
	Methanol[a]	k'[b]	α	Methanol[a]	k'[b]	α
Ala	30	1.00	1.19	35	1.31	1.49
Asp	10	0.27	1.33	15	0.80	1.37
Ser	5	4.88	1.00	10	5.84	1.31
Thr	10	5.14	1.15	15	6.90	1.80
His	30	0.30	1.00	35	0.73	1.11
Tyr	30	1.62	1.27	35	1.31	1.34
Val	40	1.48	1.28	45	1.82	2.10
Met	40	1.85	1.05	45	1.51	1.64
Ile	40	2.84	1.29	45	2.87	2.13
Phe	40	2.36	1.04	45	2.25	1.47
Leu	40	4.58	1.07	45	3.72	1.80
Lys	40	12.28	1.00	45	12.10	1.56
Gln	30	0.16	1.00	35	0.23	1.53
Trp	40	1.42	1.41	45	1.30	1.40
Arg	25	0.64	1.00	30	1.66	1.37
Asn	10	2.13	1.05	15	2.62	1.32
Glu	10	1.17	1.00	15	1.67	1.60
α-Ph-Gly	40	2.14	1.10	45	2.38	1.40
α-Me-Val	40	2.45	1.15	45	6.60	1.34
α-Me-Leu	40	4.41	1.04	45	4.52	1.15
α-Me-Phe	35	9.07	1.09	40	8.63	1.20
α-Me-α-Ph-Gly	40	3.13	1.08	45	3.76	1.07

[a] Percentage of methanol in the mobile phase.
[b] Capacity factor of the first-eluted diastereomer.

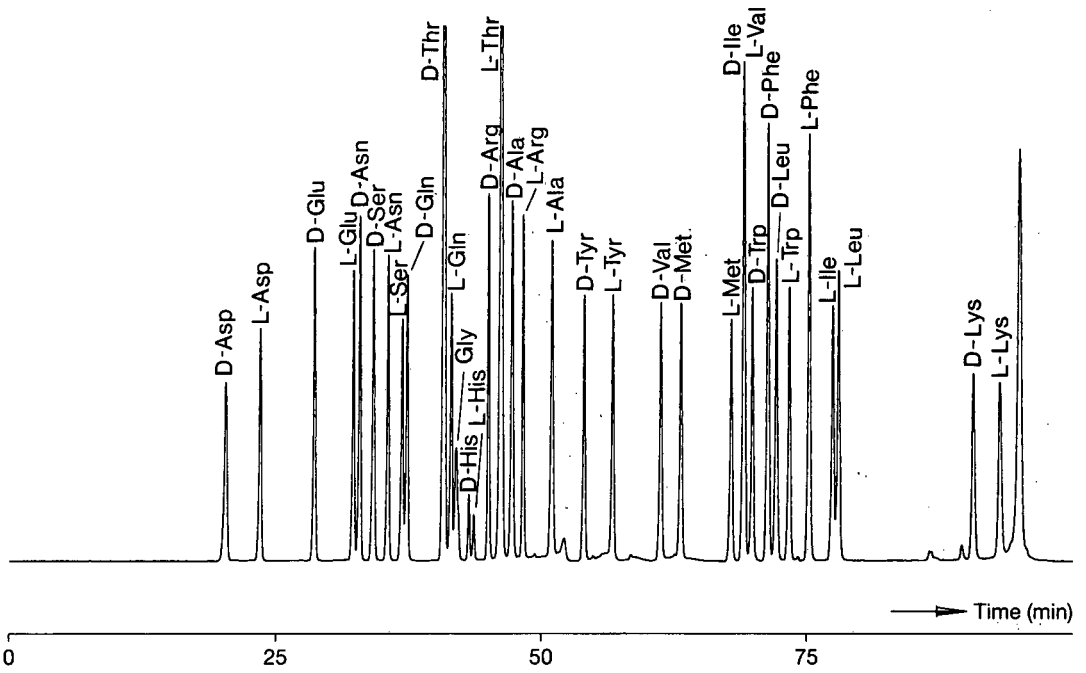

Fig. 2. Enantioseparation of an amino acid standard mixture consisting of seventeen pairs of AAs and the non-chiral Gly. Mobile phase: (A) 50 m*M* sodium acetate buffer (pH 6.0); (B) acetonitrile; gradient: 100% A, 0–10 min; 0–37.5%, 10–110 min. For other conditions, see Experimental.

tives of α-alkyl-α-AAs (Table I) showed lower α-values than the corresponding AAs. Compared with NAC, equal or better enantioselectivity was obtained with MMPA.

The k' and α-values for the OPA–MMPA and OPA–NAC derivatives of AAs-NH_2 and α-alkyl-α-AAs-NH_2 are given in Table III. For all the AAs-NH_2 investigated, enantioseparation occurred with

TABLE III

CAPACITY FACTORS (k') AND SELECTIVITIES (α) OF OPA–L-NAC AND OPA–D-MMPA DERIVATIVES OF α-AA-NH_2 COMPOUNDS

For chromatographic conditions, see Experimental.

AA-NH_2	Reagent					
	OPA–L-NAC			OPA–D-MMPA		
	Methanol[a]	k'[b]	α	Methanol[a]	k'[b]	α
Val-NH_2	40	4.88	1.17	45	11.26	1.48
Ala-NH_2	30	2.87	1.21	35	4.46	1.42
Leu-NH_2	40	10.70	1.18	45	11.46	1.51
Ser-NH_2	10	13.44	1.13	15	22.40	1.25
Phe-NH_2	40	11.35	1.00	45	9.55	1.33
α-Ph-Gly-NH_2	40	6.15	1.11	45	7.88	1.32
α-Me-Val-NH_2	40	4.81	1.23	45	5.46	1.06
α-Me-Leu-NH_2	40	8.69	1.10	45	10.00	1.03
α-MePhe-NH_2	35	20.53	1.22	40	20.43	1.06

[a] See Table II.

MMPA as selector. Analogously to the AAs, the highest α-values were obtained for the aliphatic AAs-NH_2, *i.e.*, Val-NH_2 and Leu-NH_2. The α-values obtained for the OPA–MMPA derivatives of the AAs-NH_2 are lower than those of the corresponding AAs. With respect to the elution order of the AAs-NH_2, the D-form always eluted before the L-form with MMPA, whereas for NAC both DL and LD orders occurred. As can be seen in Table III, the enantioselectivity obtained for OPA–MMPA derivatives of AAs-NH_2 is higher in all instances than for the OPA–NAC derivatives. With MMPA as selector, lower α-values were obtained for the α-alkyl-α-AAs-NH_2 in comparison with the AAs-NH_2.

The results for MMPA and NAC as selector for the enantioseparation of β-amino alcohols and the alkylated analogues are presented in Table IV. Using MMPA, resolution of the enantiomers could be obtained in all instances. For the β-amino alcohols tested, the elution order was D before L. Analogously to the AAs and AAs-NH_2, the alkylated analogues of the β-amino alcohols showed a lower enantioselectivity. For the whole series of amino alcohols, MMPA proved to be a better selector than NAC.

The rates of derivative formation of OPA–MMPA with an AA, AA-NH_2, α-alkyl-α-AA, α-alkyl-α-AA-NH_2 and β-amino alcohol were studied as a function of the reaction time. The results are presented in Fig. 3. In the two graphs, the molar fluorescence intensity for D-Val, L-Val-NH_2, L-Me-Val, D-Me-Val-NH_2 and L-Val-ol are shown at different reaction times. For D-Val, L-Val-NH_2 and L-Val-ol, maximum fluorescence was reached within 3 min, whereas L-Me-Val and D-Me-Val-NH_2 reached their maximum after 30 min. The difference in reaction rate between α-alkyl-α-amino compounds and the corresponding α-H analogues has also been observed for OPA in combination with other thiol compounds [14,27–29]. An explanation for this phenomenon may be steric hindrance of the α-alkyl substituent in the nucleophilic attack of the amine on the carbonyl function of OPA.

After their plateau value had been reached, a comparison of the molar fluorescence intensity of the compounds studied was performed. It was found that the molar fluorescence intensity increased in the order L-Val-ol > D-Val > L-Me-Val > D-Me-Val-NH_2 > L-Val-NH_2. The stability of the derivatives investigated can be seen from the right part of the graphs in Fig. 3. For up to 5 h, the derivatives of D-Me-Val-NH_2, L-Me-Val and L-Val-NH_2 show excellent stability. For D-Val, a slight decrease in the fluorescence with time is observed, *i.e.*, 1%/h. L-Val-ol formed an unstable derivative with OPA–MMPA; after 5 h only 10% of the initial fluorescence response was left. The alcohol functionality may play an important role in the instability of the derivative formed, as degradation of OPA–thiol adducts of β-amino alcohols has also been noted in other studies [4,10]. However, a possible degradation route for β-amino alcohols can-

TABLE IV

CAPACITY FACTORS (k') AND SELECTIVITIES (α) OF OPA–L-NAC AND OPA–D-MMPA DERIVATIVES OF β-AMINO ALCOHOLS

For chromatographic conditions, see Experimental.

β-Amino alcohols	Reagent					
	OPA–L-NAC			OPA–D-MMPA		
	Methanol[a]	k'[b]	α	Methanol[a]	k'[b]	α
Val-ol	40	8.53	1.04	45	11.60	1.27
Phe-ol	45	7.11	1.08	50	6.58	1.26
β-Me-Val-ol	45	10.09	1.21	50	7.98	1.38
α-Ph-Gly-ol	40	10.40	1.02	45	11.64	1.27
α-Me-Val-ol	45	4.75	1.03	50	4.86	1.21
α-et-Phe-ol	45	14.80	1.00	50	14.32	1.05

[a,b] See Table II.

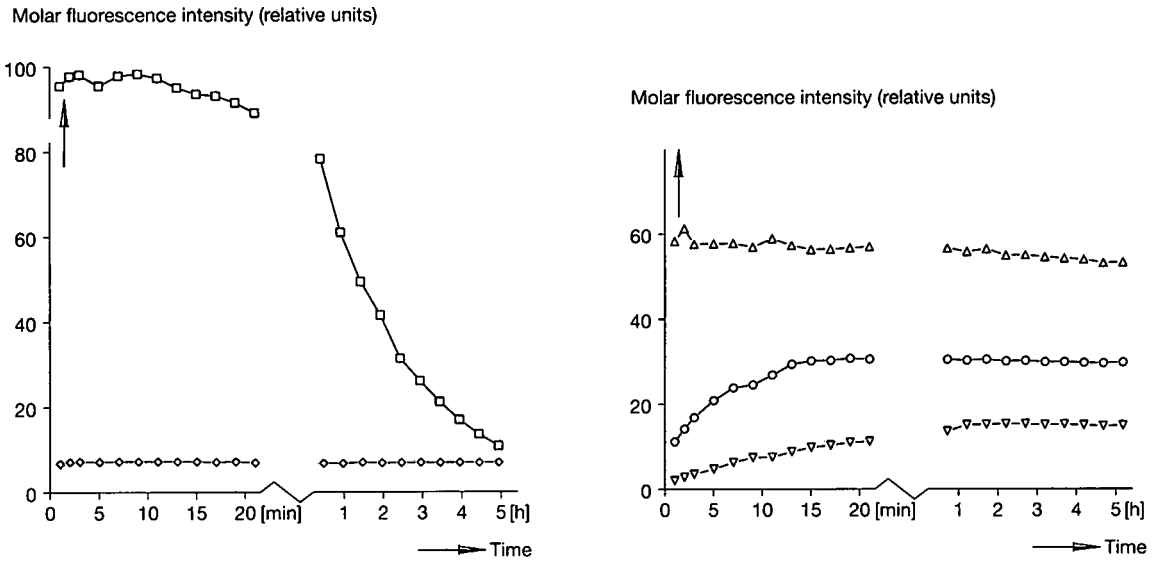

Fig. 3. Molar fluorescence response of the OPA–MMPA derivatization as a function of reaction time for (▽) D-Me-Val-NH_2 (Me = methyl), (○) L-Me-Val, (△) D-Val, (◇) L-Val-NH_2 and (□) L-Val-ol. The molar excess of OPA and MMPA was 100-fold and 10-fold, respectively, with respect to the compounds studied.

not be deduced from degradation mechanisms described earlier for isoindoles [30,31].

In our search for applications of the OPA–MMPA reaction, we noted that the OPA–chiral thiol approach has not been reported for monofunctional amines, *i.e.*, compounds possessing no other heteroatom apart from the primary amino group. As we were interested in the question of whether OPA–MMPA could be applied to this type of chiral amine, we selected α-methylbenzylamine as a model compound. Using the OPA–MMPA reagent, enantioseparation of racemic α-methylbenzylamine could be obtained (Fig. 4). Compared with other α-substituted benzylamines used in this study, *i.e.*, α-Ph-Gly-ol, α-Ph-Gly-NH_2 and α-Ph-Gly, the following ranking for the enantioselectivity can be made: α-Ph-Gly (COOH substituent; α = 1.40) > α-Ph-Gly-NH_2 ($CONH_2$ substituent; α = 1.32) > α-Ph-Gly-ol (CH_2OH substituent; α = 1.27) > α-methylbenzylamine (methyl substituent; α = 1.07).

The higher enantioselectivities obtained for α-Ph-Gly, α-Ph-Gly-NH_2 and α-Ph-Gly-ol compared with α-methylbenzylamine may be attributed to the type of α-substituent. Both the amino acid and amino acid amide and amino alcohol possess α-substituents that are capable of forming intramolecular hydrogen bonds. As this type of bond may play an important role in the diastereoselectivity obtained for the isoindole derivatives, the absence of this bonding site in α-methylbenzylamine may explain the low α-value observed.

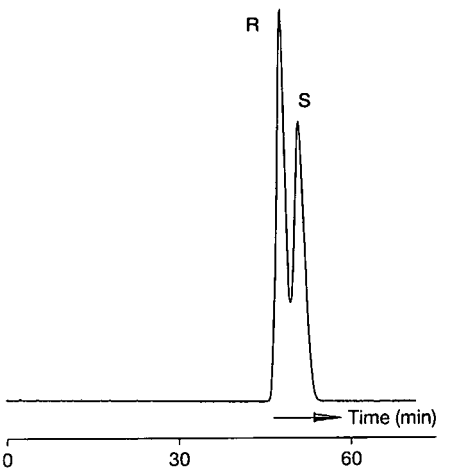

Fig. 4. Chromatogram of the OPA–MMPA derivatives of (*R,S*)-α-methylbenzylamine.. Mobile phase: 50 m*M* sodium acetate buffer (pH 6.0)–methanol (55:45, v/v). For other conditions, see Experimental.

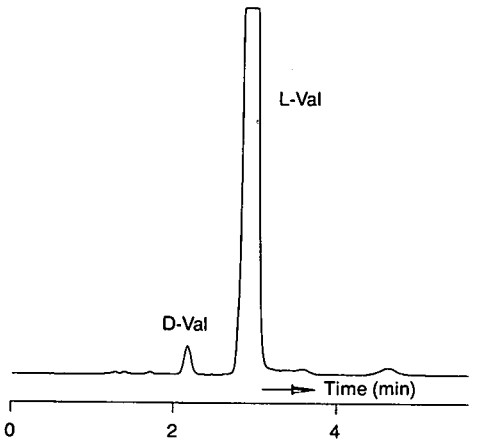

Fig. 5. Chromatogram of a sample from L-Val synthesis. Mobile phase, 50 m*M* sodium acetate buffer (pH 6.0)–methanol (55:45, v/v); flow-rate, 2 ml/min; temperature, 50°C. For other conditions, see Experimental.

Quantitative analysis

For most of the compounds studied, the diastereomeric OPA–MMPA derivatives exhibited different specific fluorescence intensities. Differences of up to 25% were obtained for some AAs-NH_2. Therefore, quantitative measurements were made by comparing the peak areas of compounds of the same enantiomeric form.

As an example of the linearity and precision of the method, these data are given for Val. The linearity of the amount *versus* response relationship was established over the range 4–67 pmol for each of the enantiomers. Linear regression analysis from the calibration graphs indicated that the correlation coefficient was 0.9999 for both enantiomers. The within-run precision of the assay gave a relative standard deviation < 2% (n = 5; 67-pmol level) and < 4% (n = 5; 4-pmol level) for both enantiomers.

As an application, a representative chromatogram of a sample from a chemo-enzymatic reaction performed on laboratory scale is given in Fig. 5.

CONCLUSIONS

It has been demonstrated that with the use of MMPA in combination with OPA, good enantioselectivity can be obtained for a broad range of amino compounds. As optically pure MMPA can be readily obtained from the commercially available S-acetylated analogue by simple hydrolysis, it may prove to be a valuable selector in other studies on the enantioselective analysis of chiral amino compounds.

ACKNOWLEDGEMENTS

We thank Mr. G. Kwakkenbos for the LC–thermospray MS analysis and Mr. H. Linssen for the ^1H NMR measurements.

REFERENCES

1 D. W. Aswad, *Anal. Biochem.*, 137 (1984) 405.
2 R. H. Buck and K. Krummen, *J. Chromatogr.*, 315 (1984) 279.
3 N. Nimura and T. Kinoshita, *J. Chromatogr.*, 352 (1986) 169.
4 R. H. Buck and K. Krummen, *J. Chromatogr.*, 387 (1987) 255.
5 H. Brückner, R. Wittner and H. Godel, *J. Chromatogr.*, 476 (1989) 73.
6 M. R. Euerby, L. Z. Partridge and W. A. Gibbons, *J. Chromatogr.*, 483 (1989) 239.
7 H. Brückner, R. Wittner and H. Godel, in G. Lubec and G. A. Rosenthal (Editors), *Amino Acids: Chemistry, Biology and Medicine*, ESCOM Sci. Publ., Leiden, 1990, pp. 143–151.
8 S. Einarsson, S. Folestad and B. Josefsson, *J. Liq. Chromatogr.*, 10 (1987) 1589.
9 A. Jegorov, T. Tríska, T. Trnka and M. Cerný, *J. Chromatogr.*, 434 (1988) 417.
10 A. Jegorov, T. Trnka and J. Stuchlík, *J. Chromatogr.*, 558 (1991) 311.
11 H. Goetz and B. Glatz, *Hewlett-Packard Application Note*, No. 12-5954-8911, 1987.
12 J. Florance, A. Galdes, Z. Konteatis, Z. Kosarych, K. Langer and C. Martucci, *J. Chromatogr.*, 414 (1987) 313.
13 M. Maurs, F. Trigalo and R. Azerad, *J. Chromatogr.*, 440 (1988) 209.
14 A. Duchateau, M. Crombach, J. Kamphuis, W. H. J. Boesten, H. E. Schoemaker and E. M. Meijer, *J. Chromatogr.*, 471 (1989) 263.
15 H. Brückner, I. Bosch, S. Kühne and S. Zivny, in G.R. Marshall (Editor), *Peptides: Chemistry and Biology*, ESCOM Science, Leiden, 1988, pp. 195–197.
16 S. Lam and G. Malikin, *J. Chromatogr.*, 368 (1986) 413.
17 H. Brückner, S. Kühne, S. Zivny, M. Langer, Z.J. Kaminski and M.T. Leplawy, in A. Aubry, M. Marraud and B. Vitoux (Editors), *Second Forum on Peptides*, John Libbey Eurotext, London, 1989, pp. 291–295.
18 M. R. Euerby, L. Z. Partridge and P. Rajani, *J. Chromatogr.*, 447 (1988) 392.
19 M. R. Euerby, P. B. Nunn and L. Z. Partridge, *J. Chromatogr.*, 466 (1989) 407.
20 M. R. Euerby, L. Z. Partridge and P. B. Nunn, *J. Chromatogr.*, 469 (1989) 412.
21 S. Lam, *J. Chromatogr.*, 355 (1986) 157.

22 F. Federici, A. M. Girelli, A. Messina, I. Nicoletti and M. Sinibaldi, *Anal. Lett.*, 23 (1990) 1565.
23 W. Lindner, in M. Zief and L. J. Crane (Editors), *Chromatographic Chiral Separations* (*Chromatographic Science Series*, Vol. 40), Marcel Dekker, New York, 1988, Ch. 4, p. 116.
24 J. Kamphuis, H. F. M. Hermes, J. A. M. van Balken, H. E. Schoemaker, W. H. J. Boesten and E. M. Meijer, in G. Lubec and G. A. Rosenthal (Editors), *Amino Acids: Chemistry, Biology and Medicine*, ESCOM Science, Leiden, 1990, pp. 119–125.
25 R. G. J. van Leuken and G. T. C. Kwakkenbos, *J. Chromatogr.*, in press.
26 S. S. Simons and D. F. Johnson, *J. Am. Chem. Soc.*, 98 (1976) 7098.
27 S. Weinstein and N. Grinberg, *J. Chromatogr.*, 318 (1985) 117.
28 H. Brückner, I. Bosch, T. Graser and P. Fürst, *J. Chromatogr.*, 368 (1986) 413.
29 J. R. Cronin, S. Pizzarello and W. E. Gandy, *Anal. Biochem.*, 93 (1979) 174.
30 S. S. Simons and D. F. Johnson, *J. Org. Chem.*, 43 (1978) 2886.
31 J. F. Stobaugh, A. J. Repta, L. A. Sternson and K. W. Garren, *Anal. Biochem.*, 135 (1983) 495.

Journal of Chromatography, 623 (1992) 247–254
Elsevier Science Publishers B.V., Amsterdam

CHROM. 24 464

High-performance liquid chromatographic separation of purine deoxyribonucleoside monophosphate–benzo[*a*]pyrene adducts

Kimmo Peltonen, Karen Canella and Anthony Dipple

Chemistry of Carcinogenesis Laboratory, ABL-Basic Research Program, NCI-Frederick Cancer Research and Development Center, Frederick, MD 21702 (USA)

(First received April 7th, 1992; revised manuscript received July 1st, 1992)

ABSTRACT

Chromatographic methods that allow the separation of adducts of purine nucleoside 3'-phosphates with the pure enantiomers of the *anti*-dihydrodiol epoxide of benzo[*a*]pyrene are developed. The optimization procedure includes evaluation of the effect of buffer molarity, the pH of the buffer, and the role of organic modifiers. The method can be utilized to prepare standards with known absolute configuration that can be further used in the Randerath ^{32}P-postlabeling procedure.

INTRODUCTION

The potent mutagen and carcinogen benzo[a]pyrene (BP) is a widely spread environmental pollutant that is also present in cigarette smoke and certain working environments [1,2]. It is generally believed that BP, like many other carcinogens, induces cancer by causing heritable changes in the genetic material of the cell. Of various methods available for monitoring polycyclic aromatic hydrocarbon DNA adducts in biological systems, the Randerath ^{32}P-postlabeling method [3] is perhaps the most widely used at present. In order to enhance the utility of this method, we sought to prepare markers of the various adducts of purine deoxyribonucleoside 3'-phosphates that might arise from the key DNA-binding metabolite of BP, the *anti*-7,8-dihydrodiol 9,10-epoxide [4–12]. The various products that can arise are shown in Fig. 1 where it can be seen that a single reaction gives rise to a pair of *cis–trans* isomers. The development of separations for these isomers is described in the present paper. The isomers are hybrid molecules with both lipophilic and hydrophilic components and, therefore, were neither separable by the chromatographic procedures usually used for normal nucleotides [13–15] nor by the reversed-phase procedures, without buffer or salts, usually used for hydrocarbon–nucleoside adducts [16–19].

Correspondence to: Dr. K. Peltonen, Institute of Occupational Health, Topeliuksenkatu 41 aA, SF-00250 Helsinki, Finland (present address).

EXPERIMENTAL

Chemicals

Acetonitrile, tetrahydrofuran and methanol (J. T. Baker, Phillipsburg, NJ, USA) were HPLC grade. Potassium hydrogenphosphate, potassium hydroxide (Sigma, St. Louis, MO, USA) and acetone (J. T. Baker) were all analytical-grade reagents. The water used in buffers and eluents was double-distilled. Racemic *anti*-benzo[*a*]pyrene-7,8-dihydrodiol 9,10-epoxide was obtained from the NCI Chemical Carcinogen Repository (Kansas City, MO, USA) and used as a freshly prepared solution (1 mg/ml) in acetone. Both (+)- and (−)-*anti*-benzo[*a*]pyrene-

0021-9673/92/$05.00

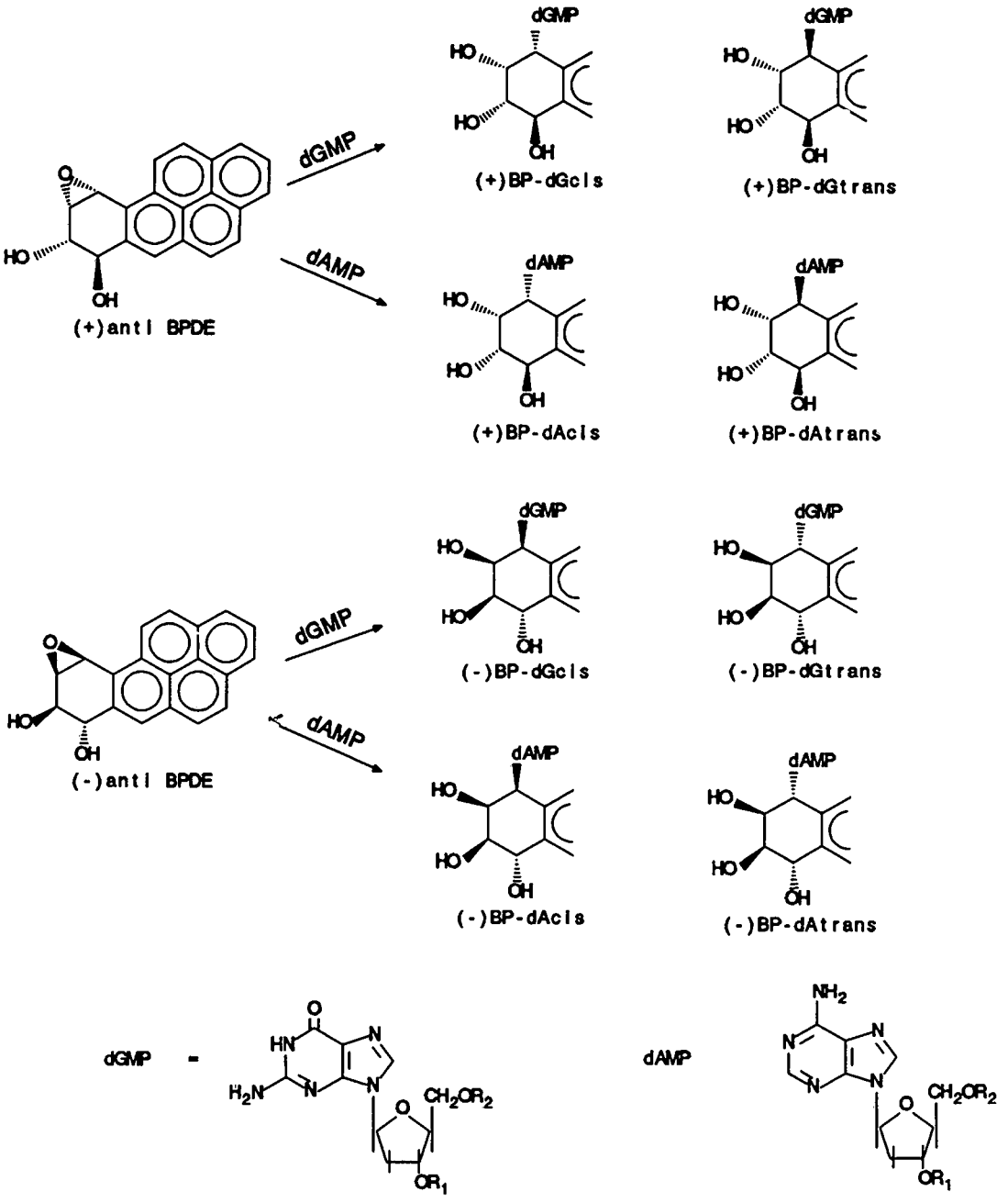

Fig. 1. Structures of adducts formed in reaction of each enantiomer of the *anti*-dihydrodiol epoxide of BP (BPDE) with the exocyclic amino groups of either deoxyguanosine (dG) or deoxyadenosine (dA) 3'- or 5'-phosphates. Each reaction results in both *cis* and *trans* opening of the epoxide ring.

dihydrodiol epoxides were purchased from Chemsyn Science Labs. (Lenexa, KS, USA) as solutions (0.7 mg/ml) in tetrahydrofuran–triethylamine (19:1, v/v). All unmodified nucleotides were purchased commercially and utilized as solutions in 0.1 *M* Tris buffer, pH 7.0 (40 and 10 mg/ml for the 5′- and 3′-phosphates, respectively).

Apparatus

The HPLC system consisted of a Hewlett-Packard Model 1090 equipped with a diode-array detector (Hewlett-Packard, Rockville, MD, USA). Ultraviolet spectra were also recorded off-line on a Milton Roy Spectronic 3000 diode-array spectrophotometer (Milton Roy, Durham, NC, USA) and circular dichroism (CD) spectra were recorded on a Jasco J-500A spectropolarimeter (Jasco, Easton, MD, USA). All CD spectra were normalized by dividing each spectrum by the ultraviolet absorbance at 343 nm.

Preparation of modified nucleotides

Solutions of nucleotides (1 ml) were separately mixed with a solution (100 μl) of the racemic or the (+)- or (−)-dihydrodiol epoxide. After initial mixing, all reactions were kept in the dark at 37°C for 4 h.

To remove the hydrolysis products of the dihydrodiol epoxides, the reaction mixtures were extracted three times with water-saturated ethyl acetate (1 ml) and then three times with diethyl ether to remove the ethyl acetate. Finally, the solutions were flushed for 5 min with nitrogen. Removal of the unreacted nucleotide was achieved by loading the reaction mixtures on reversed-phase Sep-Pak cartridges (Waters, Milford, MA, USA) and washing each cartridge with water (20 ml). Lipophilic products were then eluted with methanol (3 ml). The methanol fractions were concentrated to dryness and redissolved in 0.05 *M* potassium phosphate buffer, pH 7.1 (1 ml).

Chromatography

An Ultrasphere ODS column (250 × 4.6 mm, 5 μm particle size) was used (Beckman Instruments, Columbia, MD, USA). The mobile phase consisted of aqueous potassium phosphate with methanol, acetonitrile or a mixture of acetonitrile–tetrahydrofuran as an organic modifier. Different proportions of organic modifiers and different pH and molarity values for the aqueous eluent were tested in order to optimize the chromatographic conditions. The optimum condition established was a linear gradient from 2 to 40% of organic modifier over 60 min. For some separations, pure acetonitrile was used as the organic component, whereas in others, 50% tetrahydrofuran in acetonitrile was necessary. The phosphate buffer was filtered through a Millipore GF 0.22-μm filter. The mobile phase flow-rate was 1.0 ml/min, and elution was monitored using three independent channels (245, 285 and 346 nm, respectively). The chromatograph was operated at ambient temperature, and samples of 20 μl were injected.

RESULTS AND DISCUSSION

Since we have previously characterized all of the eight adducts shown in Fig. 1 at the deoxyribonucleoside level [20], we could identify nucleotide adducts either by comparison of the CD spectra of the nucleoside and nucleotide adducts [21] or by comparison of retention times of the modified nucleotides after dephosphorylation with those of the fully characterized nucleoside standards.

As can be seen in Fig. 1, the purine mononucleotides can be either 3′- or 5′-phosphates. Although only modified 3′-monophosphates are suitable as standards in the Randerath postlabeling assay, we carried out experiments with both 3′- and 5′-monophosphates to develop the chromatographic separations described here, because, for unknown reasons, the 5′-monophosphates generally give higher yields than the 3′-phosphates when reacted with dihydrodiol epoxides. Similarly, because of readier availability, we initially examined reactions of the racemic *anti*-dihydrodiol epoxide with these nucleotides but eventually had to undertake studies with the separate optically active enantiomers.

Reactions of the racemic dihydrodiol epoxide with the 5′-phosphates were used to optimize the molarity and the pH of the aqueous component of the eluent. When the molarity of potassium phospate buffer, pH 7.2 (the aqueous component of a gradient of 2–40% acetonitrile in buffer over 60 min), was varied in the range 10–350 m*M*, the resultant capacity factors for the separation of adducts from deoxyadenosine or deoxyguanosine 5′-phosphates showed little variation (data not shown), in

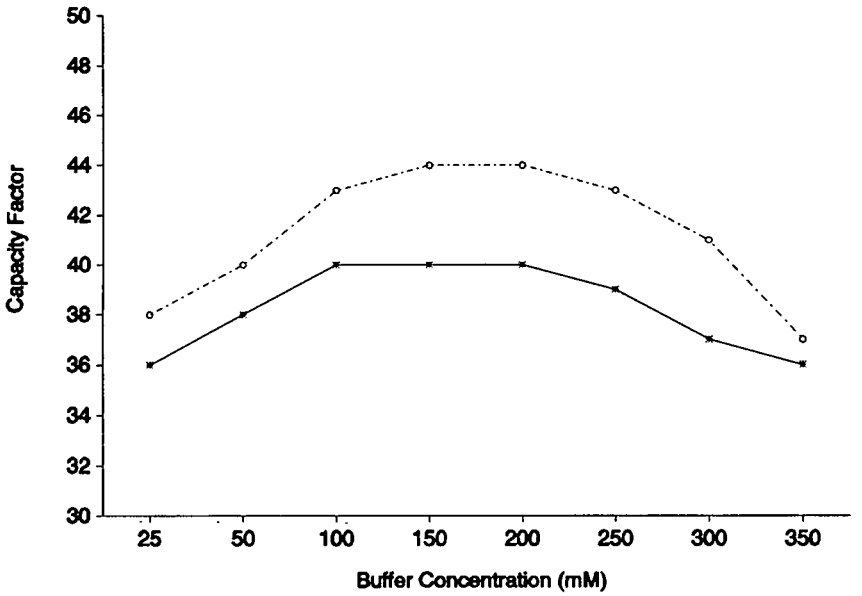

Fig. 2. Effect of the pH of the buffer on the capacity factor for racemic dihydrodiol epoxide adducts with deoxyguanosine 5'-phosphate (*) and deoxyadenosine 5'-phosphate- (O). Buffer molarity was 0.05 *M* and buffers at pH 4 and 5 were prepared from sodium acetate and those at pH 2, 3, 6, and 7 were made from potassium phosphate. The buffer was the aqueous component of a gradient of 2–40% acetonitrile in buffer over 60 min.

contrast to findings for non-modified nucleotides [15].

The analysis of non-modified nucleotides in the reversed-phase mode are normally carried out with acidic aqueous buffers. In our hands the first trials with acidic-pH (pH 3–4) buffers were not successful and led to poor separation of the analytes. Therefore, a range of pH values were tested. Because all buffers have a limited effective buffering range (*i.e.* $pK_a \pm 1$ pH unit), it was not possible to use the same buffer through a wide pH range. At pH 2, 3, 6, and 7, phosphate buffer was used and at pH 4 and 5, acetate buffer was used. The capacity factor as a function of pH is graphically presented in Fig. 2. These results clearly demonstrate that, with the column used in these experiments, the pH of the buffer had a substantial impact on the chromatography of these hybrid compounds. It was also clear that the capacity factor of this column was more affected by pH than by buffer concentration. The data also showed that the optimum pH was approximately 7. At pH values higher than 7.2, silica-based C_{18} columns are not stable for extended times. Since our studies showed that these analytes did not need a high buffering capacity, any buffer, even one outside its effective buffering range, could give satisfactory results if the pH were appropriate.

Preliminary experiments with organic modifiers showed that methanol gave low resolution when compared with acetonitrile and acetonitrile–tetrahydrofuran mixtures (data not shown). Therefore, the properties of acetonitrile and acetonitrile–tetrahydrofuran were studied further. Fig. 3 shows the effect of 50% tetrahydrofuran in the organic modifier on the chromatographic profiles of racemic BP-dihydrodiol epoxide adducts with deoxyguanosine 5'-phosphate (compare A and B) and 3'-phosphate (compare C and D) and on those of deoxyadenosine 5'-phosphate (compare E and F) and 3'-phosphate (compare G and H). Addition of tetrahydrofuran to the acetonitrile improved the separation (but did not give baseline separation) in all cases except for the deoxyadenosine 5'-phosphate adducts, where the presence of tetrahydrofuran caused a loss of the excellent separation seen with acetonitrile alone (Fig. 3E). In this latter case, the individual adducts could be identified on the basis of their CD spectra as shown in the figure with the abbreviations de-

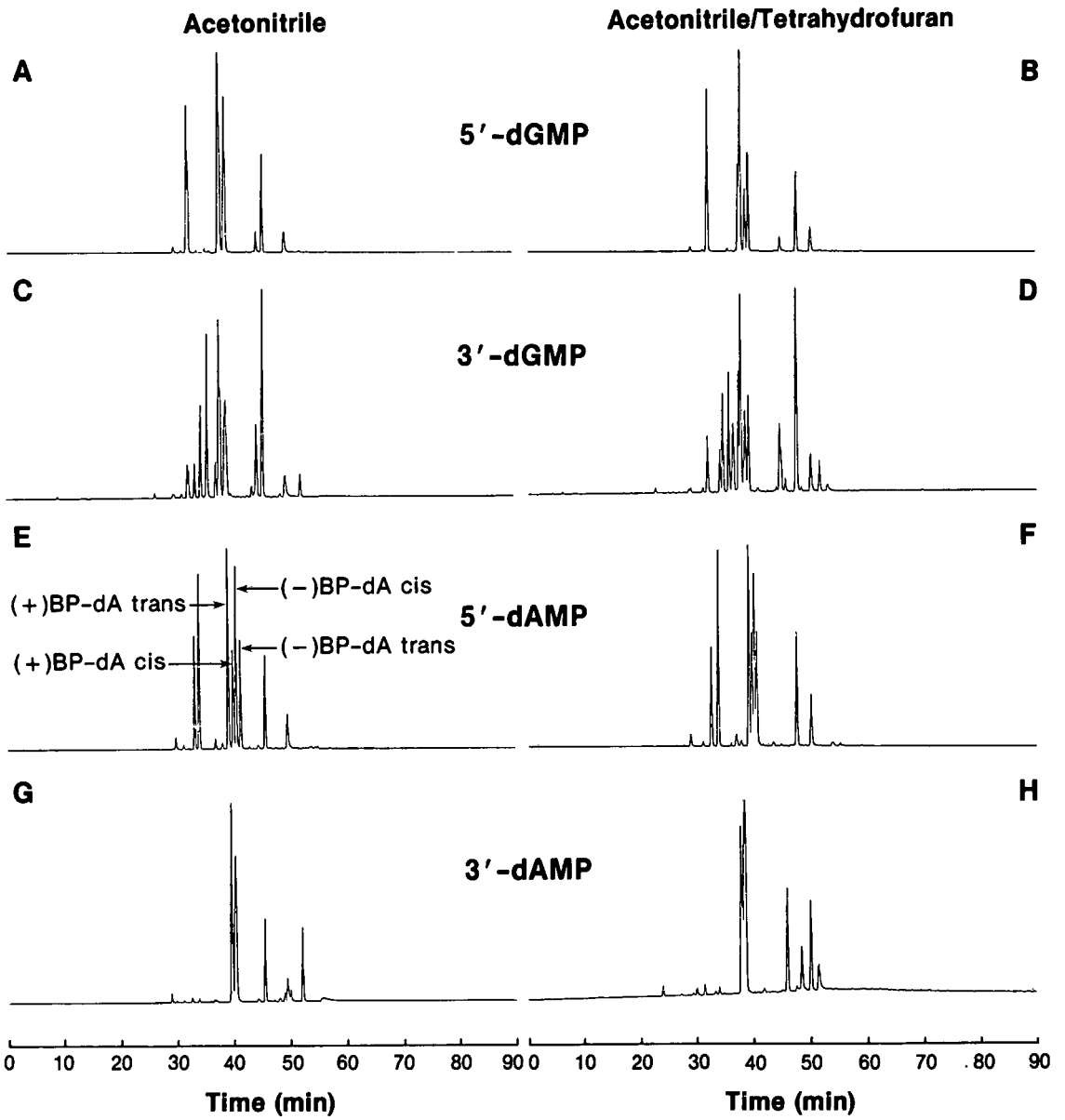

Fig. 3. Elution profile for products from reaction of the racemic dihydrodiol epoxide with deoxyguanosine 5′-phosphate (A and B) and deoxyadenosine 5′-phosphate (dA) (E and F). C and D present the elution profile of analogous products from deoxyguanosine 3′-phospate and G and H from deoxyadenosine 3′-phosphate. All separations involved a gradient of 2–40% organic modifier in buffer over 1 h. In A, C, E and G the organic modifier was acetonitrile whereas in B, D, F and H it was 50% tetrahydrofuran in acetonitrile.

fined in Fig. 1. In the other cases, the location of the adducts in the chromatogram could be determined from the UV absorption spectra of the various peaks, and these products appeared between retention times of 36 and 42 min in all cases. Some unknown products with a characteristically different UV spectrum [21] eluted ahead of these adducts, and tetraol hydrolysis products of the dihydrodiol epoxide eluted after these adducts. It was notable that the adducts from deoxyadenosine 3′-phosphate

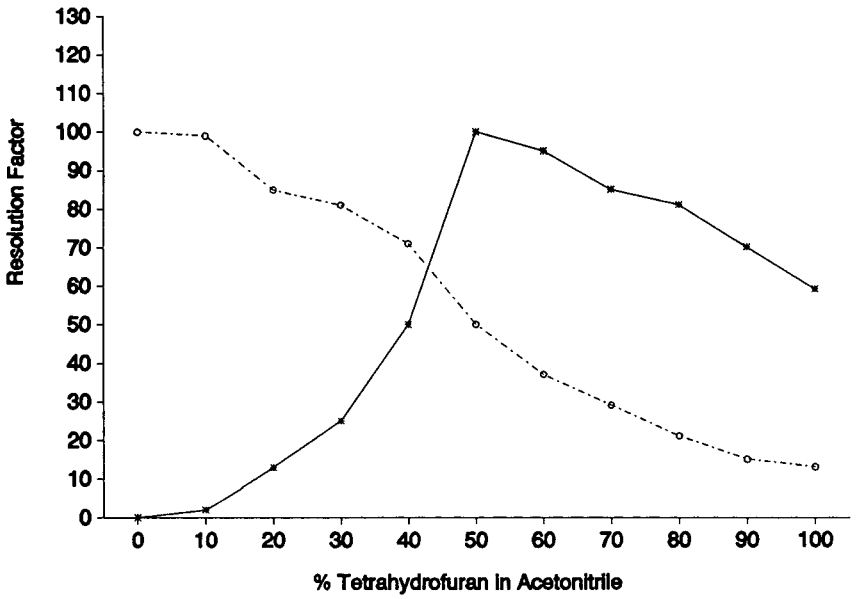

Fig. 4. Effect of the concentration of tetrahydrofuran in acetonitrile on the resolution [$R = 1.18\ (t_2 - t_1)/(w_1 + w_2)$, where R = resolution, t_1 and t_2 are retention times of adjacent peaks and w_1 and w_2 are peak widths at half height] for reactions of racemic dihydrodiol epoxide with deoxyguanosine 5′-phosphate (∗) and deoxyadenosine 5′-phosphate (○). The buffer used was 50 mM potassium phosphate, pH 7.2, and a gradient from 2 to 40% organic modifier was run over 60 min.

were less well resolved than those from the corresponding 5′-phosphate.

A systematic study of the resolution for deoxyguanosine and deoxyadenosine 5′-phosphate adducts as a function of tetrahydrofuran concentration in acetonitrile was undertaken (Fig. 4). Firstly, the resolution of the deoxyguanylic acid adducts, measured with the two most abundant peaks in the middle of the chromatogram of Fig. 3A, increased to an optimum at 50% tetrahydrofuran, after which the separation deteriorated. The decreasing resolution when 50% tetrahydrofuran in acetonitrile was exceeded was due to peak broadening and loss of peak symmetry. However, the deoxyadenylic acid adducts behaved differently. For these, the resolution monitored with the (+)-BP–deoxyadenosine *trans* and (+)-BP–deoxyadenosine *cis* peaks in Fig. 3E decreased almost linearly as a function of tetrahydrofuran and the best separation was achieved using pure acetonitrile.

The results from the experiments done with racemic BP-dihydrodiol epoxide showed that completely pure standards could not be obtained with the 3′-phosphates. With optically pure dihydrodiol epoxides, only *cis–trans* isomers need to be separated. The elution profiles from the reactions of (+)- and (−)-dihydrodiol epoxide of BP with deoxyguanosine 3′-phosphate and deoxyadenosine 3′-phosphate are shown in Fig. 5. The effects of tetrahydrofuran addition to the acetonitrile eluent can be seen by comparing the panels on the right (B, D, F and H) with those on their immediate left (A, C, E and G, respectively). For the deoxyguanylic acid reactions, only minor effects on the separations were seen, and the separations were good in all cases. However, for the deoxyadenylic acid reactions, tetrahydrofuran led to improved separation in the case of the products from the (−) enantiomer (Fig. 5G and H) yet worsened the separation of the (+) enantiomer adducts (Fig. 5E and F).

Given the good separations achieved in one or other solvent conditions for each reaction, it was possible to measure CD spectra of individual adduct peaks and, thereby, to identify them through comparison with known nucleoside adducts [20,21]. It was then clear that the order of elution of *cis* and *trans* adducts was different for products from different enantiomers of the dihydrodiol epoxide. Thus,

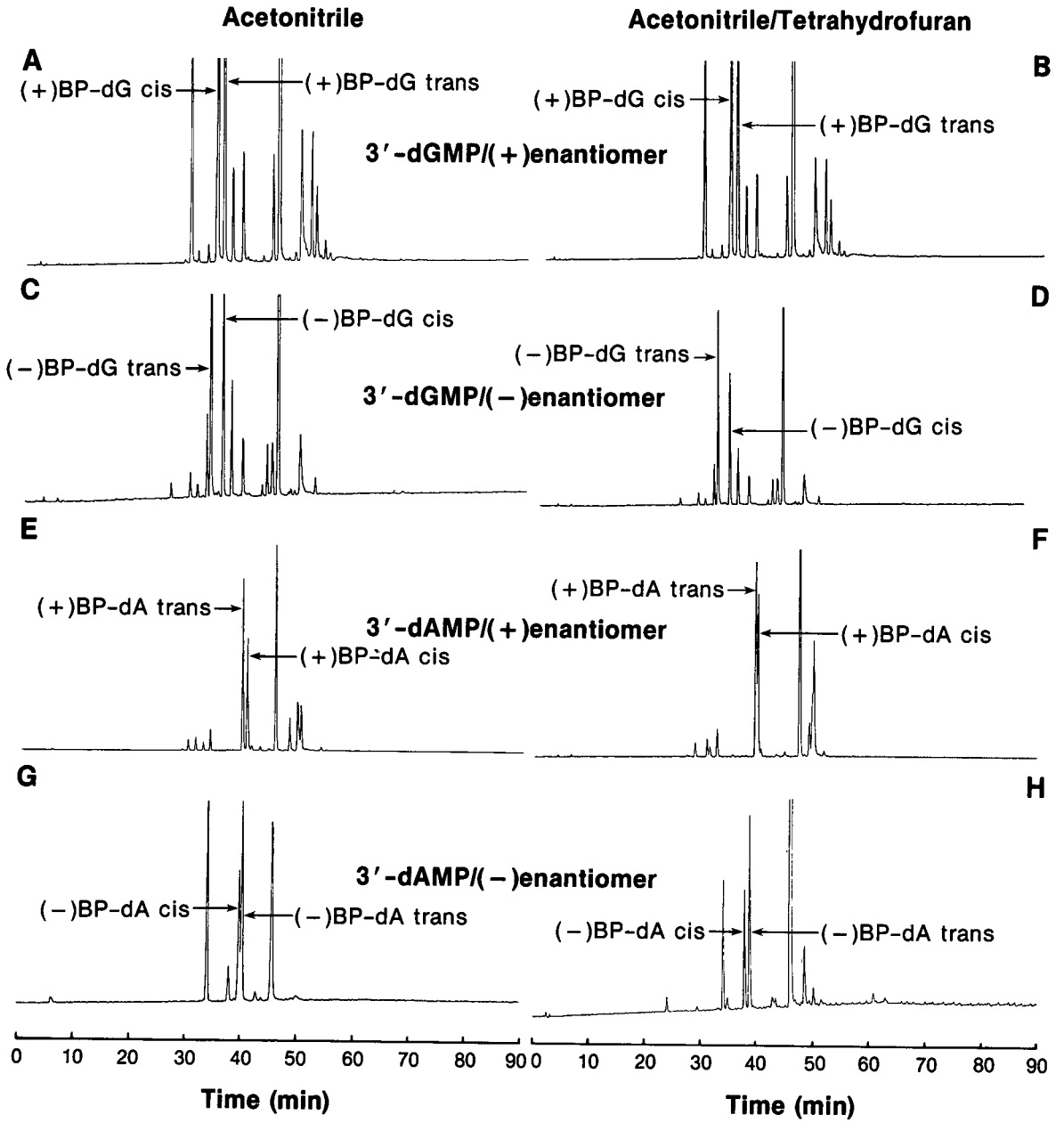

Fig. 5. Elution profile of deoxyguanosine 3′-phosphate (dG) and deoxyadenosine 3′-phosphate (dA) modified by optically active dihydrodiol epoxides of BP. In A, C, E and G the organic modifier was acetonitrile and in B, D, F and H it was 50% tetrahydrofuran in acetonitrile. A–D are for deoxyguanosine 3′-phosphate modified by the (+) enantiomer (A and B) and the (−) enantiomer (C and D). E–H are for deoxyadenosine 3′-phosphate modified with the (+) enantiomer (E and F) and the (−) enantiomer (G and H). The structure abbreviations are defined in Fig. 1.

for the deoxyguanylic acid adducts, *cis* adducts eluted before *trans* adducts for the (+) enantiomer but the reverse was found for the (−) enantiomer. In the case of the deoxyadenylic acid adducts, *trans* adducts eluted before *cis* adducts in the (+)-dihydrodiol epoxide case and *vice versa* for the (−) enantiomer.

In conclusion, chromatographic methods were developed that allowed the separation of the purine nucleoside 3′-phosphate adducts formed by reaction with the pure enantiomers of the *anti*-dihydrodiol epoxide of BP. In the case of the deoxyguanosine 3′-phosphate adducts good separations were achieved using a 2–40% acetonitrile gradient over 60 min in 0.05 *M* potassium phosphate buffer, pH 7.2. For the deoxyadenosine 3′-phosphate adducts, a good separation was achieved for the (+) enantiomer adducts with acetonitrile alone but tetrahydrofuran addition to the acetonitrile optimized the separation of the adducts from the (−) enantiomer.

ACKNOWLEDGEMENTS

Research was sponsored by the National Cancer Institute, DHHS, under Contract No. NO1-CO-74101 with ABL. The contents of this publication do not necessarily reflect the views or policies of the Department of Health and Human Services, nor does mention of trade names, commercial products, or organizations imply endorsement by the US Government.

REFERENCES

1 A. Dipple, R. C. Moschel and C. A. H. Bigger, in C. E. Searle (Editor), *Chemical Carcinogens*, American Chemical Society, Washington, DC, 2nd ed., 1984.
2 R. Newbold, P. Brookes and R. Harvey, *Int. J. Cancer*, 24 (1979) 203.
3 R. C. Gupta, M. V. Reddy and K. Randerath, *Carcinogenesis*, 3 (1982) 1081.
4 M. Topal, *Carcinogenesis*, 9 (1988) 691.
5 F. Beland and M. Poirier, *The Pathobiology of Neoplasia*, Plenum Press, New York 1989.
6 P. Brookes and P. Lawley, *Nature*, 202 (1964) 781.
7 E. Miller and J. Miller, *Cancer*, 47 (1981) 2327.
8 P. Sims, P. Grover, A. Swaisland and A. Hewer, *Nature*, 252 (1974) 326.
9 P. Grover, A. Hewer, K. Pal and P. Sims, *Int. J. Cancer*, 18 (1976) 1.
10 E. Huberman, L. Sachs, S. Yang and H. Gelboin, *Proc. Natl. Acad. Sci. U.S.A.*, 73 (1976) 607.
11 A. Conney, *Cancer Res.*, 42 (1982) 4875.
12 P. Brookes and M. Osborne, *Carcinogenesis*, 3 (1982) 1223.
13 A. Werner, W. Schneider, W. Siems, T. Grune and C. Schreiter, *Chromatographia*, 27 (1989) 639.
14 L. McLaughlin, *Chem. Rev.*, 89 (1989) 309.
15 G. Liu, *Chromatographia*, 28 (1989) 493.
16 S. Cheng, A. Prakash, M. A. Pigott, B. D. Hilton, H. Lee, R. G. Harvey and A. Dipple, *Carcinogenesis*, 9 (1988) 1721.
17 R. Nair, R. Gill, C. Cortex, R. Harvey and J. DiGiovanni, *Chem. Res. Toxicol.*, 2 (1989) 341.
18 K. Peltonen, B. D. Hilton, J. Pataki, H. Lee, R. G. Harvey and A. Dipple, *Chem. Res. Toxicol.*, 4 (1991) 305.
19 K. Peltonen, S. C. Cheng, B. D. Hilton, H. Lee, C. Cortez, R. G. Harvey and A. Dipple, *J. Org. Chem.*, 56 (1991) 4181.
20 S. C. Cheng, B. D. Hilton, J. Roman and A. Dipple, *Chem. Res. Toxicol.*, 2 (1989) 334.
21 K. Canella, K. Peltonen and A. Dipple, *Carcinogenesis*, 12 (1991) 1109.

Journal of Chromatography, 623 (1992) 255–263
Elsevier Science Publishers B.V., Amsterdam

CHROM. 24 465

Characterization of abscisic acid and metabolites by combined liquid chromatography–mass spectrometry with ion-spray and plasma-spray ionization techniques☆

Lawrence R. Hogge

Plant Biotechnology Institute, National Research Council of Canada, 110 Gymnasium Place, Saskatoon, Saskatchewan S7N 0W9 (Canada)

Garth D. Abrams

Prairie Malt Ltd., P.O. Box 1150, Biggar, Saskatchewan S0K 0M0 (Canada)

Suzanne R. Abrams

Plant Biotechnology Institute, National Research Council of Canada, 110 Gymnasium Place, Saskatoon, Saskatchewan S7N 0W9 (Canada)

Pierre Thibault

Marine Biosciences Institute, National Research Council of Canada, 1411 Oxford Street, Halifax, Nova Scotia B3H 3Z1 (Canada)

Steven Pleasance

Sciex Division of MDS Health Group Ltd., 55 Glen Cameron Road, Thornhill, Ontario L3T 1P2 (Canada)

(First received May 5th, 1992; revised manuscript received June 16th, 1992)

ABSTRACT

Liquid chromatographic–mass spectrometric methods have been developed for the characterization of abscisic acid (ABA) and metabolites in plant cell cultures using plasma-spray and ion-spray ionization techniques. Both techniques provide useful mass spectral data for ABA and its acidic metabolites. The most intense ions in these spectra are represented by $[M + H]^+$ and $[M + H - H_2O]^+$ The limit of detection for ABA, using plasma-spray and ion-spray was 5 and 9 ng, respectively, for full scans and 0.5 and 1 ng, respectively, for selected-ion recording of *m/z* 265, the protonated molecular ion. Ion-spray also provided intense protonated molecular ions for the neutral ABA metabolites whereas plasma-spray did not. Spectra acquired using both techniques showed intense ions indicating the presence of the ABA moiety in these neutral conjugates.

INTRODUCTION

The plant hormone abscisic acid (ABA, **1**) (see Fig. 1) is implicated in regulating many developmental processes in higher plants and in triggering

Correspondence to: Lawrence R. Hogge, Plant Biotechnology Institute, National Research Council of Canada, 110 Gymnasium Place, Saskatoon, Saskatchewan S7N 0W9, Canada.

☆ NRC Publication No. 33 536.

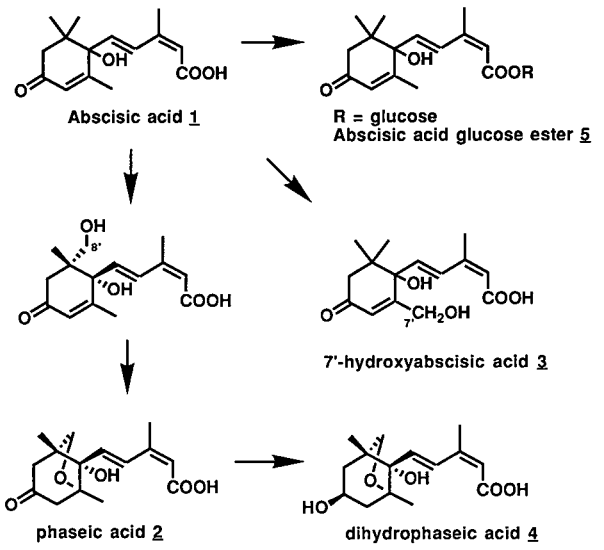

Fig. 1. Structures of ABA and ABA metabolites (products of oxidation of ring methyl groups and/or conjugation with sugar molecules).

plant responses to environmental stresses [1]. Numerous analytical methods have been developed to measure levels of endogenous ABA found in plant tissues, and newer physico-chemicals methods have been recently reviewed by Parry and Horgan [2]. Gas chromatography–mass spectrometry (GC–MS) of the methyl ester derivative with selected ion monitoring (SIM) and the use of deuterated internal standards has proved to be a powerful method for quantifying ABA [2]. Immunochemical methods, verified by GC–MS, have become popular with plant physiologists studying ABA responses in plants [3].

The currently known principal metabolites of ABA in plants are products of oxidation of ring methyl groups and/or conjugation to sugar molecules (Fig. 1). Of the acidic metabolites, phaseic acid (PA, **2**), like ABA, is known to be active in inhibiting barley embryo germination [4] while the roles of other metabolites, 7′-hydroxyabscisic acid (7′-OH-ABA, **3**) [5] and dihydrophaseic acid (DPA, **4**) have been less well studied [1,6].

As the role of these metabolites in the developmental process of plants is of interest to an increasing number of plant physiologists, there is a need for analytical methods providing information on the entire ABA metabolic profile within a single experiment. Direct analysis of crude plant extracts has been accomplished using desorption chemical ionization (DCI) and secondary-ion MS in conjunction with linked scanning at constant B/E, where B is the magnetic field strength and E is the electrostatic sector voltage [7]. The detection limit for these compounds using DCI is very low but linked scanning is very difficult to perform because of the short-lived nature of the ion current [7]. Secondary-ion MS or fast atom bombardment (FAB) is more amenable to linked-scanning MS–MS because this technique does possess a much longer ion current life time. Unfortunately, detection limits for secondary-ion MS or FAB are much higher than for DCI, often requiring more than a microgram of analyte [8].

High-performance liquid chromatography (HPLC) has been most valuable for the separation and quantitation of ABA and ABA metabolites [2,9]. This technique provides the advantage of analyzing directly the ABA-related compounds without derivatization and therefore fewer manipulations. This is an important considerization, as many ABA metabolites (including ABA conjugates) are prone to decomposition or isomerization [10,11].

However, there is a need for a better method of detection and characterization of the HPLC eluates. Until now, detection of compounds has been either by UV or, in cases in which labelled ABA has been supplied to plant material, by radioactivity detection. The combination of HPLC to separate compounds of interest, coupled with MS for structure identification, has not yet been reported for analysis of ABA and metabolites [2].

We have undertaken to develop HPLC–MS for our studies on metabolism of supplied ABA and related compounds by plant cell cultures. Our current studies have involved two different ionization techniques, plasma-spray and ion-spray, on instruments fitted with HPLC–MS interfaces. We have determined the sensitivities of both ionization techniques for the detection of ABA as well as the feasibility of characterizing both acidic and neutral metabolites of ABA using these methods of analysis. We now report the results of our investigations.

EXPERIMENTAL

ABA and ABA metabolite mixtures

Racemic ABA was purchased from Sigma

(A-2784). A stock solution containing 0.05 μg/ml ABA in methanol was prepared for the purpose of determining the detection limit and quantitative response for each mode of ionization.

Mixtures of unconsumed ABA and its acidic metabolites were obtained by ethyl acetate extraction of acidified filtrates from bromegrass cell suspension cultures fed racemic ABA, followed by back extraction of the acidic substances into aqueous $NaHCO_3$, as previously described [12]. Neutral metabolites were obtained from the ethyl acetate solution by washing with saturated aqueous NaCl, drying with Na_2SO_4, filtration, and evaporation of the solvent from the filtrate under reduced pressure.

Mass spectrometry

Plasma-spray LC–MS. LC separation was performed using a Waters system consisting of two pumps, Models 590 and 510, controlled by a Model 680 gradient controller. Sample injections of 20 μl were made on a Vydac 218TP54 C_{18} column (150 mm × 4 mm I.D.) using a linear gradient elution [10–40% acetonitrile in aqueous 0.1% trifluoroacetic acid (TFA) over 20 min] at a flow-rate of 0.8 ml/min.

The LC system was interfaced to a VG Analytical 70-250 SEQ hybrid mass spectrometer equipped for plasma-spray analysis. The probe temperature was 220°C and the source temperature 250°C Spectra were obtained by scanning from *m/z* 500 to 100 (resolution of 1000) at a rate of 3 s per decade. SIM experiments were performed by monitoring *m/z* 265.1442 using a dwell time of 80 ms and a settling time of 20 ms at a mass resolution of 4000.

Ion-spray LC–MS. LC separation was performed using a Hewlett-Packard 1090 high-pressure liquid chromatograph equipped with a diode-array detector. Sample injections of 5 μl were made on a Vydac 218TP52 C_{18} column (150 mm × 2 mm I.D.) using the gradient elution mentioned above at a flow rate of 0.2 ml/min.

The LC system was interfaced to a Sciex API/111 triple quadrupole mass spectrometer equipped with an ion-spray source. Spectra were obtained by scanning from either *m/z* 100 to 300 in 3 s (ABA full-scan calibration curve) or *m/z* 100 to 500 in 3 s (acidic and neutral extracts). For SIM experiments, *m/z* 265 was monitored using a dwell time of 200 ms.

RESULTS AND DISCUSSION

Detection of ABA by HPLC–MS

Racemic ABA was used to assess the usefulness of both plasma-spray and ion-spray for the characterization of natural ABA and its metabolites in plant cell cultures. Fig. 2A and B shows representative spectra obtained for ABA (approximately 200 ng sample size) using plasma-spray and ion-spray, respectively. These spectra are very similar with intense ions at *m/z* 265 (the protonated molecular ion) and the base ion at *m/z* 247 (the loss of water from the protonated molecular ion). However, the plasma-spray spectrum contains ions at *m/z* 306 and 288 that are not present in the ion-spray spectrum. These are adduct ions due to the addition of acetonitrile (from the mobile phase) to the intense ions mentioned above (*m/z* 265 and 247). On the other hand, the ion-spray spectrum contains an adduct ion at *m/z* 282 which is not present in the plasma-spray spectrum. The nature of this ion is not yet fully understood, but appears to be equivalent to the addition of an NH_4^+ ion which could be formed during the ion evaporation process either from trace amounts of ammonia in the mobile phase or in the air. Similar observations have been noted in the analysis of other compounds containing carboxylic acid moieties such as okadaic acid [13].

Limit of detection for ABA

The limit of detection for ABA using both ionization techniques (plasma-spray and ion-spray) was determined by analyzing known amounts under isocratic LC–MS conditions. The results obtained for full scan acquisitions are shown in Fig. 3, the plot of peak heights (arbitrary units) for the ABA protonated molecular ion (*m/z* 265) *versus* amount of ABA injected for the plasma-spray and ion-spray LC–MS systems. For plasma-spray the limit of detection was 5 ng (signal-to-noise ratio of approximately 8) with a linear response that ranged to 1000 ng while with ion-spray the limit of detection was 9 ng with a similar range of linear response.

Fig. 2C and D show the respective mass spectrum obtained from plasma-spray and Ion spray at the lower detection limit. The expected major ions at *m/z* 265 ($[MH]^+$) and *m/z* 247 ($[MH - H_2O]^+$) are present in both spectra. However, it should be

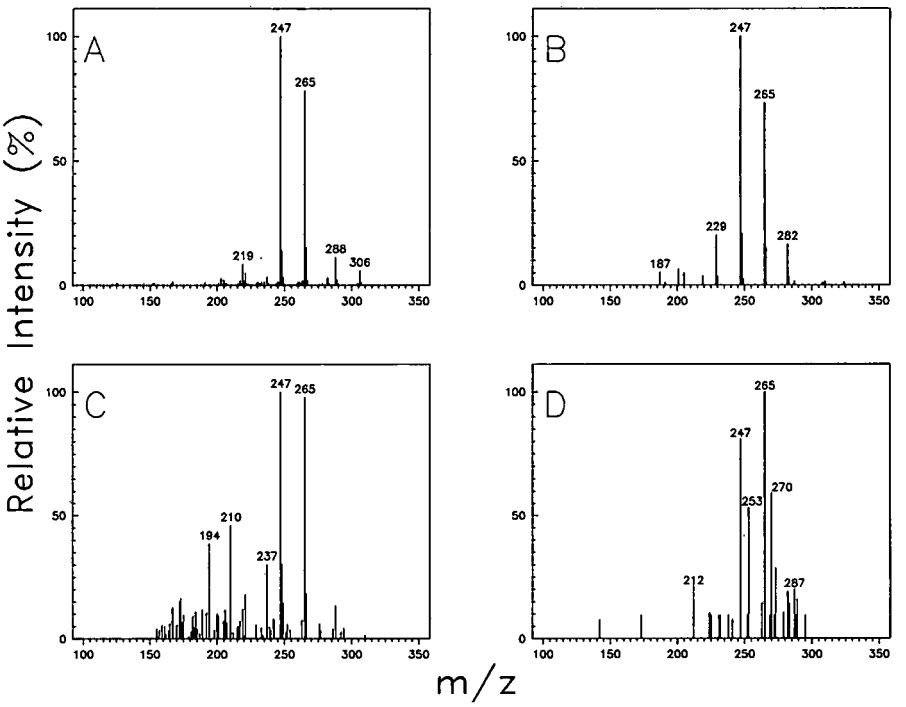

Fig. 2. Plasma-spray (A) and ion-spray (B) mass spectra of approximately 200 ng of ABA. (C) Plasma-spray limit of detection mass spectrum for ABA (5 ng) and (D) ion-spray limit of detection mass spectrum for ABA (9 ng).

noted that not all the background ions could be subtracted in these spectra (see Fig. 2A and B).

Detection limits were also determined using the SIM mode. Fig. 4 shows the calibration curve for both techniques, a plot of peak heights of the protonated molecular ion (*m/z* 265) *versus* the amount of ABA injected. Ion-spray SIM experiments were carried out at unit mass resolution. However, because the plasma-spray was installed on a double-focusing magnetic system, which has the advantage of operating with higher mass resolution and therefore providing a greater degree of specificity, a mass resolution of 4000 was used for these experiments. As shown, the limit of detection was 500 pg for plasma-spray and 1 ng for ion-spray (signal-to-noise ratio of 5). The linear response for the amount of ABA injected was similar to that obtained with the full scan experiments.

It should be noted that although plasma-spray appears to have slightly lower detection levels under these experimental conditions, the results should not be seen as proof that one of the above techniques is more sensitive than the other as the chromatographic conditions used were quite different. For example, the different injection volumes, column sizes and flow rates used would produce differ-

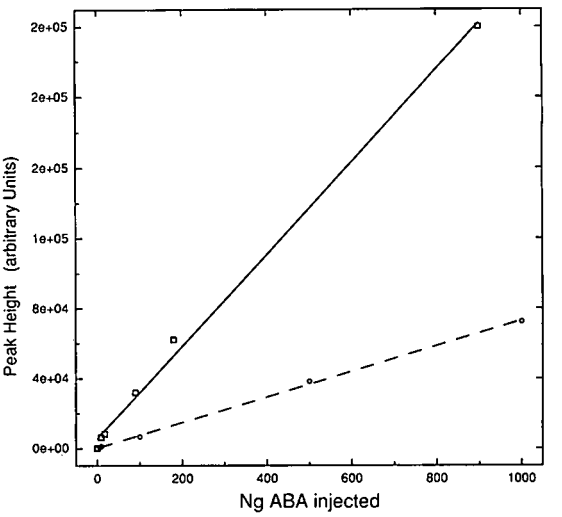

Fig. 3. Plot of peak heights for the ABA protonated molecular ion (full-scan acquisitions) *versus* amounts (ng) of ABA injected on the LC column. □ = Ion-spray; ○ = plasma-spray.

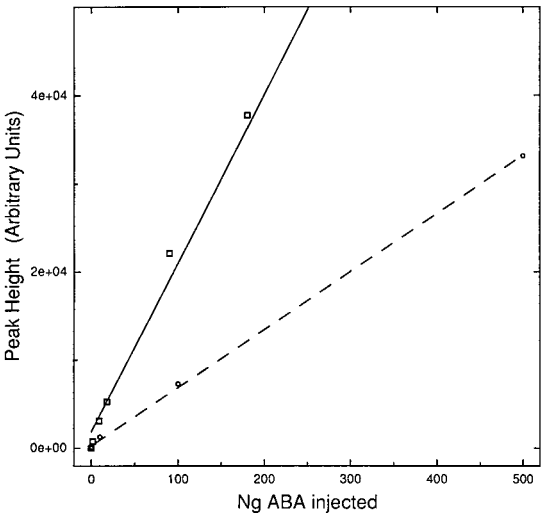

Fig. 4. Plot of peak heights for the ABA protonated molecular ion (selected ion recording) *versus* amount (ng) of ABA injected on the LC column. □ = Ion-spray; ○ = plasma-spray.

ent concentration levels of the analyte even though the absolute amounts injected were the same. As plasma-spray and ion-spray have different flow constraints, direct comparisons of concentration levels are difficult. However, the results do show the practical limits of detection for each of the techniques using experimental conditions that are typical for that particular interface.

LC–MS of acidic metabolites isolated from plant cell cultures fed racemic ABA

Plasma-spray and ion-spray LC–MS was used to confirm the identity of the major ABA metabolites produced in the ABA-fed bromegrass tissue cultures and to determine the usefulness of these techniques for the characterization of other ABA metabolites or ABA analogue metabolites for future plant tissue culture feeding experiments. In previous work in this laboratory, the major ABA metabolites as well as ABA in this culture extract were identified as DPA (**4**), PA (**2**), 7′-OH-ABA (**3**) and ABA (**1**) [5] (see Fig. 1). Fig. 5 shows the LC chromatogram obtained with UV detection as well as the limited ion chromatograms obtained from plasma-spray and ion-spray LC–MS with the major components identified in each chromatogram. The ion chromatograms show similar profiles to the UV trace. Although the ion-spray chromatogram appears more attractive from a chromatographic point of view, it should be noted that the amount of sample injected was over three times that injected in the plasma-spray experiment.

Mass spectral data (plasma-spray and ion-spray) for the four major components are summarized in Table I, a listing of the masses and intensities for the diagnostically important ions along with their proposed assignments. These data show that the four major acidic components have very intense ions similar to those of ABA. They include the protonated molecular ion, solvent adduct ions, and ions due to the loss of water for each of the components. It should be noted that the protonated molecular ion for DPA is of low intensity (less than 1%) in the ion-spray spectrum. However, the spectrum does exhibit an adduct ion ($[M + NH_4]^+$), confirming the molecular mass. Furthermore, the most intense ion in the spectrum corresponds to the loss of water from DPA which contains both a secondary and tertiary hydroxyl group. In contrast, the plasma-spray-generated protonated molecular ion for PA has a much lower intensity than the protonated molecular ion obtained from the ion-spray analysis (12% *versus to* 74%).

PA and 7′-OH-ABA are isomeric and give similar fragmentation patterns in both ionization modes. Although the intensities of the protonated molecular ions of the specific isomers (relative to the base peak) do vary significantly, particularly in the plasma-spray spectra, it is more reliable to distinguish the isomers using their specific chromatographic elution times.

The plasma-spray spectra for ABA and 7′-OH-ABA and the ion-spray spectrum of ABA also contain an ion at *m/z* 219 with intensities of 8.5%, 52.5% and 3.9%, respectively. This ion may be the result of the loss of formic acid from the protonated ABA molecular ion or in the case of 7′-OH-ABA, the loss of water and carbon dioxide. The ion-spray spectrum of 7′-OH-ABA also contains an intense ion at *m/z* 233 (56.6%) not observed in the plasma-spray spectrum. This ion is likely formed as a result of the loss of neutral molecules of methanal and water from the protonated molecular ion.

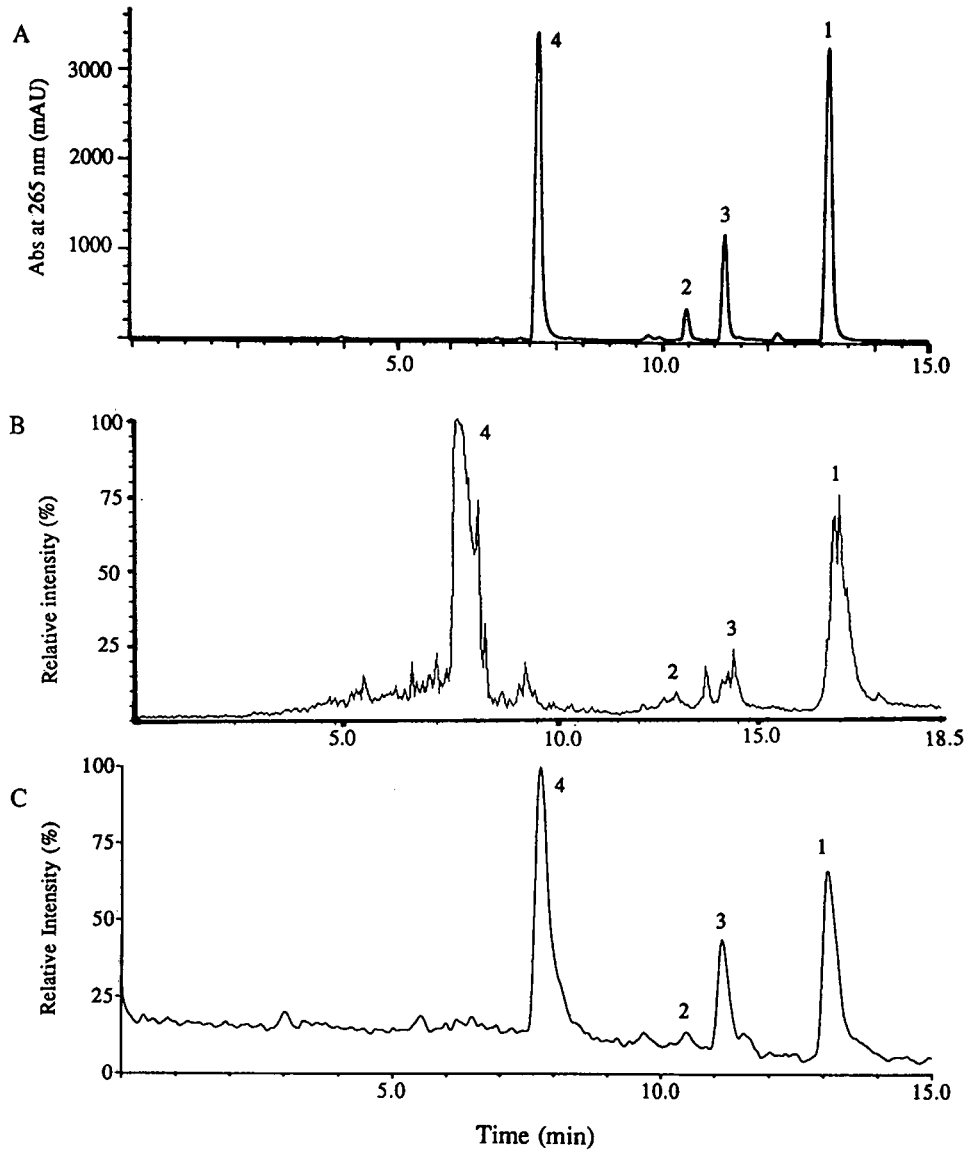

Fig. 5. Analysis of the acidic fraction of ABA-treated bromegrass plant cell extract. (A) LC–UV chromatogram, 5 μl injection; (B) LC–MS with plasma-spray, 3 μg injection, reconstructed ion chronmatogram (RIC) for *m/z* 250–430; (C) LC–MS with ion-spray, 10 μg injection, RIC for *m/z* 250–430. Separation conditions: (A, C) Vydac 218TP52 HPLC column, flow-rate 0.20 ml/min, linear gradient from 10 to 40% acetonitrile in aqueous 0.1% TFA in 20 min; (B) Vydac 218TP54 HPLC column, flow-rate 0.80 ml/min linear gradient as in A and C, peaks: **4** = DPA; **2** = PA; **3** = 7'-OH-ABA, **1** = ABA.

LC–MS of neutral metabolites isolated from plant cell cultures fed ABA

The analysis of the neutral metabolites showed different results for the two ionization techniques. Fig. 6 shows the LC chromatogram obtained with UV detection as well as the limited ion chromatograms obtained from the plasma-spray and ion-spray LC–MS analyses. These chromatograms indicate there is one major neutral metabolite. This metabolite was identified as the glucose ester of

TABLE I

DIAGNOSTIC IONS FROM PLASMA-SPRAY AND ION-SPRAY ANALYSIS OF ACIDIC ABA METABOLITES

Component	Proposed structure (percent relative intensity)							
	Plasma-spray				Ion-spray			
	$[MH]^+$	$[MH + CH_3CN]^+$	$[MH - H_2O]^+$	$[MH - H_2O + CH_3CN]^+$	$[MH]^+$	$[M + NH_4]^+$	$[MH - H_2*]^+$	$[MH - 2H_2O]^+$
DPA	283 (4.89)	324 (8.06)	265 (100)	306 (0.97)	283 (<0.5)	300 (8.44)	265 (100)	247 (8.00)
PA	281 (11.6)	322 (1.48)	263 (100)	304 (5.64)	281 (74.1)	298 (85.4)	263 (100)	245 (0.0)
7′-OH-ABA	281 (44.1)	322 (0.0)	263 (100)	304 (3.34)	281 (55.6)	298 (35.9)	263 (100)	245 (33.8)
ABA	265 (78.3)	306 (5.81)	247 (100)	288 (11.3)	265 (74.5)	282 (17.4)	247 (100)	229 (19.9)

TABLE II

DIAGNOSTIC IONS FOR PLASMA-SPRAY AND ION-SPRAY LC–MS ANALYSIS OF NEUTRAL ABA METABOLITE

Component	Proposed structure (percent relative intensity)							
	Plasma-spray				Ion-spray			
	$[MH]^+$	$[MH + CH_3CN]^+$	$[MH - \text{glycone}]^+$	$[MH - \text{glycone} - H_2O]^+$	$[MH]^+$	$[M + NH_4]^+$	$[MH - \text{glycone}]^+$	$[MH - \text{glycone} - H_2O]^+$
ABA glucose ester	427 (0.0)	468 (0.0)	265 (63.8)	247 (100)	427 (99.4)	444 (18.3)	265 (100)	247 (41.2)

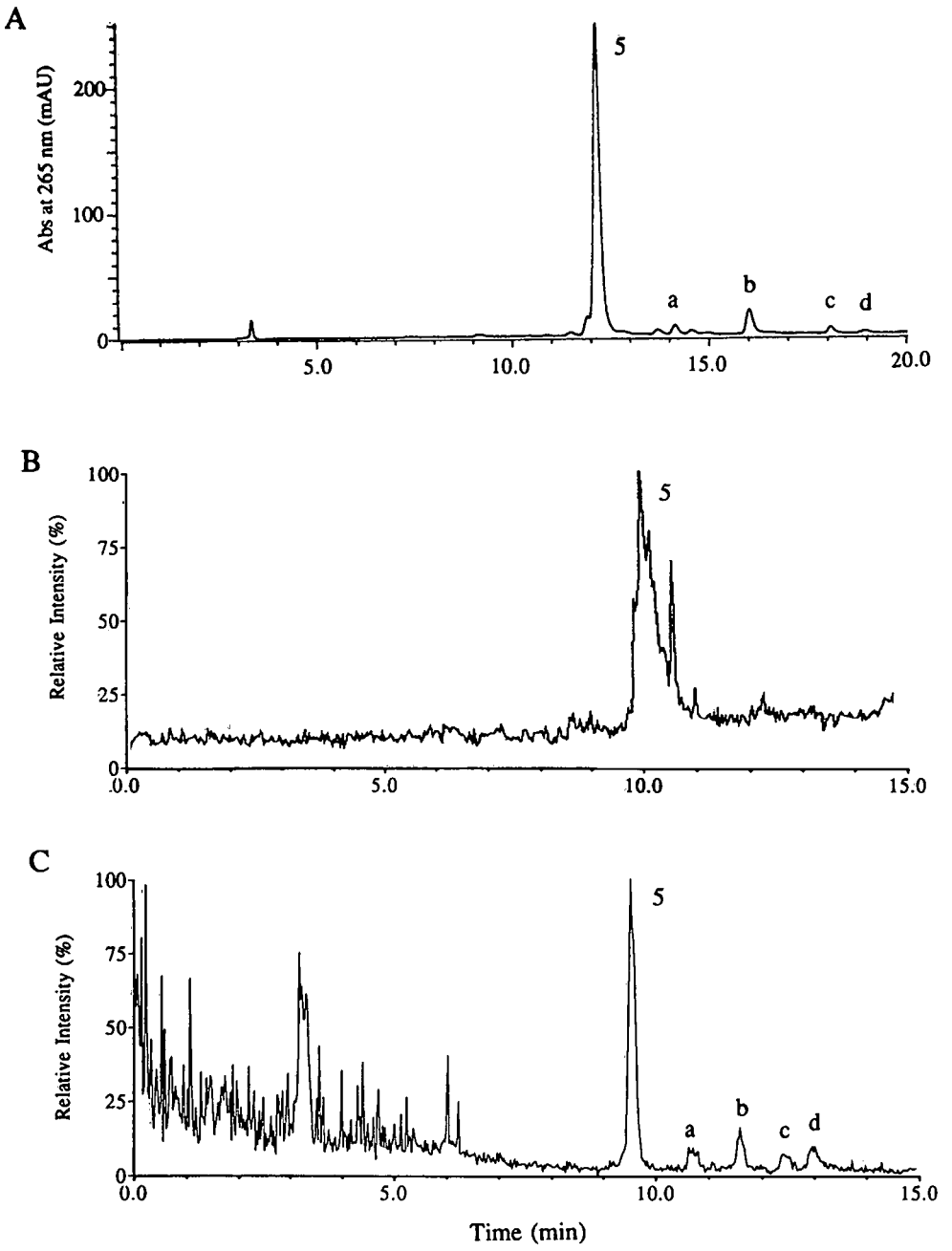

Fig. 6. Analysis of the neutral fraction of ABA-treated bromegrass plant cell extract. (A) LC–UV chromatogram, 1 μg injection; (B) LC–MS with plasma-spray, 0.5 μg injection, RIC for *m/z* 200–450; (C) LC–MS with ion-spray, 1 μg injection, RIC for *m/z* 200–450. Separation conditions: (A, C) Vydac 218TP52 HPLC column, flow-rate 0.20 ml/min, linear gradient from 10 to 35% acetonitrile in aqueous 0.1% TFA in 20 min; (B) Vydac 218TP54 HPLC column, flow-rate 0.80 ml/min, linear gradient as in A and C. Peaks: **5** = ABA glucose ester; a, b, c and d = ABA conjugates.

ABA by comparing its LC elution time, UV spectrum and mass spectrum to an authentic standard of ABA glucose ester (5) synthesized in this laboratory. Details of the confirmation of the identity of this glucose ester which is known to exist in plants [10] will be given in a future publication. As with the acidic fraction (Fig. 5), the ion-spray chromatogram appears chromatographically more appealing. This may be in part due to the amount of sample injected (1 μg *versus* 0.5 μg in the plasma-spray experiment). However, there are more significant differences in the mass spectral data. Table II lists the diagnostically important ions produced from each ionization technique for the glucose ester. There are no protonated or other adduct ions observed in the plasma-spray analysis while very intense protonated molecular ions (99%) as well as $[M + NH_4]^+$ adduct ions are observed in the ion-spray analysis.

In addition, the ion-spray analysis indicates that other neutral ABA conjugates are present in minor amounts (see Fig. 6C, components a, b, c and d). Although the structures of these minor components have not yet been determined, the mass spectral data suggest that all contain an intact ABA moiety and two (components a and b) likely have a molecular mass of 410 daltons, 16 units less than the ABA glucose ester.

CONCLUSION

LC–MS using either plasma-spray or ion-spray is a practical method for the separation and characterization of ABA and ABA metabolites extracted from plant tissue cultures. Information obtained from the elution times and mass spectral data allow for qualitative analysis of these components. Calibration curves done with full scan acquisition and selected ion recording showed a linear response for up to 1000 ng of ABA injected on the column. The preparation and use of deuterated internal standards should therefore make quantitative analysis possible. With the LC–MS instrumentation and chromatographic conditions used in this study, detection levels were slightly lower for ABA and its acidic metabolites using plasma-spray, while ion-spray provided more useful mass spectral data (intense protonated molecular ions) for the ABA glucose ester and other neutral ABA conjugates.

REFERENCES

1 J. A. A Zeevaart and R. A. Creelman, *Ann. Rev. Plant Physiol. Plant Mol. Biol.*, 39 (1988) 439.
2 A. D. Parry and R. Horgan, in W. J. Davis and H. G. Jones (Editors), *Abscisic Acid Physiology and Biochemistry*, Bios Scientific, Cambridge, 1991, p. 5.
3 M. K. Walker-Simmons and S. R. Abrams, in W. J. Davis and H. G. Jones (Editors), *Abscisic Acid Physiology and Biochemistry*, Bios Scientific, Cambridge, 1991, p. 53.
4 R. D. Hill, D. Durnin, L. A. K. Nelson, G.D. Abrams, L. V. Gusta and S. R. Abrams, *Plant Physiol.*, in press.
5 C. R. Hampson, M. J. T. Reaney, G. D. Abrams, S. R. Abrams and L. V. Gusta, *Phytochemistry*, 31 (1992) 2645.
6 L. A. K. Nelson, A. C. Shaw and S. R. Abrams, *Tetrahedron*, 47 (1991) 3259.
7 N. Takeda, K. Harada, M. Suzuki, A. Tatematsu, N. Hirai and K. Koshimizu, *Agric. Biol. Chem.*, 51 (1987) 2351.
8 J.R. Chapman, in *Practical Organic Mass Spectrometry*, John Wiley, Chichester, pp.122–129.
9 R. A. Creelman and J. A. D Zeevaart, in H. F. Linskens and J. F. Jackson (Editors), *Modern Methods of Plant Analysis*, Vol. 5, Springer-Verlag, Berlin, 1987 pp. 39–51.
10 B. V. Millborrow and R. Mallaby, *J. Exp. Bot.*, 26 (1975) 741.
11 S. J. Neill, R. Horgan and J. K. Heald, *Planta*, 157 (1983) 371.
12 S. R. Abrams, M. J. T. Reaney, G. D. Abrams, T. Mazurek, A. C. Shaw and L. V. Gusta, *Phytochemistry*, (1989) 2885.
13 P. Thibault, S. Pleasance and P. G. Sim, unpublished results.

Journal of Chromatography, 623 (1992) 265–276
Elsevier Science Publishers B.V., Amsterdam

CHROM. 24 411

Low ng/l-level determination of twenty N-methylcarbamate pesticides and twelve of their polar metabolites in surface water via off-line solid-phase extraction and high-performance liquid chromatography with post-column reaction and fluorescence detection

A. de Kok and M. Hiemstra

Food Inspection Service, Department of Pesticide Analysis, Burgpoelwaard 6, 1824 DW Alkmaar (Netherlands)

U. A. Th. Brinkman

Department of Analytical Chemistry, Free University, De Boelelaan 1083, 1081 HV Amsterdam (Netherlands)

(First received March 12th, 1992; revised manuscript received June 5th, 1992)

ABSTRACT

Reversed-phase high-performance liquid chromatography (HPLC) was used for the determination of twenty parent N-methylcarbamate pesticides and twelve major metabolites in surface water. A 50-ml water sample was passed through a disposable solid-phase extraction cartridge, packed with 500 mg of low-carbon C_{18}-bonded silica (C_{18}/OH, 40 μm particle size), which selectively retained polar compounds. The preconcentrated analytes were eluted with acetonitrile, reconstituted in 1 ml of water and 100 μl were injected into the HPLC system. The carbamates were separated via a water–methanol–acetonitrile gradient. Detection was performed via postcolumn hydrolysis on a solid-phase (anion-exchange) catalyst, derivatization of the methylamine formed with *o*-phthalaldehyde–2-mercaptoethanol and fluorescence detection of the isoindole derivative. The detection limits for surface water were between 20 and 30 ng/l. Recoveries were determined for thirteen carbamates and ten metabolites at the 0.1 and 1 μg/l level and generally ranged from 76 to 106% with relative standard deviations (R.S.D.s) of 0.5–8.5%. Only the sulphoxide metabolite of ethiofencarb and thiofanox had lower recoveries and correspondingly higher R.S.D.s.

INTRODUCTION

The worldwide increase in the use of pesticides during the last two decades has led to the presence of residues of these pesticides not only on the crops to which they are applied but also, owing to leaching into and run-off from the soil, in ground water and surface waters, respectively. Because of the proven or suspected toxicity of many of these pesticides, their monitoring is needed from both the regulatory and the consumer points of view. Surveillance by governmental agencies of pesticide residues on crops has become routine since the discovery of DDT residues in the early 1960s. However, only in the last 5 years has monitoring of pesticides in ground and surface waters been performed on a regular basis, especially since high residue levels were reported for various ground and well waters. In the USA the National Pesticide Survey project was initiated to conduct a statistically based survey

Correspondence to: Dr. A. de Kok, Food Inspection Service, Department of Pesticide Analysis, Burgpoelwaard 6, 1824 DW Alkmaar, Netherlands.

0021-9673/92/$05.00

of pesticide contamination of drinking-water wells [1].

In crop analysis, emphasis is generally laid on the determination of insecticides (organochlorine and organophosphorus compounds, carbamates) and fungicides (benzimidazoles, phthalimides), whereas in water analysis herbicides (triazines, phenoxycarboxylic acids, phenylureas) are often the target compounds. This is reflected in the availability of analytical methods for these typical matrix–pesticide combinations. Especially in Europe, the analysis of water samples for N-methylcarbamates has only attracted increased attention in recent years.

Since the development of a high-performance liquid chromatographic (HPLC) analysis for N-methylcarbamates by Moye *et al.* [2], based on post-column hydrolysis, followed by derivatization with *o*-phthaladehyde (OPA) reagent and fluorescence detection, this method is now used routinely for food analysis in the FDA laboratories in the USA. The application to food samples has been elaborated by Krause [3,4] in the USA and by de Kok and co-workers [5–7] in the Netherlands. We have further improved the former method by the incorporation of a rapid and effective solid-phase extraction (SPE) clean-up [5] and optimized postcolumn reaction technology [6] based on the efficient hydrolysis of the N-methylcarbamates on a solid phase, *e.g.*, a strong anion-exchange material or magnesium oxide. The method has ultimately been fully automated by combining automated SPE with on-line gradient elution HPLC analysis and data processing [7].

After the occasional detection of some individual carbamates in ground and river water samples, drinking water laboratories in the Netherlands showed increased interest in the possible application of our method for crop samples to surface water samples, after some necessary adaptations. This prompted us to investigate various water sample preparation techniques for the extraction and preconcentration of N-methylcarbamates in water.

HPLC methods for N-methylcarbamates are now generally preferred over gas chromatographic (GC) methods, which will not be considered here. For HPLC, no derivatization is required for the thermolabile N-methylcarbamates and the aqueous samples, analysed either directly or after preconcentration, are very compatible with reversed-phase HPLC. It should be noted that in the early 1980s only residue methods for single, or a limited number of, compounds were developed. Aldicarb and its metabolites [8–12] and, to a lesser extent, carbofuran and its metabolites [12,13], carbaryl and its metabolites [14] and oxamyl and its metabolites [15] have been predominantly studied. These methods have in common that sample preparation was performed either by repetitive extraction of 100–1000-ml samples with dichloromethane [8,10,12,15,16] and dissolution of the evaporated extract in the mobile phase solvent or direct injection [9,11,13,14] of large volumes (0.2–5 ml). UV detection at the absorption maxima (190–205 nm) or secondary absorption maxima (220, 247 or 280 nm) was routinely used. The detection limits ranged between 1 and 10 μg/l.

More recently, both direct large-volume aqueous injections [17–22] and off-line [23–25] and on-line [26–31] SPE techniques have gained in popularity. Using these preconcentration methods, improved detection limits have been obtained. Modern UV detectors or the postcolumn reaction detection principle followed by sensitive fluorescence detection [17–21,25–27] have also led to improved detection limits. Finally, real multi-residue methods for up to twelve N-methylcarbamates have been developed for water analysis [16–21] analogous to the approach for crop sample analysis [3–7].

Notwithstanding these improvements, several shortcomings still exist. The most studied water types are ground, well, pond and drinking waters. Heavily polluted river or surface water samples have hardly been investigated. Method detection limits have decreased to the 0.1–1.0 μg/l range, but owing to the stringent European Community (EC) Directive imposing a tolerance level for all pesticides of 0.1 μg/l, a further increase in sensitivity is still required.

Marvin and co-workers [28,29] reported determination limits between 0.01 and 0.07 μg/l using on-line preconcentration on 3 cm × 4.6 mm I.D. columns. Samples of 100 ml of drinking water could be concentrated for the determination of a group of eleven pesticides, including four N-methylcarbamates (aminocarb, propoxur, carbaryl and carbofuran). The same group [30] developed an advanced, automated SPE method with disposable C_{18} SPE cartridges, using a Waters Millilab Work-

station for the analysis of several tap and surface water samples. Determination limits for propoxur, carbofuran and carbaryl were 0.13, 0.14 and 0.02 μg/l, respectively. In a recent study, Marvin *et al.* [31] applied their on-line preconcentration method to the relatively more polar N-methylcarbamates aldicarb, aldicarb sulphoxide and aldicarb sulphone. Instead of 100 ml, now only 10 ml could be preconcentrated, because greater sample volumes resulted not only in the loss of the polar aldicarb metabolites due to breakthrough, but also gave a poorer separation of these two early eluting analytes. The determination limits that could be obtained for these carbamates were correspondingly higher, namely 7–11 μg/l.

Both McDonald *et al.* [19] and Dong *et al.* [20] have evaluated a promising multipesticide method based on direct aqueous injections with determination limits down to 0.2 μg/l. However, only distilled and well water, respectively, were analysed. The same principle was used by Edgell *et al.* [21] in a collaborative study on the determination of ten carbamates in finished drinking water with reported estimated detection limits of 0.5–4.0 μg/l.

The aim of this study was to develop a considerably extended multi-residue method for virtually all N-methylcarbamates and to include the important sulphoxide and sulphone metabolites of aldicarb, methiocarb, ethiofencarb, butocarboxim and thiofanox. The method should be able to detect the analytes at levels which are a factor 3–5 below the EC tolerance limit of 0.1 μg/l, and it should be applicable to heavily polluted water samples. This has been achieved by combining SPE of water samples with HPLC separation of the carbamates and fluorescence detection after solid-phase-catalysed hydrolysis and derivatization of methylamine with OPA reagent.

EXPERIMENTAL

Chemicals

HPLC-grade acetonitrile and dichloromethane were purchased from Rathburn (Walkerburn, UK) and water was purified with an ElgaStat UHQ water-purification system (Elga, High Wycombe, UK). *o*-Phthalaldehyde (OPA), 2-mercaptoethanol and disodium tetraborate (anhydrous) were obtained from Merck (Darmstadt, Germany).

OPA reagent was prepared by dissolving 2.0 g of disodium tetraborate in *ca.* 500 ml of purified water in a 1-l volumetric flask, adding 250 mg of OPA (dissolved in 1 ml of acetonitrile) and 0.1 ml of 2-mercaptoethanol and diluting to volume with water. The OPA reagent solution and the HPLC mobile phase solvents were degassed under vacuum prior to use.

Carbamate pesticide and metabolite standards were supplied by Promochem (Wesel, Germany) or by the Environmental Protection Agency Repository (Research Triangle Park, NC, USA). Stock solutions (1 mg/ml) were prepared by dissolving *ca.* 10 mg of standard in a suitable volume of dichloromethane. Standard mixtures were prepared by transferring 100 μl of standard solutions, by means of an injection syringe, into a 100-ml volumetric flask and diluting to volume with dichloromethane. The standard solutions are kept in a freezer at −18°C, where they are stable for at least 1 year. For fortification studies, an appropriate volume (10–100 μl) of the standard mixture in dichloromethane was allowed to evaporate in air and the residue was dissolved in blank surface water samples.

Apparatus

Chromatographic separations were effected with a Hewlett-Packard HP 1050 pumping system using a ternary gradient, a variable-volume injector (with a 100-μl loop), a temperature-controlled analytical column compartment (35°C), a Model 7910 (reactor) column oven (Jones Chromatography, Little, CO, USA), a Hewlett-Packard HP 1050 isocratic reagent-delivery pump provided with a special low-pressure pulse damper (Free University, Amsterdam, Netherlands) for postcolumn reagent delivery, a vortex mixing tee-piece (Kratos, Ramsey, NJ, USA) and a Hewlett-Packard HP 1046A double monochromator fluorescence detector.

Analytical separations were performed on a Merck LiChroCART 250 × 4.0 mm I.D. cartridge column packed with Supersphere RP-8 (4 μm) from Merck.

The postcolumn carbamate hydrolysis column (50 × 4.0 mm I.D.) was packed in our laboratory [6] with Aminex A-27 (15 μm) from Bio-Rad Labs. (Richmond, CA, USA) and kept at a reaction temperature of 120–140°C. The optimum hydrolysis efficiency was obtained when the peak height of

methomyl was as high as that of oxamyl.

After the catalytic hydrolysis reactor, OPA reagent was added to the column effluent at a flow-rate of 0.1 ml/min. The methylamine reacted with the OPA reagent in a 20 cm × 0.12 mm I.D. PTFE capillary connecting the vortex tee-piece with the fluorescence detector inlet. No extra precautions such as cooling the solvent stream prior to fluorescence detection were necessary. The excitation and emission wavelengths were 340 and 445 nm, respectively. The monochromator slit widths were 20 and 15 nm, respectively. It should be noted that with fluorescence detectors from different manufacturers, depending on the flow cell construction and volume and/or the detector outlet capillary length and inner diameter, a back-pressure regulator (*ca.* 10 bar) may be required to prevent boiling of the mobile phase.

Ternary gradient elution runs were as follows. The mobile phase solvents were (A) acetonitrile–water (20:80), (B) methanol–water (20:80) and (C) Acetonitrile–water (60:40) with the following conditions:

Gradient run time (min)	A (%)	B (%)	C (%)
0	65	35	0
5	65	35	0
25	0	0	100
30	0	0	100
32	65	35	0
40	65	35	0

The mobile phase flow-rate was 0.75 ml/min.

Water sample preparation

Water samples were collected from the rivers Rhine and Meuse and, for fortification studies, from the Dutch lake IJsselmeer. In order to prevent degradation of some of the more labile carbamates, the water samples should be conserved [21], *e.g.*, by adding glacial acetic acid to obtain a pH of 3. Samples were stored in a refrigerator (4°C). Filtration of the water samples prior to SPE is not required, provided that the water is allowed to settle.

Liquid–liquid extraction. A 250-ml volume of surface water sample was extracted with three separate 100-ml portions of dichloromethane using a separating funnel and vigorous shaking. The organic phases were combined and concentrated in a rotary evaporator under vacuum to *ca.* 5 ml, then transferred into a centrifuge tube. The extract was evaporated to dryness with a gentle stream of nitrogen and the residue was taken up in 1 ml of distilled water.

Liquid–solid extraction. Bond-Elut SPE cartridges containing 500 mg of adsorbent were obtained from Varian/Analytichem (Harbor City, CA, USA). Three different phases were used: C_8-, C_{18}- and low-carbon C_{18}/OH-bonded silica (particle size 40 μm). SPE experiments were executed by means of a Varian/Analytichem Vac-Elut system, applying a vacuum of 15 kPa. The SPE columns were attached to the vacuum manifold and 75-ml reservoirs were placed on top of the SPE cartridges. The cartridges were conditioned by passing 2 ml of acetonitrile followed by 3 ml of water. Then 50 ml of water sample were passed through the cartridge, which was washed with an extra 3 ml of water. When the water level just reached the top of the column packing, 2 ml of acetonitrile were applied to elute the N-methylcarbamates in a calibrated centrifuge tube, to which 10 μl of an internal standard solution (1 μg/ml landrin in dichloromethane) had already been transferred. The extract was evaporated with nitrogen until *ca.* 200 μl of residual water were left. The extract was made up to 1.0 ml with distilled water.

HPLC analysis

From the final 1-ml SPE extract, 100 μl were injected into the HPLC system. The carbamate concentrations were calculated via the internal standard method. Peak areas of carbamates relative to the peak area of landrin were calculated for both sample extracts and standard mixtures, each containing the same absolute amount of internal standard. Data acquisition and processing were performed via a Hewlett-Packard Chem Station. The fluorescence detector response was linear for injected amounts of 0.1–100 ng for all carbamates studied, with correlation coefficients of between 0.995 and 1.000.

RESULTS AND DISCUSSION

HPLC analysis

Various workers [7,17,20,21] have shown that a multi-pesticide mixture of nine to twelve N-methyl-

carbamates can be separated using a binary gradient of water with methanol or acetonitrile; McDonald *et al.* [19] further improved the critical resolution between the early eluting aldicarb sulphoxide, aldicarb sulphone, oxamyl and methomyl by applying a more complex ternary water–methanol–acetonitrile gradient. Our task however, was, to separate a mixture of 34 compounds including the sulphoxide and sulphone metabolites of aldicarb, butocarboxim, ethiofencarb, methiocarb and thiofanox, and also 3-hydroxy- and 3-ketocarbofuran. These metabolites are relatively polar and emerge in the front part of the chromatogram. With real water samples interferences mostly show up in this region. Therefore, we further optimized the reversed-phase HPLC separation using a linear water–methanol–acetonitrile gradient with an initial isocratic part of 5 min. The relative retention times of all analytes are presented in Table I. Six pairs of carbamates remain unresolved on Supersphere C_8-bonded silica. Studies on stationary phases with different selectivities, which are especially important for confirmatory purposes, are in progress.

In Fig. 1, the HPLC of a standard mixture of twelve N-methylcarbamates and ten of the sulphoxide and sulphone metabolites is shown. The separation time is less than 30 min. The additional equilibration at the initial mobile phase composition results in a total analysis time of 40 min. The N-methylcarbamates are detected via postcolumn reaction detection based on the hydrolysis of N-methylcarbamates to methylamine, which is reacted with OPA reagent to form a fluorescent isoindole. This derivative can be detected very selectively and sensitively. Detection limits calculated for a signal-to-noise ratio 3:1 are, on average, 100 pg, as can also be seen from Fig. 1.

TABLE I

RETENTION TIMES OF TWENTY N-METHYLCARBAMATE PESTICIDES AND TWELVE METABOLITES IN THE REVERSED-PHASE HPLC SYSTEM SUPERSPHERE RP-8 (4 μm) WITH AN ACETONITRILE–METHANOL–WATER GRADIENT

See Experimental for further details.

Peak No.	Carbamate/metabolite	Retention time (min)
1	Butocarboxim sulphoxide	5.90
2	Aldicarb sulphoxide	6.28
3	Butocarboxim sulphone	7.38
4	Aldicarb sulphone	7.85
5	Oxamyl	8.85
6	Methomyl	10.67
7	Ethiofencarb sulphoxide	12.76
8	Thiofanox sulphoxide	13.27
9	Ethiofencarb sulphone	13.81
	3-Hydroxycarbofuran	14.17
10	Methiocarb sulphoxide	14.86
	Tranid	15.00
	Dioxacarb	15.49
11	Thiofanox sulphone	15.63
12	Methiocarb sulphone	17.51
13	Butocarboxim	18.27
	3-Ketocarbofuran	18.85
14	Aldicarb	18.97
	Cloethocarb	21.15
15	Propoxur	21.47
	Bendiocarb	21.62
16	Carbofuran	21.75
17	Carbaryl	22.82
18	Ethiofencarb	23.27
	Thiofanox	23.46
	Isoprocarb	24.35
19	Landrin	24.35
20	Carbanolate	24.90
21	Methiocarb	26.49
	Fenobucarb	26.57
22	Promecarb	27.41
	Bufencarb	32.15

Catalytic solid-phase hydrolysis

Postcolumn hydrolysis of the N-methylcarbamates is usually performed by the addition of NaOH solution to the HPLC column effluent by means of a reagent pump. In order to simplify the postcolumn reaction, McGarvey [32] combined a KOH hydrolysis with the OPA reaction in a one-stage reaction, thereby eliminating one reagent pump. In spite of this elegant method and its potential advantages, applications to real sample analysis were not shown. Therefore, this approach may not have gained widespread acceptance.

In 1983, Nondek and co-workers [33,34] proposed the use of a solid-phase catalyst to replace the NaOH hydrolysis. Efficient hydrolysis was shown for six carbamates on Aminex-28, a strong anion exchanger. This principle was also adopted by She *et al.* [27] for the determination of carbaryl and by Jansen *et al.* [35], who miniaturized the postcolumn system for the narrow-bore HPLC of four N-methylcarbamates. Unfortunately, only brief applica-

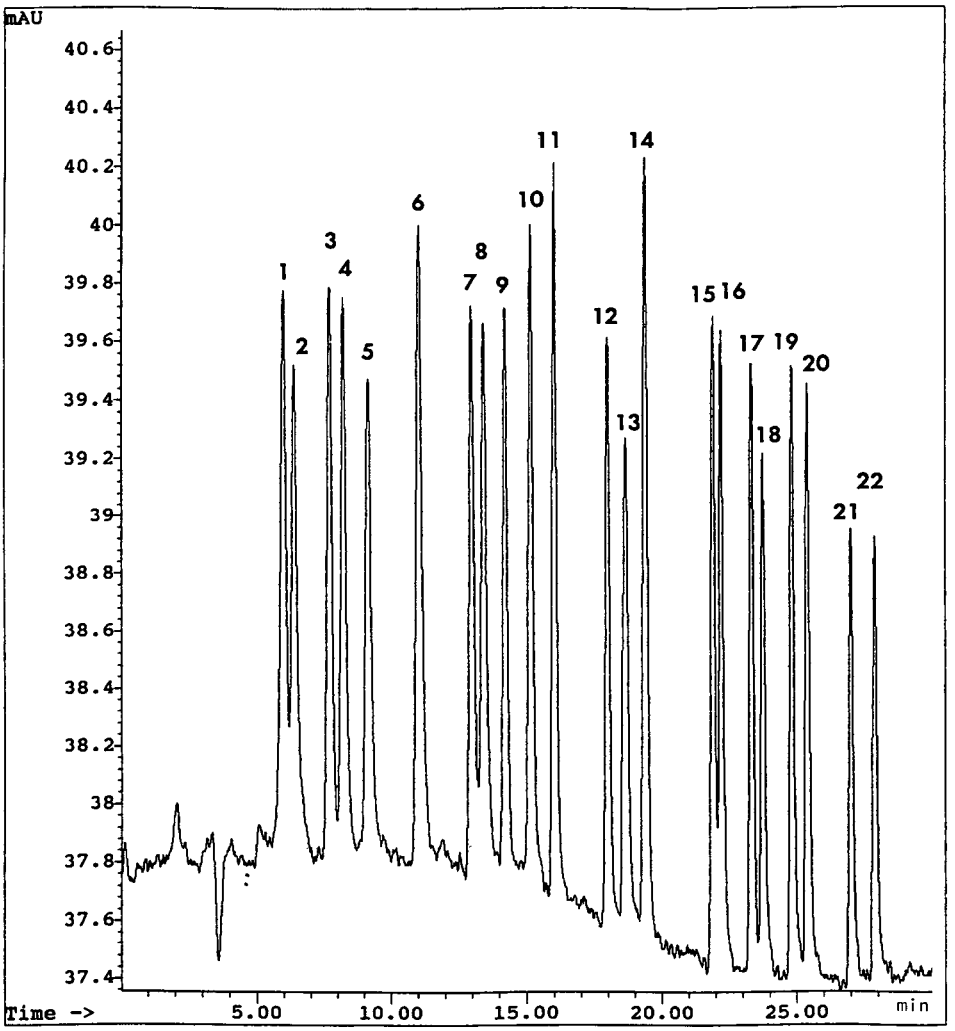

Fig. 1. HPLC of a standard mixture of twelve N-methylcarbamates and ten metabolites using Supersphere RP-8 (4 μm) with an acetonitrile–methanol–water gradient. Injected amounts: 1.0 ng of each carbamate. Fluorescence detection: excitation, 340 nm; emission, 445 nm. Peak numbers correspond to those in Table I. For further details, see Experimental.

tions for the analysis of water samples were described by these workers, which has hampered wider use by others. In 1990, de Kok *et al.* [6] examined various basic solid-phase materials and discovered that, apart from the strong anion-exchange material Aminex-27, the inexpensive, general-purpose magnesium oxide (MgO) has very favourable catalytic characteristics for the hydrolysis of N-methylcarbamates. The postcolumn solid-phase hydrolysis could be extended to include the whole group of more than 30 compounds tested [6]. In practice, the only problem with MgO is the relatively rapid blockage of the hydrolysis column due to the wide range of particle sizes from 100 μm down to 5 μm and the presence of fines. In routine crop analysis, the solid-phase hydrolysis principle has now been in use for more than four years in our laboratory [7], using the anion exchanger Aminex A-27, which has a narrow particle size range (15 ± 2 μm).

The major advantage of solid-phase hydrolysis compared with NaOH solution hydrolysis is the omission of an extra reagent pump, which means that no dilution of the HPLC column effluent takes place, thereby avoiding extra band broadening and retaining optimum resolution and peak sensitivity. Eliminating the NaOH hydrolysis also prevents unnecessary problems such as the occasional leaking of the reagent pump seals or blockage of the hydrolysis reaction capillary due to the build-up of crystallized NaOH reagent. In addition, daily preparation of NaOH reagent has become redundant. The lifetime of a well packed reactor column can be as long as 6 months, because the reaction is purely catalytic, which means that the solid phase is not consumed. Although ion exchangers are known for their incompatibility with drastic solvent changes, we have shown in a recent study [7] that gradient elution may be used without any problems at the prevalent reactor temperature of 120–140°C. Special care is required, however, if one changes to a very low flow-rate (0.05 ml/min), *e.g.*, overnight, to save solvent. The reactor column should first be allowed to cool nearly to room temperature, otherwise the ion-exchange resin will be deformed by the high temperature and blockage of the reactor column will occur.

Water sample analysis

Various research groups [17,19–21] use direct injection of large volumes of aqueous samples in their multi-residue methods for N-methylcarbamates. The AOAC recently adopted this technique for official first action [21]. The principle of large-volume injection is based on the on-column concentration of the analytes on an apolar stationary phase, which are injected dissolved in a purely aqueous phase. Subsequent gradient elution allows the normal separation of the mixture of analytes. Low determination limits in the range 0.2–4 μg/l can be obtained, especially in combination with sensitive postcolumn derivatization and fluorescence detection. Sample clean-up, other than filtration, is not required owing to the high selectivity of the HPLC detection system, and therefore virtually no recovery losses can occur. However, large injection volumes (> 500 μl) often broaden peaks and reduce the resolution, particularly for the early eluting peaks. Matrix peaks typically show up in the same part of the chromatogram, that is, matrix effects cannot be totally excluded.

In initial experiments, we also studied direct large-volume injection of surface water samples fortified with N-methylcarbamates. Volumes of 500 μl appeared to be the practical limit for good resolution of the polar sulphoxide and sulphone metabolites of butocarboxim and aldicarb, and therefore the ultimate determination limits on average were 0.2 μg/l. Keeping the EC tolerance limit (0.1 μg/l) in mind, further research had to be executed to achieve our aim of determination limits in the 0.02–0.03 μg/l range.

Liquid–liquid extraction

In the interest of efficiency and cost effectiveness in processing large numbers of environmental samples, it is highly desirable to determine as many pesticides as possible using a single extract, from which aliquots can be taken for subsequent analyses via GC, GC–mass spectrometry (MS), LC or LC–MS. For water samples, dichloromethane is widely accepted as an extraction solvent [36]. Typically, 1 l of water is extracted, the solvent evaporated and the residue dissolved in a small volume of a suitable solvent before chromatographic analysis. In our laboratory, crop sample analysis is performed according to Luke *et al.*'s method [37], followed by the recently developed, automated SPE clean-up on amino-bonded silica cartridges [7]. For SPE, the sample extract has to be evaporated and redissolved in dichloromethane. Hence, this clean-up procedure and on-line HPLC analysis seemed appropriate to combine with a dichloromethane extraction of water samples. The use of this combined method in initial experiments resulted in very clean chromatograms, even with highly polluted water samples from the rivers Rhine and Meuse. Surprisingly, omitting the SPE step also yielded satisfactory chromatograms, probably because of the selective postcolumn derivatization with fluorescence detection.

On the other hand, recoveries for the more polar carbamates after extraction of spiked surface water samples were insufficient. As a typical indicator of the polar carbamate metabolites, aldicarb sulphoxide was studied. When water volumes of 250–1000 ml were used, the recovery of aldicarb sulphoxide never exceeded 20%. This is caused by the unfa-

vourable partition coefficient in water–dichloromethane [7]. Bellar and Budde [36] also reported a recovery of 19% when a 1-l sample was extracted with three 60-ml portions of dichloromethane.

Higher extraction yields for (relatively) polar compounds can only be obtained by improving the ratio of organic to aqueous phase and/or increasing the number of (repetitive) extractions. As an example, in Table II the recovery results are shown for a 250-ml surface water sample fortified with sixteen N-methylcarbamates and/or metabolites at the 0.1 μg/l level, after three extractions with 100 ml of dichloromethane each. For aldicarb sulphoxide a 62% recovery was obtained. Most recoveries were well above 80% with relative standard deviations (R.S.D.s) below 10%, particularly for the parent compounds. However, the sulphoxides and sulphones were insufficiently extracted. The (extremely) low recoveries and high R.S.D.s for methiocarb sulphone and ethiofencarb sulphone can be ascribed to the fast degradation of these analytes in aqueous solution, which already starts when the samples are waiting for analysis in an autosampler queue. Acidification of the samples to pH 3 partly eliminates the problem. However, the overall result was unacceptable in terms of extraction recoveries, repeatability, sample preparation time and volumes of harzardous organic solvent used. Therefore, we decided to explore the potential of SPE for the concentration of N-methylcarbamates.

Liquid–solid extraction

We first investigated off-line SPE, because it can be applied in every laboratory without the necessity of purchasing expensive column-switching apparatus. In addition, it offers the opportunity to apply on-site field sampling and conservation of the analytes on the solid-phase material, which helps in stabilizing the labile carbamates. Finally, the validated HPLC method for N-methylcarbamate analysis can be used without any modification.

Off-line SPE has been used for the preconcentration of carbofuran [23], aldicarb [25] and carbaryl [24] and their respective metabolites. Sample volumes were 100, 10–20 and 1 ml, respectively, and determination limits were 0.4, 1 and 0.5 μg/l, respectively. Marvin *et al.* [30] concentrated 100-ml drinking water samples and obtained determination limits as low as 0.02–0.14 μg/l for carbaryl, propoxur and carbofuran, but this could only be achieved because of the relatively apolar nature of these three N-methylcarbamates. In their more recent study [31], breakthrough of the more polar aldicarb, aldicarb sulphoxide and aldicarb sulphone occured if water sample volumes exceeded 10 ml. Consequently, higher determination limits (7–11 μg/l) were obtained for these compounds. C_{18}-bonded [23,24,30,31] or C_8-bonded [25,31] silica phases were used in these studies. The sample volumes that can be preconcentrated on these apolar phases without breakthrough of the carbamates are strongly dependent on the polarity of the carbamate or metabolite studied. This means that the polar sulphoxides and sulphones are the critical compounds in SPE method development. We mainly focused our attention on these metabolites.

Most researchers use C_{18}-bonded silica cartridges to preconcentrate medium-polarity pesticides such as triazines and phenylurea herbicides from water. For more polar pesticides such as the N-methylcarbamates and, more so, their metabolites, this sorbent is not necessarily the best choice, as was shown by, *e.g.*, Lesage [25] and Chaput [26] in off-line and on-line SPE, respectively. They obtained significantly higher recoveries for aldicarb sulphoxide on C_8 than on C_{18}-bonded silica. This typical behaviour may be explained by selective sorption of the polar aldicarb sulphoxide on the free silanol groups of the silica, which are more accessible on the C_8 than the C_{18}-bonded material. To confirm these findings, we compared C_8- and C_{18}-bonded silica SPE cartridges from Analytichem that had not previously been tested for N-methylcarbamates.

The results obtained for real surface water samples from the IJsselmeer are given in Table II. The samples were fortified with a standard mixture of thirteen N-methylcarbamates and the ten most polar metabolites at two fortification levels (0.1 and 1.0 μg/l). When a sample volume of 50 ml was passed through the SPE cartridges, the recoveries for C_8- and C_{18}-bonded silica were in the range 34–108% (R.S.D. 0.7–7.5%) and 44–110% (R.S.D. 1.4–11.8%), respectively, at the 1.0 μg/l level. Recoveries at the 0.1 μg/l level were very similar, namely 32–112% and 40–109% for C_8- and C_{18}-bonded silica, respectively. Surprisingly, we did not notice higher recoveries on the C_8 phase for the more polar compounds (the first six peaks in the

TABLE II

AVERAGE PERCENT RECOVERIES [WITH R.S.D. (n = 5) IN PARENTHESES] OF N-METHYLCARBAMATES AND METABOLITES FROM SURFACE WATER, FORTIFIED AT 0.1 and 1.0 μg/l LEVELS, AFTER LIQUID–LIQUID OR SOLID-PHASE EXTRACTION

Carbamate/metabolite	Dichloromethane extraction (250 ml)[a]	Solid-phase extraction (0.1 μg/l) (50 ml)[a]			Solid-phase extraction (1.0 μg/l)			
					50 ml[a]			100 ml[a]
		C_8	C_{18}	C_{18}/OH	C_8	C_{18}	C_{18}/OH	C_{18}/OH
Butocarboxim sulphoxide		32	40	76 (3.9)	34 (6.1)	44 (4.9)	82 (3.9)	70 (4.8)
Aldicarb sulphoxide	62 (9.6)	37	45	83 (6.2)	42 (6.3)	55 (3.3)	93 (1.9)	78 (6.2)
Butocarboxim sulphone		41	46	80 (6.4)	47 (7.2)	49 (3.8)	88 (7.6)	42 (5.8)
Aldicarb sulphone		50	45	83 (6.5)	52 (5.7)	57 (4.1)	91 (8.5)	44 (3.7)
Oxamyl	82 (2.4)	83	83	89 (5.0)	86 (3.6)	87 (4.0)	111 (1.2)	74 (5.7)
Methomyl	91 (4.4)	58	65	81 (2.7)	60 (7.5)	72 (4.6)	90 (3.2)	46 (2.8)
Ethiofencarb sulphoxide	74 (9.4)	107	88	55 (4.8)	108 (3.2)	110 (10.2)	59 (10.3)	76 (4.7)
Thiofanox sulphoxide		110	91	42 (7.3)	105 (2.7)	107 (11.8)	38 (12.7)	54 (7.2)
Ethiofencarb sulphone	66 (24.2)	113	109	98 (4.5)	107 (2.9)	102 (3.1)	106 (2.4)	102 (2.8)
Methiocarb sulphoxide	89 (5.6)	111	106	80 (4.5)	108 (2.5)	101 (4.0)	77 (4.5)	95 (1.6)
Tranid		112	108	99 (3.2)	107 (2.2)	100 (2.1)	106 (1.4)	100 (1.8)
Thiofanox sulphone	91 (4.4)	112	109	102 (5.1)	105 (3.7)	102 (2.8)	106 (1.9)	101 (1.6)
Methiocarb sulphone	26 (26.0)	104	101	100 (2.6)	107 (3-3)	103 (2.6)	106 (1.9)	105 (2.7)
Butocarboxim		106	104	93 (1.0)	97 (1.9)	99 (1.7)	99 (1.4)	100 (1.3)
Aldicarb	69 (8.6)	101	99	95 (1.5)	100 (2.4)	99 (1.8)	103 (1.1)	99 (1.1)
Propoxur	89 (7.9)	102	103	98 (1.4)	102 (2.8)	100 (1.9)	104 (0.9)	100 (2.6)
Carbofuran	89 (7.8)	105	103	98 (1.8)	101 (3.4)	99 (3.2)	101 (0.5)	100 (2.7)
Carbaryl	89 (6.7)	104	104	104 (4.1)	102 (4.1)	102 (3.7)	102 (0.6)	99 (4.2)
Ethiofencarb		93	92	108 (3.1)	98 (3.1)	96 (3.6)	100 (2.7)	95 (3.7)
Carbonolate	82 (9.9)	97	97	89 (1.1)	99 (0.6)	97 (1.8)	100 (0.5)	98 (3.3)
Methiocarb	83 (8.4)	103	109	98 (3.0)	96 (2.9)	96 (3.4)	98 (2.1)	99 (2.7)
Promecarb	88 (5.7)	100	100	100 (2.6)	96 (0.7)	94 (1.4)	96 (2.2)	97 (2.4)
Bufencarb	82 (6.1)	95	99	96 (4.0)	93 (1.7)	87 (2.5)	92 (4.5)	97 (5.2)

[a] The volumes indicate the sample volumes extracted.

chromatogram). Apparently, the typical bonding chemistry and resulting surface characteristics of the C_8- and C_{18}-bonded phases from various manufacturers play an important role, which cannot easily be explained. Despite the incomplete recoveries due to breakthrough, the repeatability was encouraging.

In order to investigate further the influence of the free silanol groups of the solid-phase material on the recovery of polar carbamate metabolites, a new low-carbon C_{18}-bonded silica (C_{18}/OH), specially designed for polar metabolites of pharmaceuticals, was studied. Volumes of 50 ml of fortified water were concentrated on the C_{18}/OH phase. In general, recoveries at both fortification levels (76–111%) were better on this new sorbent than on the C_8- or C_{18}-bonded phases, as can be seen from Table II. The repeatability was very goood, with R.S.D.s of 0.5–8.5% and 1.0–7.3% for the 1.0 and 0.1 μg/l fortification levels, respectively. Only two exceptions

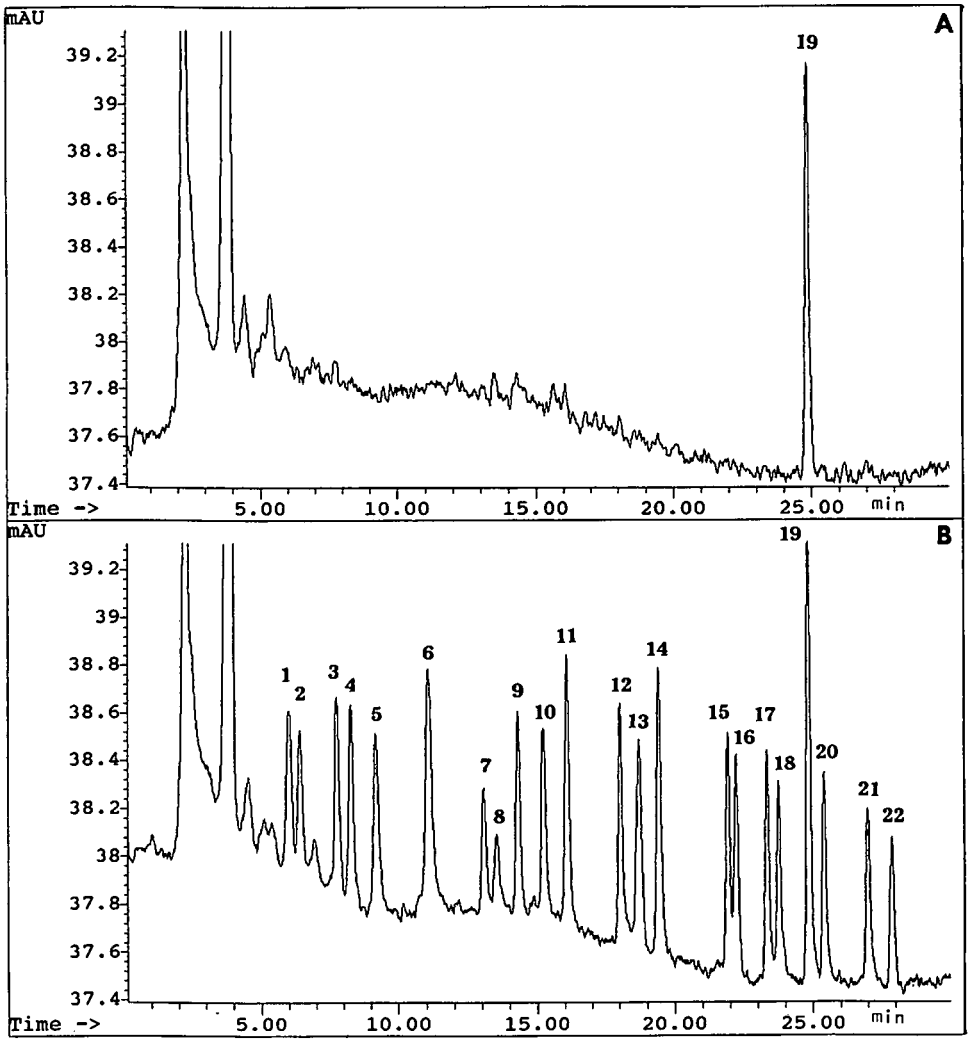

Fig. 2. HPLC of lake IJsselmeer surface water samples after SPE of 50 ml of (A) a blank water sample and (B) a water sample fortified with eleven N-methylcarbamates and ten metabolites at the 0.1 μg/l level on 500 mg C_{18}/OH cartridges. Landrin (peak 19; 1.0 ng injected) was used as an internal standard. In the case of 100% recovery, the injected amount (in 100 μl) of all other carbamates is 0.5 ng. Numbers above the peaks correspond to those given in Table I. For more details, see Experimental, Fig. 1 and text.

were noted, namely ethiofencarb sulphoxide and thiofanox sulphoxide, with recoveries in the 40–60% range with R.S.D.s slightly over 10% at the 1.0 μg/l level. Surprisingly, these two compounds were completely recovered on the other alkyl-bonded phases studied. This deviating behaviour is difficult to explain, because the recoveries were not significantly different at the two fortification levels or when a higher sample volume (100 ml) was concentrated. Increasing the sample volume from 50 to 100 ml resulted in breakthrough and hence, lower recoveries for the first six carbamates; however, the R.S.D.s remained very satisfactory. It is remarkable that the R.S.D.s are very low, irrespective of the sample volumes or the analyte concentrations. Even at the 0.1 μg/l level, which is a factor of *ca.* 3 above the determination limits, the R.S.D.s never exceed 10%.

It can be concluded that the C_{18}/OH phase has a special selectivity for the more polar carbamates oxamyl and methomyl and the sulphoxide and sulphone metabolites of aldicarb and butocarboxim, which can possibly be ascribed to the number and/or accessibility of the free silanol groups on the surface of the sorbent. In this context, one should note that the C_{18}/OH phase with its long alkyl chain concentrates the polar compounds better than does the C_8 phase with its shorter alkyl chain.

A chromatogram of an IJsselmeer surface water sample, fortified with eleven parent N-methylcarbamates and ten metabolites at a concentration of 0.1 μg/l and extracted on a 500-mg C_{18}/OH cartridge, is shown in Fig. 2. Landrin (peak 19), an older carbamate that has been taken out of production, was tentatively used as internal standard, and added after the acetonitrile elution step of the SPE procedure. A chromatogram of the corresponding blank surface water is included in Fig. 2 for comparison. The chromatograms are remarkably free from interfering peaks. The large peak with a retention time of *ca.* 3.5 min elutes well in front of the first carbamate metabolite. It originates from acetic acid, which is added to the water sample for conservation. Acidification (pH 3) of the water samples is important because many N-methylcarbamates and their metabolites are unstable under neutral or basic conditions.

With the optimized procedure, for all the N-methylcabamates listed in Table I, minimum detectable concentrations (signal-to-noise ratio = 3:1) were in the range 0.02–0.03 μg/l. These concentrations correspond to amounts injected into the HPLC system of 100–150 pg. This is surprisingly close to the detection limits of about 100 pg, obtained when standards are injected. Obviously, the clean-up and detection system are highly efficient and selective.

CONCLUSIONS

The multi-residue method described in this paper allows the detection of all twenty N-methylcarbamates and twelve polar metabolites studied in surface water down to the level of 20–30 ng/l using 50 ml of sample. Clean-up and preconcentration on selective C_{18}/OH SPE cartridges is a simple and rapid pretreatment step. The method is superior to conventional liquid–liquid extraction in terms of accuracy, precision and analysis time.

Off-line SPE allows the water samples to be concentrated on the cartridges at the collection site, which facilitates transportation and analyte conservation and is convenient when sophisticated laboratory facilities are not available. The method also lends itself to full automation with commercially available equipment such as the ASPEC (Gilson), as we have shown recently for crop samples [7]. A sample throughput of 36 samples per 24 h can then be achieved. Our current research is aimed at setting up such an automated system for water analysis.

ACKNOWLEDGEMENT

We are grateful to Hewlett-Packard (Waldbronn, Germany) for the loan of the HPLC equipment and computer system.

REFERENCES

1 D. J. Munch, R. L. Graves, R. A. Maxey and T. M. Engel, *Environ. Sci. Technol.*, 24 (1990) 1446–1451.
2 H. A. Moye, S. J. Scherer and P. A. St. John, *Anal. Lett.*, 10 (1977) 1049–1058.
3 R. T. Krause, *J. Assoc. Off. Anal. Chem.*, 68 (1985) 726–733.
4 R. T. Krause, *J. Assoc. Off. Anal. Chem.*, 68 (1985) 734–741.
5 A. de Kok, M. Hiemstra and C. P. Vreeker, *Chromatographia*, 24 (1987) 469–476.
6 A. de Kok, M. Hiemstra and C. P. Vreeker, *J. Chromatogr.*, 507 (1990) 459–472.
7 A. de Kok and M. Hiemstra, *J. Assoc. Off. Anal. Chem.*, (1992) in press.

8 L. H. Wright, M. D. Jackson and R. G. Lewis, *Bull. Environ. Contam. Toxicol.*, 28 (1982) 740–747.
9 C. J. Miles and J. J. Delfino, *J. Chromatogr.*, 299 (1984) 275–280.
10 A. T. Lemley and W.-Z. Zhong, *J. Agric. Food Chem.*, 32 (1984) 714–719.
11 L.Y. Lin and W. T. Cooper, *J. Chromatogr.*, 390 (1987) 285–295.
12 W. P. Cochrane, M. Lanouette and S. Trudeau, *J. Chromatogr.*, 243 (1982) 307–314.
13 P. H. Cramer, A. D. Drinkwine, J. E. Going and A. E. Carey, *J. Chromatogr.*, 235 (1982) 489–500.
14 A. S. Jones, L. A. Jones and F. L. Hastings, *J. Agric. Food Chem.*, 30 (1982) 997–999.
15 J. L. Prince, *J. Agric. Food Chem.*, 32 (1984) 1184–1186.
16 E. Grou, V. Radulescu and A. Csuma, *J. Chromatogr.*, 260 (1983) 502–506.
17 K. M. Hill, R. H. Hollowel and L. A. Dal Cortivo, *Anal. Chem.*, 56 (1984) 2465–2468.
18 C. J. Miles and H. A. Moye, *Chromatographia*, 24 (1987) 628–632.
19 P. D. McDonald, W. P. Leveille, A. E. Sims, W. J. Wildman, V. R. Zener and A. D. Scarchilli, *Advances in Water Analysis and Treatment, Water Quality Technology Conference Proceedings, Philadelphia, PA, 1989*, AWWA, Denver, CO, 1990, pp. 631–649.
20 M. W. Dong, F. L. Vandemark, W. M. Reuter and M. V. Pickering, *Am. Environ. Lab.*, 2 (1990) 14–27.
21 K. W. Edgell, L. A. Biederman and J. E. Longbottom, *J. Assoc. Off. Anal. Chem.*, 74 (1991) 309–317.
22 C. H. Marvin, I. D. Brindle, C. D. Hall and M. Chiba, *J. Chromatogr.*, 555 (1991) 147–154.
23 K. W. Beauchamp, Jr., D. D. W. Liu and E. J. Kikta, Jr., *J. Assoc. Off. Anal. Chem.*, 72 (1989) 845–847.
24 J. R. Strait, G. C. Thornwall and M. Ehrich, *J. Agric. Food Chem.*, 39 (1991) 710–713.
25 S. Lesage, *LC · GC*, 7 (1989) 268 and 271.
26 D. Chaput, *J. Assoc. Off. Anal. Chem.*, 69 (1986) 985–989.
27 L. K. She, U. A. Th. Brinkman and R. W. Frei, *Anal. Lett.*, 17A (1984) 915–931.
28 C. H. Marvin, I. D. Brindle, C. D. Hall and M. Chiba, *J. Chromatogr.*, 503 (1990) 167–176.
29 C. H. Marvin, I. D. Brindle, R. P. Singh, C. D. Hall and M. Chiba, *J. Chromatogr.* 518 (1990) 242–249.
30 C. H. Marvin, I. D. Brindle, C. D. Hall and M. Chiba, *Anal. Chem.*, 62 (1990) 1495–1498.
31 C. H. Marvin, I. D. Brindle, C. D. Hall and M. Chiba, *J. Chromatogr.*, 555 (1991) 147–154.
32 B. D. McGarvey, *J. Chromatogr.*, 481 (1989) 445–451.
33 L. Nondek, R. W. Frei and U. A. Th. Brinkman, *J. Chromatogr.*, 282 (1983) 141–150.
34 L. Nondek, U. A. Th. Brinkman and R. W. Frei, *Anal. Chem.*, 54 (1983) 1466–1470.
35 H. Jansen, U. A. Th. Brinkman and R. W. Frei, *Chromatogrpahia*, 20 (1985) 453–460.
36 T. A. Bellar and W. L. Budde, *Anal. Chem.*, 60 (1988) 2076–2083.
37 M. A. Luke, J. E. Froberg, G. M. Doose and H. T. Masumoto, *J. Assoc. Off. Anal. Chem.*, 64 (1981) 1187–1195.

Journal of Chromatography, 623 (1992) 277–287
Elsevier Science Publishers B.V., Amsterdam

CHROM. 24 457

Study of amphiphilic behaviour of alkylglycoside surfactants using reversed-phase liquid chromatography

M. Lafosse, P. Marinier, B. Joseph and M. Dreux

Laboratoire de Chimie Bioorganique et Analytique (LCBA), URA 499, Université d'Orléans, B.P. 6759, 45067 Orléans Cedex 2 (France)

(First received February 25th, 1992; revised manuscript received June 30th, 1992)

ABSTRACT

Alkylglycosides are biological surfactants used to solubilize membrane proteins. A large series of these compounds (commercial or synthesized) were chromatographed using reversed-phase liquid chromatography to study their amphiphilic properties. The latter were found to depend on the length of the alkyl chain, the nature of the polar head and the bonding nature between the sugar and alkyl chain. A comparison with hexaethylene glycol monoalkyl ethers was made. This chromatographic system with evaporative light-scattering detection allows excellent separations of all the compounds.

INTRODUCTION

Surfactants required for the solubilization and purification of intrinsic membrane proteins showed possess the following properties: high solubilizing power, no denaturation of proteins, optical transparency allowing spectrophotometric detection of purified membrane proteins, chemical purity and easy removal by dialysis necessary for the assay of the protein activity. Among the usual non-ionic surfactants, alkylglycosides are preferred because they have a high critical micelle concentration (CMC) which facilitates their easy removal by dialysis [1,2] and their non-denaturing properties make them very mild surfactants [3,4].

Surfactant properties depend on the nature of the polar head (hydrophilic sugar moiety), the length of the non-polar hydrocarbonaceous chain, the α- and β-anomeric form [3] and the bonding nature between the sugar and alkyl chain. Saito and Tsuchiya [5,6] have shown that octylthioglucoside is superior to octylglucoside and very useful in membrane biochemistry.

These surfactants are often synthesized from the corresponding long-chain alcohols. To produce such compounds on an industrial scale, mixtures of alcohols can be used and purification of the alkylglycosides obtained is difficult because their chromatographic separation in a normal-phase system is very poor, depending on the chain length [4,7]. It was therefore of interest to develop a selective chromatographic method that allows analysis during their synthesis and that resolves a mixture of surfactants according to their non-polar moieties and polar heads. Moreover, a better characterization of the hydrophilic–lipophilic behaviour of these non-ionic surfactants may permit their comparison in order to modify alkyl-bonded silicas and achieve hydrophilic shielding to prevent proteins from being adsorbed while analysing small molecules [8].

In this work we examined these surfactants using reversed-phase liquid chromatography (RPLC). As retention mechanisms of neutral substances in RPLC are principally based on Horváth's solvophobic theory [9], this chromatographic method permits an evaluation of the hydrophobic properties of solutes

Correspondence to: Dr. M. Lafosse, Laboratoire de Chimie Bioorganique et Analytique (LCBA), URA 499, Université d'Orléans, B.P. 6759, 45067 Orléans Cedex 2, France.

0021-9673/92/$05.00

[10–12], which is useful because of the high hydrophobicity of the membrane proteins. The retention behaviour in RPLC can thus reflect the hydrophobic associations of the alkyl chains observed in the CMC that characterizes the properties of a surfactant. In the same manner, Dinten *et al.* [13] used reversed-phase thin-layer chromatography for the determination of lipophilicity values of neutral carriers as liquid membrane components.

EXPERIMENTAL

LC system

Chromatography was carried out using a Spectra-Physics (San Jose, CA, USA) Model 8800 ternary pump, a Rheodyne (Cotati, CA, USA) Model 7125 valve, a Shimadzu CR 6A integrator (Touzart et Matignon, Vitry-sur-Seine, France) and a Model Sedex 45 light-scattering detector (Sedere, Vitry-sur-Seine, France). This detector uses the following principle: the effluent is nebulized by an inert gas and the solvent is vaporized in a warm tube. The non-volatile solutes give a mist of small particles which scatter the light. Scattered light is measured at 120° to the collimated light source. This permits a universal detection method for solid and liquid solutes with or without a chromophore and is compatible with gradient elution [14].

Columns

The columns used were LiChrospher 100 RP-8 (125 × 4 mm I.D.), LiChrospher 100 RP-18 (125 × 4 mm I.D.) and LiChrospher 100 RP-18 end-capped (125 × 4 mm I.D.), purchased from Merck (Nogent-sur-Marne, France), Zorbax octyl (150 × 4.6 mm I.D.) and Zorbax phenyl (150 × 4.6 mm I.D.), purchased from DuPont (Wilmington, DE, USA) and Asahipak ODP-50 (150 × 6 mm I.D.), purchased from Asahi Chemical Industry (Kawasaki, Japan).

Reagents

The mobile phase solvents used were reversed-phase HPLC-grade methanol (Prolabo, Paris, France), HPLC-grade acetonitrile (Merck) and distilled water (Cooperation Pharmaceutique Française, Melun, France). 1-O-Hexyl-β-D-glucopyranoside (C6Glu), 1-O-octyl-β-D-glucopyranoside (C8Glu), 1-O-decyl-β-D-glucopyranoside (C10Glu), 1-O-dodecyl-β-D-glucopyranoside (C12Glu), 1-O-decyl-β-D-maltoside (C10Mal), hexaethylene glycol monodecyl ether (C10E6), hexaethylene glycol monododecyl ether (C12E6), hexaethylene glycol monotetradecyl ether (C14E6) (Fluka, Mulhouse, France), 1-O-dodecyl-β-D-maltoside (C12Mal) and 1-S-octyl-β-D-thioglucopyranoside (C8TGlu) (Aldrich, Mulhouse, France) were all used as received.

1-O-Octyl-β-D-galactose (C8Gal), 1-O-octyl-β-D-cellobiose (C8Cell), 1-O-octyl-β-D-thiocellobiose (C8TCell), 1-O-octyl-β-D-fucose (C8Fuc) and 1-O-octyl-β-D-xylose (C8Xyl) were synthesized in the laboratory. The main structures of the alkylglycosides are shown in Fig. 1.

Void volume (V_0) determination

A knowledge of V_0 is required for the determination of capacity factors, k'. Linearization of the retention data was obtained using a homologous series [15,16] (*e.g.*, alkylglycosides or hexaethylene glycol monoalkyl ethers) with the following equation [17]:

$$V_0 = \frac{V_3 V_1 - V_2^2}{V_3 + V_1 - 2V_2}$$

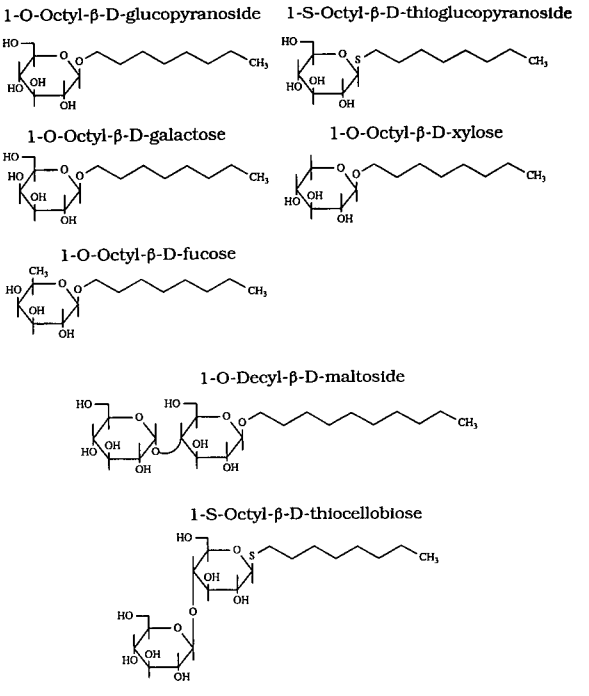

Fig. 1. Main structures of the various alkylglycosides.

where V_1, V_2 and V_3 are the retention volumes of three consecutive homologous surfactants. The value of V_0 obtained was slightly higher than that found when sodium nitrate, fructose or glucose was used as the void volume marker.

RESULTS AND DISCUSSION

In order to elucidate the amphiphilic properties of surfactants, allowing solubilization of highly hydrophobic membrane proteins, the chromatographic behaviour of various alkylglycosides having different alkyl chains and polar heads was investigated. Hexaethylene glycol monoalkyl ethers (RE6) were also tested as these non-ionic surfactants have been widely used for the solubilization of membrane proteins. They are extremely difficult to separate from isolated proteins because of their low CMC and high affinities for membrane proteins [1]. In addition, the number of oxygen atoms in their polar heads is similar to that of alkylglycosides with only one glycosylic group and their hydrophylic–lipophilic balance (HLB) is nearly identical (see Table I).

Influence of polar and non-polar moieties of surfactants on retention

In Fig. 2, the logarithm of the measured capacity factor is plotted against the carbon number of the alkyl chain of alkylglycosides (RGlu), alkylmaltosides (RMal) and RE6 surfactants.

TABLE I

HYDROPHILIC-LIPOPHILIC BALANCE (HLB) AND CRITICAL MICELLE CONCENTRATION (CMC) OF SURFACTANTS

Solute[a]	HLB[b]	CMC (mM)	Ref.
C6Glu	13.6	–	
C8Glu	12.3	25	30
C10Glu	11.2	2.2	4
C12Glu	10.3	0.19	4
C10Mal	14.1	–	
C12Mal	13.4	0.16	4
C10E6	12.9	0.92	31
C12E6	12.0	0.082	31
C14E6	11.3	0.0104	31

[a] For abbreviations, see Experimental.
[b] HLB: weight % polar head / 5.

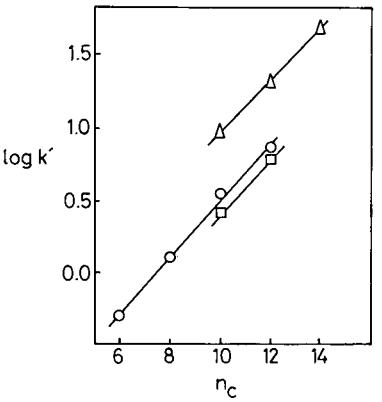

Fig. 2. Experimental plot illustrating the relationship between log k' and carbon number, n_c, of non-ionic surfactants in methanol–water (70:30) on a LiChrospher RP-8 column. Solutes: △ = RE6, ○ = RGlu; □ = RMal.

For a given alkyl chain (C_{10} or C_{12}), the order of retention is RMal < RGlu ≪ RE6, showing the effect of the polar head. For a given mobile phase, the retention of homologues increases with increasing carbon number, n_c, as follows [18]:

$$\log k' = \log \beta + n_c \log \alpha \quad (1)$$

where $\log \beta$ is the specific contribution of the polar moiety to the retention (extrapolation to $n_c = 0$) and $\log \alpha$ is the non-specific contribution of the methylene group (α is the ratio of the capacity factors of two consecutive homologous solutes); α is proportional to the free energy of transfer of a hydrophobic group, methylene, between the mobile and stationary phases [19] and characterizes the solvophobic effect [20].

Table II gives the $\log \alpha$ and $\log \beta$ values with a methanol–water (75:25) mobile phase obtained on various hydrocarbonaceous stationary phases. The selectivity α between two homologous compounds of each series (RGlu, RMal, RE6) is similar on a given stationary phase. This value is smaller on Zorbax phenyl (average value of $\log \alpha$ with three families = 0.119) than on octyl phases (average value of $\log \alpha = 0.171$ on Zorbax C_8 and 0.163 on LiChrospher RP-8). Hence this non-specific contribution is similar with a multi-layer octyl (LiChrospher RP-8) and monolayer octyl (Zorbax C_8) phases. As already noted [20,21], the largest value is obtained on octadecyl phases [average value 0.221 with

a relative standard deviation (R.S.D.) of 4.7% on the seven values] and this value is similar to the means (0.218) reported by Colin *et al.* [22]. These results show that log α does not depend on packing characteristics (specific area, bonding mode, residual silanol groups). This selectivity α depends more on the nature of the hydrocarbonaceous moiety of the stationary phase than on that of the family of solutes for a given mobile phase.

The log β term, a measure of the polar moiety contribution, shows a poor contribution to the retention of glucose and maltose ($n_c = 0$). The average log β values for glucose and maltose are -1.83 (R.S.D. 4%) on the three octadecyl-bonded phases, -1.52 (R.S.D. 9%) on the octyl-bonded phases and -1.3 on Zorbax phenyl. These values determined from eqn. 1 correspond to a retention volume close to the void volume observed on the non-polar bonded phases in the methanol–water mobile phases.

The log β term for the E6 moiety is larger than that for the sugar moiety: the hydrophobic contribution of the polar head is larger with hexaethylene glycol than with sugar.

Table III shows for a given mobile phase (methanol–water, 75:25) the capacity factors of various surfactants on octyl-bonded (LiChrospher RP-8) and octadecyl-bonded phases (LiChrospher RP-18, LiChrospher RP-18 end-capped and Asahipak ODP-50). Octadecyl-bonded phases with end-capped residual silanol groups (LiChrospher) or without silanol groups (Asahipak) involve larger retentions. This effect indicates that the interactions between the sugar moiety of the surfactant and silanol groups are very weak; this is confirmed by the small values of log β (Table II).

Comparison of retention mechanisms

From the results in Table III, a comparison of the separation on a pair of stationary phases j and j' can be made based on the log k'_{ij} *versus* log $k'_{ij'}$ relationship, where k'_{ij} is the capacity factor of the ith solute (alkyl surfactant) in the jth chromatographic system. According to Melander *et al.* [23],

$$\log k'_{ij} = a_{jj'} \log k'_{ij'} + C^t \qquad (2)$$

where r (correlation coefficient) and $a_{jj'}$ (proportionality factor) allow the retention mechanism on the stationary phases to be classified as follows: homoenergetic (the same) if $r > 0.95$ and $0.90 < a < 1.10$, homeoenergetic (similar) if $r > 0.95$ and $a < 0.90$ or $a > 1.10$ and heteroenergetic (different) if $r < 0.95$.

For the column pair with j = LiChrosphr RP-18 end-capped and j' = LiChrospher RP-18, the slope $a_{jj'}$ of log k'_{ij} *vs.* log $k'_{ij'}$ is 0.96 ($r = 0.995$), showing a homoenergetic (the same) mechanism, and the $a_{jj'}$ value for the column pair with j = Asahipak and j' = LiChrospher RP-18 end-capped is 0.99 ($r = 0.995$) and also indicates a homoenergetic mechanism. This illustrates a poor interaction of the hydrophilic moiety of the surfactant with silanol groups of the octadecyl phases.

For the column pair with j = RP-18 and j' = RP-8, the value $a_{jj'}$ is 1.19 ($r = 0.988$), showing a homeoenergetic (similar) mechanism with a larger lipo-

TABLE II

VALUES OF LOG α AND LOG β OF EQN. 1 IN METHANOL–WATER (75:25)

Stationary phase	RGlu		RMal		RE6	
	Log α	Log β	Log α	Log β	Log α	Log β
Zorbax phenyl	0.122	−1.30	0.110	−1.31	0.126	−0.79
Zorbax C_8	0.163	−1.49	0.178	−1.72	0.171	−1.07
LiChrospher RP-8	0.166	−1.43	0.161	−1.45	0.162	−0.92
LiChrospher RP-18	0.231	−1.92	0.209	−1.74	0.206	−1.24
LiChrospher RP-18 end-capped	0.228	−1.82	0.218	−1.77	–	–
Asahipak ODP-50	0.231	−1.82	0.227	−1.89	–	–

TABLE III

VALUES OF CAPACITY FACTORS ON ALKYL-BONDED STATIONARY PHASES IN METHANOL–WATER (75:25)

Solute	k'			
	LiChrospher RP-18	LiChrospher RP-18 end-capped	Asahipak ODP-50	LiChrospher RP-8
C8Glu	0.833	1.075	1.077	0.803
C8Gal	0.808	1.058	0.983	–
C8Xyl	1.183	1.733	1.774	–
C8TGlu	1.033	1.400	1.500	–
C10Glu	2.475	2.950	3.107	1.712
C10Mal	2.233	2.567	2.360	1.492
C10E6	6.642	9.600	8.187	4.576
C12Glu	6.967	7.933	9.011	3.530
C12Mal	5.850	6.992	6.702	3.136
C12E6	17.183	–	–	9.652

philicity (larger k') on the octadecyl-bonded phase owing to the alkyl chain, which is longer than on the octyl phase.

Based on the average capacity factor ($k'_j = \Sigma k_{ij}/n$) of the values of Table III on the octyl- and octadecyl-bonded phases, the order of the "hydrophilic power" of the polar head is Gal > Glu ≫ ThioGlu > Xyl and Mal > Glu ≫ E6. In fact, the selectivity $\alpha_{RE6,RGlu}$ is 2.74 (average of the six values of the selectivities C12E6–C12Glu and C10E6–C10Glu on the four alkyl phases, R.S.D. = 9.7%; see Table IV) and $\alpha_{RGlu,RMal}$ is 1.19 (average of the eight values of the selectivities C12Glu–C12Mal and C10Glu–C10Mal on the four alkyl phases, R.S.D. = 7.6%).

In the same manner, selectivity is more linked to the number of hydroxylic groups ($\alpha_{C8Xyl,C8Glu}$ = 1.56 with R.S.D. = 7.8%) than to their spatial configurations ($\alpha_{C8Gal,C8Glu}$ = 0.95 with R.S.D. = 4%).

The presence of S-bonding decreases the hydrophilicity of the polar head ($\alpha_{C8TGlu,C8Glu}$ = 1.31 with R.S.D. 5.8%) and this can be taken in combination with the CMC [4] of C8TGlu, which is lower (9 mM) than that of the C8Glu (25 mM). In a similar

TABLE IV

SELECTIVITY (α) ON ALKYL-BONDED STATIONARY PHASES IN METHANOL–WATER (75:25)

For capacity factors, see Table III.

Pair	α			
	LiChrospher RP-18	LiChrospher RP-18 end-capped	Asahipak ODP-50	LiChrospher RP-8
C8Xyl–C8Glu	1.420	1.612	1.647	–
C8Gal–C8Glu	0.970	0.984	0.913	–
C8TGlu–C8Glu	1.240	1.302	1.393	–
C10E6–C10Glu	2.684	3.254	2.635	2.673
C12E6–C12Glu	2.466	–	–	2.734
C10Glu–C10Mal	1.108	1.149	1.316	1.147
C12Glu–C12Mal	1.191	1.135	1.344	1.126

manner, the lipophilicity of S-bonding is larger than that of O-bonding from the Rekker constants [24] in the determination of partition coefficient P in octanol–water.

Influence of the nature of the mobile phase

By varying the volume fraction φ of the organic modifier, a nearly linear relationship between log α or log β and φ was usually observed according to [20]

$$\log \alpha = \alpha_0 - \alpha_1 \varphi \quad (3)$$

and

$$\log \beta = \beta_0 - \beta_1 \varphi \quad (4)$$

Fig. 2 shows a comparison of the selectivity, log α, between the neighbouring members of the RGlu series for three non-polar supports in the methanol–water and acetonitrile–water mobile phases. The theory [20] predicts very low values of the coefficient β_1 for a homologous series with strongly polar end groups, so that log β may not vary significantly over a certain range of the composition of mobile phases. For example, a decrease in β_1 with increasing polarity of the end group was found experimentally [18] with almost constant log β for n-alkanols. Consequently, a nearly constant value of log β is not inconsistent with the validity of eqn. 4. Log β for the RGlu series remains relatively constant (R.S.D. *ca.* 4–7%) for a given stationary phase whatever be the volume fraction φ. The average value of log β on a given column is underlined on each curve in Fig. 3. The low values of β indicate that the specific interactions between the polar head and the stationary phase are very weak.

Fig. 3 shows that the similar behaviour of the octyl-bonded phases, observed in the Table I, with a methanol modifier is maintained with any mobile phase. With an acetonitrile modifier there is a small difference between the octyl phases.

Moreover, a comparison of the curves in Fig. 3 shows that for the same volume fraction φ of an organic solvent (*e.g.*, $\varphi = 0.6$), log α values for hydrophobic interactions in an acetonitrile–water mixture are about half those with methanol mixtures. Indeed, the surface tension of the acetonitrile–water mixture is lower than that of the methanol–water mixture [9], decreasing the hydrophobicity of the solute and consequently the retention [10]. Schoenmakers *et al.* [25] has also shown that on a non-polar

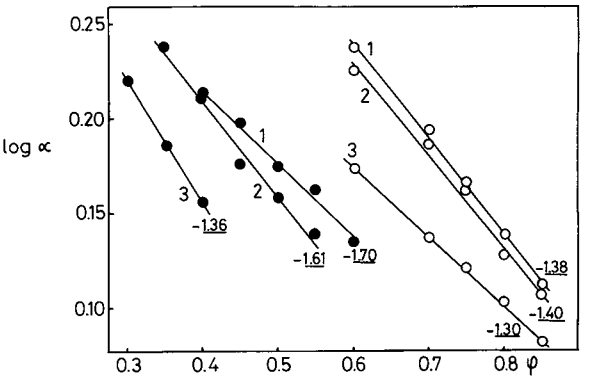

Fig. 3. Log α of alkylglycosides as a function of the volume fraction, φ, of organic modifier in (○) methanol–water and (●) acetonitrile–water mixtures. Columns: 1 = LiChrospher RP-8; 2 = Zorbax C_8; 3 = Zorbax phenyl. The underlined numbers are the average values of log β.

stationary phase for a given composition, acetonitrile is more sorbed, yielding a decrease in the lipophilic interactions of the solute with a non-polar stationary phase and consequently the retention.

Thus the elution of alkylglycosides on Zorbax phenyl requires a higher content in the mobile phase than on octyl-bonded phases. This is even more so when an acetonitrile–water mobile phase is used. In preparative chromatography, an octyl-bonded (or octadecyl-bonded) phase used with a methanol–water mixture would be better as the mobile phase would be richer in organic modifier, thus avoiding the precipitation of large amounts of the injected solute.

Because the members of these homologous series are not numerous, the values of log α and log β are not sufficiently accurate for a detailed study. We therefore investigated the relationship between the capacity factor of each solute and the volume fraction of the organic modifier.

Characterization of the hydrophobicity of the surfactant

Fig. 4 shows the plot of log k' *vs.* φ for different solutes on LiChrospher RP-8 in various binary mobile phases containing methanol–water. The dependence of the capacity factor of the solute on the volume fraction of organic solvent in the mobile phase can be described by a linear relationship [26]:

$$\log k' = a - m\varphi \quad (5)$$

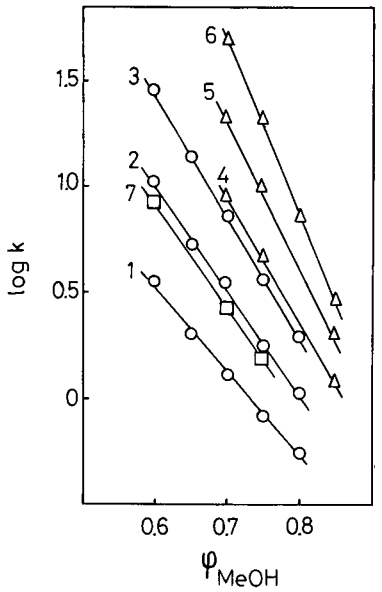

Fig. 4. Experimental plot illustrating the relationship between log k' and the volume fraction, φ, of methanol (MeOH) in the mobile phase on LiChrospher RP-8. Solutes: 1 = C8Glu; 2 = C10Glu; 3 = C12Glu; 4 = C10E6; 5 = C12E6; 6 = C14E6; 7 = C10Mal.

This equation, a simplified form of a quadratic relationship, is often adequate for a limited range of the volume fraction φ [26]. The constants a and m for the three homologous series in each organic modifier and on the three stationary phases are given in Table V. They were derived by linear regression analysis (correlation coefficient $r \geqslant 0.990$).

The intercept value a makes it possible to calculate the extrapolated k' value in pure water and the slope m represents the decrease in retention on increasing the organic modifier content. Jandera [20] has shown that the dependences of the constants a and m on n_c are linear.

The CMC, illustrating the hydrophobicity of a surfactant, is also proportional to n_c, following the linear relationship [27]

$$\log \text{CMC} = An_c + B \quad (6)$$

As the value of m represents the increase in retention as the water content in the mobile phase is increased, it permits an evaluation of the solvophobicity of the solutes. Thus a combination of m and log CMC (Table I) yields Fig. 5a, which illustrates the relationship between the solvophobicity measured by HPLC (m) and the hydrophobicity evaluated by CMC.

In the same manner, Fig. 5b illustrates the relationship between the extrapolated k' value in pure water (a) and CMC. In each instance, two distinct series, one with alkylglycosides and the other with RE6, can be obtained. As in the plot of log k' *vs.* log P of Sabatka *et al.* [11] for another family of compounds, each curve is related to solutes giving hydrogen bonding or not.

TABLE V

VALUES OF CONSTANTS a AND m IN EQN. 5

Solute	LiChrospher RP-8				Zorbax C_8				Zorbax phenyl			
	CH_3OH–water		ACN–water		CH_3OH–water		ACN–water		CH_3OH–water		ACN–water	
	m	a	m	a	m	a	m	a	m	a	m	a
C6Glu	2.793	1.689	–	–	2.826	1.658	–	–	2.171	1.099	3.605	1.020
C8Glu	3.879	2.836	3.127	1.246	3.669	2.590	2.902	1.170	3.040	1.916	4.560	1.743
C10Glu	4.925	3.953	3.952	2.046	4.632	3.625	3.803	1.943	3.691	2.646	5.863	2.564
C12Glu	5.734	4.874	4.734	2.799	5.602	4.673	4.662	2.733	4.430	3.430	7.340	3.477
C10Mal	5.819	4.451	4.690	2.179	4.554	3.524	4.560	2.184	3.822	2.694	5.950	2.425
C12Mal	6.558	5.290	5.255	2.829	5.325	4.422	4.921	2.692	4.517	3.440	7.383	3.296
C10E6	5.819	5.018	4.473	3.028	5.659	4.880	3.776	2.680	4.485	3.824	2.935	2.037
C12E6	6.862	6.121	5.472	3.875	6.550	5.876	4.358	3.330	5.755	5.020	3.232	2.433
C14E6	8.382	7.581	6.384	4.687	7.852	7.198	4.935	3.990	6.803	6.079	3.724	2.965

TABLE VI

REGRESSION CONSTANTS AND CORRELATION COEFFICIENTS OF EXPERIMENTAL PLOTS LOG CMC *vs.* *m* AND LOG CMC *vs.* *a* (SEE FIG. 5)

Mobile phase	Slope	Intercept	*r*	Series	Plot	Relationship
Methanol–water	−1.136	2.845	9.997	RGlu	Fig. 5a	*vs.* *m*
	−0.737	1.111	0.987	RE6 + C12Mal	Fig. 5a	*vs.* *m*
	−0.942	1.050	0.992	RGlu + C12Mal	Fig. 5b	*vs.* *a*
	−0.752	0.657	0.992	RE6	Fig. 5b	*vs.* *a*
Acetonitrile–water	−1.318	2.531	0.999	RGlu	Fig. 5a	*vs.* *m*
	−1.023	1.544	0.999	RE6 + C12Mal	Fig. 5a	*vs.* *m*
	−1.380	0.134	0.999	RGlu + C12Mal	Fig. 5b	*vs.* *a*
	−1.174	0.500	0.999	RE6	Fig. 5b	*vs.* *a*

From the results of the linear regression analysis of these plots (Table VI), C12Mal appears to belong to the RE6 family (Fig. 5a) or the RGlu family (Fig. 5b). This shows that RMal family have a particular behaviour but the lack of CMC data of this series prevents a more precise correlation.

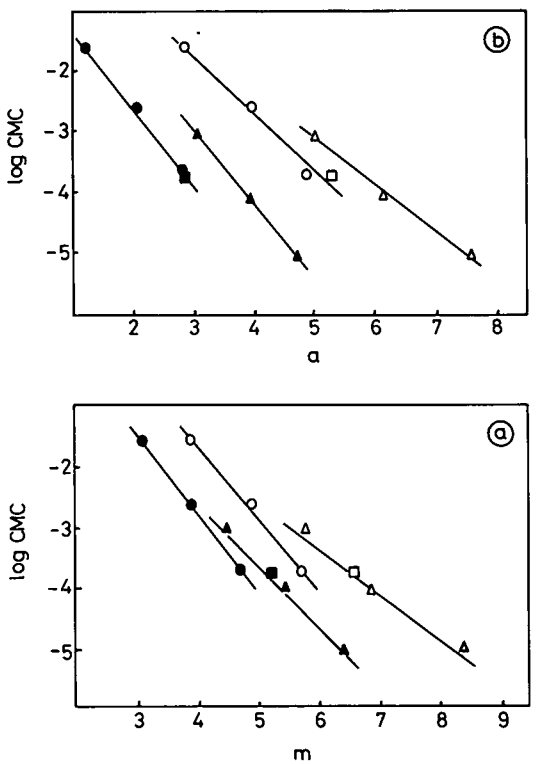

Fig. 5. Correlation between log CMC of surfactant and the slope *m* or the intercept *a* of eqn. 5. Solutes: ▲,△ = RE6; ●,○ = RGlu; ■,□ = RMal. Organic modifier: closed symbols, acetonitrile; open symbols, methanol.

It should be possible to determine the CMC of a new surfactant by its chromatographic behaviour. Fig. 5 shows linear relationships for both organic modifiers. These slopes illustrate a difference in solvophobicity. For a given CMC value, the solvophobicity derived from *m* is larger in methanol–water, corresponding to higher values of the surface tension of the liquid phase in the range of volume fraction studied [9].

Chromatographic separation

As a linear dependence of *a* and *m* on the number of methylene groups n_c, of each solute has been observed, the following relationship [20] between *m* and *a* can be obtained after elimination of n_c:

$$m = q + pa \quad (7)$$

From the values in Table V, plots of *m* *vs.* *a* are shown in Figs. 6 and 7 for both organic modifiers.

As shown in Fig. 6a, a positive correlation ($r = 0.995$) exists between *m* and *a* in methanol–water mixtures. The resulting values of this correlation are 0.93 for *p* and 1.25 for *q* (see eqn. 7). These values are similar to those found by Jandera [28] on Silasorb C_8 with the same mobile phase; they are slightly higher than those obtained by Schoenmakers *et al.* [29] on an RP-18 stationary phase for various solutes without a large alkyl chain.

The correlation observed for all the data points in Fig. 7 is the consequence of small differences between the coefficients *q* in methanol–water. On the other hand, Fig. 6 shows the absence of a

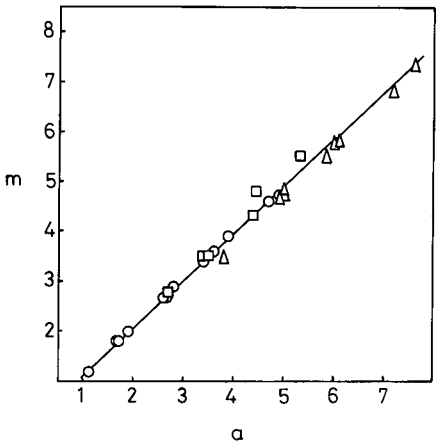

Fig. 6. Correlation between the slope m and the intercept a of eqn. 5 in methanol modifier system. Symbols as in Fig. 5.

TABLE VII

COMPARISON OF THE CONSTANTS q AND p IN EQN. 7 IN ACETONITRILE–WATER MOBILE PHASE FOR VARIOUS HOMOLOGOUS SERIES AND STATIONARY PHASES

Stationary phase	Homologous series	q	p
Zorbax phenyl	RE6	1.180	0.854
Zorbax C_8	RE6	1.407	0.885
LiChrospher RP-8	RE6	0.992	1.152
LiChrospher RP-8	RGlu	1.837	1.035
Zorbax C_8	RGlu	1.595	1.126
Zorbax C_8	RMal	3.010	0.711
LiChrospher RP-8	RMal	2.796	0.869
Zorbax phenyl	RGlu	1.974	1.530
Zorbax phenyl	RMal	1.960	1.645

correlation ($r = 0.65$) with acetonitrile–water. A similar scattered plot was also observed by Schoenmakers *et al.* [29]. According to both plots (Figs. 6 and 7), the nature of the organic modifier significantly improves the difference in the behaviour between these non-ionic surfactants. In fact, the absence of a correlation in Fig. 7 is only apparent; eqn. 7 is theoretically valid only for a given type of homologous surfactant and stationary phase.

The values of q and p were calculated for homologous series and various stationary phases and are listed in Table VII. Except for RGlu and RMal on Zorbax phenyl, the average value of p is 0.95 (R.S.D. = 17%) as in Fig. 6, showing the small difference in the system. In contrast, the constants q differ much more significantly from one another for different homologous series and stationary phases (R.S.D. *ca.* 40%). The difference in q explains the apparent scattering of the plot in Fig. 7.

Fig. 8 illustrates (for alkylglycosides) similar selectivities to those already seen for both the octyl-bonded silicas. In contrast, Fig. 9 shows the influence of the organic modifier on changing the selectivity. In fact, we can observe a better separa-

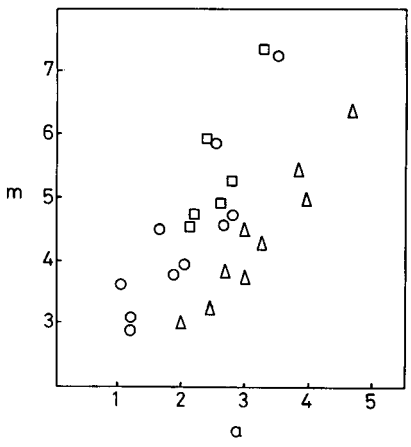

Fig. 7. Correlation between the slope m and the intercept a of eqn. 5 in acetonitrile modifier system. Symbols as in Fig. 5.

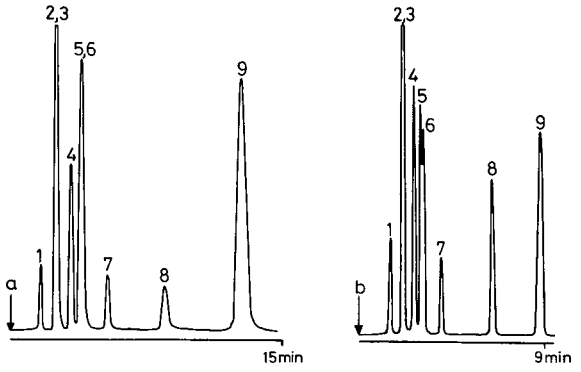

Fig. 8. Chromatograms of alkylglycosides. (a) Column, LiChrospher RP-8; mobile phase, acetonitrile–water (40:60); flow-rate, 1 ml min^{-1}. (b) Column, Zorbax C_8; mobile phase, acetonitrile–water (40:60); flow-rate, 1.5 ml min^{-1}; detector vaporization tube temperature, 45°C. Peaks: 1 = C6Glu; 2 = C8Gal; 3 = C8Glu; 4 = C8TGlu; 5 = C8Xyl; 6 = C10Mal; 7 = C10Glu; 8 = C12Mal; 9 = C12Glu.

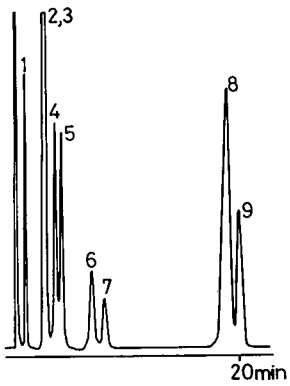

Fig. 9. Chromatogram of alkylglycosides. Column, LiChrospher RP-8; mobile phase, methanol–water (60:40); flow-rate, 1.5 ml min^{-1}. Detector conditions and peaks as in Fig. 8.

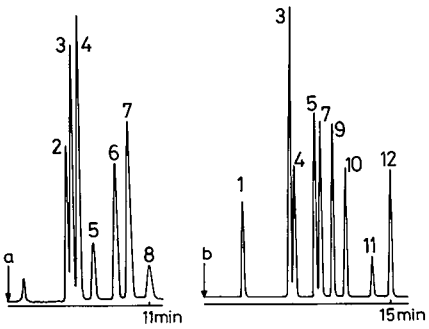

Fig. 10. Chromatograms of alkylglycosides. Column, LiChrospher RP-8. (a) Mobile phase, acetonitrile–water (30:70); flow-rate, 1 ml min^{-1}. (b) Linear gradient elution: acetonitrile–water from 25:75 to 55:45 in 15 min; flow-rate, 1 ml min^{-1}. Detector conditions as in Fig. 8. Peaks: 1 = C6Glu; 2 = C8Cell; 3 = C8Gal; 4 = C8Glu; 5 = C8TGlu; 6 = C8TCell; 7 = C8Xyl; 8 = C8Fuc; 9 = C10Mal; 10 = C10Glu; 11 = C12Mal; 12 = C12Glu.

tion between the C8Xyl–C10Mal pair with methanol–water (60:40) (Fig. 9), and the selectivity between C12Glu and C12Mal is higher with acetonitrile–water on LiChrospher RP-8 (Fig. 8).

On increasing the water content in the mobile phase, the C8Glu–C8Gal pair is separated. In fact, in acetonitrile–water (40:60) these compounds were not separated (t_R = 2.84 and 2.72 min, respectively; Fig. 8a), whereas in acetonitrile–water (30:70) t_R = 6.65 and 5.79, respectively (Fig. 10a). The same influence of increasing the water content on the resolution is illustrated by comparing Figs. 8a and 10b for C10Mal and C8Xyl.

Following Schoenmakers *et al.* [29], the value of p determines the shape of the optimum gradient programme such that all solutes elute with the same peak width. When $0 < p < 1$, *i.e.*, with a methanol modifier, a convex gradient curve will be optimum. On the other hand, acetonitrile–water affords no correlation and therefore optimum gradients are linear. As our apparatus does not permit a convex gradient, an acetonitrile–water mobile phase with a linear gradient was chosen, resulting in good chromatograms with constant peak widths and a good distribution of peaks (Fig. 10). No baseline drift was observed during the gradient elution due to light-scattering detection. On comparing Fig. 10a and b, a higher retention of alkylthioglycosides is noted (see C8Cell and C8TCell and C8Glu and C8TGlu) and the retention increases as the number of hydroxyl group of the head polar decreases (see C8Cell, C8Glu, C8Xyl and C8Fuc).

CONCLUSIONS

Reversed-phase liquid chromatography appears to be a good means of comparing the amphiphilic behaviour of non-ionic surfactants. The behaviour of alkylglycosides depends not only on the length of the alkyl chain, but also the nature of the glycoside and S- or O-bonding. A study by molecular modelling of the spatial configuration of these surfactants in water is in progress to elucidate this behaviour.

REFERENCES

1 C. Baron and T. E. Thompson, *Biochim. Biophys. Acta*, 382 (1975) 276.
2 P. Lundahl and Q. Yang, *J. Chromatogr.*, 544 (1991) 283.
3 P. Rosevear, T. Van Aken, J. Baxter and S. Ferguson-Miller, *Biochemistry*, 19 (1980) 4108.
4 W. J. DeGrip and P. H. M. Bovee-Geurts, *Chem. Phys. Lipids*, 23 (1979) 321.
5 S. Saito and T. Tsuchiya, *Biochem. J.*, 222 (1984) 829.
6 T. Tsuchiya and S. Saito, *J. Biochem.*, 96 (1984) 1593.
7 M. Dreux, M. Lafosse and L. Morin-Allory, presented at the *3rd Meeting, Groupe Français de Bio-Chromatographie, Biochromatography and Molecular Affinity, Dijon, May 1990.*
8 C. Desilets, M. Rounds and F. Regnier, *J. Chromatogr.*, 544 (1991) 25.
9 Cs. Horvath, W. Melander and I. Molnár, *J. Chromatogr.*, 125 (1976) 129.
10 M. T. W. Hearn and B. Greco, *J. Chromatogr.*, 203 (1981) 349.

11 J. J. Sabatka, D. T. Minick, T. K. Shumaker, G. L. Hodgson, Jr. and D. A. Brent, *J. Chromatogr.*, 384 (1987) 349.
12 J. C. Kraak, H. H. Van Rooij and J. L. G. Thus, *J. Chromatogr.*, 352 (1986) 455.
13 O. Dinten, H. Spichiger, N. Chaniotakis, P. Gehrig, B. Rusterholz, W. Morf and W. Simon, *Anal. Chem.*, 63 (1991) 596.
14 S. Brossard, M. Lafosse and M. Dreux, *J. Chromatogr.*, 591 (1992) 149.
15 B. Bidlingmeyer, F. Warren, A. Weston, C. Nugent and P. Froehlich, *J. Chromatogr. Sci.*, 29 (1991) 275.
16 H. Wätzig and S. Ebel, *Chromatographia*, 31 (1991) 544.
17 M. L. Peterson and J. Hirsh, *J. Lipid Res.*, 1 (1959) 132.
18 H. Colin, A. Krstulovic, M. F. Gonnord, G. Guiochon, Z. Yun and P. Jandera, *Chromatographia*, 17 (1983) 9.
19 P. C. Sadek, P. W. Carr and M. J. Ruggio, *Anal. Chem.*, 59 (1987) 1032.
20 P. Jandera, *J. Chromatogr.*, 314 (1984) 13.
21 A. Krstulovic, H. Colin, A. Tchapla and G. Guiochon, *Chromatographia*, 17 (4) (1983) 228.
22 H. Colin, G. Guiochon, Z. Yun, J. C. Diez-Masa and J. Jandera, *J. Chromatogr. Sci.*, 21 (1983) 179.
23 W. Melander, J. Stoveken and Cs. Horváth, *J. Chromatogr.*, 199 (1980) 35.
24 R. F. Rekker, *The Hydrophobic Constant*, Elsevier, Amsterdam, 1977.
25 P. Schoenmakers, H. Billiet and L. de Galan, *J. Chromatogr.*, 282 (1983) 107.
26 L. Snyder, J. Dolan and J. Gant, *J. Chromatogr.*, 165 (1979) 3.
27 K. Shinoda (Editor), *Colloid Surfactants, Some Physicochemical Properties*, Academic Press, New York, 1963.
28 P. Jandera, *J. Chromatogr.*, 352 (1986) 91.
29 P. Schoenmakers, H. Billiet and L. de Galan, *J. Chromatogr.*, 185 (1979) 179.
30 K. Shinoda, T. Yamaguchi and R. Hori, *Bull. Chem. Soc. Jpn.*, 34 (1961) 237.
31 M. J. Schick (Editor), *Non-Ionic Surfactants*, Vol. 1, Marcel Dekker, New York, 1966.

Journal of Chromatography, 623 (1992) 289–295
Elsevier Science Publishers B.V., Amsterdam

CHROM. 24 463

Fast evaluation of the polarity of gas chromatographic columns using the difference in apparent carbon number of linear alkanes and alcohols with the same retention

Gianrico Castello* and Giuseppina D'Amato

Istituto di Chimica Industriale, Università, Corso Europa 30, 16132 Genova (Italy)

(First received February 18th, 1992; revised manuscript received June 30th, 1992)

ABSTRACT

A method for the measurement of the polarity order of gas chromatographic columns (liquid-packed, porous polymer beads, capillary) which does not require reference to standard phases and many probes, is suggested. The method is based on ΔC, *i.e.* the difference in apparent carbon number of linear alkanes and alcohols with the same retention time. The graphical measurement or mathematical calculation of the horizontal distance between the straight lines obtained by plotting the logarithm of the retention of linear alkanes and alcohols as a function of their number of carbon atoms allows the importance of hydrogen bonding with respect to the dispersion forces to be evaluated. All the retention data (adjusted retention times and volume, relative retention, adjusted, net and specific retention volumes) can be used for the calculations. The method is useful for the determination of the change in polarity of mixed or serially linked columns, for the evaluation of the performance of porous polymer beads with respect to liquid stationary phases and for the comparison of packed and bonded-phase capillary columns when polyglycol or polydimethylsiloxane phases are used.

INTRODUCTION

The classification of more than 200 liquid phases currently used in gas chromatography has been attempted using many methods which were found to be more or less adequate depending on the type of liquid phase. The methods cannot be applied with the same confidence to packed or capillary columns, to bonded liquid phases and to various adsorption phases such as carbon black and porous polymers.

An early empirical approach was derived from the classification of many organic compounds by Ewell *et al.* [1] on the basis of the probability of forming hydrogen bonds. The classification of stationary phases and solutes according to Ewell *et al.*'s method was carried out by McNair and Bonelli [2].

Kovats' retention index scheme for quantifying retention [3] has been used as the basis for the methods of Rohrschneider [4] and McReynolds [5] the latter being the most popular classification used by the producers of liquid phases to characterize their products and to establish when two or more phases show a similar behaviour, thus decreasing the stock of columns in the laboratory. The overall polarity of the phases can be obtained by the sum of some of the McReynolds' constants, the most common choice being those obtained with the probes benzene, *n*-butanol, 2-pentanone, 1-nitropropane and pyridine, indicated as $\sum_{MR}^{5}$. Unfortunately, some porous polymer beads react with nitro compounds, and therefore nitromethane and nitropropane cannot be used; with these columns the $\sum_{MR}^{4}$ sum is therefore reported [6]. A method based on the ratios of the retention index (I) values instead of the differ-

Correspondence to: Dr. G. Castello, Instituto di Chimica Industriale, Universita, Corso Europa 300, 16132 Genova, Italy.

0021-9673/92/$05.00

ences has also been suggested [7] and is known as the "retention polarity" method.

The main problem with these procedures is the normalization with respect to squalane as the reference phase and to *n*-alkanes as the reference homologous series. Squalane (temperature limit 100–120°C) could be replaced with the synthetic phase $C_{87}H_{176}$ Apolane [8,9] for high-temperature analysis, whereas the use of linear alkanes has been criticized for polar phases and for porous polymers [10–12] because the difference in the *I* values is due to the change in retention of the reference value (smaller for polar phases and greater for porous polymers) rather than to the change in the retention of the probes. The use of different series of homologues or special probes [13–17] does no solve the problem, which is related to the fundamental concept of the methods which are essentially "relative" with respect to the reference stationary phase and the polarity probes. For the classification of the polarity of capillary columns, a method that in theory may be extended to packed columns was suggested by Chrompack International [18]. The "CP index" requires the determination of the ΔI values with squalane used as the lowest polarity limit and OV-275 cyanosilicone as the highest limit, with increasing complexity as it requires two reference columns.

In the classification of porous polymers negative values were obtained when squalane was used as the reference phase [9,19]. At the low temperatures used for gas analysis, classification methods based on the separation of C_2 hydrocarbons and CO_2 [20,21] and on McReynolds' probes with respect to the reference phase Chromosorb 106 [22], which was found to be the column with the lowest polarity, were suggested.

The selectivity triangle suggested for liquid chromatography by Snyder [23,24] was extended to gas–liquid chromatography by Klee *et al.* [25]. Only three probes (*n*-butanol, 1-nitropropane and 1,4-dioxane) were used, but this trio of solutes seems to be poor for gas chromatographic applications as they plot low-polar phases as SE-30 near to highly polar Carbowaxes. The choice of 1-nitropropane as one of the probes may exaggerate the contribution of the polarizability of the stationary phase, as it has a large dipole moment (3.7 Debye). Other solutes were used [26,27] but the calculation of McReynolds' relative ΔI values with respect of squalane are still necessary for the use of the selectivity triangle. Hepp and Klee [28] applied the same procedure to porous polymers by using as the reference phase graphitized carbon black, considered as representing the basic separation mechanism of the porous polymers and giving retention values due primarily to non-specific dispersive forces.

All the listed "relative" methods require reference phases and many reference probes. An "absolute" method, based only on the retention values of *n*-alkanes, was suggested by Fernandez-Sanchez *et al.* [29] which used Kováts' coefficient, K_c, used by Tarjan *et al.* [30], the ratio between the intercept and the slope of the straight line obtained by plotting the logarithm of the specific retention volume of the *n*-alkanes, V_g, as a function of the number of carbon atoms. Linear alkanes only are necessary as probes, and no reference column is used, but the calculation of V_g values is complex as it requires knowledge of the exact amount of liquid phase in the column and the application of the pressure correction factors of James and Martin [31], only the effect of dispersive forces is taken into account, whereas most of the "polarity" of a liquid phase is often due to hydrogen bonding. Swoboda [32] introduced the concept of the functional retention index, as similar substitution in similar compounds increases the retention index by the same amount for a given stationary phase [33]. Therefore comparison between the behaviour of linear alkanes, reference compounds of the Kováts index system, and of another homologous series may allow the measurement of different interaction parameters with respect to purely dispersive forces.

In a previous paper [34] a method based on the determination of the behaviour of linear-alkanes and alcohols was suggested for the evaluation of the change in polarity when different capillary columns were connected in series. This method can be easily applied to packed and capillary columns and to porous polymers.

EXPERIMENTAL

Analyses of samples of linear alkanes (C_4–C_{12}) and alcohols (C_2–C_8) were carried out at 100, 120, 140 and, when allowed by the temperature limit of the phase, at 160°C on different lengths and diame-

ters of columns filled with various liquid phases (20% concentration) on Chromosorb W, 80–100 mesh; a high concentration of liquid phase was used to allow comparison with McReynolds' data [35] ("m" in Table I), and to minimize interfacial and adsorption effects on the solid support. Phase loadings of 10% were also used for some liquid phases (polysiloxanes, polyglycols) and small effects on the results were observed.

Analyses were also carried out on columns filled with various porous polymer beads (Porapak N, P, Q, R, S, 80–100 mesh) and on wide-bore (60 m × 0.75 mm I.D.) glass capillary columns of different polarity, used alone or serially connected with the flow in the polar to non-polar and in the reversed direction. All the columns used are listed in Table I, and are indicated by "e". Some of the capillary results have been published previously and are given here to show how the proposed method allows a comparison of the behaviour of packed and capillary columns.

Fig. 1 (left) shows the linearity of the logarithm of the retention values of *n*-alkanes and *n*-alcohols on three stationary phases of low, intermediate and

TABLE I

ΔC AND $\sum_{MR}^{5}$ VALUES FOR VARIOUS COLUMNS (PACKED, POLYMER BEADS AND WIDE-BORE CAPILLARY) AND THEIR SELECTIVITY PARAMETERS WITH RESPECT TO BUTANOL, x_b, 1-NITROPROPANE, x_n AND DIOXANE, x_d

Temperature, 120°C.

	Column	Notes[a]	ΔC	$\sum_{MR}^{5}$	$\sum \Delta I_i$	x_b	x_n	x_d
1	Squalane	e	1.48	0	0			
2	Porapak Q	e	1.82	−82		0.276[a]	0.366	0.358
3	Apiezon L	e, m	1.90	143	85	0.260	0.376	0.365
4	Porapak P	e	2.20	530		0.259[a]	0.371	0.371
5	Porapak R	e	2.25	177		0.290[a]	0.404	0.306
6	SE 30	e	2.43	217	161	0.329	0.400	0.273
7	SE 52	e	2.48	334	237	0.304	0.413	0.283
8	Porapak S	e	2.50	44		0.300[a]	0.374	0.326
9	OV 101	e	2.51	229	170	0.335	0.394	0.270
10	DC 200	e	2.52	227	169	0.337	0.390	0.272
11	Capillary SPB-1 (NP)	e, 1	2.55					
12	Porapak N	e	2.79	345		0.305[a]	0.375	0.320
13	DC 550	m	2.89	663	449	0.276	0.421	0.303
14	Dioctyl sebacate	m	3.42	651	454	0.370	0.397	0.233
15	Diisodecyl pthalate	m	3.43	767	521	0.332	0.418	0.249
16	Didecyl pthalate	e, m	3.43	1159	777	0.328	0.412	0.260
17	Dioctyl pthalate	m	3.49	831	562	0.331	0.420	0.249
18	QF 1	e	3.67	1500	976	0.239	0.474	0.287
19	Capillary NP + P	e, 2	4.40					
20	Hallcomid M18	m	4.46	945	596	0.450	0.372	0.178
21	Capillary P + NP	e, 3	5.00					
22	Tricresylphosphate	e, m	5.01	1420	949	0.338	0.394	0.268
23	Neopenthylglycol adipate	m	5.65	1870	1249	0.340	0.370	0.290
24	Neopenthylglicol succinate	e, m	6.14	2115	1425	0.328	0.378	0.294
25	Carbowax 20 M	e, m	6.93	2308	1542	0.348	0.371	0.281
26	Carbowax 6000	e, m	7.28	2320	1554	0.347	0.371	0.281
27	Ethylglycol adipate	m	7.35	2692	1784	0.324	0.367	0.308
28	Diethylglycol adipate	m	7.71	2764	1822	0.331	0.365	0.304
29	Capillary Supelcowax (P)	e, 4	7.75					
30	Carbowax 1000	e	7.85	2587	1726	0.352	0.363	0.286
31	Carbowax 400	e	8.20	2642	1731	0.352	0.363	0.287
32	Diethyl glycol succinate	m	9.89	3430	2271	0.323	0.367	0.310

[a] e = Experimental data; m = McReynolds' data [34]; 1 = non-polar wide-bore capillary (see text); 2,3 = series connection of capillary columns, polar + non-polar or reversed order; 4 = polar wide-bore capillary; a = calculated from Betts [27].

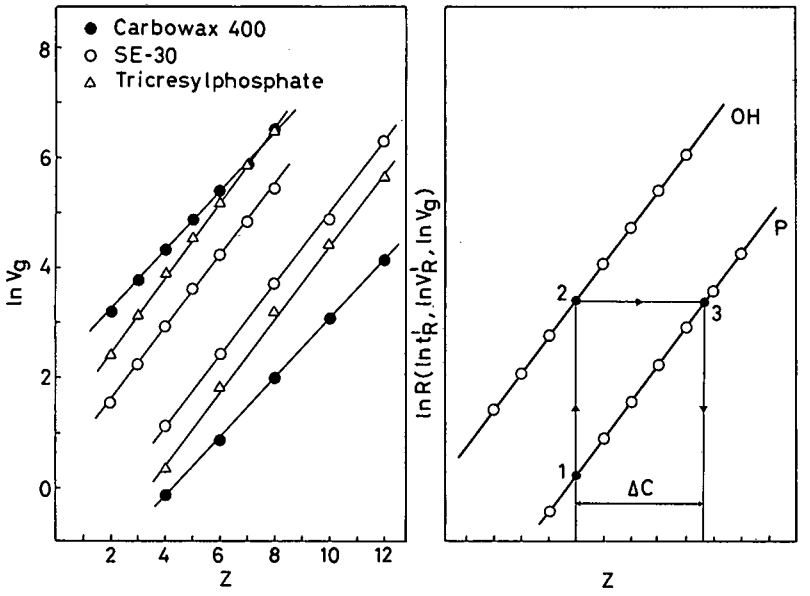

Fig. 1. Left: linear behaviour of the logarithm of the retention values of *n*-alkanes and *n*-alcohols on some columns at 120°C as a function of the number of carbon atoms in the molecule, Z. Right: schematic diagram showing the definition of ΔC values: (1) given linear akane; (2) linear alcohol with the same Z value as 1; (3) hypothetical alkane with the same retention as alcohol 2; ΔC = difference of Z value between alkanes 3 and 1.

high polarity as a function of the number of carbons atoms, Z:

$$\ln R_p = a_p + b_p Z \quad (1)$$

$$\ln R_{OH} = a_{OH} + b_{OH} Z \quad (2)$$

where R_p for paraffins and R_{OH} for alcohols may be adjusted retention times, t'_R, adjusted retention volumes, V'_R, and specific retention volumes, V_g. In fact, the following relationships hold:

$$V'_R = \phi_n t'_R \quad (3)$$

$$V_g = \phi j \frac{273}{TW} t'_R = K t'_R \quad (4)$$

where ϕ is the carrier gas flow-rate and K is a constant that contains the contribution of the compressibility factor of James and Martin, j, the absolute temperature, T, and the weight of stationary phase in the column, W. On a logarithmic scale the constant parts of eqns. 3 and 4 only shift the lines of Fig. 1 in vertical directions, without changing their horizontal distance.

$$\ln V'_R = \ln \phi + \ln t'_R = \text{const} + \ln t'_R \quad (5)$$

$$\ln V'_g = \ln \kappa + t'_R = \text{const} + \ln t'_R \quad (6)$$

The lines for different homologous series on the same column are parallel, as previously found by Hawkes [36], whereas a difference exists between different columns. For the three columns shown in Fig. 1, the values of b_p and b_{OH} are, respectively: Carbowax 400, 0.597 and 0.593; tricresylphosphate, 0.667 and 0.672; SE-30, 0.609 and 0.614. The horizontal distance between the two straight line (ΔC) is therefore a measure of the difference in behaviour of the non-polar and of the polar homologous series. This distance can be measured directly parallel to the abscissa: the experimental values of Fig. 1 (left) are 8.2 for Carbowax 400, 5.0 for tricresylphosphate and 2.4 for SE-30. They can be calculated:

$$a_{OH} - a_p = \Delta a \quad (7)$$

$$(b_{OH} + b_p)/2 = b^0 \quad (8)$$

$$\Delta C = \Delta a / b^0 \quad (9)$$

The averaged b^0 values are used to compensate the slight experimental fluctuations in the slopes due to measurement of the retention times of peaks that may have different shapes due to the different polarities of the samples.

RESULTS AND DISCUSSION

The ΔC value can be considered as the difference of apparent carbon number between linear alkanes and alcohols with the same retention or as the number of methylene groups that should be theoretically added to a linear alkane with Z carbon atoms to obtain an hypothetical alkane with the same retention of a linear alcohol with Z carbon atoms (see Fig. 1, right). The concept of apparent or equivalent carbon number or chain length was used as a means for the classification of the elution characteristics of various substances by James [37] and was replaced by the Kováts' retention index concept [3]. The ΔC values calculated with the above formulas from experimental or literature data are shown in the second columns of Table I. In the same table are also reported the values of the $\sum^5_{MR}$ (sum of the McReynolds constants for benzene, *n*-butanol, 2-pentanone, 1-nitropropane and pyridine), $\sum \Delta I_i$ (sum of the McReynolds' constants for *n*-butanol, 1-nitropropane and 1,4-dioxane, *i.e.* the divisor in Snyder's formula for the calculation of the selectivity parameter, which gives a measure of the importance of hydrogen bonds and dipole interactions with respect to the dispersive forces) and the selectivity parameters x_b, x_n and x_d calculated for the three probes used to obtain the position of each column on the selectivity triangle [23,24].

Fig. 2 compares the $\sum^5_{MR}$ and the ΔC values; the

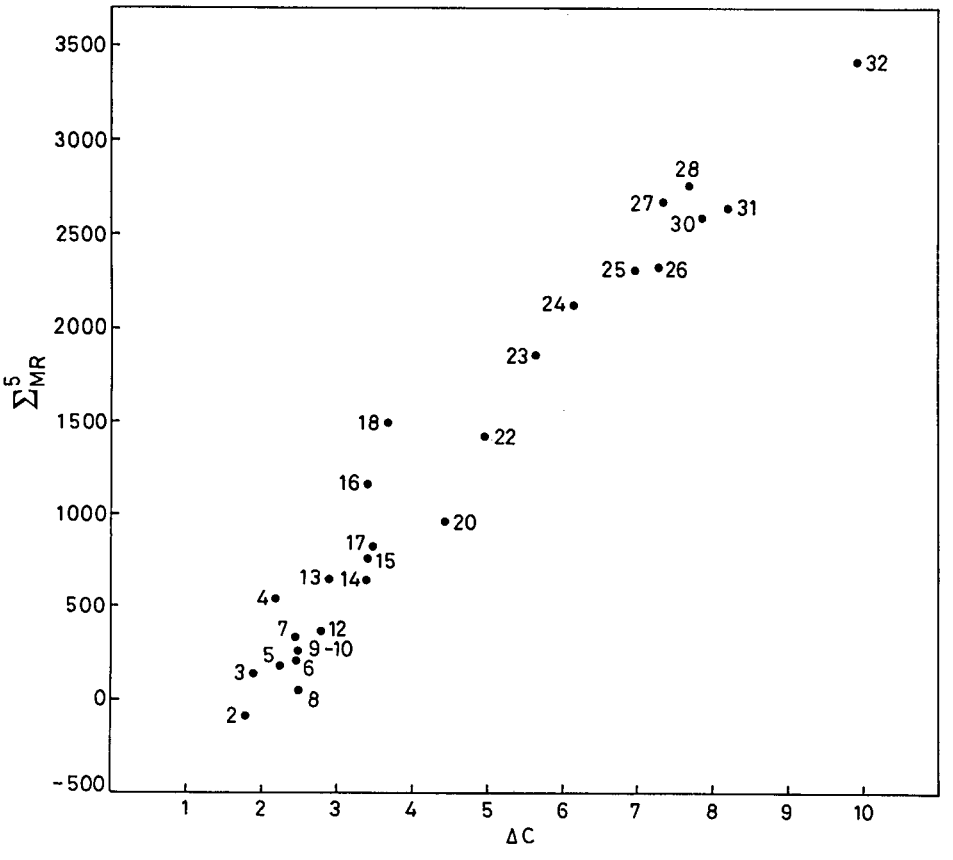

Fig. 2. Values of the sum of McReynold's constants, $\sum^5_{MR}$, for the five probes benzene, *n*-butanol, pentan-2-one, nitropropane and pyridine as a function of the ΔC values at 120°C.

general trend of the polarity measured with the two methods is similar. Some characteristics of the liquid phases are equally expressed by both methods, but some differences are better shown by the ΔC values.

For example, the different polarity of the Carbowaxes with different molecular weights [38] is shown by ΔC, whereas the $\sum_{MR}^{5}$ and the selectivity parameter are fairly similar. The polarity of the capillary column Supelcowax (polyglycol), which cannot be measured with the ΔI values, is easily obtained with the ΔC method and lies between CW6000 and CW1000. Phase 18 (QF 1) shows a very high polarity value with both the methods of McReynolds and Snyder due to the prevailing effect of the polarizability measured by 1-nitropropane. The analysis of pesticides and haloalkanes showed that a behaviour similar to that of esters is more probable. Again, phases 6, 7, 9 and 10 are chemically similar and the difference of $\sum_{MR}^{5}$ values is not justified. The ΔC value of the non-polar SPB-1 capillary column is very similar to that of methylsilicone-packed columns.

The ΔC value shows the changes in polarity that are obained when the flow direction in serially coupled columns is reversed, with the upstream column having a greater influence. This is clearly shown by the ΔC values for the NP + P and P + NP arrangements shown in Table I, compared with the ΔC values for the two separated columns.

A further advantage of the use of ΔC is that this parameter is obtained directly by injecting only two linear alkanes and two linear alcohols with a convenient difference of Z on the column to be classified, without any reference to the standard non-polar phase squalane, which cannot be used at high temperatures or with a bonded-phase capillary column. The use as the non-polar reference phase of methylsilicone-bonded phase columns (SE 30, BP-1) suggested as an alternative to squalane, gives fair results for high-polarity phases (*e.g.* polyglycols or cyanosilicones) but is misleading for other methyl and low phenyl polymers, as methylsilicones show a hydrogen bonding capacity due to the lone pairs of electrons on the oxygen atoms of the Si–O–Si bonds, and their McReynolds constants differ appreciably from zero. This was also confirmed by the greater polarity of silanized versions of Porapak P (Porapak PS) found by Hepp and Klee [28] with respect to the non-silanized version. It is evident that the presence of Si–O–Si bonds with lone electrons pairs on the oxygen atom will increase the polar interactions with respect to the behaviour of simple Porapak P, a pure polystyrene cross-linked polymer, whose possibility of hydrogen bonding with alcohols is only restricted to the limited availability of π electrons from the aromatic rings.

The application of the method to porous polymer columns also gives positive values for all phases, thus avoiding the negative polarity values obtained by applying McReynolds' method with respect to squalane [9,19].

All the retention values (t_R, V_R, V_g) can be used directly and previously tabulated retention data of alkanes and alcohols allow the ΔC values of any column to be obtained. Published values of I can also be used, as the knowledge of the retention times of two *n*-alkanes and the application of the reversed Kovát's equation allow the t'_R or V'_R values to be easily calculated. The ΔC value depends on column temperature, but can be calculated by knowing the slope of the Arrhenius plot (logarithm of the retention as a function of the reciprocal of the absolute column temperature) for alkanes and alcohols on the various phases.

An objection to the generalized use of the ΔC values for the classification of all stationary phases is that only the effects of dispersive forces (measured by the behaviour of the alkanes) and of the hydrogen bonding (alcohols) are considered, and that columns whose action mainly depends on dipole interactions are not correctly classified. The trend in bonded phase capillary column technology is to try to obtain any possible intermediate polarity by the connection of various lengths of polydimethylsiloxane and polyglycol columns, by developing theoretical approaches [39] that allow the prediction of retention times in serially linked open-tubular columns and the optimization of column length. The validity of this approach was confirmed for narrow-bore and wide-bore columns [40]. In this mixed-phase system the hydrogen acceptor, donor and dispersive forces are the prevailing phenomena that control the separation, and therefore the use of the easily measured ΔC values allows the comparison of different column systems, rather than simple liquid phases, as it also considers the interaction with Si–O–Si bonds of the glass wall, of the support

and of the silanizing agents. It also allows an evaluation of the change in polarity due to column ageing and contamination or that obtained by connecting different lengths of polar and non-polar columns.

ACKNOWLEDGEMENT

This work was supported by the Italian Ministry of University and Scientific and Technological Research.

REFERENCES

1 R. N. Ewell, J. M. Harrison and L. Berg, *Ind. Eng. Chem.*, 36 (1944) 871.
2 H. M. McNair and E. J. Bonelli, *Basic Gas Chromatography*, Varian Aerograph, Walnut Creek, CA, 1965, p. 40.
3 E. Kováts, *Helv. Chim. Acta*, 41 (1958) 1915.
4 L. Rohrschneider, *J. Chromatogr.*, 22 (1966) 6.
5 W. O. McReynolds, *J. Chromatogr. Sci.*, 8 (1970) 685.
6 G. Castello and G. D'Amato, *J. Chromatogr.*, 366 (1986) 51.
7 Z. Szentirmai, G. Tarjan and J. Takacs, *J. Chromatogr.*, 73 (1972) 11.
8 F. Riedo, D. Fritz, G. Tarjan and E. Kováts, *J. Chromatogr.*, 126 (1976) 63.
9 G. Castello and G. D'Amato, *J. Chromatogr.*, 269 (1983) 153.
10 C. F. Poole and S. K. Poole, *Chem. Rev.*, 89 (1989) 377.
11 C. F. Poole, S. K. Poole, R. M. Pomaville and B. R. Kersten, *J. High Resolut. Chromatogr. Chromatogr. Commun.*, 10 (1987) 640.
12 J. Li, A. J. Dallas and P. W. Carr, *J. Chromatogr.*, 517 (1990) 103.
13 G. Castello, G. D'Amato and E. Biagini, *J. Chromatogr.*, 41 (1969) 313.
14 G. Castello and G. D'Amato, *J. Chromatogr.*, 54 (1971) 157.
15 G. Castello and G. D'Amato, *J. Chromatogr.*, 150 (1978) 319.
16 T. J. Betts, G. J. Finucane and H. A. Tweedie, *J. Chromatogr.*, 213 (1981) 317.
17 M. B. Evans and J. K. Haken, *J. Chromatogr.*, 472 (1989) 93.
18 *General Catalog*, Chrompack International, Middelburg, 1986, p. 7.
19 G. Castello and G. D'Amato, *J. Chromatogr.*, 366 (1986) 51.
20 G. Castello, G. D'Amato and G. Canciani, *Ann. Chim. (Rome)*, 68 (1978) 255.
21 G. Castello and G. D'Amato, *J. Chromatogr.*, 196 (1980) 245.
22 G. Castello and G. D'Amato, *J. Chromatogr.*, 254 (1983) 69.
23 L. R. Snyder, *J. Chromatogr.*, 92 (1974) 223.
24 L. R. Snyder, *J. Chromatogr. Sci.*, 16 (1978) 223.
25 M. S. Klee, M. A. Kaiser and K. B. Laughlin, *J. Chromatogr.*, 279 (1983) 681.
26 T. J. Betts, *J. Chromatogr.*, 354 (1986) 1.
27 T. J. Betts, *J. Chromatogr.*, 504 (1990) 186.
28 M. A. Hepp and M. S. Klee, *J. Chromatogr.*, 404 (1987) 145.
29 E. Fernandez-Sanchez, A. Fernandez-Torres, J. A. Garcia-Dominguez and J. M. Santiuste, *Chromatographia*, 31 (1991) 75.
30 G. Tarjan, S. Nyiredy, M. Györ, E. R. Lombosi, T. S. Lombosi, M. V. Budahegyi, S. T. Meszaros and J. M. Takacs, *J. Chromatogr.*, 472 (1982) 1.
31 A. T. Kames and A. J. P. Martin, *Biochem. J.*, 50 (1952) 679.
32 Swoboda, in M. van der Swaay (Editor), *Gas Chromatography 1960*, Butterworths, London 1962, p. 36.
33 E. sz. Kováts, *Adv. Chromatogr.*, 1 (1965) 239.
34 G. Castello, A. Timossi and T. C. Gerbino, *J. Chromatogr.*, 522 (1990) 329.
35 W. O. McReynolds, *Gas Chromatographic Retention Data*, Preston Technical Abstract, Evanston, IL, 1966.
36 St. J. Hawkes, *Chromatographia*, 25 (1988) 87.
37 A. T. James, in D. Glick (Editor), *Methods of Biomedical Analysis*, Interscience, New York, 1960.
39 J. R. Jones and J. H. Purnell, *Anal. Chem.*, 62 (1990) 2300.
40 T. C. Gerbino and G. Castello, in P. Sandra (Editor), *Proceedings of 13th International Symposium on Capillary GC, Riva del Garda, 1991*, Vol. I, Hüthig, Heidelberg, p. 889.

Journal of Chromatography, 623 (1992) 297–304
Elsevier Science Publishers B.V., Amsterdam

CHROM. 24 466

Gas chromatographic study of the inclusion properties of dibenzo-24-crown-8 ether

P. Mňuk, E. Smolková-Keulemansova and L. Feltl

Department of Analytical Chemistry, Charles University, Albertov 2030, 128 40 Prague 2 (Czechoslovakia)

(First received March 31st, 1992; revised manuscript received June 24th, 1992)

ABSTRACT

The inclusion properties of dibenzo-24-crown-8 ether were studied in gas–solid chromatography (GCS) and gas–liquid chromatography (GLC) systems. Substances potentially capable of interacting with the cavity of the crown ether —homologous series of alkanes, alcohols, ethers, aromatics and halogenated hydrocarbons— were used as the sorbates and solutes. It was found that inclusion compounds are formed with methanol, ethanol, dichloromethane, trichloromethane, 1,2-dichloroethane, diiodomethane and the aromatic nucleus of aromatics under conditions used in the GSC system and with dichloromethane, trichloromethane, 1,2-dichloroethane, diiodomethane and the aromatic nucleus of aromatics in the GLC system.

INTRODUCTION

Crown ethers, which are macrocyclic polyethers, are primarily used for selective binding of metal cations in order to transfer the cations into non-polar media. However, many crown ethers also form inclusion compounds with organic molecules [1,2].

This study of the inclusion properties of dibenzo-24-crown-8 ether (DB-24-C-8) (Fig. 1) is a continuation of the previous work [3], in which the formation of inclusion compounds of dibenzo-18-crown-6 and tribenzopyridine-21-crown-7 ethers with lower *n*-alcohols was demonstrated under gas chromatographic conditions. The use of DB-24-C-8 ether in gas chromatography is rare [4,5].

The aim of the present work was to study the inclusion properties of crown ethers with a cavity size of 0.3 × 0.6 nm [6], which is large enough for the inclusion of simple organic molecules.

EXPERIMENTAL

The stationary phases for gas–solid chromatography (GSC) were prepared by dissolving the crown ether in N,N-dimethylformamide, coating Chromosorb W (60–80 mesh) with this solution and evaporating the solvent at 55°C *in vacuo* (10–20 Pa). The stationary phase obtained, containing 8% (w/w) DB-24-C-8 ether, was used to fil micropacked glass columns (1.6 m × 1 mm I.D.). The stationary phas-

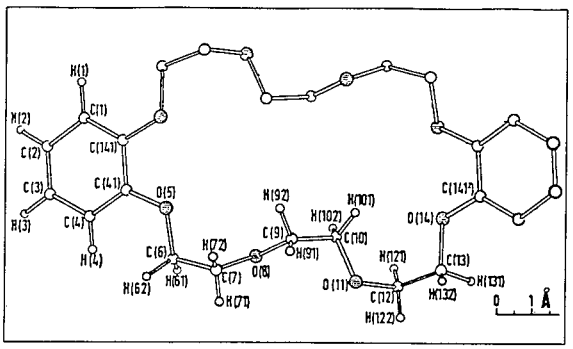

Fig. 1. Crystal structure of the molecule of dibenzo-24-crown-8 ether. The centrally symmetrical atoms are denoted by a superscript I. (according to Ref. 4).

Correspondence to: Dr. E. Smolková-Keulemansová, Department of Analytical Chemistry, Charles University, Albertov 2030, 128 40 Prague 2, Czechoslovakia.

0021-9673/92/$05.00

es for gas–liquid chromatography (GLC) were prepared by separately dissolving the crown ether and methylsilicone gum SE-30 in chloroform, mixing the two solutions, coating the mixture on Chromosorb W (CHS) 60–80 mesh and evaporating the solvent at 55°C under atmospheric pressure. The stationary phase thus obtained, containing 8% DB-24-C-8 ether and 4% SE-30 (w/w, CHS), was used to fill a micropacked glass column (1.5 m × 1 mm I.D.).

The measurements were carried out on a CHROM 61 gas chromatograph equipped with a flame ionization detector (Laboratorní přístroje, Prague, Czechoslovakia). The column temperature was 70°C and the flow-rate of the nitrogen carrier gas was 6.7 ml/min. Head-space sample injection was used, with Hamilton microsyringes. All the substances used were of analytical reagent purity.

RESULTS AND DISCUSSION

The formation of inclusion compounds of DB-24-C-8 ether was studied with homologous series of alkanes, alcohols, ethers, aromatics and halogenated hydrocarbons. The steric effects on the retention of these substances were found from the dependence of the logarithm of the capacity ratio on the boiling temperatures or the volumes of the test molecules. The effect of the pure supporting material was considered. The effect of the methylsilicone component (SE-30) in the GLC stationary phase was eliminated by using the difference in the capacity ratios (dk) between the phase used (SE-30 + DB-24-C-8) and pure SE-30. The results obtained were critically evaluated by comparing the size of the DB-24-C-8 ether cavity with the sizes of the solute molecules.

Retention behaviour of alkanes and alkenes

The alkane and alkene homologues are eluted in order of their boiling temperatures. Dispersion interactions predominate; with alkenes, interactions between the π-electrons of the multiple bond and the electron-deficient $-CH_2-CH_2-$ groupings of the polyether ring in the crown ether also play a role. No steric preference was observed.

Retention behaviour of alcohols

In the GSC system, the values for methanol and ethanol deviate considerably from the log k *versus* boiling temperature linear dependence in the *n*-alcohol homologous series (Fig. 2). The dependence of log k on the polarizability of the solutes also indicates an increased retention of the two substances (Fig. 3). A comparison of the sizes of the molecules and the DB-24-C-8 ether cavity demonstrates that methanol and ethanol are included into the DB-24-C-8 ether cavity in the GSC system. Higher alcohols are not included, but their retention behaviour is affected by the position of the hydroxyl group in the chain. The presence of the multiple bond in alkenols exerts no substantial influence on their retention, as hydrogen bonding between the alcohol hydroxyl group and the electron-donor oxygen atoms in the polyether ring remains the predominating interaction. The coating of the relatively active surface of Chromosorb W with the crown ether eliminates the specific interaction sites in the surface, which leads to a perceptible improvement in the column efficiency in separations of alcohols and also of many other polar substances.

In contrast to the GSC system, the GLC system exhibited no steric preference in the retention of homologous alcohols.

Retention behaviour of ethers

Acyclic homologous ethers are eluted in order of their boiling temperatures in GSC. Cyclic tetrahydrofuran is more retained, and the stereochemistry of this molecule suggests possible inclusion in the DB-24-C-8 ether cavity.

The ethers behave similarly in the GLC system. However, information about the system (especially about the DB-24-C-8 ether structure in the SE-30 medium) is not sufficient for deciding whether inclusion is the predominating factor in increased retention of cyclic ethers.

Retention behaviour of aromatics

It is evident from Fig. 4 that aromatics are more retained in the GSC system than with cyclohexane/cyclohexene. The sterically most likely cause of this behaviour is inclusion of the aromatic nucleus in the DB-24-C-8 ether cavity. Increased retention of *o*-xylene and decreased retention of *p*-xylene and *p*-ethyltoluene (Figs. 5 and 6) make it possible to estimate a probable steric arrangement of these molecules during interaction with DB-24-C-8 ether. Xy-

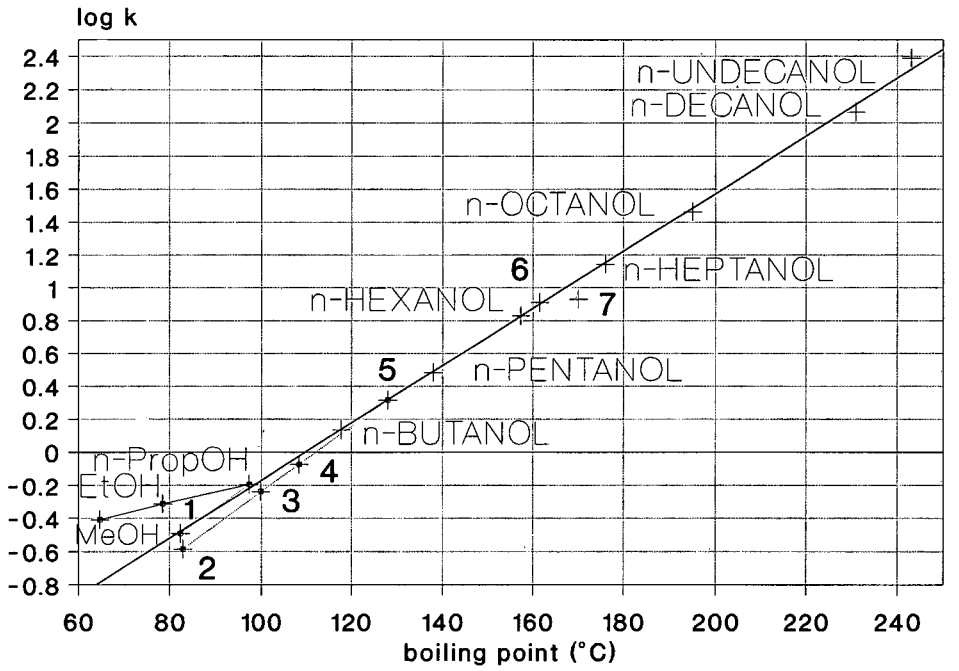

Fig. 2. Retention behaviour of alcohols in the GSC system: relationship between the logarithm of the capacity ratio and the boiling point. 1 = 2-propanol; 2 = *tert.*-butanol; 3 = *sec.*-butanol; 4 = isobutanol; 5 = isopentanol; 6 = cyclohexanol; 7 = methylcyclohexanol. MeOH = Methanol; EtOH = ethanol; n-PropOH = *n*-propanol.

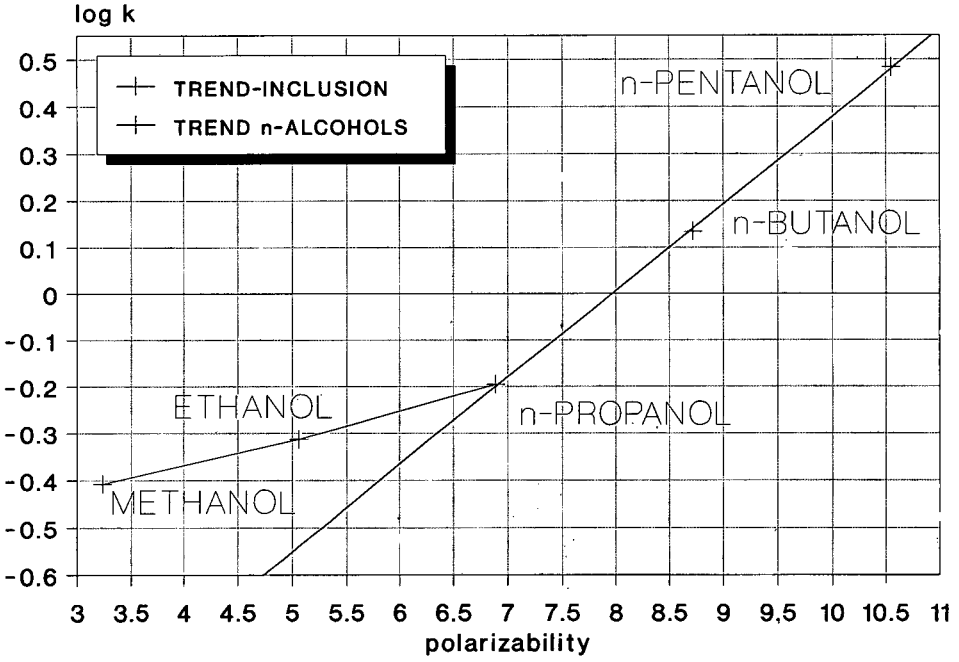

Fig. 3. Retention behaviour of lower alcohols in the GSC system: relationship between the logarithm of the capacity ratio and the polarizability.

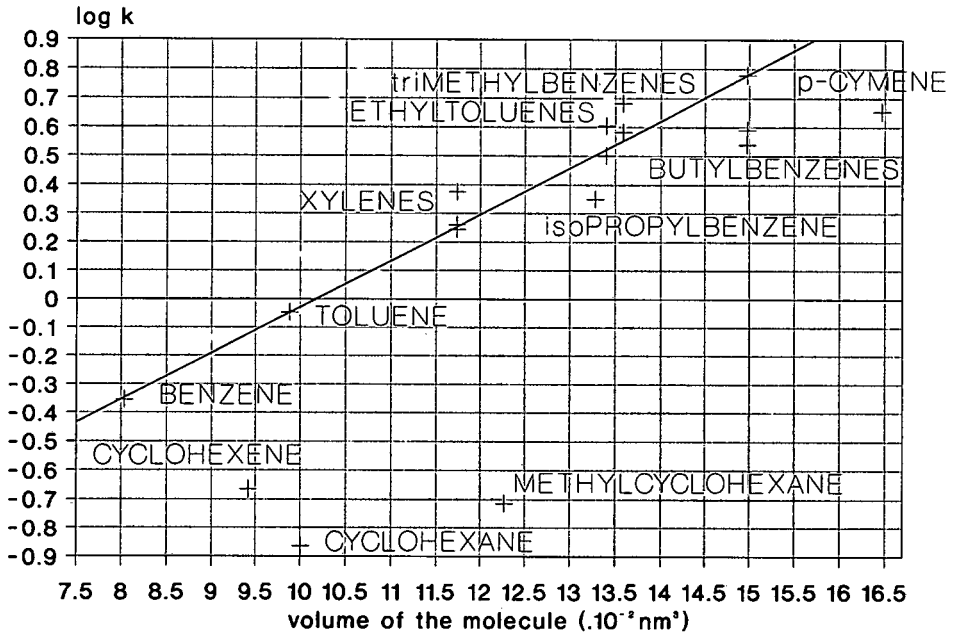

Fig. 4. Retention behaviour of aromatics in the GSC system: relationship between the logarithm of the capacity ratio and the volume of the molecule.

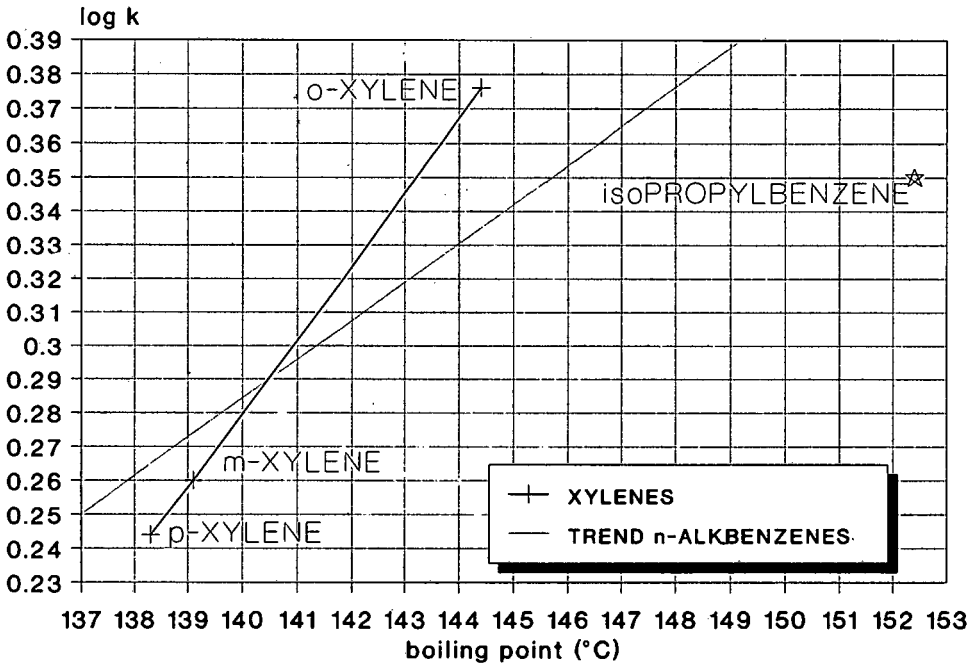

Fig. 5. Retention behaviour of xylenes in the GSC system: relationship between the logarithm of the capacity ratio and the boiling point. Alk. = Alkyl.

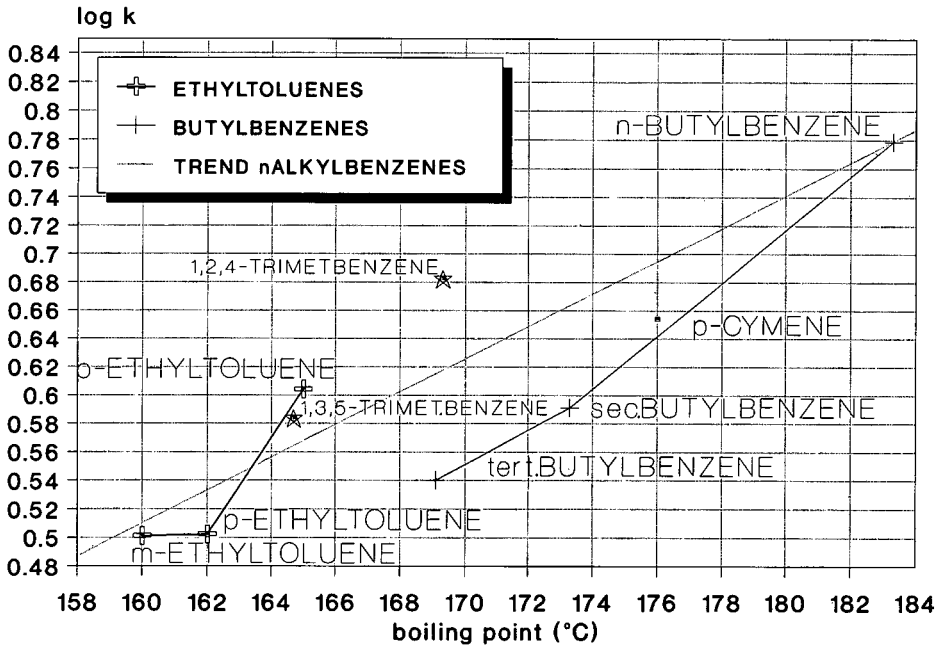

Fig. 6. Retention behaviour of ethyltoluenes and butylbenzenes in the GSC system: relationship between the logarithm of the capacity ratio and the boiling point. Met. = Methyl.

lenes and ethyltoluenes can, at least partially, enter the DB-24-C-8 ether cavity and thus form inclusion complexes. It is likely that the six-fold symmetry axis of the benzene ring in xylene (the guest) is oriented at right angles to the line connecting the aromatic rings of DB-24-C-8 ether (the host) and lies approximately in the plane of the polyether ring of DB-24-C-8 ether during the inclusion process. The π-electron system of the guest interacts with the electrophilic atom grouping at the C-9, C-10, C^{I}-6 and C^{I}-10 carbons (see Fig. 1). The electrophilic methyl/ethyl group interacts with the two strongly nucleophilic sites formed by the aromatic rings of DB-24-C-8 ether and the oxygen atoms O-5, O^{I}-14 or O-14, O^{I}-5. With this mutual orientation, inclusion is sterically easiest with the *ortho* isomer and the greatest steric hindrance is encountered with the *para* isomer (Fig. 7). The butyl derivatives of benzene interact in the same way, the electrophilic butyl chain interacting with the nucleophilic space around the DB-24-C-8 ether aromatic nucleus. The interaction is sterically easiest with the *n*-butyl chain and most difficult with *tert.*-butyl ones.

The mixture of acyclic (C_5–C_7), cyclic (C_6) and aromatic (benzene, *o*-xylene, *p*-xylene, 1,3,5-trimethylbenzene and *n*-butylbenzene) hydrocarbon compounds was injected onto a DB-24-C-8 column on the GSC system at a column temperature 32°C and flow-rate of 6.0 ml/min. Separation of aromatic hydrocarbons from the acyclic and cyclic hydrocarbons was achieved.

The aromatic nucleus is also completely or partially included in the DB-24-C-8 ether cavity in the GLC system (Fig. 8). It can be assumed from the steric preference of *p*-xylene over the *ortho* and *meta* derivatives (Fig. 9) that methylsilicone medium probably favours interaction between the weakly electron-deficient methyl groups and the electron-

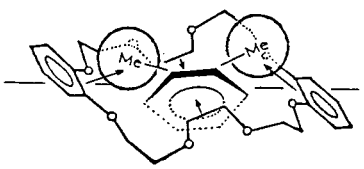

Fig. 7. Probable steric arrangement of inclusion complex of *o*-xylene and dibenzo-24-crown-8 ether (schematic).

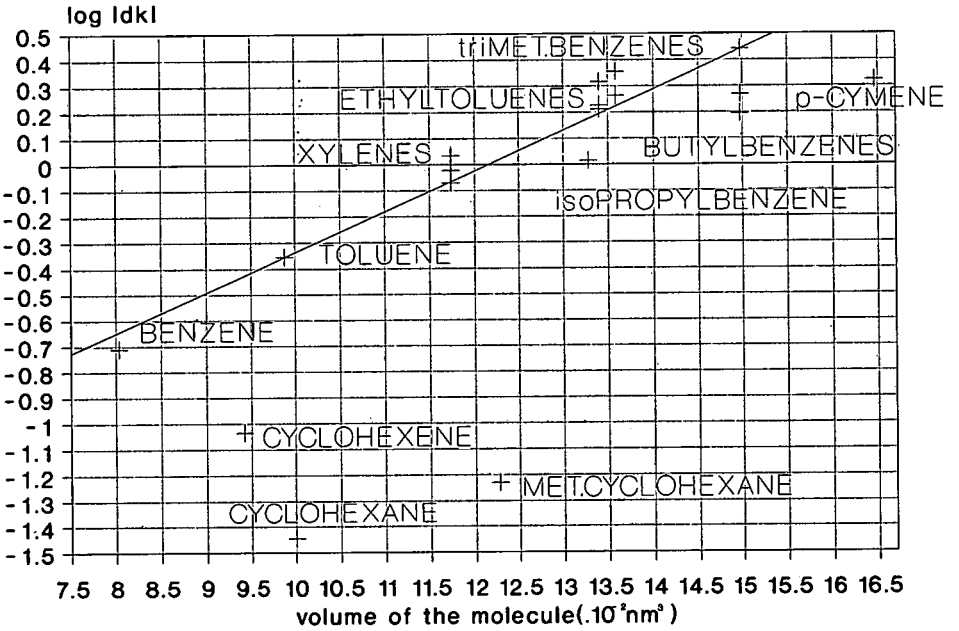

Fig. 8. Retention behaviour of aromatics in the GLC system: relationship between the logarithm of the difference in the capacity ratios (dk) of the phase used (SE-30 + DB-24-C-8) and pure SE-30 and the volume of the molecule.

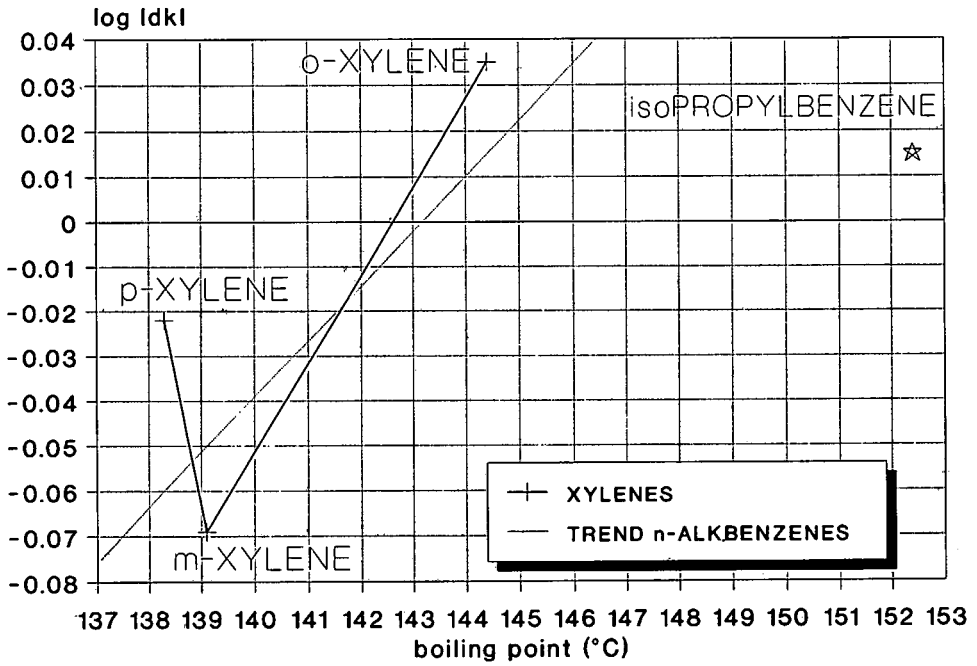

Fig. 9. Retention behaviour of xylenes in the GLC system: relationship between log dk and the boiling point.

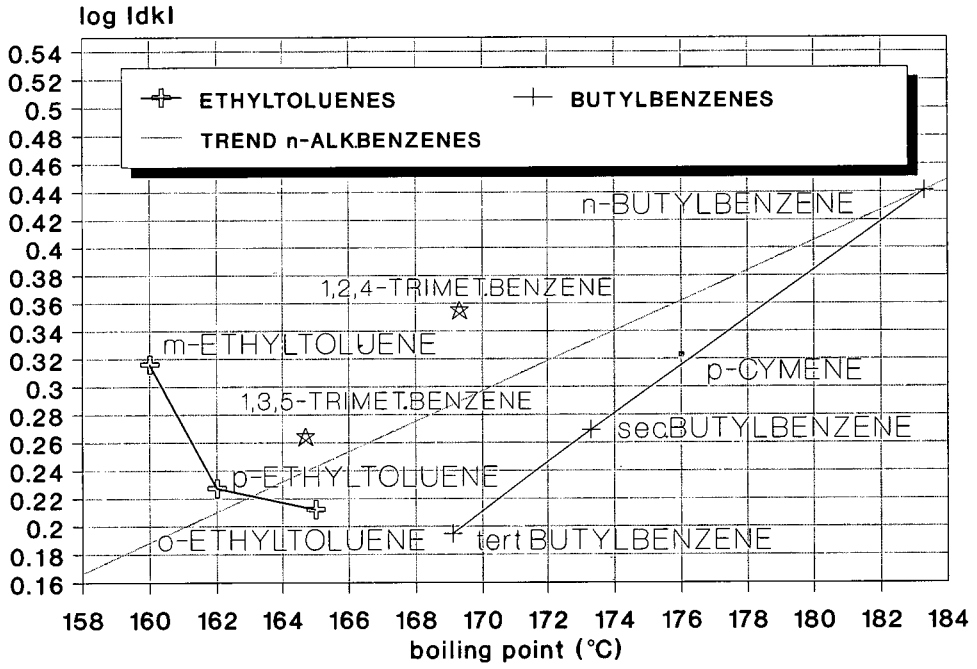

Fig. 10. Retention behaviour of ethyltoluenes and butylbenzenes in the GLC system: relationship between log dk and the boiling point.

donor areas of the benzene nuclei in DB-24-C-8 ether prior to complete inclusion of the xylene molecule in the DB-24-C-8 ether cavity. Under these conditions, the *para* position is the most favourable arrangement of the methyl substituents. The retention of ethyltoluenes and butylbenzenes in the GLC system can be seen in Fig. 10. The highest retention of the *meta* isomer can be caused by interaction of the alkyl substituents with the DB-24-C-8 ether benzene nuclei, as described above, which accompanies partial inclusion of the *m*-ethyltoluene benzene nucleus into the DB-24-C-8 ether cavity. This accompanying interaction is more likely with the *meta* isomers than with the para isomer, provided that the two interacting molecules have a suitable spatial arrangement. The group of butylbenzenes exhibits similar interactions to the GSC system.

Retention behaviour of halogen derivatives

Fig. 11 summarizes the retention behaviour of halogen derivatives in the GSC system. The compounds fall into two groups. The first group includes rather small molecules: dichloromethane, trichloromethane, 1,2-dichloroethane and diiodomethane. The other group involves compounds with large molecules or long alkyl chains: tetrachloromethane, tetrachloroethane, *n*-heptyl-, *n*-octyl- and *n*-decylchloride. The compounds from the first group are retained substantially more strongly than those from the other group. This fact cannot be satisfactorily explained using only a purely electrostatic model of interaction. On the basis of a stereochemical study of these substances, the retention behaviour can be explained by inclusion of the molecules from the first group into the DB-24-C-8 ether cavity. The behaviour of halogen derivatives is identical in the GLC system.

CONCLUSION

The results obtained indicate that gas chromatographic measurement can significantly contribute to the evaluation of the properties of dibenzo-24-crown-8 ether and to the characterization of its interactions with various organic substances. Dibenzo-24-crown-8 ether can be classified among the

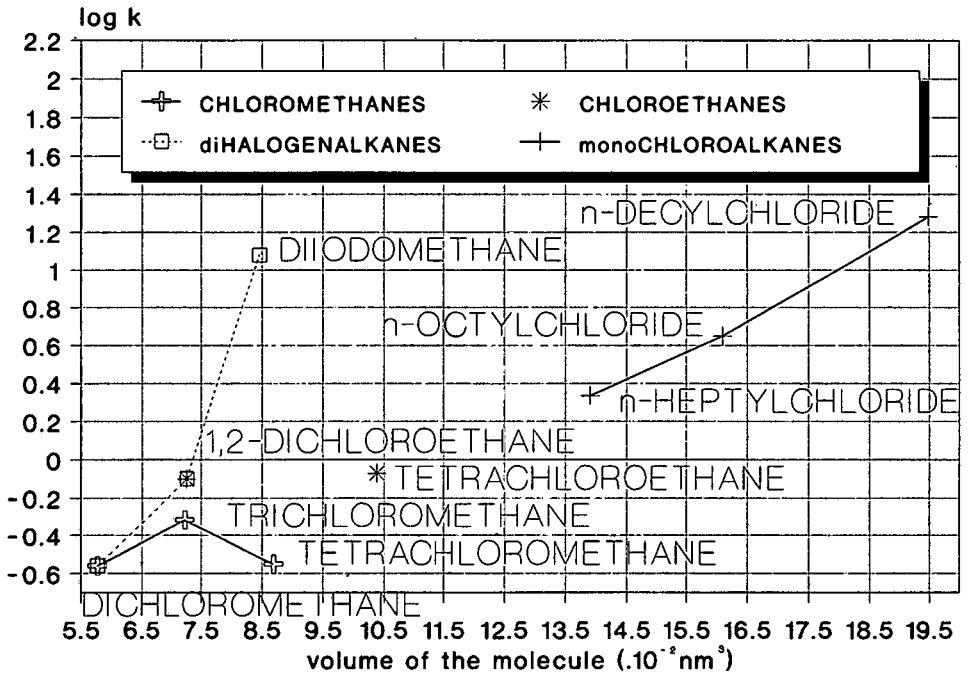

Fig. 11. Retention behaviour of halogen derivatives in the GSC system: relationship between the logarithm of the capacity ratio and the boiling point.

substances whose specific spatial interactions with benzene derivatives can be used to study inclusion phenomena in gas chromatography. In contrast to α-cyclodextrin, dibenzo-24-crown-8 ether also specifically interacts with methanol and ethanol in GSC systems.

REFERENCES

1 H. M. Colquhoun, S. M. Doughty, J. F. Stoddart, A. M. Slawin and D. J. Williams, *J. Chem. Soc., Perkin Trans. 2*, (1986) 253.
2 H. M. Colquhoun, E. P. Goodings, J. M. Maud, J. F. Stoddart, D. J. Williams and J. B. Wolstenholme, *J. Chem. Soc., Chem. Commun.*, (1983) 1140.
3 A. Kohoutová, E. Smolková-Keulemansova and L. Feltl, *J. Chromatogr.*, 471 (1989) 139.
4 R. Li, *Sepu*, 4 (1986) 304.
5 N. R. Ayyangar, A. S. Tambe and S. S. Biswas, *J. Chromatogr.*, 543 (1991) 179.
6 I. R. Hanson, D. I. Hughes and M. R. Truter, *J. Chem. Soc., Perkin Trans. 2*, (1976) 972.

Journal of Chromatography, 623 (1992) 305–313
Elsevier Science Publishers B.V., Amsterdam

CHROM. 24 436

Taguchi design experiments for optimizing the gas chromatographic analysis of residual solvents in bulk pharmaceuticals

Pascal Billot

Analytical Department, Roussel-Uclaf, 93230 Romainville (France)

Bruno Pitard

Compiègne University of Technology, 60206 Compiègne (France)

(First received February 6th, 1992; revised manuscript received June 12th, 1992)

ABSTRACT

Taguchi design experiments were conducted in order to identify and optimize the parameters that yield a maximum separation of 26 solvents commonly found in bulk pharmaceuticals. Wide-bore columns with chemically cross-linked stationary phases of different polarities were retained owing to their sensitivity and specificity in optimizing the analysis via a simple response function based on information theory.

INTRODUCTION

For several years, the search for a general method applicable to the evaluation of solvent residues in bulk pharmaceuticals has received great attention. Several procedures based on packed-column or wide-bore column separation have been published [1–4]. The US and European Pharmacopoeias propose standard procedures employing porous polymer packings or silicone phases [5,6] with direct injection or headspace sampling.

These techniques require a high-boiling solvent such as octanol or benzyl alcohol to dissolve the sample. The solubility of pharmaceuticals in these solvents is poor, $\leqslant 1\%$, thus adversely affecting the detection limits. After each analysis it is necessary to maintain the column at its highest temperature limit to eliminate the dissolving solvent and its impurities. Benzyl alcohol contains by-products such as methanol, toluene, oxidation products and benzene generated during injection. Dimethylformamide, which has been termed the universal organic solvent, seems to be a better choice.

Many strategies for the optimization of gas chromatography have been used, such as the sequential simplex method [7,8], window diagrams [9], response surface method [10] and computer-simulation techniques [11–14]. They all suffer from the poor number of parameters tested or from a difficulty in calculating the response function, often imprecise owing to uncertainties in the measurement of data.

For any optimization strategy, a mathematical function must be defined to reflect the quality of a chromatogram as a single number. Optimization then becomes a process of maximizing (or possibly minimizing) the numerical value of this function. It is a challenge to capture adequately the chromato-

Correspondence to: Dr. P. Billot, Analytical Department, Roussel-Uclaf, 93230 Romainville, France.

0021-9673/92/$05.00

grapher's perception of quality with a mathematical expression and, consequently, considerable effort has been devoted to the development of the response function.

Response functions such as [15]

$$Ct = \sum R_i - b(t_w - t_{max}) - d(t_{min} - t_\alpha)$$

$$\prod R_s = \prod R_i$$

where

R_i = resolution between two adjacent peaks
t_{min} = minimum time required for analysis
t_{max} = maximum time acceptable
t_α = retention time of the first peak
t_w = retention time of the last peak
b and d = weighing factors

give numbers without dimensions increasing with the quality of the chromatogram. In fact, the increase is not necessarily correlated with an improvement of the separation between two adjacent peaks, $\sum R_i$ and $\prod R_i$ being strongly dependent on the chromatograms to be compared (retention times of the same order are necessary to have R_i of the same type). The interval of variation of the response function, *i.e.*, minimum and maximum, is often not known, particularly the maximum. Some workers [16] have introduced functions such as *CRF* and *COF* that remove this last drawback:

$$CRF = \sum_{i=1}^{k} \ln P_i$$

where P_i is a measure of separation between adjacent peaks

$$COF = \sum_{i=1}^{k} A_i \ln(R_i/R_{id}) + B(t_M - t_L)$$

where R_i is the resolution of the ith pair, R_{id} is the desired resolution and A_i and B are weighing factors.

All these disadvantages, mainly the uncertainties in the measurement of the resolution, the long time necessary to analyse the chromatogram and the unknown maximum of the response functions already used, convinced us to use a response function based on information theory [15,17,18], in conjunction with Taguchi design experiments.

Orthogonal array designs are used to assign factors, *i.e.*, the analytical parameters (in our case, column, temperature, flow-rate, ...) to a series of experimental combinations whose results then can be treated by a common mathematical procedure to extract independently the main effects of these factors. Emphasis is placed on identifying controlling factors and quantifying the magnitude of effects rather than just identifying statistically significant effects.

Taguchi has simplified the application of design experiments by using a standardized library of basic designs [19,20] called orthogonal arrays along with some simple methods to modify these layouts to fit individual situations.

THEORY

Optimization criteria

Let a mixture of n components be separated by gas–liquid chromatography (GLC). The resulting chromatogram is composed of k_1 singlets, k_2 doublets, ..., k_p p-uplets with $\sum_p pk_p = n$. The quantity of specific information brought by the identification of one component is

$$Q_1 = \log_2(n/1)$$

The appearance frequency is

$$F_1 = k_1/n$$

F_1 is also the probability of one component being present as a singlet, postulating that each component could be present anywhere in the chromatogram.

The contribution of the singlets to the quantity of information is given by

$$I_1 = F_1 Q_1 = (k_1/n)\log_2(n/1)$$

In the same way, the contribution of the doublets is

$$I_2 = F_2 Q_2 = (2k_2/n)\log_2(n/2)$$

The total information brought by the chromatogram is the sum of the individual contributions of each peak groups:

$$IC = \sum_p (pk_p/n)\log_2(n/p)$$

where n is the total number of components to be separated. This function varies between zero, all the peaks together ($p = n$, $k_p = 1$) and $\log_2(n)$, all the peaks separated ($p = 1$, $k_p = n$).

For instance, let a mixture of eight components be

separated. If the resulting chromatogram is composed of four singlets and two doublets, then

$$IC = 4 \times 1/8 \times \log_2(8/1) + 2 \times 2/8 \times \log_2(8/2) = 3.5$$

EXPERIMENTAL

Materials

Samples of solvents were obtained from Merck (Nogent sur Marne, France), Prolabo (Paris, France), Riedel-de Haen (Seelze, Germany). Dimethylformamide was of high-purity grade from Merck (>99.8%)

Apparatus and conditions

The method was developed on a Varian 3400 gas chromatograph equipped with a flame ionization detector, a Varian Model 8035 autosampler and Model OCA-4/90 insert from Scientific Glass Engineering (Villeneuve-Saint-Georges, France). Chromatograms were recorded on a Spectra-Physics Chromjet system. Hydrogen and air flow-rates were 37 and 260 ml/min, respectively, and the carrier gas was nitrogen with a make-up of 30 ml/min.

The columns were 50 m × 0.53 mm I.D. fused-silica columns (Chrompack, Les Ulis, France) with the thickest chemically cross-linked stationary phases available: CP Sil 5CB and CP Sil 8CB with a 5-μm film thickness and CP Sil 13CB and CP Wax 52CB with a 2-μm film thickness.

Procedure

The standard solution used in the optimization step was prepared by dissolution in dimethylformamide at 0.02% (v/v) for each solvent. Volumes of 0.4 μl were injected. The injector and detector temperature were 130 and 250°C, respectively.

RESULTS AND DISCUSSION

The experiment is designed to determine the effect of operating conditions on the separation of 26 different solvents commonly found in bulk pharmaceuticals. A number of analytical variables influence the chromatographic results obtained for a mixture of solvents. Six main injection variables affect the solvent peak shape and resolution when using 0.53 mm I.D. columns in a packed-column injection port: injector temperature, injector volume, solvent molecular weight, injection rate, sample size and flow-rate. The column parameters length, diameter, stationary phase film thickness and type of the stationary phase coating and the oven temperature programme must also be considered.

A large number of parameters can be optimized but previous experimental results [21] have indicated that the column flow and the oven temperature programme, namely the initial oven temperature, initial time, programming rate and final oven temperature, are particularly likely to affect the quality of the chromatogram. Parameters such as polarity are difficult to introduce in design experiments because one cannot assign a significant continuous number to a polarity, thus preventing the optimization step.

In order to test these five factors and the four interactions with the flow-rate, a screening experiment was conducting using an L16 (2^{15}) Taguchi orthogonal array. This fractional factorial design, at two levels, labelled (1) and (2), (Table I), is time saving in this initial step for screening five potentially important factors. A factor at two levels corresponds to one degree of freedom (degree of freedom equals the number of levels minus one). Each interaction between two factors at two levels corresponds to one times one degree of freedom. Therefore, five factors at two levels and four interactions equal nine degrees of freedom. Consequently, the L16 orthogonal array (fifteen degrees of freedom) is the minimum fractional array to choose. Each factor is assigned to a column according to the linear graph for this Taguchi orthogonal array (Fig. 1). Circles are for the main factors and the lines between them permit the estimation of the interactions (*i.e.*, if flow-rate and initial temperature are assigned to columns 1 and 2, respectively, then column 3 contains the interaction between flow-rate and initial temperature).

The sixteen experiments were done following Table II, where flow-rate is assigned to column 1, initial temperature to column 2, initial time to column 8, programming rate to column 12 and final temperature to column 6. For instance, trial 10 corresponds to flow-rate 5.3 ml/min, initial temperature 25°C, initial time 17 mn, programming rate 15°C/min and final temperature 90°C.

In such experiments a direct estimate of the

TABLE I

L16 TAGUCHI ORTHOGONAL ARRAY

Trial	1	2	3	4	5	6	7	8	9	10	11	12	13	14	15
1	1	1	1	1	1	1	1	1	1	1	1	1	1	1	1
2	1	1	1	1	1	1	1	2	2	2	2	2	2	2	2
3	1	1	1	2	2	2	2	1	1	1	1	2	2	2	2
4	1	1	1	2	2	2	2	2	2	2	2	1	1	1	1
5	1	2	2	1	1	2	2	1	1	2	2	1	1	2	2
6	1	2	2	1	1	2	2	2	2	1	1	2	2	1	1
7	1	2	2	2	2	1	1	1	1	2	2	2	2	1	1
8	1	2	2	2	2	1	1	2	2	1	1	1	1	2	2
9	2	1	2	1	2	1	2	1	2	1	2	1	2	1	2
10	2	1	2	1	2	1	2	2	1	2	1	2	1	2	1
11	2	1	2	2	1	2	1	1	2	1	2	2	1	2	1
12	2	1	2	2	1	2	1	2	1	2	1	1	2	1	2
13	2	2	1	1	2	2	1	1	2	2	1	1	2	2	1
14	2	2	1	1	2	2	1	2	1	1	2	2	1	1	2
15	2	2	1	2	1	1	2	1	2	2	1	2	1	1	2
16	2	2	1	2	1	1	2	2	1	1	2	1	2	2	1

experimental error is not calculable because for each trial only one experiment has been done. Therefore, the residual variance was calculated with the sum of squares of columns that have not been assigned (columns 4, 5, 10, 11, 14, 15). These columns correspond to interactions with a very low probability of occurrence.

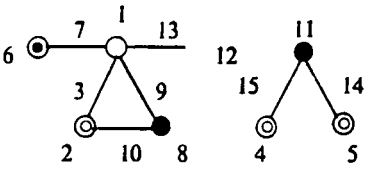

Fig. 1. Linear graph.

An analysis of variance table with pooled errors was constructed from individual contribution (*IC*) data, and it indicated that the factors initial time and final oven temperature are statistically significant at the 99.5% confidence level and initial oven temperature and programming rate at the 95% level. Column flow and the interactions between flow and the other parameters have no influence on the separation of the 26 solvents (Table III).

The most significant effects contributing to the output signal were the initial time (31.3%) and the

TABLE II

L16 TAGUCHI ORTHOGONAL ARRAY

Trial	1[a]	2[a]	3	4	5	6[a]	7	8[a]	9	10	11	12[a]	13	14	15	*IC*
1	1	1				1		1				1				4.3347
2	1	1				1		2				2				4.4406
3	1	1				2		1				2				4.0270
4	1	1				2		2				1				4.2868
5	1	2				2		1				1				4.1039
6	1	2				2		2				2				4.1039
7	1	2				1		1				2				4.1808
8	1	2				1		2				1				4.3347
9	2	1				1		1				1				4.2578
10	2	1				1		2				2				4.2578
11	2	1				2		1				2				3.9980
12	2	1				2		2				1				4.2868
13	2	2				2		1				1				4.0749
14	2	2				2		2				2				4.1808
15	2	2				1		1				2				4.0749
16	2	2				1		2				1				4.2578

[a] Column 1: Flow-rate — level 1: 2 ml/min — level 2: 5.3 ml/min
Column 2: Initial temperature — level 1: 25°C — level 2: 60°C
Column 8: Initial time — level 1: 6 min — level 2: 17 min
Column 12: Programming rate — level 1: 4°C/min — level 2: 15°C/min
Column 6: Final temperature — level 1: 90°C — level 2: 140°C

TABLE III

VARIANCE ANALYSIS

Source of variation	Sum of squares	Degrees of freedom	Mean square	Variance ratio[a]	Contribution (%)[b]
Flow-rate	$1.123 \cdot 10^{-2}$	1	$1.123 \cdot 10^{-2}$	3.93	4.7
Initial temperature	$2.086 \cdot 10^{-2}$	1	$2.086 \cdot 10^{-2}$	7.30	8.7
Initial time	$7.525 \cdot 10^{-2}$	1	$7.525 \cdot 10^{-2}$	26.34	31.3
Final temperature	$7.249 \cdot 10^{-2}$	1	$7.249 \cdot 10^{-2}$	25.37	30.1
Programming rate	$2.835 \cdot 10^{-2}$	1	$2.835 \cdot 10^{-2}$	9.92	11.8
Flow-rate/final temperature	$1.331 \cdot 10^{-2}$	1	$1.331 \cdot 10^{-2}$	4.66	5.5
Flow-rate/initial temperature	$1.479 \cdot 10^{-3}$	1	$1.479 \cdot 10^{-3}$	0.52	0.6
Flow-rate/programming rate	$2.108 \cdot 10^{-4}$	1	$2.108 \cdot 10^{-4}$	0.07	0.1
Flow-rate/initial time	$2.108 \cdot 10^{-4}$	1	$2.108 \cdot 10^{-4}$	0.07	0.1
Pooled errors (columns 4,5,10, 11,14,15)	$1.714 \cdot 10^{-2}$	6	$2.857 \cdot 10^{-3}$		

[a] Critical variance ratio is 5.99 (95% confidence), 18.6 (99.5% confidence).

[b] Contribution is sum of squares / total sum of squares.

final oven temperature (30.1%). The next most significant factors were the programming rate (11.8%) and the initial oven temperature (8.7%).

Fig. 2 shows the effect of significant factors on the response function. A low initial oven temperature, programming rate and final oven temperature will improve the response function the most. Changing the initial time from a low to a high level will also increase the response function.

The L16 orthogonal table enabled us to choose which factors are to be included in the method for determining the optimum combination of factor levels. With the important factors (initial temperature, initial time, programming rate, final oven temperature) a full factorial design at two levels (Table IV) is used to optimize the experimental conditions. Column flow-rate was left at the low level corresponding to the best HETP value. A model can be developed that relates the design variables to the measurement of experimental behaviour. This can be done by using regression methods.

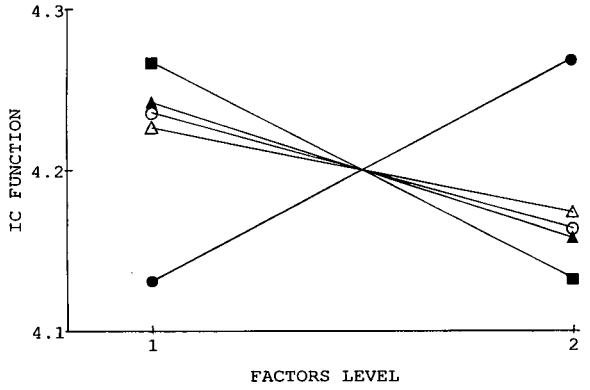

Fig. 2. Test of means (L16 Taguchi table). △ = Flow-rate (2 and 5.3 ml/min); ○ = initial temperature (25 and 60°C); ■ = final temperature (90 and 140°C); ● = initial time (6 and 17 min); ▲ = programming rate (4 and 15°C/min).

The method of steepest ascent was proposed by Box and Wilson [22]. The maximum is located by means of a series of experiments, each planned from the results of the preceding ones. First, a 2^4 full factorial design is chosen to fit a linear equation as an approximation to *IC* in the vicinity of the starting point.

The fitted linear equation in the coded scale is

$$IC = \overline{IC} + h_1(X_1) + h_2(X_2) + h_3(X_3) + h_4(X_4)$$

where $\overline{IC}$ is the mean of all the *IC* values, h_1 is the mean effect of the initial temperature, h_2 is the mean effect of the initial time, k_3 is the mean effect of the programming rate, h_4 is the mean effect of the final temperature and X_1–X_4 are the four factors being considered. The mean effect is calculated by dividing the main effect by 16, *i.e.*, the number of trials. The main effect is obtained as follows: for each trial, to the resulting *IC* is assigned the row sign (+ or −) corresponding to the column that permits the factor

TABLE IV

2^4 FULL FACTORIAL DESIGN

Trial	1[a]	2[a]	3[a]	4[a]	*IC*
1	−	−	−	−	4.33468
2	+	−	−	−	4.18083
3	−	+	−	−	4.44636
4	+	+	−	−	4.33468
5	−	−	+	−	4.18083
6	+	−	+	−	4.18083
7	−	+	+	−	4.44064
8	+	+	+	−	4.33468
9	−	−	−	+	4.25776
10	+	−	−	+	4.10391
11	−	+	−	+	4.28679
12	+	+	−	+	4.25776
13	−	−	+	+	4.02699
14	+	−	+	+	4.02699
15	−	+	+	+	4.10391
16	+	+	+	+	4.10391
Mean effect	$-5.486\ 10^{-1}$	$1.010 \cdot 10^{-1}$	$-7.984 \cdot 10^{-1}$	$-1.260 \cdot 10^{-1}$	
Mean effect	$-3.429\ 10^{-2}$	$6.314 \cdot 10^{-2}$	$-4.990 \cdot 10^{-2}$	$-7.873 \cdot 10^{-2}$	

[a] Column1: initial temperature level −: 25°C level +: 60°C
Column 2: initial time level −: 6 min level +: 17 min
Column 3: programming rate level −: 4°C/min level +: 15°C/min
Column 4: final temperature level −: 90°C level +: 140°C

estimation and the sum is obtained. The equation becomes

$$IC = 4.225 - 3.429 \cdot 10^{-2}(X_1) + 6.314 \cdot 10^{-2}(X_2) - 4.990 \cdot 10^{-2}(X_3) - 7.873 \cdot 10^{-2}(X_4)$$

where

X_1	Initial oven temperature	X_2	Initial time
−1	25°C	−1	6 min
+1	60°C	+1	17 min
X_3	Programming rate	X_4	Final oven temperature
−1	4°C/min	−1	90°C
+1	15°C/min	+1	140°C

Then the direction of the steepest ascent is calculated for each factor by the formula $h(X^+ - X^-)/2$, where h is the mean effect obtained from the 2^4 design and X^+ and X^- are high and low levels of a factor X, respectively.

The progression steps δ are chosen in such a way that the final temperature step is 5°C. The different trials are realised from the centre of the domain studied (Table V). The *IC* value is calculated for each trial until an inversion of the function is found. This occurs for the conditions corresponding to the centre plus seven times the progression steps. The resulting chromatogram is presented in Fig. 3.

Three other columns were tested in the same way and the chromatograms obtained are presented in Figs. 4–6.

The best separation is obtained on a CP-Sil 13CB column with 24 solvents separated and two co-eluted, isopropanol and diethyl ether. On the CP-Sil 8CB column the 26 solvents are visible with two groups of three peaks, acetone, isopropanol and acetonitrile and hexane, methyl ethyl ketone and diisopropyl ether. The CP-Wax 52CB column shows two groups of co-eluting solvents, 1,1,2-trichlorotrifluoroethane and diethyl ether and methanol and ethyl acetate. These three columns allowed a good separation within an analysis time between 60 and 90 min. On the other hand, the CP-Sil 5CB column shows a short analysis time of 30 min, but with a

TABLE V

OPTIMUM SEARCHING

Trial[a]	Initial temperature (°C) (δ = −1.5)[b]	Initial time (min) (δ = 0.9)[b]	Programming rate (°C/min) (δ = −0.7)[b]	Final temperature (°C) (δ = −5)[b]	*IC*
Centre	42.5	11.5	9.5	115	
Centre + 1Δ	41.0	12.4	8.8	110	4.10
Centre + 5Δ	35.0	16.0	6.0	90	4.33
Centre + 7Δ	32.0	17.7	4.6	80	4.44
Centre + 7.5Δ	31.3	18.3	4.3	77.5	4.36
Centre + 8Δ	30.5	18.7	3.9	75	4.36

[a] Centre = $(X^+ + X^-)/2$, where X^+ and X^- are high and low levels of a factor, X.
[b] δ (Final temperature) fixed at −5°C. $\delta = [-5h(X^+ - X^-)/2]/[-7.873\ \ 10^{-2}\ (140\text{-}90)/2]$ for other factors.

poorer separation; ethyl acetate and diisopropyl ether co-elute in a group of four solvents and toluene co-elutes with dimethylformamide.

An interesting feature extracted from the analysis tables of the Taguchi arrays is the different behaviour of a strictly apolar phase compared with more or less polar phases. All the phases require low initial and final temperatures and a long initial isothermal time, but a non-polar phase, unlike polar phases, needs a rapid programming rate. This could be attributed to the fact that polar interactions (dipole–dipole or hydrogen bonding) decrease in strength with increasing temperature.

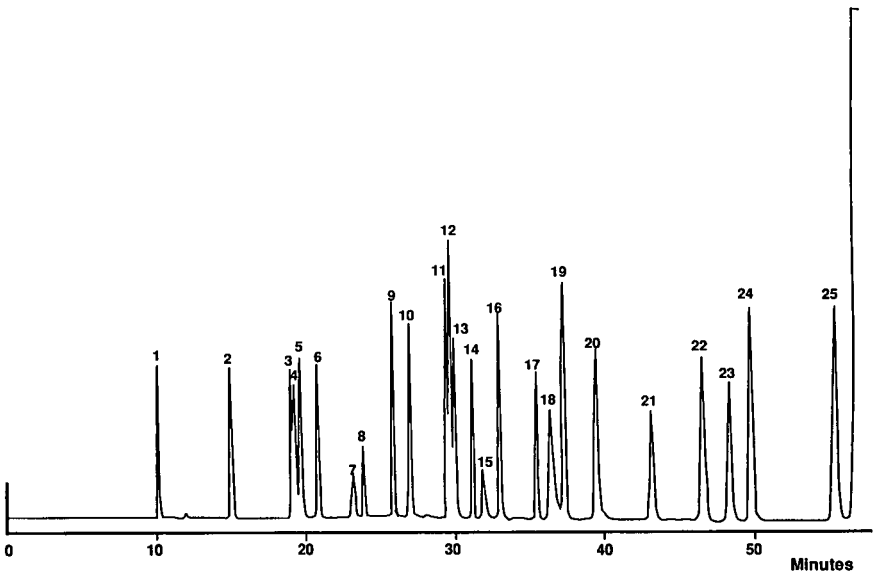

Fig. 3. Chromatogram obtained on a CP-Sil 8 CB column. Initial temperature, 32°C; initial time, 17.7 min; programming rate, 4.6°C/min; final temperature, 80°C; flow-rate, 2 ml/min. Peaks: 1 = methanol; 2 = ethanol; 3 = acetonitrile; 4 = acetone; 5 = isopropanol; 6 = diethyl ether; 7 = 1,1,2-trichlorotrifluoroethane; 8 = methylene chloride; 9 = *n*-propanol; 10 = ethyl acetate; 11 = methyl *tert.*-butyl ether; 12 = hexane; 13 = methyl ethyl ketone; 14 = diisopropyl ether; 15 = chloroform; 16 = tetrahydrofuran; 17 = methyl isobutyl ketone; 18 = *n*-butanol; 19 = cyclohexane; 20 = triethylamine; 21 = dioxane; 22 = methylcyclohexane; 23 = 1,2-dichloroethane; 24 = pyridine.

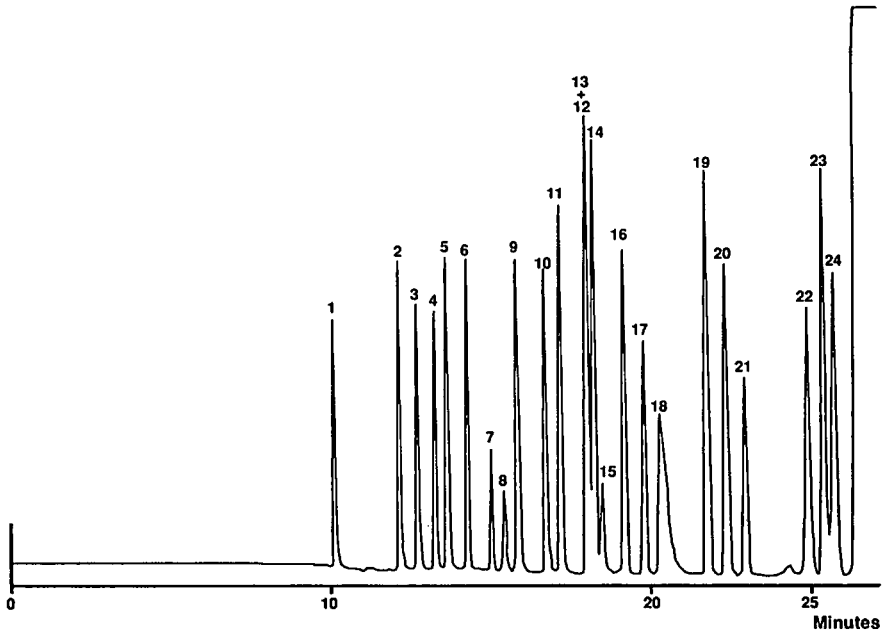

Fig. 4. Chromatogram obtained on a CP-Sil 5CB column. Initial temperature, 30°C; initial time, 5.7 min; programming rate, 12.8°C/min; final temperature, 110°C; flow-rate, 2 ml/min. Peaks: 1 = methanol; 2 = ethanol; 3 = acetonitrile; 4 = acetone; 5 = isopropanol; 6 = diethyl ether; 7 = methylene chloride; 8 = 1,1,2-trichlorotrifluoroethane; 9 = *n*-propanol; 10 = methyl *tert.*-butyl ether; 11 = methyl ethyl ketone; 12 = ethyl acetate; 13 = diisopropyl ether; 14 = hexane; 15 = chloroform; 16 = tetrahydrofuran; 17 = 1,2-dichloroethane; 18 = *n*-butanol; 19 = cyclohexane; 20 = triethylamine; 21 = dioxane; 22 = methyl isobutyl ketone; 23 = methylcyclohexane; 24 = pyridine; 25 = toluene.

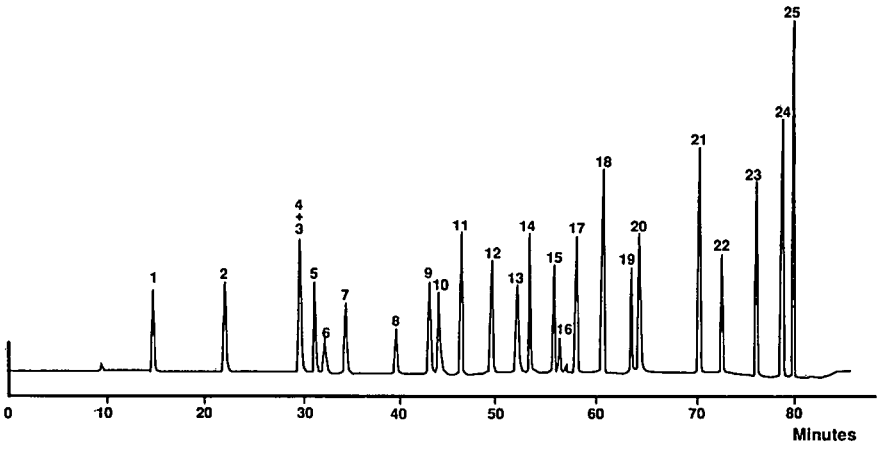

Fig. 5. Chromatogram obtained on a CP-Sil 13CB column. Initial temperature, 15°C; initial time, 30.5 min; programming rate, 1.7°C/min; final temperature, 142°C; flow-rate, 1.5 ml/min. Peaks: 1 = methanol; 2 = ethanol; 3 = diethyl ether; 4 = isopropanol; 5 = acetone; 6 = 1,1,2-trichlorotrifluoroethane; 7 = acetonitrile; 8 = methylene chloride; 9 = methyl *tert.*-butyl ether; 10 = *n*-propanol; 11 = hexane; 12 = diisopropyl ether; 13 = *n*-butanol; 14 = methyl ethyl ketone; 15 = ethyl acetate; 16 = chloroform; 17 = tetrahydrofuran; 18 = cyclohexane; 19 = 1,2-dichloroethane; 20 = triethylamine; 21 = methylcyclohexane; 22 = dioxane; 23 = methyl isobutyl ketone; 24 = pyridine; 25 = toluene.

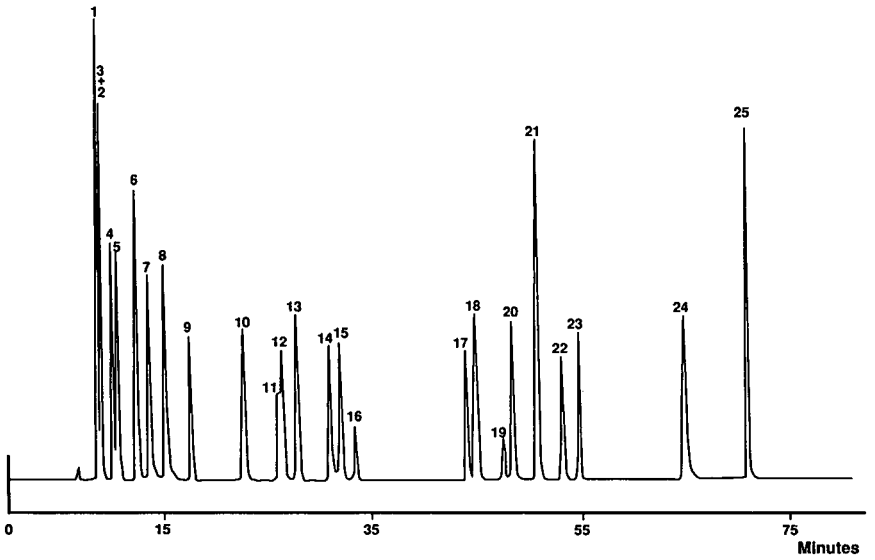

Fig. 6. Chromatogram obtained on a CP-Wax 52CB column. Initial temperature, 44°C; initial time, 23.5 min; programming rate, 1.1°C/min; final temperature, 128°C; flow-rate, 2 ml/min. Peaks: 1 = hexane; 2 = diethyl ether; 3 = 1,1,2-trichlorotrifluoroethane; 4 = diisopropyl ether; 5 = methyl *tert.*-butyl ether; 6 = cyclohexane; 7 = triethylamine; 8 = methylcyclohexane; 9 = acetone; 10 = tetrahydrofuran; 11 = methanol; 12 = ethyl acetate; 13 = methyl ethyl ketone; 14 = isopropanol; 15 = ethanol; 16 = methylene chloride; 17 = acetonitrile; 18 = methyl isobutyl ketone; 19 = chloroform; 20 = *n*-propanol; 21 = toluene; 22 = dioxane; 23 = 1,2-dichloroethane; 24 = *n*-butanol; 25 = pyridine.

CONCLUSION

The described method allowed us to optimize the separation of 26 solvents with a limited number of experiments for each column: sixteen for the L16 Taguchi table plus eight for the full factorial design. The experimental approach, unlike a traditional one (simplex method) is time saving and the simultaneous variation of all the studied factors and the study of their interactions is possible.

The best optimization could be retained as a screening method but owing to its long analysis time and low initial temperature, needing cryogenics, it could not be used as a routine analytical method.

However, a routine method could easily be extracted from the factorial design or from the modelling of *IC* to fit in with requirements such as time of analysis, detection limit or solvents for separation.

REFERENCES

1 J. E. Haky and T. M. Stickney, *J. Chromatogr.*, 321 (1985) 137.
2 D. W. Foust and M. S. Bergren, *J. Chromatogr.*, 469 (1989) 161.
3 J. C. Caire, *S.T.P. Pharma Pratiques*, 1 (1991) 267.
4 J. P. Guimbard, J. Besson, S. Beaufort, J. Pittie and M. Gachon, *S.T.P. Pharma Pratiques*, 1 (1991) 272.
5 *Pharmeuropa*, 2 (1990) 142.
6 ⟨467⟩ Organic Volatile Impurities, *Pharmacopeial Forum*, (1988), 3600.
7 Q.-S. Wang, C.-S. Zhu and B.-W. Yan, *J. Chromatogr.*, 513 (1990) 13.
8 R. J. Laub, J. H. Purnell and P. S. Williams, *J. Chromatogr.*, 155 (1978) 1.
9 D. Repka, J. Krupcik, A. Brunovska, P. A. Leclercq and J. A. Rijks, *J. Chromatogr.*, 463 (1989) 235.
10 U. Olsson, P. Kaufmann and B. G. Herslof, *J. Chromatogr.*, 505 (1990) 385.
11 E. V. Dose, *Anal. Chem.*, 59 (1987) 2420.
12 M.-G. Xie, C.-F. Zhou, X.-H. Yang and G.-Y. Ding, *Chromatographia*, 28 (1989) 274.
13 D. E. Bautz, J. W. Dolan and L. R. Snyder, *J. Chromatogr.*, 541 (1991) 1.
14 R. A. Mowery, *J. Chromatogr. Sci.*, 29 (1991) 194.
15 *Proceedings of the First European School of Chemometrics, July 4–8, 1988, Eguilles, France.*
16 J. L. Glajch, J. J. Kirkland, K. M. Suire and J. M. Minor, *J. Chromatogr.*, 199 (1980) 57.
17 Y. Hayashi and R. Matsuda, *J. Chromatogr. Sci.*, 29 (1991) 60.
18 K. Eckschlager, V. Stepanek and K. Danzer, *J. Chemometr.*, 4 (1990) 195.
19 M. G. Vigier, *Pratique des Plans d'Expérience*, Masson, Paris, 1988.
20 P. J. Oles and A. Yankovich, *LC·GC*, 7 (1989) 579.
21 P. H. Silvis, *LC·GC*, 7 (1989) 562.
22 G. E. P. Box and K. B. Wilson, *J. R. Stat. Soc. B*, 13 (1951) 1.

Journal of Chromatography, 623 (1992) 315–322
Elsevier Science Publishers B.V., Amsterdam

CHROM. 24 433

Chromatographic investigations of macromolecules in the "critical range" of liquid chromatography

II☆. Two-dimensional separations of poly(ethylene oxide–block–propylene oxide)

H. Pasch and C. Brinkmann

Deutsches Kunststoff-Institut, Schlossgartenstrasse 6, W-6100 Darmstadt (Germany)

H. Much

Centre of Macromolecular Chemistry, Rudower Chaussee 5, O-1199, Berlin (Germany)

U. Just

Federal Institute of Materials Research and Testing, Department 3, Unter den Eichen 87, W-1000 Berlin 45 (Germany)

(First received March 26th, 1992; revised manuscript received June 12th, 1992)

ABSTRACT

A polyethylene oxide–polypropylene oxide block polymer was characterized with respect to molar mass distribution and block length of the individual blocks using two-dimensional chromatographic techniques. In the first dimension the block polymer was separated according to the length of the polypropylene oxide block by liquid chromatography at the critical point of adsorption. The resulting polypropylene oxide uniform fractions were subjected to supercritical fluid chromatography or size-exclusion chromatography and the average length and the molar mass of the polyethylene oxide blocks were determined for every fraction.

INTRODUCTION

The molecular heterogeneity of a polymer is characterized by three distribution functions: the molar mass distribution, the distribution in chemical composition and the functionality type distribution. The molar mass distribution may be determined by size-exclusion chromatography (SEC) and the determination of the chemical heterogeneity is possible using liquid adsorption or precipitation chromatography [1,2]. Until recently, the functionality type distribution could be determined only via preparative chromatographic separation into functionality fractions and spectroscopic determination of the functional groups.

The development of liquid chromatography at the critical point of adsorption by Entelis and coworkers [3–5] made it possible to determine the fuctionality type distribution of telechelic oligomers and polymers. Operating in the region between exclusion and adsorption modes of liquid chromatography, retention becomes independent of the

Correspondence to: Dr. H. Pasch, Deutsches Kunststoff-Institut, Schlossgartenstrasse 6, W-6100 Darmstadt, Germany.

☆ For Part I, see ref. 9.

0021-9673/92/$05.00

length of the polymer chain and separation is accomplished exclusively by the number and type of functional groups [6–8]. Accordingly, only the functional groups and not the polymer chain contribute to the retention time, *i.e.*, the polymer chain behaves like an "invisible" part of the molecule.

In Part I [9] it was shown that the same approach can be applied to the characterization of block polymers. For example, taking a block polymer A_nB_m the block A_n can be regarded as a functional group. Therefore, using the critical conditions of B_m for the chromatographic process the chemical structure of A_n can be characterized and *vice versa*.

This paper is aimed at using two-dimensional chromatographic techniques to characterize a block polymer of ethylene oxide and propylene oxide. The first (polypropylene oxide) block will be analysed by liquid chromatography at the critical point of adsorption whereas the second (polyethylene oxide) block is to be analysed by supercritical fluid chromatography (SFC) and SEC.

EXPERIMENTAL

The SFC experiments were conducted on a Dionex SFC 600D instrument using a 10 m × 50 μm I.D. SB Biphenyl-30 capillary column (Lee Scientific). The mobile phase was carbon dioxide (Scott). Flame ionization detection (FID) at 380°C was used, the initial oven temperature being 130°C. Timed split injection was carried out using a Valco injection valve. All samples were injected as 30% (w/w) solutions in methylene chloride.

High-performance liquid chromatographic (HPLC) separations were carried out on a system consisting of a Waters Model 501 HPLC pump, a manually operated six-port injection valve (Rheodyne) and an R-401 differential refractometer (Waters). The column was Nucleosil $5C_{18}$ (250 × 4 mm I.D.) (Macherey–Nagel) with a particle diameter of 5 μm. The mobile phase was acetonitrile–water (43:57, v/v) at a flow-rate of 0.5 ml/min. A 20-μl volume of a 10% polymer solution was injected for each separation.

The SEC investigations were performed on five 300 × 8 mm I.D. columns of Ultrastyragel, 1000 Å, 2 × 500 Å and 2 × 100 Å (Waters), using tetrahydrofuran (THF) as the mobile phase at a flow-rate of 1 ml/min. A Model R-410 refractive index detector (Waters) and a Model 501 pump (Waters) were used; the molar mass calculations were based on polyethylene oxide calibration standards. Volumes of 200 μl of 0.1% (w/w) polymer solutions were injected via a Rheodyne six-port injection valve.

The block polymer was prepared at the Central Institute of Organic Chemistry, Berlin, by anionic polymerization at 110°C using potassium glycolate as initiator.

RESULTS AND DISCUSSION

Polyethylene oxide (PEO) and polypropylene oxide (PPO) and their block polymers are important precursors of polyurethanes. Their detailed chemical structure, *i.e.*, the chemical composition, block length and molar mass of the individual blocks, may be decisive for the properties of the final product.

It was shown previously [9,10] that in block

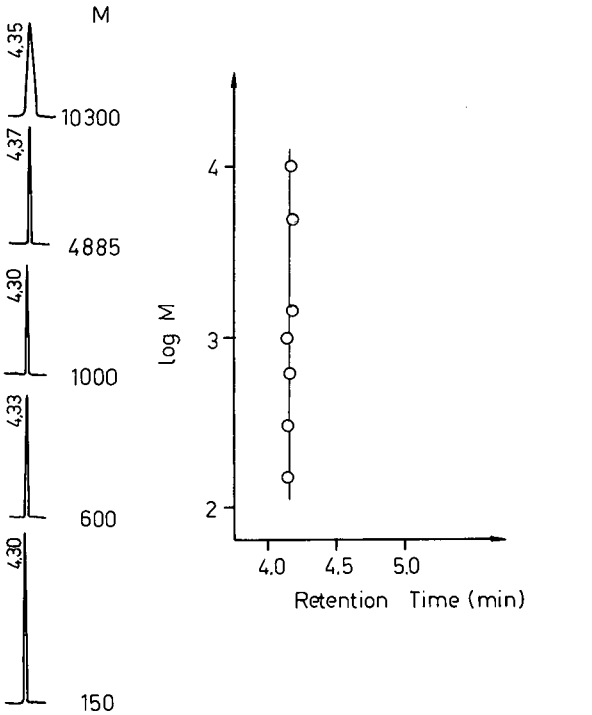

Fig. 1. HPLC of polyethylene oxide calibration standards at the critical point of adsorption and the corresponding critical diagram. Column, Nucleosil $5C_{18}$; mobile phase, acetonitrile–water (43:57, v/v); flow-rate, 0.5 ml/min; refractive index detection.

polymers the individual blocks may be characterized independently using liquid chromatography at the critical point of adsorption. Operating at the critical point of one block, the other block may be analysed and structural parameters may be calculated.

The mobile phase composition corresponding to the critical conditions for PEO was found to be acetonitrile–water (42:58, v/v) on a Chrompack RP-18 stationary phase [9]. As the present investigations were carried out on a Macherey–Nagel $5C_{18}$ column, the composition of the mobile phase had to be adjusted accordingly. Polyethylene oxide calibration standards of different molar masses were separated using acetonitrile–water of varying composition. The disappearance of the molar mass dependence of the retention time, corresponding to the critical conditions, was achieved at a composition of the mobile phase of acetonitrile–water (43:57, v/v); see Fig. 1.

Under these conditions a triblock polymer of ethylene oxide and propylene oxide, $HO(EO)_{n_1}(PO)_m(EO)_{n_2}OH$, was separated into fractions of different degrees of polymerization with respect to propylene oxide, regadless of the length of the ethylene oxide blocks (see Fig. 2). The assignment of the peaks was based on comparison with the chromatogram of a polypropylene oxide. The elution order and the retention time behaviour of the fractions, which are in agreement with the theoretically estimated distribution coefficient $K_d^{(m)} = [K_d^{(1)}]^m$ (see Part I [9]), where m is the degree of polymerization with respect to propylene oxide, suggests that the assignment given in Fig. 2 is correct.

The first peak corresponds to $m = 1$–3, the shoulder to $m = 4$, the peak at 2.5 ml to $m = 5$ and so on. Accordingly, every peak is uniform with respect to m but has a distribution in block length with respect to the polyethylene oxide blocks (n). Assuming that the refractive index responses of polyethylene oxide and polypropylene oxid oligomer series are similar, the amounts of fractions 1–8 may be determined (see Table I).

A complete picture of the microstructure of the block polymer can be provided by separating the fractions preparatively and subjecting them to a second chromatographic method. This method must separate the propylene oxide uniform fractions according to the oligomer distribution of the ethylene oxide blocks, thus providing the molar mass or

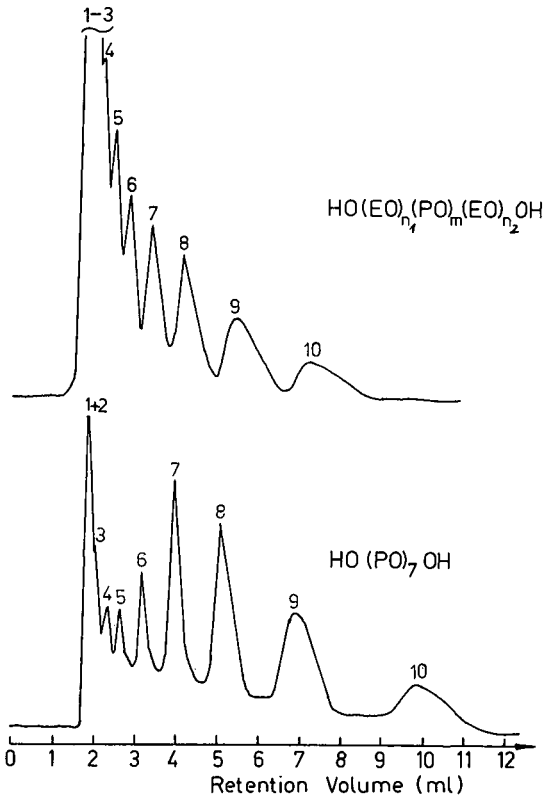

Fig. 2. HPLC of the block polymer. Chromatographic conditions as in Fig. 1.

TABLE I

RELATIVE AMOUNTS OF FRACTIONS 1–8 AFTER SEPARATION AT THE CRITICAL POINT OF ADSORPTION OF PEO

Fraction	m	Composition	Relative amount (%, v/v)
1	1	$HO(EO)_{n_1}(PO)(EO)_{n_2}OH$	41.9
	2	$HO(EO)_{n_1}(PO)_2(EO)_{n_2}OH$	
	3	$HO(EO)_{n_1}(PO)_3(EO)_{n_2}OH$	
2	4	$HO(EO)_{n_1}(PO)_4(EO)_{n_2}OH$	2.5
3	5	$HO(EO)_{n_1}(PO)_5(EO)_{n_2}OH$	8.5
4	6	$HO(EO)_{n_1}(PO)_6(EO)_{n_2}OH$	10.1
5	7	$HO(EO)_{n_1}(PO)_7(EO)_{n_2}OH$	12.1
6	8	$HO(EO)_{n_1}(PO)_8(EO)_{n_2}OH$	13.9
7	9	$HO(EO)_{n_1}(PO)_9(EO)_{n_2}OH$	9.0
8	10	$HO(EO)_{n_1}(PO)_{10}(EO)_{n_2}OH$	2.0

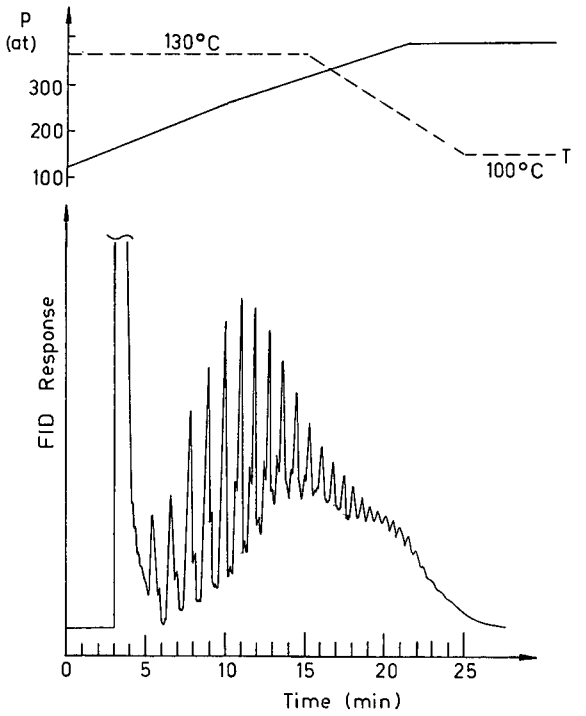

Fig. 3. SFC of fraction 1. Column, SB Biphenyl-30; mobile phase, carbon dioxide; FID.

block length distribution of the ethylene oxide blocks.

In previous investigations on the two-dimensional separation of telechelic oligomers, it was demonstrated that SFC is a very useful technique for separating polyethers according to their oligomer distribution [11,12]. Using highly efficient and selective capillary columns, oligomers may even be separated simultaneously according to the degree of polymerization and functionality.

Fig. 3 shows the SFC of fraction 1 using a pressure and temperature gradient. The oligomers are well separated and it can be seen that, in addition to the main oligomer series, peaks of minor intensity are also obtained. This is in agreement with our assumption that fraction 1 is a superposition of the oligomer series with $m = 1, 2, 3$. Based on the reaction mechanism and the retention behaviour of the fraction, it was concluded that the major peaks belong to the oligomer series with $m = 3$.

Using the same chromatographic conditions, fractions 3–8 were separated into their oligomers (see

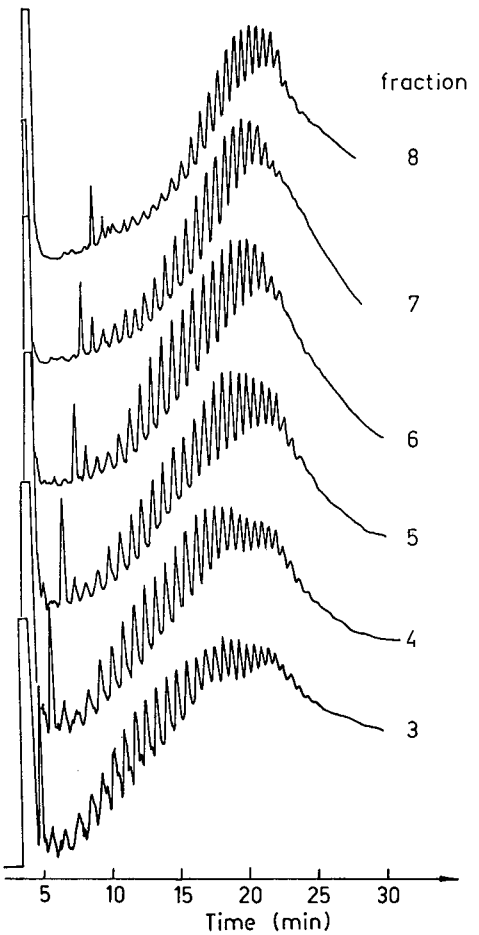

Fig. 4. SFC of fractions 3–8. Chromatographic conditions as in Fig. 3.

TABLE II

COMPARISON OF SFC RETENTION TIMES OF THE FIRST PEAKS IN FRACTIONS 3–8 WITH A COMMERCIAL PPO

n	Retention time (min)	
	$HO(^{D}O)_nOH$	First peak
5	4.57	4.77 (fraction 3)
6	5.18	5.40 (fraction 4)
7	6.00	6.15 (fraction 5)
8	6.85	6.93 (fraction 6)
9	7.62	7.67 (fraction 7)
10	8.30	8.32 (fraction 8)

TABLE III

PEAK ASSIGNMENT IN SFC OF FRACTIONS 1–8 OF THE BLOCK POLYMER $HO(EO)_{n_1}(PO)_m(EO)_{n_2}OH$

$n_1 + n_2$	Retention time (min)						
	1 ($m = 3$)	3 ($m = 5$)	4 ($m = 6$)	5 ($m = 7$)	6 ($m = 8$)	7 ($m = 9$)	8 ($m = 10$)
0	[a]	4.77	5.40	6.15	6.93	7.67	8.32
1	4.48	5.52	6.32	7.10	7.83	8.50	9.12
2	5.32	6.33	7.28	7.88	8.67	9.30	9.85
3	6.52	7.40	8.10	8.77	9.47	10.10	10.62
4	7.75	8.33	8.95	9.58	10.17	10.90	11.30
5	8.90	9.22	9.82	10.38	10.95	11.55	12.00
6	9.95	10.03	10.62	11.17	11.73	12.25	12.70
7	10.88	10.83	11.42	11.93	12.50	13.00	13.40
8	11.80	11.63	12.20	12.70	13.28	13.75	14.08
9	12.67	12.43	12.97	13.47	14.07	14.52	14.80
10	13.53	13.20	13.73	14.24	14.83	15.27	15.53
11	14.37	13.97	14.48	14.97	15.58	16.00	16.20
12	15.18	14.72	15.25	15.72	16.32	16.72	16.85
13	15.97	15.48	15.95	16.42	17.00	17.38	17.48
14	16.70	16.20	16.63	17.10	17.67	18.02	18.07
15	17.38	16.88	17.27	17.73	18.30	18.63	18.65
16	18.02	17.52	17.88	18.33	18.90	19.23	19.20
17	18.60	18.15	18.48	18.92	19.47	19.80	19.73
18	19.05	18.73	19.08	19.48	20.03	20.37	20.25
19	19.52	19.28	19.65	20.02	20.58	20.95	20.75
20	20.02	19.83	20.18	20.55	21.13	21.45	21.28
21	20.97	20.38	20.68	21.05	21.62		21.78

[a] Eluted with solvent peak.

Fig. 4). These fractions consisted nearly exclusively of one oligomer series each, indicating that the preparative separation was of good quality. Because of its low concentration and the poor separation quality, fraction 2 could not be characterized by SFC. The assignment of the peaks was based on comparison with chromatograms of PPO and the retention behaviour of PEO. Thus, the first intense peak after the solvent peak in each chromatogram was identified as the propylene oxide oligomer without ethylene oxide units. The comparison of the retention times of the first peaks with a commercial PPO in Table II shows good consistency. The next peaks in the chromatograms may then be assigned to the oligomers containing one, two, three, and so on, ethylene oxide units. Because of the high chemical similarity, SFC did not resolve oligomers of the same gross composition but different ethylene oxide distribution, *e.g.*, $HO(EO)_4(PO)_m(EO)_2OH$ and $HO(EO)_3(PO)_m(EO)_3OH$. The complete assignment of the peaks is summarized in Table III.

One of the major problems in SFC is quantification. Normally, using FID the signal depends not only on the amount of the eluted component but also on its composition and chemical structure. However, in a number of instances, namely for homologuous series, the FID response may be calculated using increment methods [13]. As was shown in a previous investigation [12], relative mass response (*RMR*) numbers of structural units may be combined to give the relative FID response of a certain molecule:

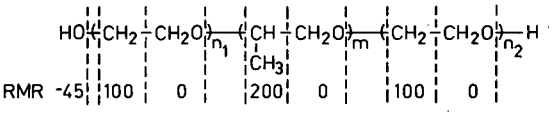

$$RMR = 200\ m - 45 + 100(n_1 + n_2)$$

Accordingly, the *RMR* numbers for every oligomer may be calculated by the following formulae:

Fraction	m	RMR
1	3	$555 + 100(n_1 + n_2)$
2	4	$755 + 100(n_1 + n_2)$
3	5	$955 + 100(n_1 + n_2)$
4	6	$1155 + 100(n_1 + n_2)$
5	7	$1355 + 100(n_1 + n_2)$
6	8	$1555 + 100(n_1 + n_2)$
7	9	$1755 + 100(n_1 + n_2)$
8	10	$1955 + 100(n_1 + n_2)$

From the relative response of each component and the peak area in the SFC trace, the number of molecules n_i and the molar mass averages (M_n = number-average molar mass; M_w = weight-average molar mass) may be calculated:

$$n_i = A_i/RMR_i$$
$$M_n = \Sigma\, n_i M_i / \Sigma\, n_i$$
$$M_w = \Sigma\, n_i M_i^2 / \Sigma\, n_i M_i$$

As can be seen from the chromatograms, the lower oligomers of each homologuous series are separated very well by SFC. Therefore, the area of every peak may be determined quantitatively. As for the higher oligomers, where complete separation could not be achieved, quantification was carried out in the SEC mode. For each fraction a separate calibration graph of log M *vs.* retention time was used, based on the retention times of the lower oligomers, and extrapolated towards higher molar masses (see Fig. 5).

Using this approach, the molar mass averages of the fractions were calculated and are summarized in Table IV. In addition, from the concentration of the individual oligomers the average block length $n_1 + n_2$ with respect to ethylene oxide was determined.

In order to verify the accuracy of these calculations, an M_n value for the total sample was calculated and compared with M_n values obtained independently by SEC and NMR:

critical chromatography/SFC	$M_n = 870$
SEC (calibration with PEO)	$M_n = 940$
^{13}C NMR	$M_n = 1100$

Taking into account, that the quantification in SFC was based on increment schemes and extrapolation was necessary for the quantification of the higher-molar-mass oligomers, the results of two-dimensional separation critical chromatography *vs.* SFC are consistent with the SEC and NMR data.

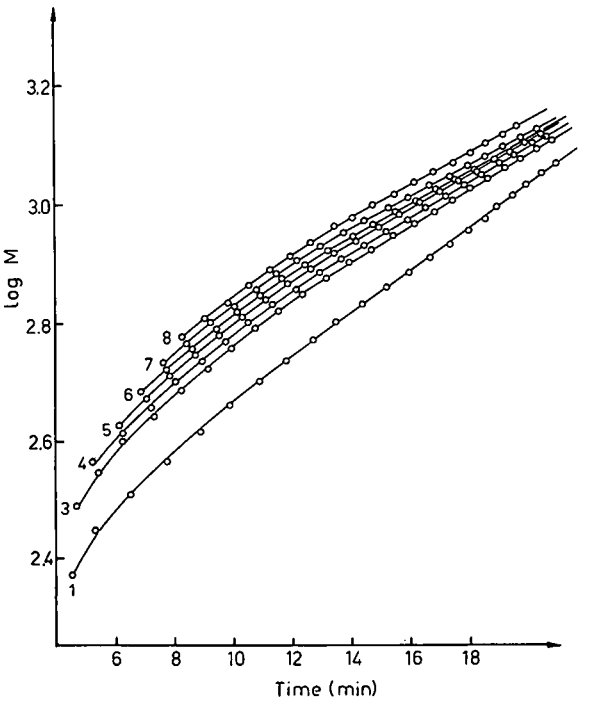

Fig. 5. SFC calibration graphs of log M *vs.* retention time for fractions 1–8.

For additional support of the results, another two-dimensional separation, but in this instance

TABLE IV

STRUCTURAL PARAMETERS OF THE BLOCK POLYMER FRACTIONS CALCULATED FROM SFC DATA, TWO-DIMENSIONAL SEPARATION CRITICAL CHROMATOGRAPHY *VS.* SFC

Fraction	$HO(EO)_{n_1}(PO)_m(EO)_{n_2}OH$		Composition	
	M_n	M_w	m	$n_1 + n_2$
1	640	770	3	10.3
3	940	1100	5	14.4
4	990	1110	6	14.1
5	1070	1170	7	14.7
6	1140	1220	8	15.0
7	1220	1290	9	15.4
8	1270	1320	10	15.2

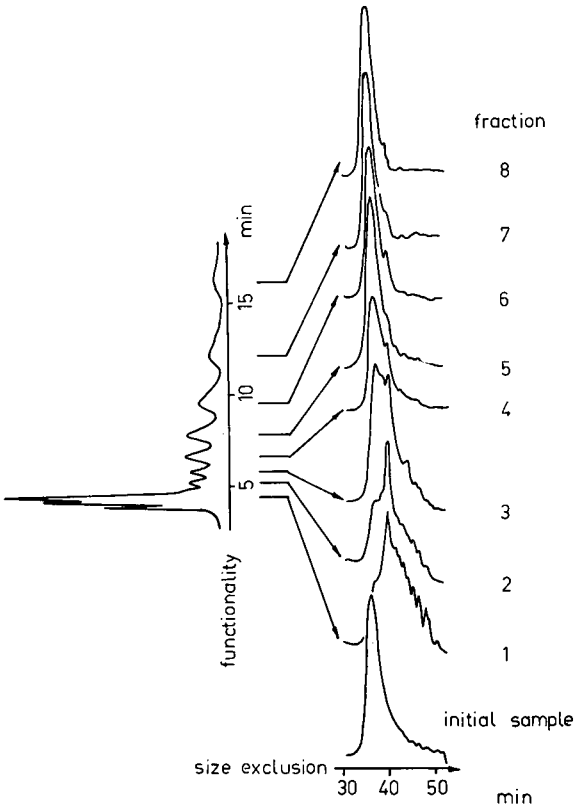

Fig. 6. Two-dimensional separation: critical chromatography *vs.* SEC of the block polymer.

critical chromatography *vs.* SEC, was performed. Again fractions were collected that were uniform with respect to the polypropylene oxide block (see Fig. 6). The fractions were subjected to SEC and the molar mass averages were calculated using a PEO calibration graph. Comparing these results with the values from the SFC experiments (see Tables IV and V), it was found that the M_w values of fractions 6–9 are significantly lower for the SFC experiments. This again might be due to poor resolution of the higher molar mass oligomers in SFC. However, comparing the calculated molar mass averages for the total sample, good agreement was obtained.

	M_n	M_w
critical chromatography *vs.* SFC	870	950
critical chromatography *vs.* SEC	830	1170

TABLE V

MOLAR MASS AVERAGES OF THE BLOCK POLYMER FRACTIONS CALCULATED FROM SEC DATA, TWO-DIMENSIONAL SEPARATION CRITICAL CHROMATOGRAPHY *VS.* SEC

Fraction	m	M_n	M_w
1	3	550	780
2	4	660	940
3	5	879	1050
4	6	900	1230
5	7	990	1500
6	8	1120	1680
7	9	1320	1780
8	10	1350	1820

CONCLUSIONS

Liquid chromatography at the critical point of adsorption has been shown to be a unique method for the separation of $A_nB_mA_n$ block polymers. Operating at the critical conditions of the first block the second block may be characterized according to the molar mass and block length. Using a second chromatographic method, preparatively separated fractions may be analysed with respect to the first block. Hence quantitative data on the molar mass distribution and the block length of the individual blocks may be obtained. Further investigations will focus on improving the accuracy and reproducibility of the chromatographic techniques. It would then be possible to determine block length distributions of the individual blocks.

REFERENCES

1 G. Glöckner, *Trends Anal. Chem.*, 7 (1988) 169.
2 S. Mori, Y. Uno and M. Suzuki, *Anal. Chem.*, 58 (1986) 303.
3 S. G. Entelis, V. V. Evreinov and A. V. Gorshkov, *Adv. Polym. Sci.*, 76 (1986) 129.
4 S. G. Entelis, V. V. Evrienov and A. I. Kuzaev, *Reactive Oligmers*, Khimiya, Moscow, 1988.
5 A. V. Gorshkov, V. V. Evreinov and S. G. Entelis, *Zh. Fiz. Khim.*, 59 (1985) 958.
6 A. V. Gorshkov, V. V. Verenikh and V. V. Evreinov, *Chromatographia*, 26 (1988) 338.

7 G. Schulz, H. Much, H. Krüger and C. Wehrstedt, *J. Liq. Chromatogr.*, 13 (1990) 1745.
8 A. V. Gorshkov, T. N. Prudskova, V. V. Guryakova and V. V. Evreinov, *Polym. Bull.*, 15 (1986) 465.
9 A. V. Gorshkov, H. Much, H. Becker, H. Pasch, V. V. Evreinov and S. G. Entelis, *J. Chromatogr.*, 523 (1990) 91.
10 H. Pasch, H. Much, G. Schulz and A. V. Gorshkov, *LC · GC Int.*, 5 (1992) 38.
11 H. Pasch, H. Krüger, H. Much and U. Just, *J. Chromatogr.*, 589 (1992) 295.
12 H. Pasch, H. Krüger, H. Much and U. Just, *Polymer*, (1992) in press.
13 R. G. Ackman, *J. Gas Chromatogr.*, 2 (1964) 173.

Journal of Chromatography, 623 (1992) 323–328
Elsevier Science Publishers B.V., Amsterdam

CHROM. 24 425

Analysis of synthetic mixtures of waxes by supercritical fluid chromatography with packed columns using evaporative light-scattering detection

S. Brossard, M. Lafosse and M. Dreux

Laboratoire de Chimie Bioorganique et Analytique (LCBA), URA CNRS 499, Université d'Orléans, B.P. 6759, 45067 Orléans Cedex 2 (France)

(First received March 17th, 1992; revised manuscript received June 10th, 1992)

ABSTRACT

The analysis of waxes, the basis of numerous cosmetic products, is frequently carried out by gas chromatography. Unfortunately, the chromatographic "fingerprints" are very complex and sometimes abnormal compositions, a sign of "doping" of waxes, remain undetected. The object of this study by supercritical fluid chromatography with packed columns was to select chromatographic conditions that characterize the majority of the different wax families and not a separation according to the hydrocarbon chain for a given family.

INTRODUCTION

Natural waxes, which are very complex mixtures mainly consisting of hydrocarbons, esters, triglycerides, alcohols and acids with long-chain alkyl groups in the range C_{20} to $>C_{50}$ (straight, branched, saturated or unsaturated), are commonly used in the cosmetics industry because of their many advantageous properties. The compositions of different waxes such as candellila or carnauba have long been known [1,2]. Their analysis by gas chromatography (GC), is often carried out on capillary [3] or packed columns [1,4], but the chromatograms remain exceedingly complex. The systematic identification of each component is lengthy and sometimes impossible. This technique often requires the derivatization of the more polar components, so that alcohols are frequently converted into their acetate derivatives after treatment with acetic anhydride and acids into their methyl esters after treatment with diazomethane [1–6]. Moreover, insufficient volatility of certain components such as triglycerides requires working at high temperatures, adding the risk of degradating certain thermally labile compounds.

Different synthetic mixtures of waxes have been analysed by supercritical fluid chromatography (SFC) using packed columns, the first objective being to obtain the chromatographic "fingerprint" whereby each family of solutes is represented by a single signal, the total representing the bulk characteristics. For this reason, the system had to be capable of resolving the functional groups and not the methylene groups.

Constituent waxes are either slightly UV absorbing or do not absorb at all. It is also necessary to use universal detection in order to avoid the preliminary derivatization steps. Evaporative light-scattering detection (ELSD) seemed to be suitable for this type of study because of its compatibility with SFC [7–9]. Also, contrary to the frequently used flame ionization detection (FID), it is possible to add one or several polar modifiers to the supercritical carbon dioxide to elute all wax compounds without any residue problems.

Correspondence to: Dr. M. Lafosse, Laboratoire de Chimie Bioorganique et Analytique (LCBA), URA CNRS 499, Université d'Orléans, B.P. 6759, 45067 Orléans Cedex 2, France.

0021-9673/92/$05.00

This paper discusses the influence of different parameters such as stationary phases, temperature and chromatographic column pressure on the elution of synthetic wax mixtures.

EXPERIMENTAL

Two sets of apparatus were used, as described below.

First apparatus

The SFC apparatus was set up as follows. Carbon dioxide was pumped with a Waters (Milford, MA, USA) Model M 501 pump. An ethanol cooling bath was used to cool the pump head in order to increase the pump-down efficiency. A polar modifier was added using a Jasco (Tokyo, Japan) Model 2510 pump. The two solvents were mixed at a controlled temperature (Jasco 860-CO oven) in a dynamic mixing chamber (Knauer, Berlin, Germany). A Rheodyne (Touzart et Matignon, France) Model 7125 injection valve, with a 20-μl loop, and the column were placed in the Jasco oven. A Touzart et Matignon Model 45 evaporative light-scattering detector with the interface adjusted to SFC was used.

Second apparatus

Carbon dioxide was pumped with a Gilson (Villiers-le-Bel, France) Model 305 piston pump. An ethanol cooling bath was used to cool the pump head. The polar modifier was added using a Gilson Model 306 piston pump. The two solvents were mixed at ambient temperature in a Gilson Model 811 mixer. A Gilson Model 821 pressure regulator, controlled by the Model 305 pump, was placed between the column and the restrictor. A Rheodyne Model 7125 injection valve with a 20-μl loop and the column were placed on the outside of the Knauer oven. A Touzart et Matignon Model 45 evaporative light-scattering detector was used.

Chromatographic column

Various stationary phases and columns were used: 7-μm LiChrosorb diol (250 mm × 7 mm I.D.); 5-μm LiChrosorb diol (150 mm × 4.6 mm I.D.); 5-μm LiChrospher 100 diol (125 mm × 4 mm I.D.) (Merck, Darmstadt, Germany); and 5-μm Zorbax diol (250 mm × 9.4 mm I.D.) (DuPont, Wilmington, DE, USA).

Chemicals and reagents

Carbon dioxide was of B 50 grade purchased from Air Liquide (Paris, France). 2-Propanol (SDS, Peypin, France) and acetone (Fisons, Loughborough, UK) were of HPLC grade and other polar modifiers were of analytical-reagent grade. Triglyceride (tripalmitine and tristearine in mixture) and stearic acid solutes were purchased from Fluka (Buchs, Switzerland), stearic alcohol from Baker (Deventer, Netherlands) and cetyl myristate from Fluka.

RESULTS AND DISCUSSION

The initial analysis and characterization of waxes were limited to determining the main components according to each chemical group rather than its alkyl chain length. Polar stationary phases were chosen even when the amount of the apolar solutes remained predominant in each family because selectivity, according to the apolar function, is poor on these phases, and therefore advantageous in the analysis of the more polar groups. Using bare silica columns involved long equilibrium times, so diol-bonded silicas (Zorbax, LiChrosorb, LiChrospher) were employed.

The first studies were carried out using carbon dioxide at a constant flow-rate of 3 ml/min (see Experimental, first apparatus). Working pressure was maintained by a specially made outlet restrictor of fused silica placed between the chromatographic column and the detector which nebulizes the fluid at its end. This system, recently employed in several studies, was preferred to Guthrie tubing [10], which is brittle, tends to clog and often requires replacement. The addition of an organic modifier to the carbon dioxide (acetone, 2-propanol, formic acid) permitted the elution of less polar compounds such as esters, triglycerides and the more polar compounds such as alcohols and acids. In spite of this and because of weak retentions of esters and triglycerides on an analytical-size column, wider diameter columns were necessary for better resolutions. The greater phase volume of these columns made it possible to vary the amount (x%) of organic modifier within a close range, thus avoiding large retentions of the more polar compounds where x was too low and too rapid elution where x was very high. Consequently, small variations in the organic modifier content help to avoid major variations in pressure and eluent density.

As shown in Fig. 1a and b, on the Zorbax diol column, an increase in 2-propanol content of the mobile phase was necessary to elute the esters, triglycerides and alcohols. On the other hand, too much 2-propanol, needed to elute the organic acid in isocratic elution, brought the risk of mixing the other three components with too rapid elution. Moreover, the peak shape of this acid was asymmetric, indicating strong adsorption. Berger and Deye [11] have recently shown that polar organic acids, such as certain basic solutes such as amines, were difficult to elute by packed-column SFC. By adding a small amount of a strong acid such as formic acid to the mobile phase, the interactions of the residual silanol groups of the stationary phase with the analytes were decreased, resulting in their elution with a good peak shape without eluting the other solutes too rapidly (Fig. 1c).

Selectivity between the four probe solutes had to be improved so that each chromatographic peak could represent a family having any hydrocarbon chain length. Therefore, acetone was tried as modifier instead of 2-propanol because of its lowest hydrogen bond solubility parameter (δ_h = 3.4 [12]) than that of 2-propanol (8.0) and its higher dipole–dipole solubility parameter (δ_p = 5.1) than that of 2-propanol (3.0). From a comparison of Figs. 2a and 1b, it can be concluded that acetone had a lower eluent strength than 2-propanol and the acid solute was not eluted. In the same way, as shown in Fig. 1c, this modifier necessitated adding a small amount of formic acid (Fig. 2b). In this instance, the same effect was obtained as with 2-propanol and the acid was eluted without changing the selectivity of the other three solutes.

In addition, if we compare the selectivities α (Table I) relating to the ester from Figs. 1c and 2b, the following observations can be made: acetone as a polar modifier eluted the carbonyl derivatives such

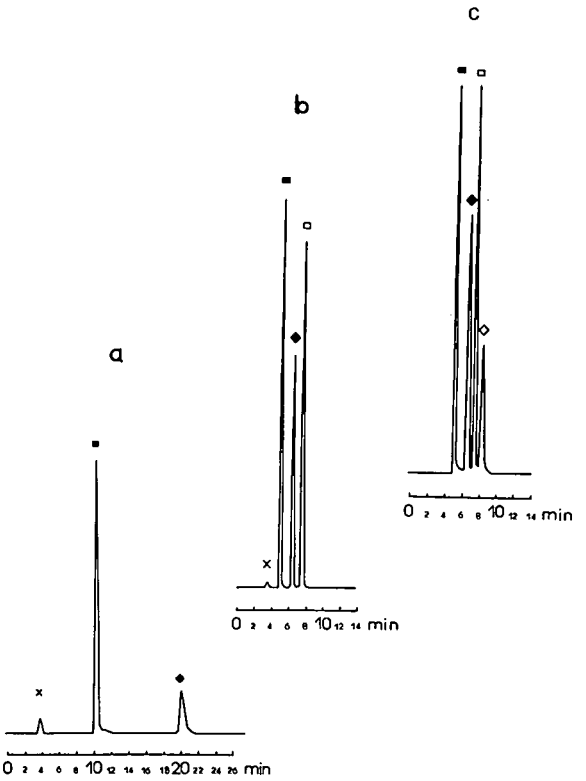

Fig. 1. Separation of (■) cetyl myristate, (◆) triglycerides (cetyl and octadecyl chain in mixture), (□) stearylic alcohol, (◇) stearic acid and (×) chloroform (injection solvent). Chromatographic conditions: column, Zorbax diol (250 mm × 9.4 mm I.D.); mobile phase, (a) carbon dioxide–2-propanol (96.8:3.2, w/w), (b) carbon dioxide–2-propanol (91:9, w/w) and (c) carbon dioxide–2-propanol–formic acid (90.9:8.8:0.3, w/w/w); flow-rate, 3.3 ml min^{-1}; pressure, 130 bar; detection, ELSD.

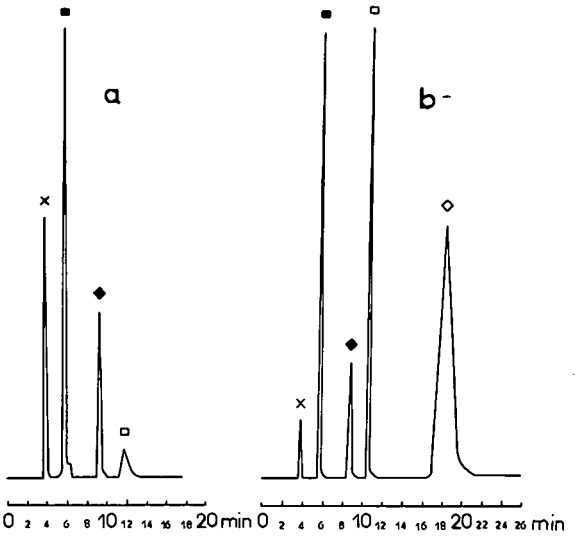

Fig. 2. Separation of (■) cetyl myristate, (◆) triglycerides (cetyl and octadecyl chain in mixture), (□) stearylic alcohol, (◇) stearic acid and (×) chloroform (injection solvent). Chromatographic conditions: column, Zorbax diol (250 mm × 9.4 mm I.D.); mobile phase, (a) carbon dioxide–acetone (91:9, w/w), (b) carbon dioxide–acetone–formic acid (90.9:8.8:0.3, w/w/w); flow-rate, 3.3 ml min^{-1}; pressure, 130 bar; detection, ELSD.

TABLE I

SELECTIVITY RELATING TO THE ESTER

For chromatographic conditions, see Figs. 1c and 2b.

Organic modifier	Content (%)	α		
		Triglycerides	Alcohol	Acid
2-Propanol	8.80	2.13	2.72	3.42
Acetone	8.80	2.66	3.60	7.70

as 2-propanol (see Table I, $\alpha_{triglycerides/ester}$ have similar values) and 2-propanol eluted the hydroxyl derivatives (alcohol and acid) more easily than acetone (see Table I). These remarks have to be considered in relation to the aforementioned components of the solubility parameters.

To avoid adding formic acid in the mobile phase, a few other diol-bonded silicas phases were tried, especially LiChrosorb in a wide-diameter column. As shown in Fig. 3, the four components were eluted with the carbon dioxide–2-propanol binary mixture and the retention decreased with an increase in 2-propanol content. With a 4.68% 2-propanol content an excellent separation was efficiently obtained (Fig. 4) in about 11 min with a reduced plate height (h/d_p) of 5 (where h and d_p are the plate height and particle size, respectively). The asymmetry factor, A_s, measuring the tailing band at 10% of the acid peak height decreases from 5 to 3 when the 2-propanol content varies from 3.17 to 4.68%.

In certain waxes where the more polar compounds such as triglycerides, alcohols and acids are in the minority, it is difficult to determine their concentrations when the less apolar components such as hydrocarbons and esters are predominant. For this reason, it is advisable to isolate the less polar derivatives in order to obtain a richer mixture. This extraction must be carried out with carbon dioxide in order to circumvent contamination by the solvents.

The following two modifications were made to avoid too long retention times on these diol-bonded silicas using carbon dioxide: wider diameter columns (250 mm × 9.4 or 7 mm I.D.) were replaced with analytical-size columns (150 mm × 4.6 mm I.D. or 125 mm × 4 mm I.D.); and a programmable Gilson pressure regulator (see Experimental, second apparatus) ensuring mobile phase flow and a constant pressure was placed at the column outlet just

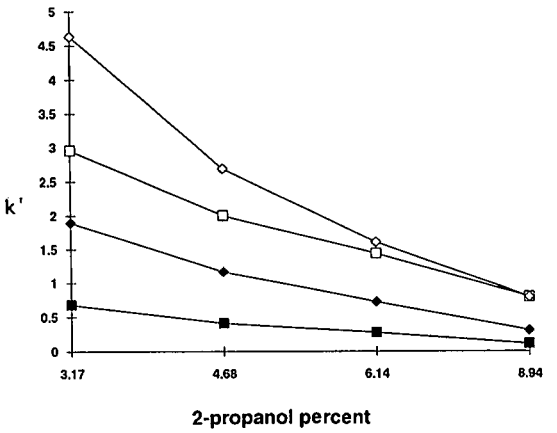

Fig. 3. Graph of *k' versus* percentage of 2-propanol. ■ = Cetyl myristate; ◆ = triglycerides (cetyl and octadecyl chain in mixture); □ = stearylic alcohol; ◇ = stearic acid. Chromatographic conditions: column, LiChrosorb diol (250 mm × 7 mm I.D.); mobile phase, carbon dioxide–2-propanol; flow-rate, 3.3 ml min^{-1}; pressure, 130 bar; detection, ELSD.

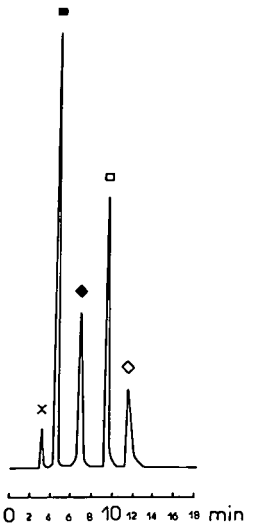

Fig. 4. Separation of (■) cetyl myristate, (◆) triglycerides (cetyl and octadecyl chain in mixture), (□) stearylic alcohol, (◇) stearic acid and (×) chloroform. Chromatographic conditions: column, LiChrosorb diol (250 mm × 7 mm I.D.); mobile phase, carbon dioxide–2-propanol (95.3:4.7, w/w); flow-rate, 3 ml min^{-1}; pressure, 140 bar; detection, ELSD.

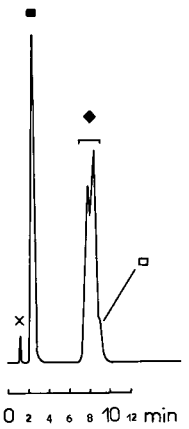

Fig. 5. Separation of (■) cetyl myristate, (◆) triglycerides (cetyl and octadecyl chain in mixture), (□) stearylic alcohol and (×) chloroform. Chromatographic conditions: column. LiChrosorb diol (150 mm × 4.6 mm I.D.); mobile phase, pressure gradient from 150 bar carbon dioxide (flow-rate 3 ml min^{-1}) to 250 bar carbon dioxide (flow-rate 4 ml min^{-1}) in 25 min; detection, ELSD.

ahead of the restrictor; because of this regulator, the carbon dioxide density and therefore its polarity could vary within wide ranges.

After a preliminary study on the satisfactory LiChrosorb diol support, we observed (Fig. 5) poor selectivities of the triglycerides and alcohols, and the acids were not eluted. However, the beginning of a triglyceride separation according to its alkyl chain length was noted. LiChrospher diol, a similar but spherical support, was chosen with seemingly more success because all four families of the components could be eluted. Fig. 6, showing the effect of the pressure on the capacity factor (k') variation, indicates that, at low pressure (166 bar), the ester was easily eluted whereas the triglycerides and acids were not fully separated. Their retentions were high and their asymmetry factor, A_s, too great. Note here the retention inversion in Fig. 4. At high pressure (290 bar), retentions decreased and no alcohols or triglycerides were separated. By programming the pressure regulator (Fig. 7), it was possible to elute the ester at low pressure and the other three polar components under higher pressures with good resolutions.

Temperature was the final parameter to be studied. Similarly to liquids, a solute at any given temperature is more soluble in a supercritical fluid than in a gas. What we observed here is different from the aforementioned effects of temperature on retentions. Huston and Berhard [13] explained that

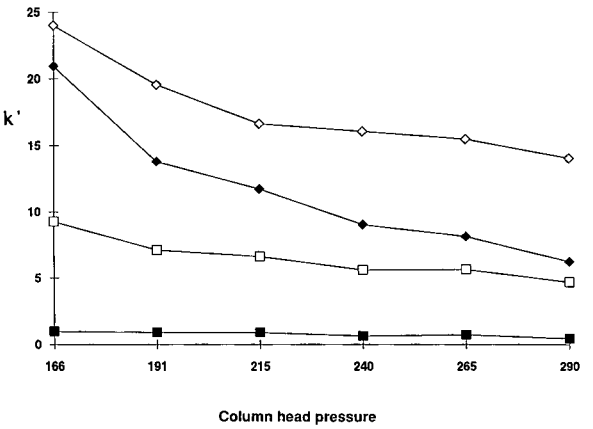

Fig. 6. Graph of k' *versus* pressure (bar). ■ = Myristyl myristate; ◆ = triglycerides (cetyl and octadecyl chain in mixture); □ = stearylic alcohol; ◇ = stearic acid. Chromatographic conditions: column, LiChrospher diol (125 mm × 4 mm I.D.); mobile phase, carbon dioxide; flow-rate, 3 ml min^{-1}; detection, ELSD.

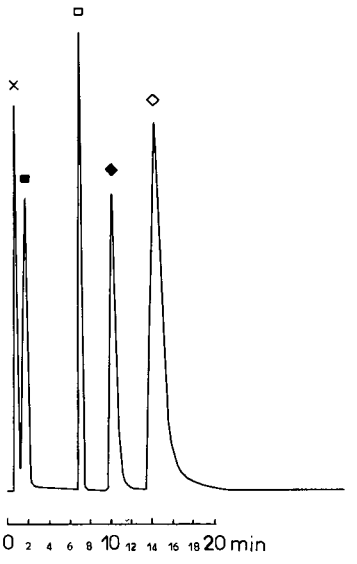

Fig. 7. Separation of (■) myristyl myristate, (□) stearylic alcohol, (◆) triglycerides (cetyl and octadecyl chain in mixture), (◇) stearic acid and (×) chloroform. Chromatographic conditions: column, LiChrospher diol (125 mm × 4 mm I.D.); mobile phase, pressure gradient from 140 to 275 bar in 10 min; flow-rate, 3 ml min^{-1}; detection, ELSD.

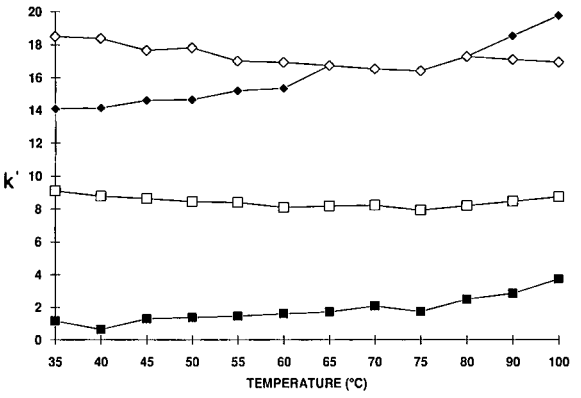

Fig. 8. Graph of k' *versus* temperature. ■ = Cetyl myristate; □ = stearylic alcohol; ◆ = triglycerides (cetyl and octadecyl chain in mixture); ◇ = stearic acid. Chromatographic conditions: column, LiChrospher diol (125 mm × 4 mm I.D.); mobile phase, carbon dioxide; flow-rate, 3 ml min^{-1}; column head pressure, 166 bar; detection, ELSD.

such a curve shows a maximum. When the temperature increases, the mobile phase density decreases. In the first part of the curve, increased retention was caused by a decrease in the solubility of the solute in the mobile phase. In the second part of the curve, beyond the retention maximum temperature, while solubility continued to decrease, a higher temperature caused an increase in volatility and so the solutes were not retained as much. A smaller variation in selectivity for the triglycerides–stearic acid solute pair could be observed from 65°C upwards (Fig. 8). None of the previous temperature effects were noted, with the only difference being that these studies were carried out with capillary columns. In conclusion, a slight evolution of the k' values indicates that temperature has less influence than pressure. The best selectivities may be obtained by working at temperatures lower than 60°C or higher than 90°C. As high temperatures are not desirable for long-term column stability and because of thermal degradation of the solutes, all subsequent experiments were performed at 45°C.

CONCLUSIONS

From these preliminary studies on polar stationary phases, chromatographic systems have been developed that make it possible to identify the main component types encountered in waxes.

The two systems employed were as follows: without pressure programming, 7-μm LiChrosorb diol column (250 mm × 7 mm I.D.), mobile phase carbon dioxide–2-propanol (96.83:3.17, w/w), flow-rate 3.1 ml min^{-1} and pressure 124 bar; and with pressure programming, 5-μm LiChrospher 100 diol column (125 mm × 4 mm I.D.), mobile phase carbon dioxide pressure initially 165 bar and flow-rate 3 ml min^{-1} to 10 min pressure 290 bar and flow-rate 3 ml min^{-1}. The latter system appears to be the most advantageous owing to a shortened column equilibrium time and the fact that FID can be used.

The application of the above method to the analysis of commercial waxes is in progress but it will probably require supercritical extraction of the major components of waxes such as hydrocarbons (not treated here) and esters in order to achieve the preconcentration of the minor species, namely triglycerides, alcohols and acids.

ACKNOWLEDGEMENT

This thesis work (S. Brossard) was supported by a grant provided by Laboratoires Parfums Christian Dior, Saint-Jean-de-Braye, France.

REFERENCES

1 A. P. Tulloch, *J. Am. Oil. Chem. Soc.*, 50 (1973) 367.
2 A. P. Tulloch, *Cosmet. Perfum.*, 89 (1974) 53.
3 S. B. Hawthorne and D. J. Miller, *J. Chromatogr.*, 388 (1987) 397.
4 J. F. Lawrence, J. R. Iyengar, B. D. Page and H. B. S. Conacher, *J. Chromatogr.*, 236 (1982) 403.
5 R. P. Phadke, K. Shakuntala Nair and U. Nandedkar, *Indian Bee J.*, 33 (1971) 3.
6 G. Valmalle and A. Karleskind, *Rev. Fr. Corps Gras*, 4 (1977) 203.
7 D. Nizery, D. Thiébaut, M. Caude, R. Rosset, M. Lafosse and M. Dreux, *J. Chromatogr.*, 467 (1989) 49.
8 M. Lafosse, P. Rollin, C. Elfakir, L. Morin-Allory, M. Martens and M. Dreux, *J. Chromatogr.*, 505 (1991) 191.
9 S. Brossard, M. Lafosse and M. Dreux, *J. Chromatogr.*, 591 (1992) 149.
10 E. J. Guthrie and H. E. Schwartz, *J. Chromatogr. Sci.*, 24 (1986) 236.
11 T. A. Berger and J. F. Deye, *J. Chromatogr. Sci.*, 29 (1991) 310.
12 A. F. M. Barton, *Chem. Rev.*, 6 (1975) 731.
13 C. K. Huston, Jr. and R. A. Bernhard, *LC · GC*, 3, No. 7 (1990) 41.

Journal of Chromatography, 623 (1992) 329–336
Elsevier Science Publishers B.V., Amsterdam

CHROM. 24 390

Enantiomer fractionation of phosphine oxides by preparative subcritical fluid chromatography

G. Fuchs, L. Doguet and D. Barth

LPCI–ENSIC, 1 rue Grandville, B.P. 451, F-54001 Nancy Cédex (France)

M. Perrut

SEPAREX, 5 rue Jacques Monod, B.P. 9, F-54520 Champigneulles (France)

(First received November 8th, 1991; revised manuscript received May 26th, 1992)

ABSTRACT

The subcritical fluid chromatographic separation of three enantiomeric pairs of phosphine oxides (two phosphanorbornadienes and 1,2,5-triphenylphospholane-1-oxide) was performed on a pilot plant equiped with a 60-mm axial compression column packed with Pirkle-type phases, the mobile phase being carbon dioxide–ethanol mixtures. With selectivities ranging from 1.1 to 1.3, both enantiomers were obtained with an optical purity greater than 95%. The resolution of one phosphanorbornadiene pair was optimized with a production rate reaching 510 mg/h with a good yield (80%).

INTRODUCTION

Traditionally, chromatography has been used to separate compounds having distinctly different chemical and physical properties. Only relatively recently has attention been focused on chiral chromatography, where selective adsorption is used to separate enantiomeric mixtures into optically pure compounds. Most investigations have been directed towards the development of highly enantioselective and broadly applicable chiral stationary phases (CSPs) [1–3]. Among the numerous classes of chiral stationary phases, those developed from Pirkle's concept are probably the best known and most widely used, essentially on an analytical scale [3,4].

The principle of chromatographic separation is based on the formation of labile diastereoisomeric complexes with a chiral complexing agent (selector) bonded on a silica support. The different stabilities of these diastereoisomers lead to selectivity. In other words, the enantioselectivity factor, α, is related to the difference in free energies of binding ($\Delta\Delta G$) to the CSP for two enantiomers by the equation

$$\Delta\Delta G = \Delta\Delta H - T\Delta\Delta S = -RT \ln \alpha \quad (1)$$

where $\Delta\Delta H$ and $\Delta\Delta S$ are bonding enthalpy and entropy differences, respectively. Consequently, the chiral recognition ability of the CSP decreases with increasing column temperature [5,6]. We have to operate at the lowest temperature possible (20°C) on our pilot plant in order to maximize selectivity.

Several workers [7,8] have reported enantiomer resolutions on a wide variety of CSP using carbon dioxide enriched with different alcohols as a subcritical eluent for analytical purposes. However, no preparative resolution has been published so far.

In this work, preparative subcritical fluid chromatography (SubFC) was used for the resolution of three tertiary phosphine oxides which play a prominent role in asymmetric catalysis, *e.g.*, the pure enantiomer of 1,2,5-triphenylphospholane 1-oxide

Correspondence to: Dr. D. Barth, LPCI–ENSIC, 1 Rue Grandville, B.P. 451, F-54001 Nancy Cédex, France.

0021-9673/92/$05.00

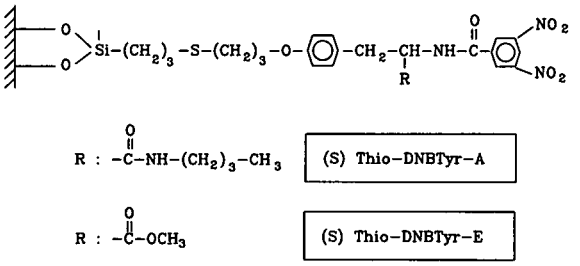

Fig. 1. Chiral stationary phases.

(compound **2**) is used as a ligand for transition metal complexes in enantioselective catalytic organic reactions [9]. Moreover, in addition, high-performance liquid chromatography (HPLC) and SubFC were compared.

Two chiral π-acceptor stationary phases derived from (*S*)-N-(3,5-dinitrobenzoyl)tyrosine (DNBTyr) covalently bonded to a γ-mercaptopropyl silica gel were used (Fig. 1). The mobile phase in SubFC was a classical mixture for a Pirkle-type phase, carbon dioxide–ethanol [8]. The three enantiomeric pairs of compounds considered were phosphine oxides (Fig. 2). Compound **1a** was fractionated on (*S*)-thio-DNBTyr A and compounds **1b** and **2** on (*S*)-thio-DNBTyr E.

EXPERIMENTAL

Analytical chromatography

HPLC. The analytical liquid chromatography consisted of a pump (Isochrom LC, Spectra-physics, Les Ulis, France) and a spectrophotometer (Model 481, Waters, Montigny-le-Bretonneux, France) connected with a computer–integrator (SP 4270, Spectra-physics).

SubFC. Liquid carbon dioxide was pumped through a cooled head metering pump (Minipump, Dosapro Milton Roy, Pont Saint-Pierre, France). Polar modifier was added through a pump (Model 510, Waters) and mixed with carbon dioxide prior to a heat exchanger. An HPLC valve (Rheodyne Model 7125, Touzart et Matignon, Vitry-sur-Seine, France) was used as an injector. The column temperature was controlled by a heat exchanger. A variable-wavelength UV detector (Spectra 100, Spectra-physics) was connected with an integrator (SP 4270, Spectra-Physics). The pressure was controlled by two manually adjustable back-pressure regulators (LTH 400, Alphagaz, Bois D'Arcy, France). Finally, the gaseous carbon dioxide was released to the atmosphere after flow-rate measurement using a rotameter (Teflinox, Wasselone, France).

Preparative subcritical fluid chromatography (PSubFC)

The PSubFC pilot plant, with total recycle of the eluent, has been under development in our laboratory since 1982 [10,11] (Fig. 3). It should be noted that eluent–product separation is performed through high-performance separators [12] and the axial compression technique is used to increase column efficiency. The column efficiencies are now at least similar to those obtained in analytical SubFC [13]. An original set-up called a saturator permits

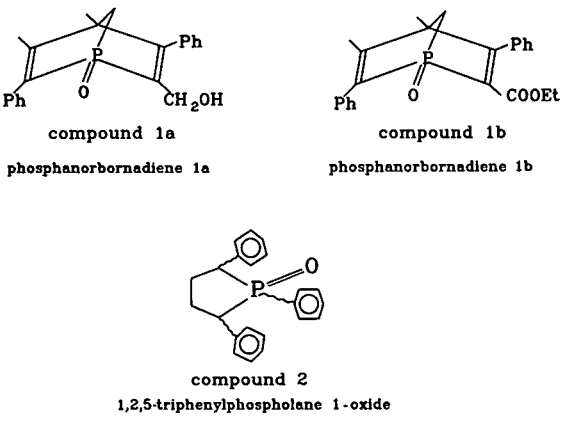

Fig. 2. Phosphine oxides.

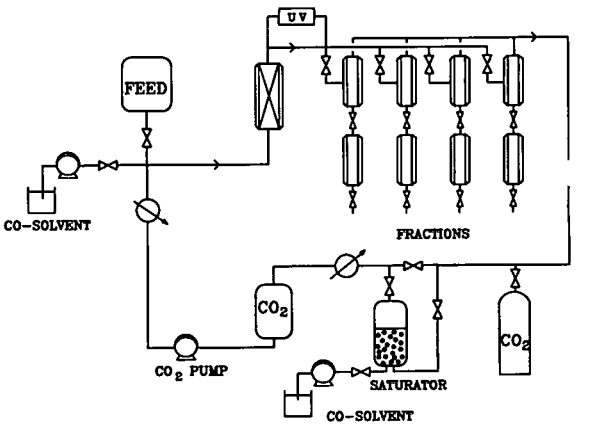

Fig. 3. PSubFC pilot plant.

TABLE I

RESOLUTION OF THREE RACEMIC PHOSPHINE OXIDES

Mobile phase: *n*-hexane–ethanol for HPLC; CO_2–ethanol, pressure 20 MPa, for SubFC. UV detection at 230 nm. Column temperature, 293 K.

Compound	Stationary phase	HPLC		Sub FC		Ethanol in mobile phase (% v/v)
		$\alpha_{1,2}$	k'_1	$\alpha_{1,2}$	k'_1	
1a	(*S*)-Thio-DNBTyr A	1.27	12	1.35	32	8
1b	(*S*)-Thio-DNBTyr E	1.19	17	1.19	17	12
2	(*S*)-Thio-DNBTyr E	1.11	22	1.15	41	8

both polar modifier addition to the mobile phase and recycled eluent cleaning [14]. The pilot plant is fully controlled by a computer which ensures periodical injection of the feed and the recovery of the different fractions.

Apparatus

Melting points (m.p.) were measured on a Kofler hot-stage apparatus (OSI, Paris, France) and are given without correction.

Optical purities were obtained using a Model 141 micropolarimeter with a 1-dm length quartz cell (Perkin-Elmer, St.Quentin en Yvelines, France).

Solvents

HPLC-grade hexane and absolute ethanol were purchased from Prolabo (Paris, France). Technical-grade carbon dioxide for preparative SubFC was supplied by Carboxyque Française (Puteaux, France) and high-purity carbon dioxide (>99.9995%) for analytical SubFC from Air Gaz (Mitry-Mory, France).

Stationary phases

The phases (*S*)thio-DNBTyr A bonded on LiChroprep Si-60 silica (10 μm, irregular) (Merck) and (*S*)-thio-DNBTyr E on LiChroprep Si-60 silica (7 μm, irregular) (Merck) have been developed recently by Tambute and Begos [15]. The stationary phase (*S*)-thio-DNBTyr A is now commercially available as ChyRoSyne A from Touzart et Matignon.

Racemic mixtures

Phosphanorbornadienes **1a** and **1b** were supplied by Le Goff (SNPE, Vert-le-Petit, France) and 1,2,5-triphenylphospholane 1-oxide by Fiaud (Institut de Chimie Moléculaire, Orsay, France). The products were dissolved in ethanol for the injection.

RESULTS AND DISCUSSION

Analytical study

The chromatographic results obtained for the direct resolution of racemic compounds under HPLC and SubFC conditions are reported in Tables I and II. For SubFC the temperature (T) was 293 K and the pressure (P) 20 MPa. The selectivity, α_{12}, is greater with the subcritical eluent than with the liquid. The capacity factor, k', is much higher in SubFC than HPLC, especially for **1a**, but the low viscosity of carbon dioxide ($\eta = 10.3 \cdot 10^{-5}$ Pa s,

TABLE II

OVERLOADING TESTS FOR THREE RACEMIC PHOSPHINE OXIDES IN SubFC

(A) Stationary phase, (*S*)-Thio-DNBTyr A; column, 250 × 4.6 mm I.D.; mobile phase, CO_2–ethanol (92:8, v/v); flow-rate, 4.42 ml/min; pressure, 20 MPa; temperature, 293 K; UV detection at 230 nm. (B) Stationary phase, (*S*)-Thio-DNBTyr E; column, 150 mm × 4.6 mm I.D.; mobile phase, CO_2–ethanol (88:12, v/v); flow-rate, 2.53 ml/min; other conditions as in (A). (C) Stationary phase, (*S*)-Thio-DNBTyr E; column, 150 mm × 4.6 mm I.D.; mobile phase, CO_2–ethanol (92:8, v/v); flow-rate, 3.88 ml/min; other conditions as in (A).

Compound	Conditions	Mass injected (mg)	R_S
1a	A	4.00	1.2
1b	B	0.32	0.9
2	C	0.15	1.0

TABLE III

PREPARATIVE SCALE COLUMN EFFICIENCIES

Column	Phase	TP/m[a]	*h* (reduced HETP)	Column length (mm)
1	(*S*)-Thio-DNBTyr A	45 000	2.2	76
2	(*S*)-Thio-DNBTyr E	56 000	2.5	100

[a] Theoretical plates per metre.

T = 293 K, P = 20 MPa) [16] permits much higher flow-rates to be used than those classicaly used in HPLC. Consequently, in SubFC the retention times are shorter (Fig. 4). It is noteworthy that the maximum amount injected in order to obtain a resolution of 1 is very low. In fact, only 19% of the initial mercaptopropyl groups have reacted with the chiral selector, which results in a small number of chiral sites and hence in a low stationary phase capacity [15].

Preparative study

The chiral stationary phases [146 g of (*S*)-thio-DNBTyr A and 184 g of (*S*)-thio-DNBTyr E] were packed successively into the column (60 mm I.D.) by axial compression (2 MPa) (Table III). The other operating conditions were as follows: column pressure 20 MPa; separator pressure, 5 MPa; column temperature, 293 K; separator temperature, 338 K; eluent, carbon dioxide–ethanol (for **1a** 92:8, for **1b** 88:12 and for **2** 92:8 v/v); and flow-rate, 10–16 l/h.

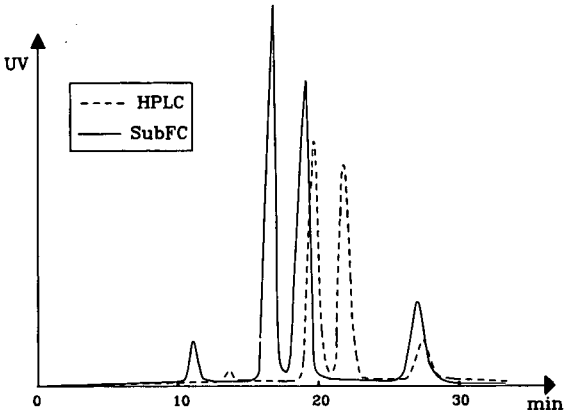

Fig. 4. Resolution of 1,2,5-triphenylphospholane 1-oxide under HPLC and SubFC conditions. HPLC conditions: stationary phase, (*S*)-thio-DNBTyr E; column, 150 mm × 4.6 mm I.D.; mobile phase, *n*-hexane–ethanol (92:8, v/v); flow-rate, 2 ml/min; column temperature, 293 K; UV detection at 230 nm. SubFC conditions: stationary phase, (*S*)-thio-DNBTyr E; column, 150 mm × 4.6 mm I.D.; pressure, 20 MPa; column temperature, 293 K; mobile phase, CO_2–ethanol (92:8, v/v); flow-rate, 3.88 ml/min; UV detection at 230 nm.

The extrapolation rules are complex and several parameters have to be taken in to account: number of theoretical plates, injection shape and peak asymmetry [17]. As a first choice, the amounts injected were linearly extrapolated with the volume of stationary phase as shown in Table IV; we shall now present the results for the three fractionations in order of increasing difficulty (**1a**, α = 1.3, **1b**, α = 1.2; **2**, α = 1.1).

*Resolution of phosphanorbornadiene **1a** enantiomers*

For the first enantiomer fractionation, the conditions of preparative separation were not optimized and small amounts of solute (100 mg) were injected in order to obtain the first and second enantiomers with purities of 100% and 97%, respectively (by HPLC). The resolution was correct (R_s = 1.1). The optical purity of each enantiomer was also measured in order to confirm the purity attainable by preparative chromatography: (+)-phosphanorbornadiene (**1a**) m.p. = 117°C, $[\alpha]_D^{22}$ = +192.26° (c = 1, $CHCl_3$); (−)-phosphanorbornadiene (**1a**) m.p.

TABLE IV

EXTRAPOLATION OF AMOUNT INJECTED FROM ANALYTICAL TO PREPARATIVE SubFC

Compound	Mass injected (mg)	
	Analytical SubFC	Preparative SubFC
1a	4.00	207
1b	0.32	36
2	0.15	17

= 123°C, $[\alpha]_D^{22}$ = −173.53° (c = 1, $CHCl_3$). The absolute configurations are not given in the literature.

Resolution of phosphanorbornadiene ***1b*** *enantiomers*

For the second enantiomer fractionation, the preparative separation parameters (flow-rate, amount injected, particle size, column length and diameter, injection frequency, cut point position) can be optimized. In fact, some parameters are imposed (column geometry, particle size). This study was performed as follows. The recovery ratio of pure enantiomer at two different flow-rates 12 and 16 l/h) was reported *versus* the injected mass, and the production rate (Tables V and VI) was quantified by

$$Q_L \text{ (mg/s)} = \frac{\text{solute recovery at each injection (mg)}}{\text{retention times of first-eluted enantiomer (s)}}$$

From 70 injections, the optimum Q_L value was determined for each flow-rate. It could be related to the fact that it is difficult to choose good cut-point positions which change with amount injected owing to non-linear adsorption isotherms. As the amount injected is increased, the band of the profile moves toward shorter retentions (Table V) owing to the non-linear elution conditions.

The fractions are considered to be correct if they reach the following enantiomeric purities: first enantiomer (+), enantiomeric excess (e.e.) = 96%; second enantiomer (−), e.e. = 94%. The enantiomeric purity and solute recovery were determined by comparing individual fractions with a standard solution containing 0.5 mg/ml of solute on an analytical column by HPLC.

According to our analytical work, the optimum amount injected is 36 mg (see Table IV). In fact, we found that the amount injected ranged from 40 to 100 mg. Consequently, direct extrapolation must be considered cautiously. This could be related to the fact that the plate number N is higher in the preparative column than in the analytical column ($N_{anal.} \approx 25\,000$ theoretical plates (TP)/m, l = 25 cm; $N_{prep.} \approx 50\,000$ TP/m, l = 10 cm), owing to the excellent performance of the axial compression technique.

For a flow-rate of 12 l/h, the mass injected is optimum around 80 mg for a recovery ratio of 90%. However, for a flow-rate of 16 l/h, the recovery ratio is lower than 90% for the same optimum mass injected.

The curves of Q_L *versus* mass injected show that higher flow-rates may lead to higher production rates (Table VI). Indeed, for a flow-rate of 16 l/h, the delay between each injection can be decreased to 7 min under such conditions, and production rate can reach 510 mg/h higher than that obtained by HPLC (250 mg/h) with a ternary mixture as eluent [18].

Although experiments with other flow-rates might lead to a better optimization, it seems that the best results are obtained at higher flow-rates. The low viscosity of carbon dioxide permits high flow-rates to be used without too high a pressure drop, which is the main advantage in PSubFC.

TABLE V

Q_L *VERSUS* MASS INJECTED FOR RESOLUTION OF PHOSPHANORBORNADIENE **1b**

Flow-rate, 12 l/h; stationary phase, (*S*)-Thio-DNBTyr E; column, 100 mm × 60 mm I.D.; mobile phase, CO_2 –ethanol (88:12, v/v); pressure, 20 MPa; column temperature, 293 K; UV detection at 230 nm.

First-eluted enantiomer				First- + second-eluted enantiomers	Second-eluted enantiomer			
Mass injected (mg)	Mass recovered (mg)	Retention time of first-eluted enantiomer (s)	Q_L	Q_L	Mass injected (mg)	Mass recovered (mg)	Retention time of first-eluted enantiomer (s)	Q_L
40	16	950	0.017	0.035	40	17	950	0.018
40	19	950	0.020	0.039	40	19	950	0.019
60	25	900	0.028	0.056	60	25	900	0.028
80	33	850	0.039	0.076	80	32	850	0.037
100	38	750	0.050	0.098	100	36	750	0.048

TABLE VI

Q_L *VERSUS* MASS INJECTED FOR RESOLUTION OF PHOSPHANORBORNADIENE **1b**

Flow-rate, 16 l/h; other operating conditions as in Table V.

First-eluted enantiomer				First- + second-eluted enantiomers	Second-eluted enantiomer			
Mass injected (mg)	Mass recovered (mg)	Retention time of first-eluted enantiomer (s)	Q_L	Q_L	Mass injected (mg)	Mass recovered (mg)	Retention time of first-eluted enantiomer (s)	Q_L
60	18	520	0.036	0.065	60	15	520	0.029
70	28	600	0.046	0.090	70	26	600	0.044
80	32	590	0.054	0.102	80	28	590	0.048

The purified enantiomers were obtained as follows: (*R,R*)-(+)-phosphanorbornadiene (**1b**), m.p. = 120°C, $[\alpha]_D^{22} = +162.6°$ (c = 1, $CHCl_3$); (*S,S*)-(−)-phosphanorbornadiene (**1b**), m.p. = 118°C, $[\alpha]_D^{22} = -154.1°$ (c = 1, $CHCl_3$). Literature data [19] are as follows: (*R,R*)-(+) -**1b**, m.p. = 139–141°C, $[\alpha]_D^{22} = +178°$ (c = 1, $CHCl_3$); (*S,S*)-(−)-**1b**, m.p. = 138–140°C, $[\alpha]_D^{22} = -172.3°$ (c = 1, $CHCl_3$).

Resolution of 1,2,5-triphenylphospholane 1-oxide enantiomers

Regarding the resolution of *trans*-1,2,5-triphenylphospholane 1-oxide, the separation of enantiomers with good enantiomeric purity is a challenge as the selectivity factor is very low (α = 1.1). The feed contains two *cis/trans* isomers (ratio 14:83 and 3% of unknown impurities); the *trans* isomer is chiral and gives the absolute configurations *R,R/S,S*, which were separated on the (*S*)-thio-DNBTyr-E stationary phase. The mass injected was fixed at 38 mg with an eluent flow-rate of 15 l/h, leading to a resolution of 1.16.

The total amount of compound fractionated on a preparative scale was *ca.* 3 g and the recovery ratios were low (*ca.* 50%) (Table VII). This result can be explained by two factors: on the one hand, the size of the pilot unit is too large in comparison with the mass injected, and on the other, the initial feed contains 17% of impurities (14% *cis* isomer + 3% impurities). Although the separation factor is low (α = 1.1), each enantiomer is obtained with high opti-

TABLE VII

RECOVERED MASS AND OPTICAL PURITIES FOR EACH INJECTION SERIES OF 1,2,5-TRIPHENYLPHOSPHOLANE 1-OXIDE

Operating conditions as in Fig. 5.

$\sum$ mass injected for each series (mg)	First fraction		Second fraction		Third fraction	
	Mass recovered (mg)	% of first enantiomer	Mass recovered (mg)	% of first enantiomer	Mass recovered (mg)	% of first
304	64	96	49	39	52	15
342	80	99	17	42	60	11
190	32	100	3	24	28	6
266	31	100	33	11	25	11
418	125	98	37	33	111	7
380	87	98	16	35	133	8
152	32	99	1	35	32	5
380	84	100	14	48	87	7
456	81	100	79	40	94	6

cal purity, as checked by HPLC (Fig. 5) (Table VII): first enantiomer (−), 100% e.e.; second enantiomer (+), 90% e.e. The enantiomeric purity of the second fraction is slightly reduced by tailing of the first band. Moreover, enantiomeric purity (>99% e.e.) could be obtained by a single recrystallization from ethanol–water (60:40) from a fraction showing 84% e.e. [9]. The (−)-enantiomer was obtained as with m.p. = 204°C and $[\alpha]_D^{22} = -150°$ (c = 1, CH_3OH).

The absolute configurations of the enantiomers are unknown. The racemate has m.p. = 170°C, which is lower than that measured for the (−)-enantiomer. Consequently, the enantiomer mixture gives a conglomerate; this is of particular interest because conglomerates are far easier to resolve than are racemic compounds by crystallization [20].

CONCLUSIONS

The separation of three enantiomer pairs with a production rate of a few hundred milligrams per hour demonstrates the great potential of PSubFC with short cycle times for difficult separations (α = 1.1) of molecules that can be eluted using subcritical carbon dioxide with a polar modifier. Moreover, preparative chromatography will become more attractive with the developement of new chiral stationary phases of greater capacity.

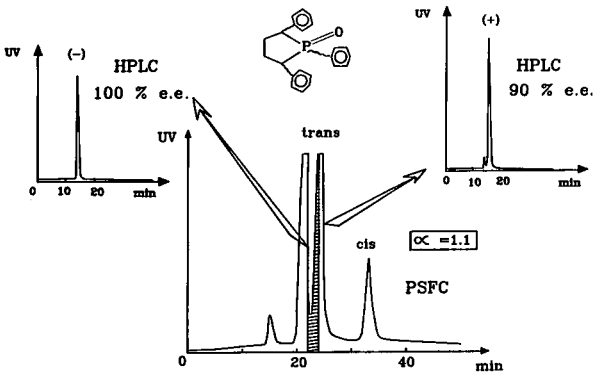

Fig. 5. Separation of *trans*-1,2,5-triphenylphospholane 1-oxide. Stationary phase, (*S*)-thio-DNBTyr E; column, 100 mm × 60 mm I.D.; mobile phase, CO_2–ethanol (92:8, v/v); flow-rate, 15 l/h; pressure, 20 MPa; column temperature, 293 K; UV detection at 230 nm; mass injected, 38 mg.

SYMBOLS

$\alpha_{ij} = k'_j/k'_i$	Selectivity
k'_i	Capacity factor
e.e. $= \frac{[R] - [S]}{[R] + [R]}$	Enantiomeric excess for R
$h = H/d_p$	Reduced height equivalent to a theoretical plate
d_p	Particle size
$H = L/N$	Height equivalent to a theoretical plate
L	Column length
N	Theoretical plates per meter

ACKNOWLEDGEMENTS

We are grateful to Dr. J. C. Fiaud, Dr. P. Le Goff and A. Tambute for providing racemic compounds and stationary phases and for helpful discussions. We thank Prochrom (Champigneulles, France) for financial support.

REFERENCES

1 W. Wairner, *Trends Anal. Chem.*, 6 (1987) 125.
2 R. Dappen, H. Arm and V. R. Meyer, *J. Chromatogr.*, 373 (1986) 1.
3 W. H. Pirkle, M. H. Hyon, A. Tsipouras, B. C. Hamper and B. Banks, *J. Pharm. Biomed. Anal.*, 2 (1984) 173.
4 W. H. Pirkle and J. Finn, *J. Org. Chem.*, 46 (1981) 2935.
5 W. H. Pirkle and T. C. Pochapsky, *Adv. Chromatogr.*, 27 (1987) 73.
6 F. Gasparini, D. Misiti and C. Villani, *J. High Resolut. Chromatogr.*, 3 (1990) 182.
7 S. Hara and A. Dobashi, *J. High Resolut. Chromatogr. Chromatogr. Commun.* 2 (1979) 531.
8 P. Macaudière, M. Caude, R. Rosset and A. Tambute, *J. Chromatogr.*, 27 (1989) 383.
9 J. C. Fiaud and J. Y. Legros, *Tetrahedon Lett.*, 32 (1991) 5089.
10 M. Perrut, *Fr. Pat.*, 2 527 934 (1982); *Eur. Pat.*, 0 099 765 (1983); *US Pat.*, 4 478 702 (1983).
11 C. Berger and M. Perrut, *J. Chromatogr.*, 505 (1990) 37.
12 M. Perrut, *Fr. Pat.*, 2 584 618 (1985); *Eur. Pat.*, 0 212 999 (1986); *US Pat.*, 4 724 087 (1986).
13 L. Doguet and M. Perrut, presented at the *2nd Symposium on Supercritical Fluids, Boston, MA, May 1991.*
14 P. Jusforgues and M. Perrut, *Fr. Pat.*, 2 601 883 (1986); *Eur. Pat.*, 0 254 610 (1987).
15 A. Tambute and A. Begos, *New J. Chem.*, 13 (1989) 625.
16 A. L. Horvath, *Physical Properties of Inorganic Compounds*, Edward Arnold, London, 1975, p. 163.
17 P. Gareil, C. Durieux and R. Rosset, *Sep. Sci. Technol.*, 18 (1983) 441.

18 A. Tambute, M. Lienne, P. Macaudière, M. Caude and R. Rosset, presented at the *1st International Symposium on Separation of Chiral Molecules, Paris, May 31 and June 1–2, 1988.*
19 A. Breque, J. M. Alcaraz, L. Ricard and F. Mathey, *New J. Chem.*, 13 (1989) 369.
20 A. Collet, M. J. Brienne and J. Jaques, *Chem. Rev.*, 80 (1980) 215.

Journal of Chromatography, 623 (1992) 337–344
Elsevier Science Publishers B.V., Amsterdam

CHROM. 24 428

Electromigration in systems with additives in background electrolytes

I. Addition of the neutral complexing agent

Eva Dubrovčáková, Bohuslav Gaš, Jiří Vacík and Eva Smolková-Keulemansová

Faculty of Science, Charles University, Albertov 2030, 128 40 Prague 2 (Czechoslovakia)

(First received March 3rd, 1992; revised manuscript received June 12th, 1992)

ABSTRACT

A mathematical model describing the electrophoretic migration of strong electrolytes in the presence of a neutral complexing agent (*e.g.*, cyclodextrin) is formulated. The model allows computer simulation of the dynamics of the electrophoretic separation in general and the calculation of the isotachophoretic steady state. The approach for the determination of stability constants and mobilities of complex compounds from the experimental isotachophoretic data is described.

INTRODUCTION

The effective mobilities of compounds in electromigration methods, *i.e.*, isotachophoresis or zone electrophoresis, can be controlled by changes in the pH of the electrolytes used or by complex formation between a separated compound and a buffering counter ion acting as a charged complexing agent. The utilization of a neutral complexing agent (NCA) is another possibility of using complex formation for separation in electromigration methods. Tazaki *et al.* [1] and Stover [2] suggested the use of cyclic crown ethers and cyclodextrins. The ability to form inclusion complexes and the chiral character of cyclodextrins allow the separation of structurally related and isomeric compounds, including enantiomers [3,4].

Neutral complexing agents have some advantages over ionic agents. They do not substantially influence the conductivity of the separation system and their molecules are not transported by migration unless they are not bound to the separated ions. These agents can be therefore used in high concentration and hence are able to influence the mobility and provide successful separations even when the stability constant is very low.

Although separations using NCAs are often utilized in analytical practice, the theoretical description of such separations has not yet been fully formulated.

Tazaki *et al.* [5] derived a relationship for the effective mobility of a compound interacting with an NCA. They also determined the stability constants of some quaternary ammonium salts with α-cyclodextrin from isotachophoretic measurements. Ionic mobilities of these complexes were not determined from experimental data, but calculated using the equation suggested by Jokl [6]. Jelínek *et al.* [7] presented the concept of effective and non-effective inclusion and also showed [8] the influence of interaction of the counter ion on separation in isotachophoresis. In our recent studies [9] some

Correspondence to: Dr. B. Gaš, Faculty of Science, Charles University, Albertov 2030, 128 40 Prague 2, Czechoslovakia.

0021-9673/92/$05.00

general ideas about the electromigration of cyclodextrin complexes of azo compounds were considered.

The purpose of this paper is to present a model of the electromigration of compounds in the presence of a neutral complexing agent. In continuation of our previous work [10] we describe the dynamics of separations in electrophoretic methods in general. The model also allows the calculation of compound concentrations in all zones in the isotachophoretic steady state. In addition, stability constants and mobilities of complex compounds can be determined from the experimental isotachophoretic data.

MATHEMATICAL MODEL

Electromigration

Let us consider n ions of strong univalent electrolytes and a neutral complexing agent present in the solution. This agent can form a complex compound with any of the ions in a 1:1 ratio. Let us assume a negligible concentration of H^+ or OH^- ions produced by ionization of water. The ionic electrophoretic mobilities are presumed to be positive numbers. The total concentration of an ion j with a relative charge z_j (*i.e.*, the concentration of free and complex ions) is denoted by c_j and the concentration of free ion is denoted by c_j^z. The relative charge of the ion can be $+1$ or -1. Further, the total concentration of the NCA (*i.e.*, the concentration of the free neutral form and charged bound form) is c_c and the concentration of the free NCA is c_c^0. It is evident that $c_c^0 = c_c - \sum_{l=1}^{n} (c_l - c_l^z)$. The formulation of electromigration equations has the same basis as previously [10]. The continuity equations, which describe the one-dimensional mass flow of an ion j in an electric field in a capillary tube, have the form

$$\frac{\partial c_j}{\partial t} = -z_j i \frac{\partial}{\partial x}\left[\frac{u_j c_j^z + m_j(c_j - c_j^z)}{\kappa}\right] \quad (1)$$

where

$$\kappa = F \sum_{l=1}^{n} [c_l^z u_l + (c_l - c_l^z) m_l] \quad (2)$$

and $j = 1, 2, \ldots, n$, n is the number of ions, t is the time, i is the current density in a capillary tube, κ is the specific conductivity, u_j is the ionic mobility of the ion j, m_j is the ionic mobility of the ion j bound on an NCA, x is the length coordinate along a capillary tube and F is the Faraday constant.

The continuity equation describing the transport of NCA can be written in a similar way. In this instance we have to remember that the agent can migrate only when it is bound to an ion and forms a complex compound:

$$\frac{\partial c_c}{\partial t} = -i \cdot \frac{\partial}{\partial x}\left[\frac{\sum_{l=1}^{n} z_l m_l (c_l - c_l^z)}{\kappa}\right] \quad (3)$$

We assume that the ionic mobilities u_j and m_j depend neither on the viscosity nor on the ionic strength of solution and therefore can be approximated by the limiting ionic mobilities. We also do not consider the electroosmotic flow and the effect of temperature.

Reaction of an ion with a ligand is mostly reversible and fast and, consequently, the rate of the reaction is controlled only by diffusion, especially when the reaction of small molecules without steric hindrance [11] is considered. Yoshida *et al.* [12,13] have studied the dynamic aspects of the inclusion reactions between alkyl-substituted hydroxyphenylazo compounds and cyclodextrins and found that the inclusion reaction is very fast when the alkyl groups are small. They have also determined the stability constants of these complexes spectroscopically.

In our model, we assume that the kinetics of complex formation do not play a considerable role in migration and the concentrations of the compounds in the system are determined by complexation equilibria. The equations describing the equilibria are of the form

$$K_j = \frac{c_j - c_j^z}{c_j^z c_c^0} \quad (4)$$

where K_j is the stability constant of the complex between the ion j and the agent.

The electroneutrality condition

$$\sum_{l=1}^{n} c_l z_l = 0 \quad (5)$$

can replace one of the equations from the set 1, preferably that which describes the migration of the counter ion.

The terms of diffusion flow can be added to the right-hand sides of the continuity equations. Values of diffusion coefficients are available only for a small number of compounds. For this reason we used the Nernst–Einstein equation, $D = uRT/(|z|F)$, which describes the relationship between the mobility u and the diffusion coefficient D of an ion with charge z (R is the gas constant and T is absolute temperature).

The Nernst–Einstein equation cannot be used for neutral compounds. Therefore, the diffusion coefficient of NCAs was interpolated from available tables of data for structurally related compounds (*e.g.*, the value of $5 \cdot 10^{-10}$ m^2 s^{-1} was estimated for β-cyclodextrin). The final form of the continuity equations (disregarding terms describing the diffusion potential gradient resulting as a cross-effect of the diffusion of ions with different mobilities [14]) is

$$\frac{\partial c_j}{\partial t} = \frac{RT}{F} \cdot \frac{\partial^2}{\partial x^2} [u_j c_j^z + m_j(c_j - c_j^z)] - z_j i \cdot \frac{\partial}{\partial x} \left[\frac{u_j c_j^z + m_j(c_j - c_j^z)}{\kappa} \right] \quad (6)$$

and

$$\frac{\partial c_c}{\partial t} = \frac{RT}{F} \cdot \frac{\partial^2}{\partial x^2} \left[\sum_{l=1}^{n} m_l(c_l - c_l^z) \right] + D \cdot \frac{\partial^2 c_c^0}{\partial x^2} - i \cdot \frac{\partial}{\partial x} \left[\frac{\sum_{l=1}^{n} z_l m_l(c_l - c_l^z)}{\kappa} \right] \quad (7)$$

The model defined by eqns. 4–7 enables the main features of the separation process to be described.

Isotachophoretic steady state

Calculation of the isotachophoretic steady state (*i.e.*, the determination of concentrations of all compounds in isotachophoretic zones) is analogous to the calculation of the steady state in the migration of weak electrolytes describe earlier [15].

Let us consider an isotachophoretic system of two zones 1 and 2. Let the first zone contain ion 1 and the second zone contain ion 2 and there is a common counter ion 3 and the NCA (which can form a complex compound with any of the ions) in both zones 1 and 2. The notation of the concentrations and mobilities of ions below consists of two subscripts, one representing a compound and the other a zone.

Our aim is to determine the parameters of the second zone in the isotachophoretic steady state, assuming we know the physico-chemical characteristics of all the compounds (the ionic mobilities and the stability constants). Let the first zone be the zone of a leading electrolyte where the concentration of a leading ion and the total concentration of an NCA are known (and as a result of the electroneutrality condition, the total concentration of the counter ion is also known). All necessary concentrations in the zone 1 can be calculated by eqns. 10 and 12, which describe the complexation equilibria.

The following five unknown parameters of zone 2 should be determined: concentrations c_{22}^z and c_{32}^z (the concentration of the free form of the ion 2 and the concentration of the free counter ion 3, respectively), concentrations c_{22} and c_{32} (the total concentrations of the free and bound forms of the ion 2 and the counter ion 3, respectively) and concentration c_{c2}^0 (the concentration of the free complexing agent).

The following equations hold:

(1) the electroneutrality condition:

$$c_{11} = c_{31} \quad (8)$$

$$c_{22} = c_{32} \quad (9)$$

(2) the equations describing complexation equilibria:

$$K_1 = (c_{11} - c_{11}^z)/(c_{11}^z c_{c1}^0) \quad (10)$$

$$K_2 = (c_{22} - c_{22}^z)/(c_{22}^z c_{c2}^0) \quad (11)$$

$$K_3 = (c_{31} - c_{31}^z)/(c_{31}^z c_{c1}^0) \quad (12)$$

$$K_3 = (c_{32} - c_{32}^z)/(c_{32}^z c_{c2}^0) \quad (13)$$

(3) the equation describing the isotachophoretic condition (the form of the equation is written in terms of the effective mobilities):

$$\bar{u}_{11}/\kappa_1 = \bar{u}_{22}/\kappa_2 \quad (14)$$

where $\bar{u}_{11}$ is the effective mobility of compound 1 in zone 1, $\bar{u}_{22}$ is the effective mobility of compound 2 in zone 2 and κ_1 and κ_2 are the specific conductivities of zone 1 and zone 2, respectively.

The conductivities of both zones can be determined from eqn. 2.

The effective mobility $\bar{u}_{ii}$ ($i = 1, 2$) is expressed as

$$\bar{u}_{ii} = [u_i c_{ii}^z + m_i(c_{ii} - c_{ii}^z)]/c_{ii} \quad (15)$$

For the last equation one can use, *e.g.*, the mass balance of the NCA, which has the form

$$c_{c1}(\bar{u}_{11} - \bar{u}_{c1})/\kappa_1 = c_{c2}(\bar{u}_{22} - \bar{u}_{c2})/\kappa_2 \quad (16)$$

where c_{c1} and c_{c2} are the total concentrations of the NCA and $\bar{u}_{c1}$ and $\bar{u}_{c2}$ are the effective mobilities of the NCA in zones 1 and 2, respectively. These effective mobilities are determined by the following equations:

$$\bar{u}_{c1} = [m_1(c_{11} - c_{11}^z) - m_3(c_{31} - c_{31}^z)]/c_{c1} \quad (17)$$

$$\bar{u}_{c2} = [m_2(c_{22} - c_{22}^z) - m_3(c_{32} - c_{32}^z)]/c_{c2} \quad (18)$$

The five unknown concentrations c_{22}^z, c_{32}^z, c_{22}, c_{32} and c_{c2}^0 can obviously be determined from eqns. 9, 11, 13, 14 and 16.

The dependence of the resistance of the sample zone on the concentration of the NCA in the leading electrolyte can be easily obtained experimentally. It permits the determination of the stability constants and the mobilities of the free and complex compounds. For this purpose, a computational program was written which iteratively fits the experimental isotachophoretic data by a simulated curve using the least-squares method.

NUMERIC METHODS

The partial differential eqns. 6 and 7 describing the electromigration was solved by the CTDS method of lines (continuous time, discrete space). The CTDS method consists in discretizing the spatial derivatives at a set of grid points to generate a set of ordinary differential equations with time as the independent variable. The finite-difference approximation is based on the first-order symmetrical difference approximation for either first and second derivatives.

Hamming's modification of the fourth-order predictor–corrector method [16] was used for the solution of the resulting set of ordinary differential equations. Simultaneously, the set of non-linear algebraic eqns. 4 must be solved at every time increment together with the sets of eqns. 6 and 7. This set of non-linear algebraic equations was solved by the Newton–Raphson iterative method [16].

For solution of the isotachophoretic steady state, the set of eqns. 9, 11, 13, 14 and 16 was solved by the Newton–Raphson method [16], instead of using of the RFQ method [17].

EXPERIMENTAL

The algorithm for solving the dynamics of electromigration and the isotachophoretic steady state was programmed in Pascal and runs on an IBM PC computer or compatible types. The results can be presented in graphical form.

The isotachophoretic measurements were made on a one-column isotachophoretic analyser consisting of the preseparation hydraulic part from a ZKI 01 instrument (Labeco, Spišská Nová Ves, Czechoslovakia) and a high-frequency contactless detector [18]. The leading ion was chloride (0.0111 *M*) and the counter ion ε-amino caproic acid; the pH of the leading electrolyte was 4.21. The terminating electrolyte was caproic acid. Chemicals used for the preparation of the leading and terminating electrolytes were of analytical-reagent grade and used without further purification. No additives were applied to decrease the electroosmotic flow. 4-Hydroxyphenylazobenzenesulphonic acid was synthesized in the Research Institute of Organic Syntheses (Pardubice, Czechoslovakia) and purified on a cellulose packed column. The complexing agent was β-cyclodextrin (Chinoin, Budapest, Hungary).

RESULTS AND DISCUSSION

NCAs are often used in capillary electromigration methods for the separation of structurally similar compounds. Compounds that originally had the same migration characteristics (*e.g.*, optical antipodes) can be separated assuming that their complexation with NCA is different.

Molecules of the NCA can migrate in an electric field only when they are bound on charged particles. In isotachophoresis, neutral complexing agents, especially cyclodextrins, are used as additives to the leading electrolyte. Fig. 1 simulates such an isotachophoretic migration where the sample contains only one ion interacting with cyclodextrin while the leading ion, the counter ion and the terminating ion do not form any complexes. In this case, the concentration of cyclodextrin remaining during migration in the terminating electrolyte is the same as in the leading electrolyte. Cyclodextrin as a whole does not move in the capillary, only the sample zone creates "a migrating bulge" on the concentration profile of cyclodextrin.

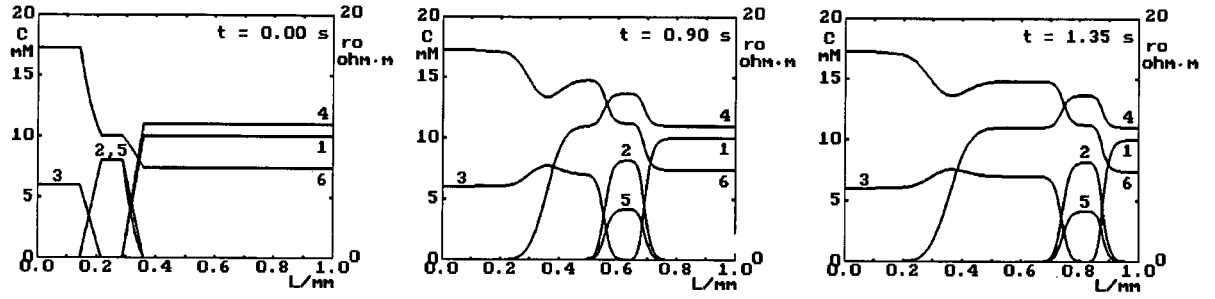

Fig. 1. Simulation of isotachophoretic migration. 1 = Leading anion; 2 = total sample; 3 = terminating anion; 4 = total cyclodextrin; 5 = free sample; 6 = specific resistance. Mobility of leading anion, $80 \cdot 10^{-9}$ m^2 V^{-1} s^{-1}; mobility of sample, $60 \cdot 10^{-9}$ m^2 V^{-1} s^{-1}; mobility of complexed sample, $30 \cdot 10^{-9}$ m^2 V^{-1} s^{-1}; mobility of terminating anion, $40 \cdot 10^{-9}$ m^2 V^{-1} s^{-1}; mobility of counter cation, $70 \cdot 10^{-9}$ m^2 V^{-1} s^{-1}; stability constant of sample, 100. L = Length coordinate of the capillary tube; C = concentration; ro = specific resistance.

When both the sample and the terminating ions interact with cyclodextrin (Fig. 2), the cyclodextrin zone moves in the zone of the terminating electrolyte in the same direction as the sample and has a higher concentration than that in the leading electrolyte.

In some instances both the counter ion and the sample can interact with a complexing agent [8]. The concentration profiles corresponding to such a situation are presented in Fig. 3. Now the cyclodextrin zone migrates in the opposite direction and has a lower concentration. The leading (Fig. 2) or trailing (Fig. 3) edge of the cyclodextrin boundary in the terminating electrolyte has interesting sharpening properties and is the subject of further studies.

Let us analyse in detail the isotachophoretic migration in a system of two migrating adjacent zones, 1 and 2. The first zone belongs to ion 1 and the second zone to ion 2 and in both zones the common counter ion 3 and NCA are present. We assume that zone 1 is the zone of the leading electrolyte with all parameters known and zone 2 is the zone of the sample. The NCA is able to interact only with ion 2. The effective mobility of the ion interacting with NCA is determined by eqn. 15. The dependence of the specific resistance ρ_2 of zone 2 ($\rho_2 = 1/\kappa_2$) on the total concentration of the NCA, c_{c2}, in zone 2 for the different values of the stability constants are presented in Fig. 4a.

The concentration c_{c2} of the agent in zone 2 is not experimentally available. However, it can be calculated using the model of the isotachophoretic steady state described above. Fig. 4b shows the dependence

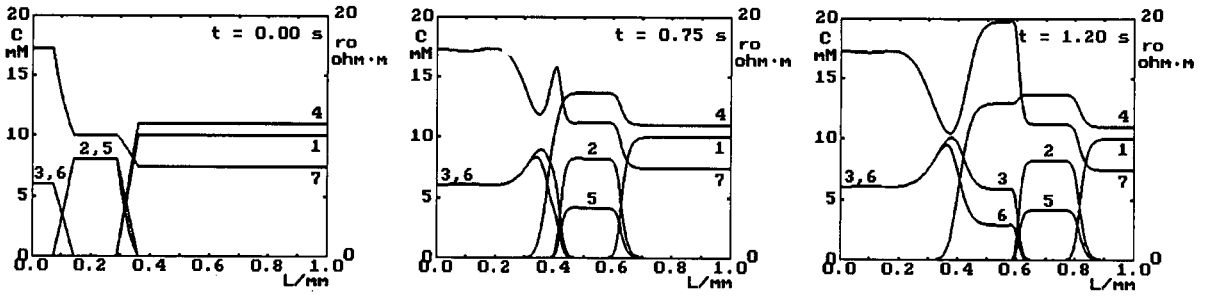

Fig. 2. Simulation of isotachophoretic migration. 1 = Leading anion; 2 = total sample; 3 = terminating anion; 4 = total cyclodextrin; 5 = free sample; 6 = free terminating anion; 7 = specific resistance. Mobility of the complexed terminating anion, $20 \cdot 10^{-9}$ m^2 V^{-1} s^{-1}; stability constant of the terminating anion, 100. Other mobilities, stability constants and symbols as in Fig. 1.

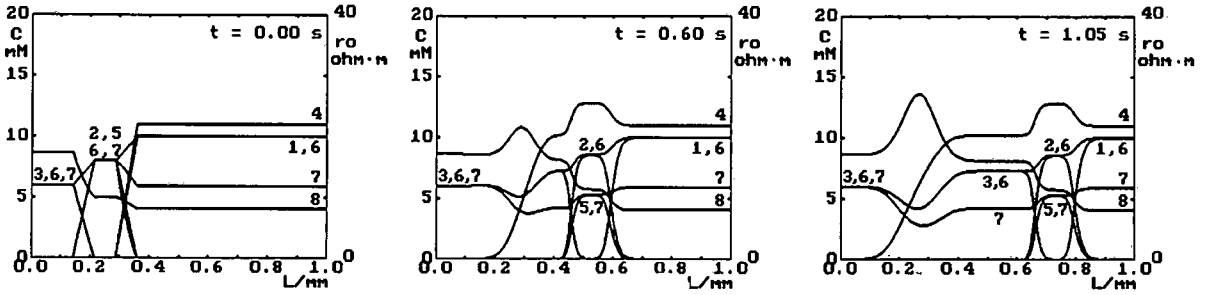

Fig. 3. Simulation of isotachophoretic migration. 1 = Leading anion; 2 = total sample; 3 = terminating anion; 4 = total cyclodextrin; 5 = free sample; 6 = total counter cation; 7 = free counter cation; 8 = specific resistance. Mobility of the complexed counter cation, $35 \cdot 10^{-9}$ m^2 V^{-1} s^{-1}; stability constant of the counter cation, 100. Other mobilities, stability constants and symbols as in Fig. 1.

of the specific resistance of zone 2 on concentration c_{c1} of the agent in the zone of the leading electrolyte for different stability constants. The existence of inflection points on the curves for higher stability constants is an interesting feature.

Let us assume that there are now two compounds A and B in the sample, both of which have the same mobilities and can interact with NCA. K_A and K_B are the stability constants of compounds A and B. The ratio $r = \bar{u}_A/\bar{u}_B$ ($\bar{u}_A$ and $\bar{u}_B$ are the effective mobilities) is the criterion of the separation ability. This ratio is also the ratio of the specific resistances of the zones, $r = \rho_B/\rho_A$, because of the validity of the isotachophoretic condition. Fig. 5a shows the graphical dependences of the ratio r on the concentration of NCA in the leading electrolyte for the same stability constants as in Fig. 4b (for curves 1 and 2, 2 and 3, ..., 6 and 7). Each curve has a maximum that corresponds to the maximum separation efficiency for the given pair of compounds and that gives the optimum concentration of NCA in the leading electrolyte. If the counter ion also interacts with the NCA, these maxima are shifted to higher concentrations (Fig. 5b).

The basic validity of the described model was verified by determination of the stability constant of the inclusion complex between 4-hydroxyazobenzenesulphonic acid and β-cyclodextrin and by the determination of the mobilities of free and complex compounds. The system with ε-aminocaproic acid as

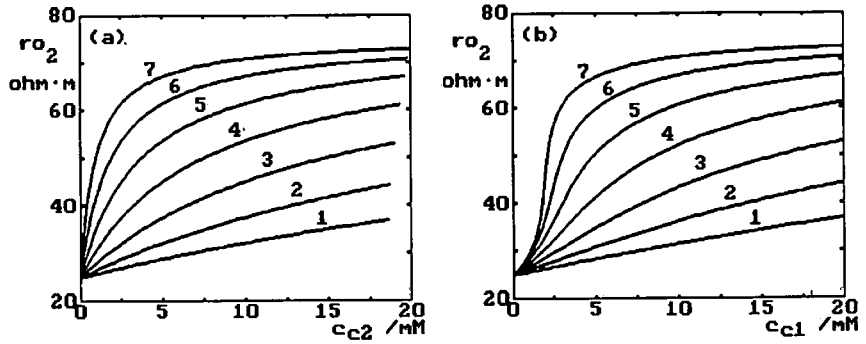

Fig. 4. Dependence of the specific resistance of the sample zone on the total concentration of complexing agent. ro_2 = Specific resistance of the sample zone. Concentration of the leading ion, 10 mM. Mobility of the leading ion, $79.1 \cdot 10^{-9}$ m^2 V^{-1} s^{-1}; mobility of the sample, $30 \cdot 10^{-9}$ m^2 V^{-1} s^{-1}; mobility of the complexed sample, $10 \cdot 10^{-9}$ m^2 V^{-1} s^{-1}; mobility of the counter ion, $30 \cdot 10^{-9}$ m^2 V^{-1} s^{-1}. Stability constant of the sample: (1) 50; (2) 100; (3) 200; (4) 400; (5) 800; (6) 1600; (7) 3200. (a) c_{c2} = Total concentration of cyclodextrin in the sample zone; (b) c_{c1} = total concentration of cyclodextrin in the leading zone.

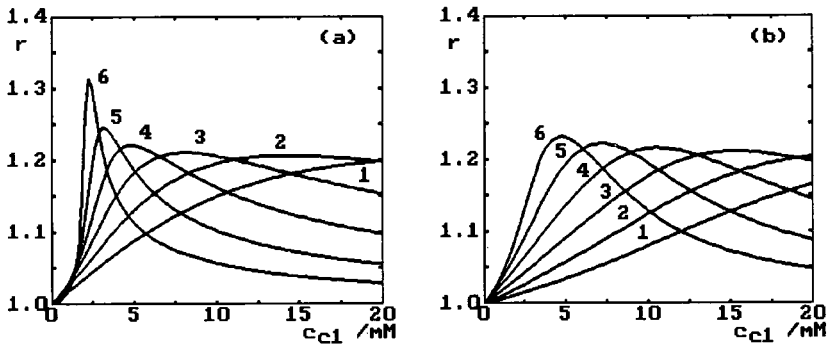

Fig. 5. Dependence of the ratio $r = \rho_B/\rho_A$ on total concentration of complexing agent in the leading zone. c_{c1} = Total concentration of cyclodextrin in the leading zone. Concentration of the leading ion, 10 mM. Mobility of the leading ion, $79.1 \cdot 10^{-9}$ m^2 V^{-1} s^{-1}; mobility of the samples A and B, $30 \cdot 10^{-9}$ m^2 V^{-1} s^{-1}; mobility of the complexed samples, $10 \cdot 10^{-9}$ m^2 V^{-1} s^{-1}; mobility of the counter ion, $30 \cdot 10^{-9}$ m^2 V^{-1} s^{-1}. Curves: (1) $K_A = 50$, $K_B = 100$; (2) $K_A = 100$, $K_B = 200$; (3) $K_A = 200$, $K_B = 400$; (4) $K_A = 400$, $K_B = 800$; (5) $K_A = 800$, $K_B = 1600$; (6) $K_A = 1600$, $K_B = 3200$. (a) Only samples A and B interact with cyclodextrin; (b) the counter ion also interacts with cyclodextrin. Mobility of the complexed counter cation, $15 \cdot 10^{-9}$ m^2 V^{-1} s^{-1}; stability constant of the counter cation, 500.

the weak buffering counter ion (pH = 4.21) with chloride as the leading ion was used. The specific resistance of the leading electrolyte is not influenced by addition of β-cyclodextrin, which implies that neither the counter ion nor the leading ion interacts with β-cyclodextrin. We can expect that 4-hydroxyazobenzenesulphonic acid will be almost totally dissociated at this pH, but ε-aminocaproic acid only *ca.* half dissociated. The model was developed for strong electrolytes only and, for this reason, we assume that the mobility of the counter ion is equal to its effective mobility. The computer simulation program [10] of the isotachophoretic separation gave $17.92 \cdot 10^{-9}$ m^2 V^{-1} s^{-1} for this effective mobility value. The limiting mobility of the leading Cl^- ion was assumed to be $79.1 \cdot 10^{-9}$ m^2 V^{-1} s^{-1}. The measured dependence of the specific resistance of the sample zone on the concentration of β-cyclodextrin in the leading electrolyte is shown in Fig. 6. The experimental points were fitted by a theoretical curve and the stability constant and the mobilities of the free and complex form of 4-hydroxyazobenzenesulphonic acid with β-cyclodextrin were iteratively determined. We obtained the following values: limiting mobility of the free anion, $21.4 \cdot 10^{-9}$ m^2 V^{-1} s^{-1}; limiting mobility of the complex anion, $10.3 \cdot 10^{-9}$ m^2 V^{-1} s^{-1}; and stability constant, 2040. Yoshida *et al.* [13] spectroscopically determined the stability constant for this compound to be 2000, which corresponds well with our result.

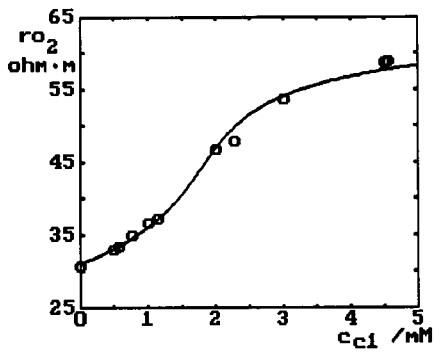

Fig. 6. Experimental data and fitting curve of the isotachophoretic measurement of 4-hydroxyphenylazobenzenesulphonic acid. Leading electrolyte, 0.0111 M Cl^-–ε-aminocaproic acid (pH 4.21); terminating electrolyte, 0.005 M caproic acid. ρ_2 = Specific resistance of the sample zone; c_{c1} = total concentration of cyclodextrin in the leading electrolyte. Circles = experimental data; full line = fitting curve.

CONCLUSION

The model presented in this paper describes all the basic features of the migration of strong monovalent electrolytes in the presence of a neutral complexing agent. It allows the determination of mobilities and stability constants and the prediction of the optimum separation conditions. In the future work this model should be extended to weak electrolytes and

their interaction with the neutral complexing agent and further it should also include the Debye–Hückel–Onsager theory of the dependence of mobilities on the ionic strength of the solution.

REFERENCES

1 M. Tazaki, M. Tagaki and K. Ueno, *Chem. Lett.*, (1982) 639.
2 F. S. Stover, *J. Chromatogr.*, 298 (1984) 203.
3 J. Snopek, I. Jelínek and E. Smolková-Keulemansová, *J. Chromatogr.*, 438 (1988) 211.
4 E. Smolková-Keulemansová, in O. Huber and J. Szejtli (Editors), *Proceedings of the 4th International Symposium on Cyclodextrins*, Kluwer, Dordrecht, 1988, p. 451.
5 M. Tazaki, T. Hayashita, Y. Fujino and M. Tagaki, *Bull. Chem. Soc. Jpn.*, 59 (1986) 3459.
6 V. Jokl, *J. Chromatogr.*, 13 (1964) 454.
7 I. Jelínek, J. Snopek, J. Dian and E. Smolková-Keulemansová, *J. Chromatogr.*, 470 (1989) 113.
8 I. Jelínek, J. Snopek and E. Smolková-Keulemansová, *J. Chromatogr.*, 557 (1991) 215.
9 E. Dubrovčáková, B. Gaš, J. Vacík and E. Smolková-Keulemansová, in Å. Sopková (Editor), *Proceedings of the 4th International Seminar on Inclusion Complexes, Stará Lesná, 17–21 June, 1991*, Slovak Chemical Society, Bratislava, 1991, p. P17.
10 B. Gaš, J. Vacík and I. Zelenský, *J. Chromatogr.*, 545 (1991) 225.
11 W. Saenger, in O. Huber and J. Szejtli (Editors), *Proceedings of the Fourth International Symposium on Cyclodextrins, Munich, April 20–22, 1988*, Kluwer, Dordrecht, 1988, p. 159.
12 N. Yoshida, A. Seiyama and M. Fujimoto, *J. Phys. Chem.*, 94 (1990) 4246.
13 N. Yoshida, A. Seiyama and M. Fujimoto, *J. Phys. Chem.*, 94 (1990) 4254.
14 T. Erdey-Gruz, *Transport Phenomena in Aqueous Solutions*, Akadémiai Kiadó, Budapest, 1974.
15 V. Kašička, J. Vacík and Z. Prusík, *J. Chromatogr.*, 320 (1985) 33.
16 A. Ralston, *A First Course in Numerical Methods*, McGraw-Hill, New York, 1965.
17 J. L. Beckers, *Thesis*, Technical University of Eindhoven, Eindhoven, 1973.
18 B. Gaš, J. Zuska and J. Vacík, *J. Chromatogr.*, 470 (1989) 69.

Journal of Chromatography, 623 (1992) 345–355
Elsevier Science Publishers B.V., Amsterdam

CHROM. 24 454

Analytical and micropreparative separation of peptides by capillary zone electrophoresis using discontinuous buffer systems

Christine Schwer and Friedrich Lottspeich

Department of Protein Chemistry, Max-Planck-Institute for Biochemistry, D(W)-8033 Martinsried (Germany)

(First received April 8th, 1992; revised manuscript received June 10th, 1992)

ABSTRACT

The tiny injection volumes that are usually necessary to maintain the high efficiency of capillary zone electrophoresis present a major problem if only limited sample amounts are available. To increase the sample load, discontinuous buffer systems were developed that allow the on-column concentration of dilute samples. Injection volumes can be increased in this way by at least a factor of 30. These stacking systems were applied to the analysis of tryptic peptides, to the purity checking of high-performance liquid chromatographic fractions and for the micropreparative separation of peptides with subsequent amino acid sequence analysis.

INTRODUCTION

Owing to its high efficiency and ease of automation, capillary zone electrophoresis (CZE) has found much interest in the field of biochemistry. In capillary gel electrophoresis of oligonucleotides more than 10^7 theoretical plates have been reported [1]. In the analysis of peptides, owing to its lower charge [2], the theoretical plates obtained are of the order of several hundred thousand. To maintain the extremely high efficiency of CZE, care has to be taken that extra-column effects do not contribute to peak dispersion. For the injection volume it follows that it may not exceed a few nanolitres for a capillary of 100 μm I.D. Although these very tiny sample volumes can be of advantage in specific applications, *e.g.*, single cell analysis [3], in most instances the limited sample load presents a major drawback as high sample concentrations are required. Using a UV detector the detection limit for, *e.g.*, peptides, is of the order of several tens of femtomoles. As the volume necessary for injection is usually 5–10 μl, a sample amount of several tens of picomoles is needed for an analytical separation. The detection limit can be improved by several orders of magnitude by using a laser-induced fluorescence detector, but as only a small number of analytes exhibit native fluorescence, derivatization has to be carried out. This leads to all the problems already known from high-performance liquid chromatography (HPLC) such as derivatization of highly diluted samples or the formation of more than one defined product.

In peptide and protein chemistry, in most instances further structural information on the separated components, such as amino acid sequence or amino acid composition, is desired, *i.e.*, a micropreparative separation has to be carried out. To be able to separate 10 pmol of a peptide, the initial sample amount has to be about 10 nmol dissolved in 5–10 μl under the usual injection conditions. This presents no problem with synthetic peptides, but in the analysis of biological samples such high concentrations are unrealistic.

If CZE is to be coupled with mass spectrometry

Correspondence to: Dr. C. Schwer, Department of Protein Chemistry, Max-Planck-Institute for Biochemistry, D(W)-8033 Martinsried, Germany.

0021-9673/92/$05.00

(MS), higher sample concentrations are also needed. For a single ion electropherogram only several tens of femtomoles are necessary, but if the whole mass range is scanned or if even MS–MS experiments are to be carried out, sample amounts of several picomoles have to be separated.

Many of these problems can be overcome by increasing the injection volume and performing a concentration step prior to the separation. This can be achieved by applying a gradient in the electric field strength. The easiest approach for concentrating a sample zone is by injecting a sample that is dissolved only in water without any ionic matrix present [4–6]. Owing to the low conductivity in the sample zone, the electrical field strength in this zone is increased, which results in concentration of the analytes at the front. However, the requirement that the conductivity of the sample has to be much lower than that of the carrier electrolyte also represents the major drawback of this concentration technique, as realistic samples are very seldom free from ionic contaminants. Therefore, in these instances isotachophoresis can be used for sample stacking. Experimentally this preconcentration can be realised in a single- or a dual-coulmn mode. In the coupled column arrangement the analytes are isotachophoretically concentrated in the first column and are then transferred to the second column, where they are separated zone electrophoretically [7,8]. In this way a sample load of about 10 μl is easily reached. As these systems are not available commercially, discontinuous buffer systems may be applied for sample stacking, as generally used in classical sodium dodecyl sulphate polyacrylamide gel electrophoresis (SDS-PAGE) [9,10]. So far these systems have been described in CZE only for the separation of proteins at high pH [11,12]. In this work discontinuous buffer systems at low pH were introduced for the analysis of peptides, but which are also applicable for the separation of proteins and many other substances at that pH.

The concentration of the dilute sample zone in a discontinuous system is caused by the fact that the buffer electrolytes are chosen such that at the beginning of the separation isotachophoretic conditions are created. In this way the concentration of the sample zone is adapted to the concentration of the preceding zone according to Kohlrausch's regulating function [13]. After the concentration step the analytes are separated zone electrophoretically as the buffer composition changes and the isotachophoretic conditions no longer hold for the sample components.

EXPERIMENTAL

Instrumentation

CZE measurements were carried out on a P/ACE System 2100 instrument (Beckman, Palo Alto, CA, USA) equipped with a UV detector. The absorbance of the peptides was detected at 200 nm in all instances. The separation capillary made of fused-silica (CS, Chromatographie Service, Langerwehe, Germany) had an I.D. of 100 μm and an effective length of 50 cm (57 cm total length). The inner wall of the capillary was coated with linear polyacrylamide according to the procedure described by Hjertén [14] in order to suppress electroosmosis and adsorption of the analytes. Injection was carried out by pressure, an injection time of 1 s corresponding to a volume of about 25 nl. Separation was carried out at a constant voltage of 20 kV, the capillary being thermostated at 30°C.

The different electrolyte solutions forming a discontinuous buffer system were filled into the capillary by applying a low pressure in the same way as hydrodynamic injection is carried out. A volume of about 25 nl is introduced when a low pressure is applied for 1 s at the inlet of a capillary of the above dimensions. The different volumes of the individual buffer solutions are shown in Fig. 1.

Fractions were collected electrophoretically by changing the outlet vials, which were filled with 10 μl of the separation buffer. The time windows for collecting the single fractions were calculated from the migration velocities determined in a previous run as described [15].

N-Terminal amino acid sequence analysis was carried out on a Model 477A gas-phase sequencer (Applied Biosystems, Foster City, CA, USA) as published [16].

Chemicals

All reagents were of analytical-reagent grade except β-alanine (for biochemistry) and ε-aminocaproic acid (for synthesis) (E. Merck, Darmstadt, Germany). β-Casein (from bovine milk) was obtained from Sigma (Deisenhofen, Germany), the

five standard peptides from Bachem (Heidelberg, Germany) and trypsin (sequencing grade) from Boehringer (Mannheim, Germany). As standard peptides the following basic, neutral and acidic peptides were used: (1) Leu–Trp–Met–Arg; (2) Leu–Trp–Met–Arg–Phe; (3) Leu–Trp–Met–Arg–Phe–Ala; (4) Tyr–Gly–Gly–Phe–Leu; and (5) Val–Leu–Ser–Glu–Gly. They were dissolved in water or the corresponding buffer electrolyte at concentrations ranging from 1 to 50 ng/ml.

The tryptic digest of β-casein was carried out in 50 m*M* Tris–HCl (pH 8.5). Water was purified in a Milli-Q Plus system (Millipore, Bedford, MA, USA). The buffer solutions in the electrode vessels were refilled after every 2–3 runs.

RESULTS AND DISCUSSION

"Three-buffer" stacking system

The classical stacking system used in SDS-PAGE applies a pH gradient and an amphoteric buffer component [9], which first acts as a terminating electrolyte but then overtakes the sample ions as the pH changes. Analogously a stacking system was developed for CZE for the separation of cationic peptides at an acidic pH of about 4.8. Its composition and arrangement of the electrolytes in the separation system is shown in Fig. 1a. It consists of three buffer electrolytes: a leading electrolyte and a stacking electrolyte, having the same constituents but different pH, and a terminating electrolyte. In this system tris(hydroxyethyl)aminomethane (Tris) acts as the leading ion whereas ε-aminocaproic acid (EACA) acts as the terminating ion when it is in a zone of high pH (>6), as formed by the stacking electrolyte. Under these conditions the mobility of EACA is very low, as it is almost a zwitterion at this pH. Hence, if the sample ions have a mobility between those of the leading and terminating electrolytes, its concentration is adapted to the concentration of the leading electrolyte, that is, concentration of the dilute sample occurs. As EACA enters a zone of lower pH, the dissociation of the carboxylic group is suppressed and it gains a higher positive charge and therefore a higher electrophoretic mobility. Hence it can overtake the analytes, which are then separated by zone electrophoresis in the EACA buffer.

In Fig. 2a and b the separation of three basic peptides dissolved in buffer electrolyte is shown without stacking and in the above stacking system. In the discontinuous system the sample is diluted tenfold, but at the same time the injection time is increased by a factor of ten compared with the non-stacking system, where injection was carried out for only 3 s. It can be clearly seen that in the discontinuous system, in spite of the high injection volume of 750 nl, a higher efficiency and a higher sensitivity

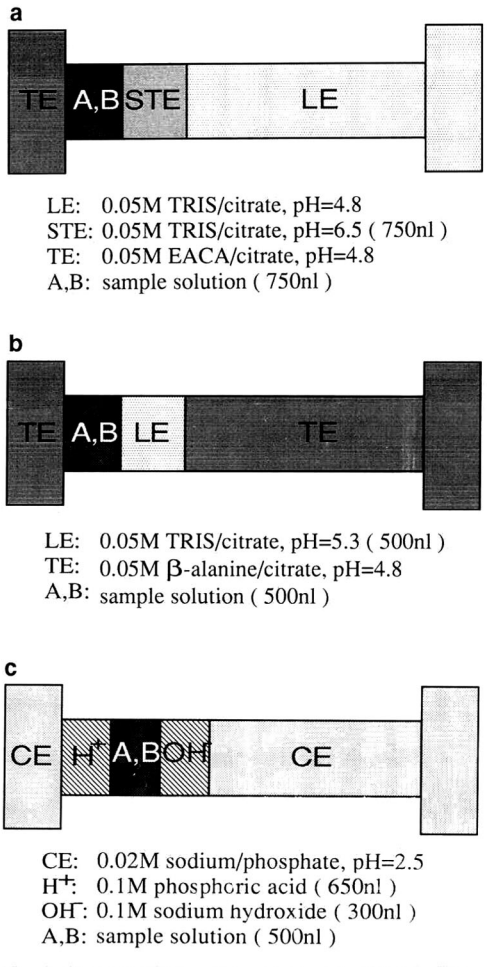

Fig. 1. Composition and arrangement of the buffer solutions of the different discontinuous systems in the separation unit. In parentheses the approximate volumes of the different zones for a 100-μm capillary, having a volume of about 4.5 μl, are given. LE = Leading electrolyte; STE = stacking electrolyte; TE = terminating electrolyte; CE = carrier electrolyte. (a) "Three-buffer" stacking system; (b) "two-buffer" stacking system; (c) "one-buffer" stacking system.

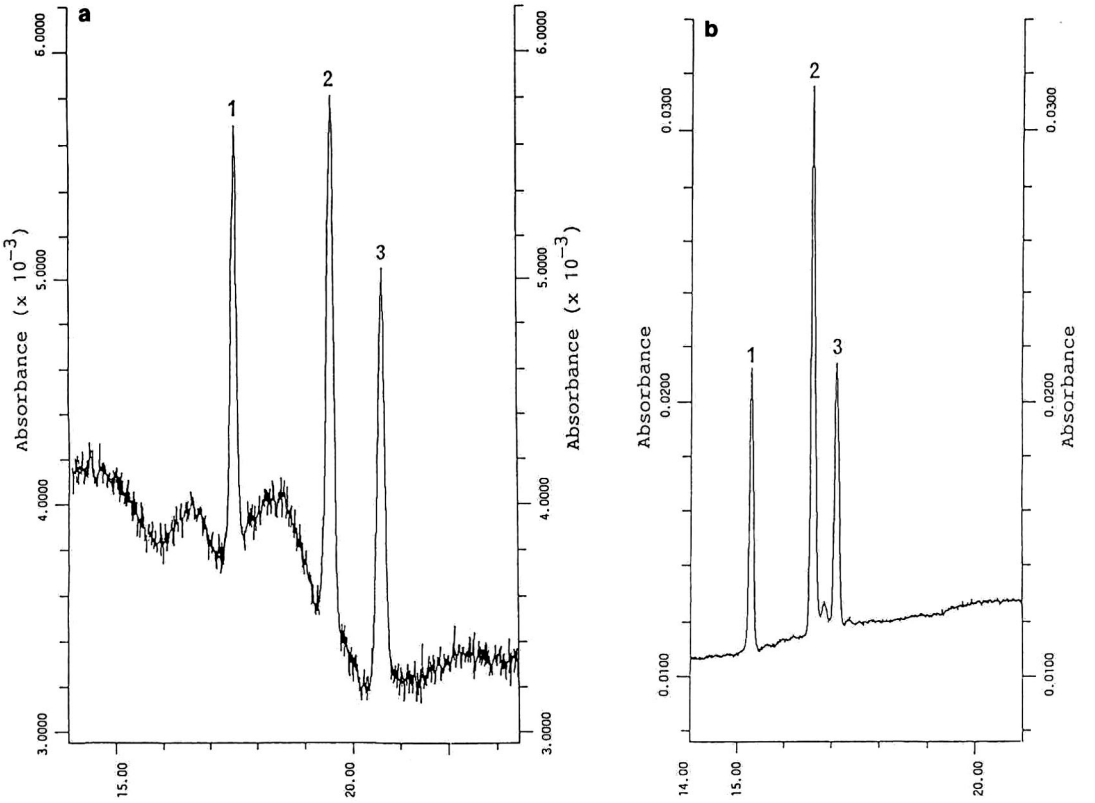

Fig. 2. Separation of three basic peptides: (a) without stacking in the EACA buffer of pH 4.8; (b) under stacking conditions in a three-buffer system. Concentrations of the peptides that were dissolved in the EACA buffer: (a) 10 ng/μl; (b) 1 ng/μl. Injection time: (a) 3 s; (b) 30 s. The sequence of the peptides is given under Experimental. For details of the electrolyte system, see Fig. 1a.

are obtained compared with the system without stacking.

The precision of the quantification under stacking conditions is comparable to that without stacking. The migration times obviously change in the discontinuous systems and are dependent on the length and conductivity of the injection zone.

To compare the different modes of injection, in Fig. 3 the peak width, expressed by the standard deviation, σ_z, based on length, is shown as a function of the injection time for the above separation of the three basic peptides. If a sample dissolved in buffer electrolyte is injected without stacking for 1 s, corresponding to a volume of about 25 nl, the maximum efficiency is not reached, *i.e.*, the contribution of injection to peak broadening is not negligible. For even higher injection times a steep increase in peak width, that is, a tremendous loss of efficiency, is observed. If injection is carried out from a sample dissolved only in water, about ten times the volume can be loaded without a decrease in efficiency. With the sample dissolved in buffer and using a discontinuous system, at least a 30 times higher sample load can be achieved compared with the non-stacking system. It can be seen that the peak widths remain constant over the whole injection range studied. In this way about 750 nl of sample can be introduced into the capillary, the volume being mainly limited by the dimensions of the capillary.

This kind of classical stacking system has the slight disadvantage that the choice of the terminating electrolyte sometimes presents a problem, as its mobility has to be lower than that of all the analytes at one pH and at the other pH it has to be higher, so

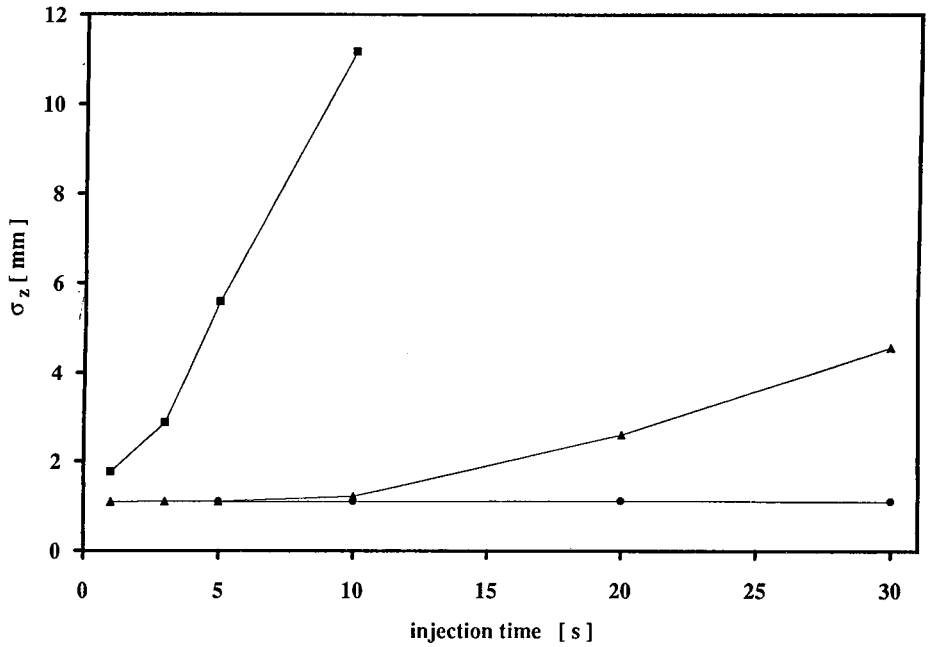

Fig. 3. Dependence of the peak width, expressed by the standard deviation based on length, σ_z, on the injection time for the different modes of injection. ■ = Injection of a sample dissolved in buffer electrolyte without stacking; ▲ = injection of a sample dissolved in water; ● = injection of a sample dissolved in buffer electrolyte under stacking conditions. The peak widths were calculated from the separation of basic peptides as shown in Fig. 2.

it can overtake the analytes. Especially with peptides, covering a wide range of mobilities, some problems may arise if other pH values are chosen. However, for the separation of basic peptides in the above system good stacking and destacking are observed.

"Two-buffer" stacking system

To facilitate the buffer selection, a stacking system, that requires no pH gradient, consisting of only two electrolytes, was developed as shown in Fig. 1b. The capillary is filled with an electrolyte of very low mobility, acting as a terminator, and just in front of the sample is placed a zone having a very high mobility, which will act as a leading electrolyte. The sample concentration is now increased as it is adapted to the concentration of the leading zone. Because this leading electrolyte is placed behind an electrolyte of lower mobility, it itself migrates zone electrophoretically in the terminating electrolyte and moves away from the sample ions. The analytes then are also separated by zone electrophoresis in the terminating electrolyte. In Fig. 4a and b the separations of three basic peptides without a leading electrolyte and in the presence of a leading electrolyte placed in front of the sample zone are shown. Injection was carried out for 20 s (*ca.* 500 nl). Without stacking the efficiency is lost and no resolution is observed. With the stacking system, high efficiency, sensitivity and resolution are obtained.

This stacking effect is also observed if a sample containing a high concentration of a mobile salt is separated in a buffer of very low mobility. Under these conditions the highly mobile salt ions may act as a leading electrolyte, resulting in sample concentration [17].

The reverse arrangement of the two electrolytes, the capillary being filled with leading electrolyte and a zone of a terminating electrolyte being placed behind the sample zone, may also lead to concentration of the analytes.

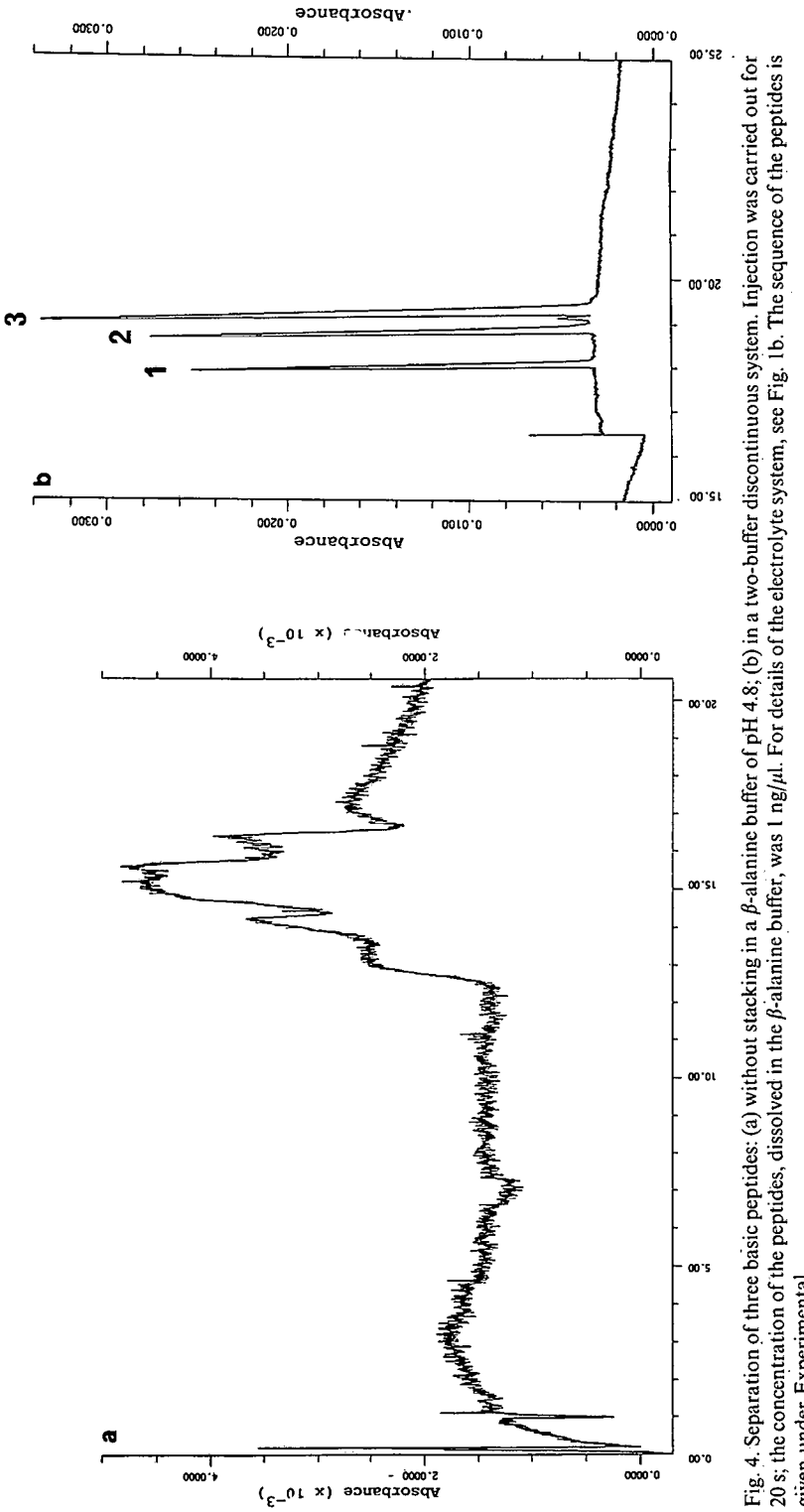

Fig. 4. Separation of three basic peptides: (a) without stacking in a β-alanine buffer of pH 4.8; (b) in a two-buffer discontinuous system. Injection was carried out for 20 s; the concentration of the peptides, dissolved in the β-alanine buffer, was 1 ng/μl. For details of the electrolyte system, see Fig. 1b. The sequence of the peptides is given under Experimental.

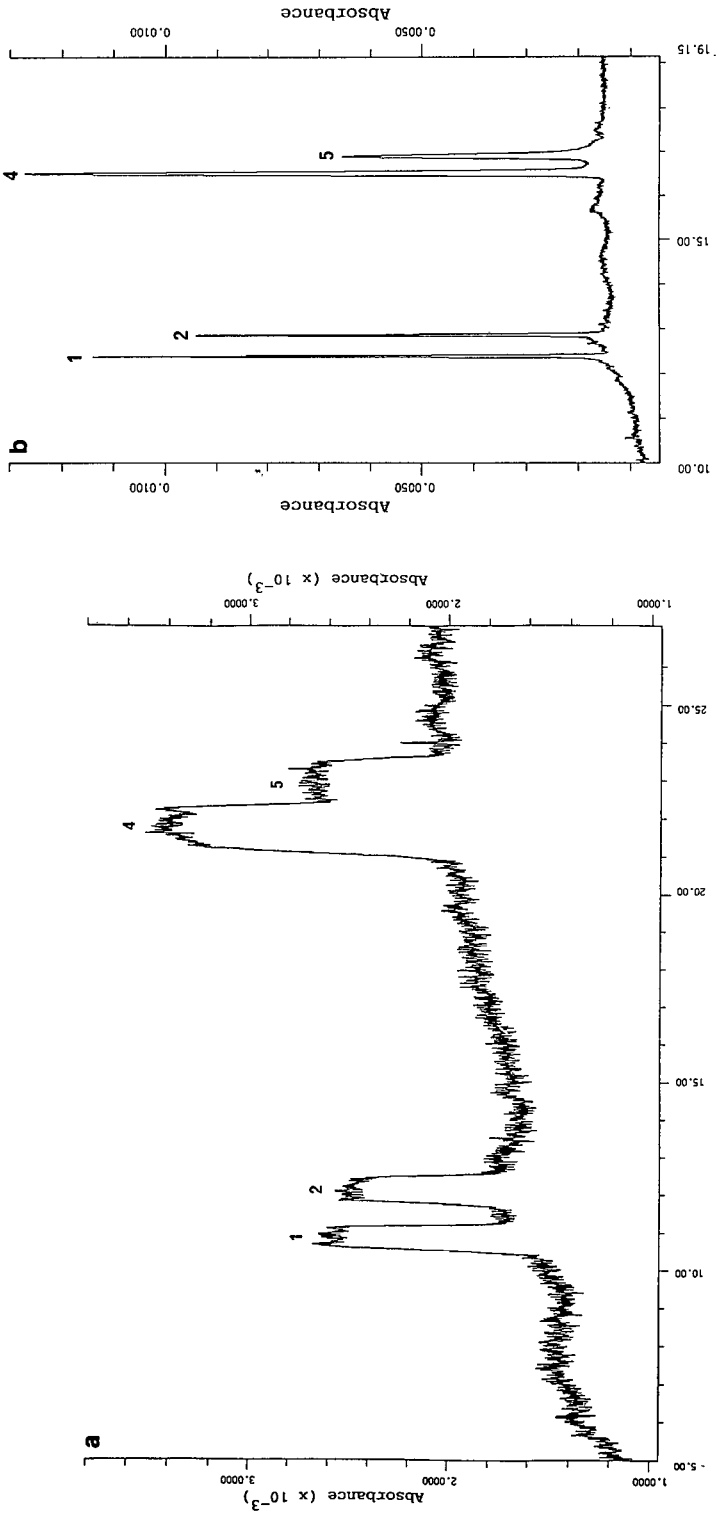

Fig. 5. Separation of four standard peptides in a phosphate buffer of pH 2.5; (a) without stacking; (b) sample sandwiched between a zone of H^+ and OH^-. Injection was carried out for 20 s; the concentration of the peptides, dissolved in the running buffer, was 2 ng/μl. The peptide code is explained under Experimental. For details of the electrolyte system, see Fig. 1c.

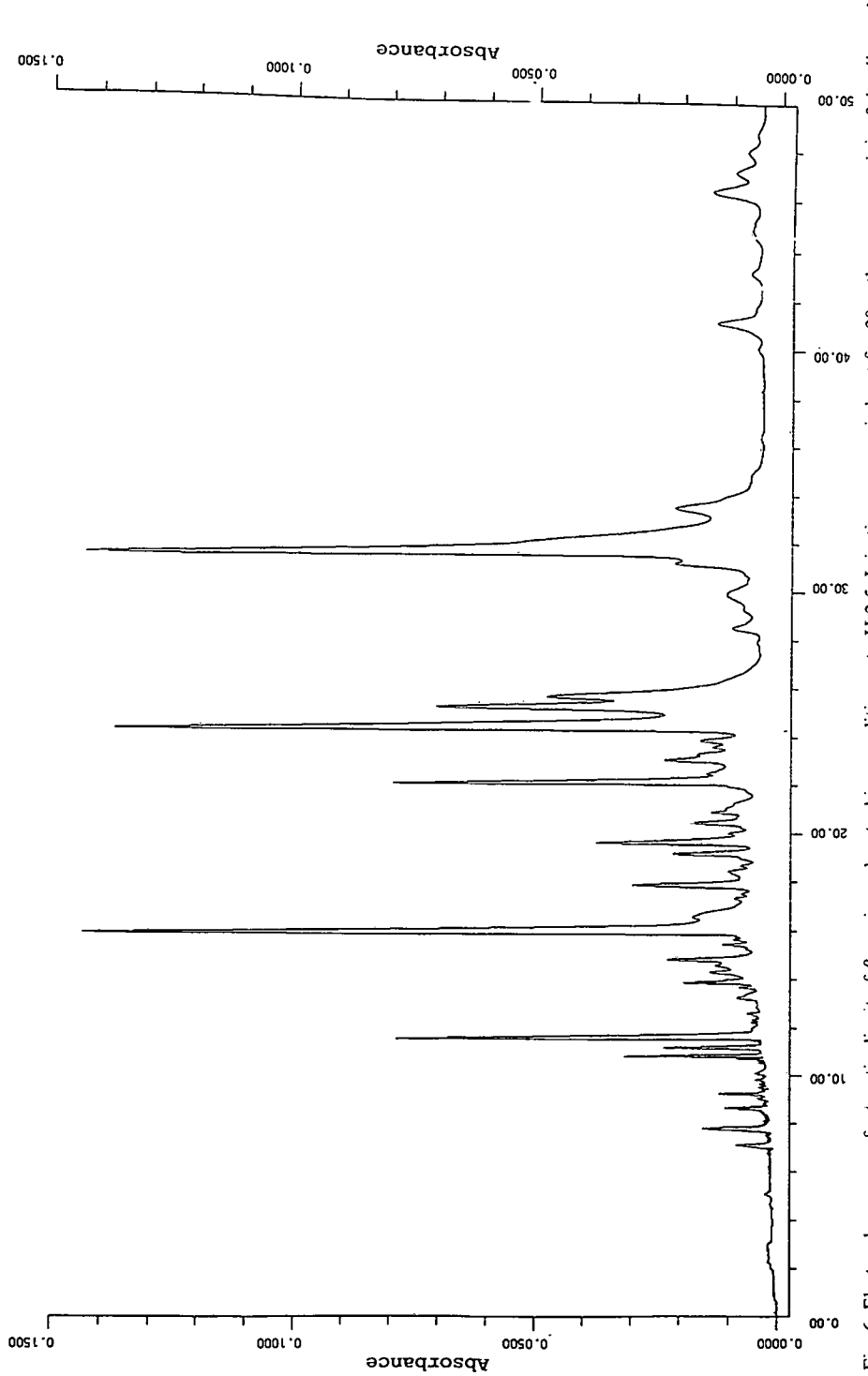

Fig. 6. Electropherogram of a tryptic digest of β-casein under stacking conditions at pH 2.5. Injection was carried out for 20 s; the concentration of the digested protein was 10 pmol/μl. For details of the electrolyte system, see Fig. 1c.

"One-buffer" stacking system

A disadvantage of the above stacking systems is that they do not work at extreme pH values. If peptides are to be analysed at a very low pH of about 2.5, so that all peptides migrate cationically, another stacking method has to be developed. Stacking of the analytes is achieved by sandwiching the sample between a zone of OH^- and H^+ as shown in Fig. 1c. As OH^- and H^+ are migrating towards each other, a zone of low conductivity is formed, as can be observed by a decrease in the electric current for a certain time at the beginning of the separation. Further OH^- and H^+ may act as a terminator. leading to isotachophoretic concentration of the analytes. Care has to be taken that the OH^- and H^+ zones are not too long, as overheating due to the high electric field strength in the low-conductivity zone formed may become a problem. In Fig. 5a and b the separation of four standard peptides (two basic, one neutral and one acidic) is shown in phosphate buffer of pH 2.5. Stacking leads to highly increased sensitivity and efficiency compared with a separation without stacking conditions.

This stacking system is not only applicable for the concentration of selected standard peptides but also for realistic samples, *e.g.*, a tryptic digest of β-casein as shown in Fig. 6. Injection was carried out for 20 s (*ca.* 500 nl) from a solution containing about 10 pmol/μl of digested protein. The peptide pattern obtained under stacking conditions is identical with that observed when a smaller volume of a more concentrated sample is injected without stacking. This means that with the described stacking system all peptides are recorded and none are lost.

With this system peptide fractions collected from HPLC can also be checked for purity with increased sensitivity. Fig. 7 shows an electropherogram obtained under stacking conditions of an HPLC fraction collected from a separation of tryptic peptides of β-casein. The fractions obtained from the RP-HPLC separation of 100 pmol of digested protein in an acetonitrile gradient containing 0.1% trifluoroacetic acid were directly injected into the CZE system without any preconcentration. Owing to the orthogonal separation principles of HPLC and CZE, a single peak in the chromatogram is resolved by CZE into several components.

A further aim with these stacking systems is to increase the sample load such that micropreparative

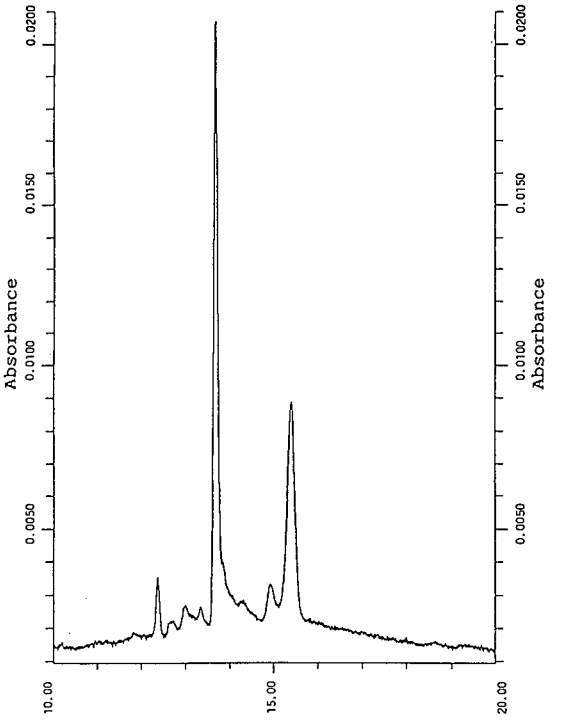

Fig. 7. Electropherogram of an HPLC fraction collected from the separation of digested β-casein. About 100 pmol of digest were separated by HPLC. Injection was carried out for 20 s. For details of the electrolyte system, see Fig. 1c.

separations also become possible with limited sample amounts. In Fig. 8 the separation of four standard peptides in phosphate buffer of pH 2.5 under stacking conditions is shown. The concentration of the analytes was 50 ng/μl (less than 100 pmol/μl). Injection was carried out for 20 s. From this electropherogram time windows were calculated for fraction collection of the four peptides. During the two following separation runs fractionation of the four peptides was carried out. To check the purity, the single fractions were reinjected also under stacking conditions as shown in Fig. 9. It can be seen that the first three peptide fractions were obtained almost pure, whereas the last fraction still contained a significant amount of the preceding peptide. This is probably caused by the fact that the calculation of the migration time from the detector to the end of the capillary is impeded by gradients in the electric field strength present in the separation system. This is the case when stacking systems are used for sam-

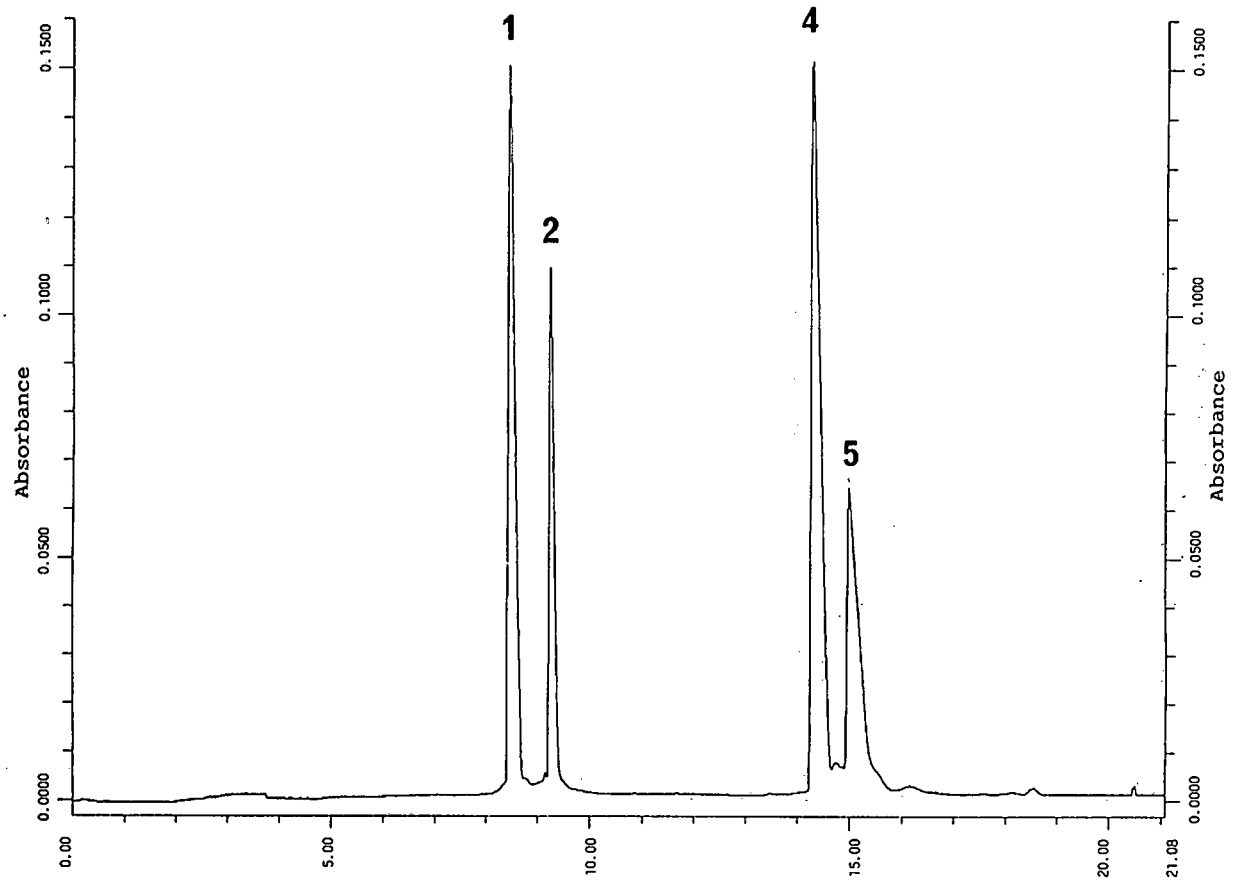

Fig. 8. Micropreparative separation of four standard peptides in phosphate buffer of pH 2.5 under stacking conditions. Injection was carried out for 20 s; the concentration of the peptides was 50 ng/μl. The peptide code is explained under Experimental. For details of the electrolyte system, see Fig. 1c.

ple concentration, or even if larger volumes of a low-conductivity sample are injected. More exact mobility values could be obtained using a double-detector system [18]. The purity of the single fractions may also be improved using other methods of collection [19].

From the re-injection, the sample amount collected was determined. It corresponded to a concentration of about 5 ng/μl, that is, about 50 ng of the single peptides were collected. The three pure peptide fractions were used for amino acid sequence analysis. An initial yield of about 40 pmol was found, corresponding well with the amount collected.

CONCLUSIONS

Discontinuous systems were introduced that allow the analysis of peptides and other analytes with an increased sample load of at least a factor of 30. These stacking systems can be applied for the concentration of dilute samples in commercially available instruments, making a micropreparative separation of moderately concentrated samples possible. Fractions can be collected from these separations and can be further characterized, *e.g.*; by amino acid sequence analysis, as was successfully demonstrated.

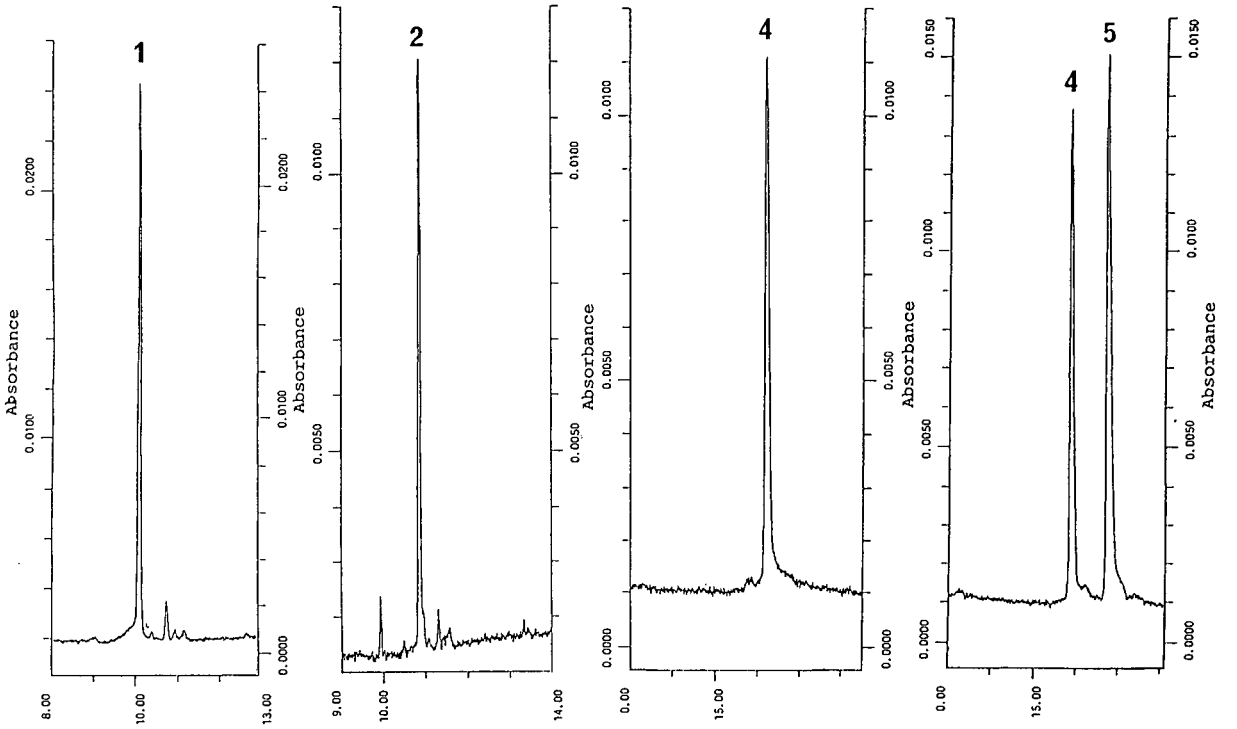

Fig. 9. Purity check of the fractions collected from the separation of four standard peptides as shown in Fig.8. The experimental conditions were the same as for the micropreparative run.

ACKNOWLEDGEMENT

The authors thank Beckman Instruments for providing the P/ACE 2100 CZE instrument. This work was supported by a bursary from the Commission of the European Communities.

REFERENCES

1 A. Guttman, A. S. Cohen, D. N. Heiger and B. L. Karger, *Anal. Chem.*, 62 (1990) 137.
2 E. Kenndler and Ch. Schwer, *Anal. Chem.*, 63 (1991) 2499.
3 T. M. Olefirowicz and A. G. Ewing, *J. Neurosci. Methods*, 34 (1990) 11.
4 H. Haglund and A. Tiselius, *Acta Chem. Scand.*, 4 (1950) 957.
5 F. E. P. Mikkers, F. M. Everaerts and Th. P. E. M. Verheggen, *J. Chromatogr.*, 169 (1979) 11.
6 D. S. Burgi and R.-L. Chien, *Anal. Chem.*, 63 (1991) 2042.
7 D. Kaniansky and J. Marak, *J. Chromatogr.*, 498 (1990) 191.
8 D. S. Stegehuis, H. Irth, U. R. Tjaden and J. Van der Greef, *J. Chromatogr.*, 538 (1991) 393.
9 L. Ornstein, *Ann. N.Y. Acad. Sci.*, 121 (1964) 321.
10 T. M. Jonvin, *Biochemistry*, 12 (1973) 871.
11 S. Hjertén, K. Elenbring, F. Kilar, J.-L. Liao. A. J. C. Chen, C. J. Siebert and M.-D. Zhu, *J. Chromatogr.*, 403 (1987) 47.
12 S. Hjerten, *Electrophoresis*, 11 (1990) 665.
13 F. Kohlrausch, *Ann. Phys. Chem.*, 62 (1897) 209.
14 S. Hjertén, *J. Chromatogr.*, 347 (1985) 191.
15 R. Biehler and H.E. Schwartz, *Technical Information Bulletin, TIBC-105*, Beckman, Palo Alto, CA, 1991.
16 C. Eckerskorn, W. Mewes, H. Goretzki and F. Lottspeich, *Eur. J. Biochem.*, 176 (1988) 509.
17 D. Kaniansky and J. Marak, presented at the *4th International Symposium on High Performance Capillary Electrophoresis*, Amsterdam, February 9–13, 1992.
18 J. L. Beckers, Th. P. E. M. Verheggen and F. M. Everaerts, *J. Chromatogr.*, 452 (1988) 591.
19 S. Hjertén and M.-D. Zhu, *J. Chromatogr.*, 327 (1985) 157.

Journal of Chromatography, 623 (1992) 357–365
Elsevier Science Publishers B.V., Amsterdam

CHROM. 24 446

Rapid isoelectric focusing of proteins in hydrolytically stable capillaries

Thomas J. Nelson

Neural Systems Section, National Institute of Neurological Disorders and Stroke, National Institues of Health, Bethesda, MD 20892 (USA)

(First received April 14th, 1992; revised manuscript received June 11th, 1992)

ABSTRACT

Three new types of capillary coatings for capillary isoelectric focusing that avoid siloxane chemistry, resulting in hydrolytically stable coatings, are described and tested: phenyl–silica, acrylamide-reacted vinyl–silica, and pure PTFE. Capillaries of these three types were compared using standard proteins and a biological mixture of proteins similar to what might be encountered in actual use. Of these, the acrylamide-coated capillary produced the highest-quality results. In contrast to capillaries prepared using siloxane reactions, the capillaries described herein exhibited greatly enhanced stability at high pH.

INTRODUCTION

Capillary zone electrophoresis (CZE) and capillary isoelectric focusing (cIEF) are high-resolution analytical techniques that can be used for separation of proteins [1,2], peptides [3,4], DNA [5], and other biological materials. Because of its high speed compared with slab gel electrophoresis, CZE is ideally suited for rapid analysis of proteins in their native state. One promising use is as a rapid assay at intermediate stages during purification for proteins which do not exhibit a specific measurable enzymatic activity. One limitation of CZE is that, although very minute quantities of solute molecules can be detected, in terms of concentration sensitivity, the current generation of UV detectors produces results slightly inferior to those achieved by high-performance liquid chromatography (HPLC). Additionally, injection of large sample volumes without stacking, or with dilute buffer stacking, reduces the plate count [6]. Thus, for free solution CZE it is necessary to concentrate dilute samples to very small volumes (≈ 1 μl). For proteins, this can cause sample precipitation or aggregation which cause loss of sample, clogging of the capillary, and spurious spikes in the electropherogram caused by particulates.

In principle, cIEF is not subject to this limitation, because the focusing process automatically concentrates the sample during the analysis. Thus, the entire capillary can be filled with sample at a low concentration. In addition, cIEF can provide an indication of a useful physical parameter, the protein's isoelectric point.

To date, however, only relatively few studies have used cIEF to analyze proteins [7–11]. In cIEF, a coated capillary is generally used in order to reduce or eliminate electroosmotic flow (EOF). Alternatively, polymer additives can be added to reduce EOF and wall adsorption by shielding interactions with the capillary wall or increasing solvent viscosity [12,13]. EOF acts to physically pump solvent toward the cathode, and thus interferes with the establishment of a stable pH gradient. Unfortunately, most of the coatings currently in use for CZE of proteins either do not sufficiently reduce EOF, or

Correspondence to: Dr. T. J. Nelson, Neural Systems Section, National Institute of Neurological Disorders and Stroke, Park-5/435, National Institutes of Health, Bethesda, MD 20892, USA.

utilize silane derivatives to covalently attach an uncharged organic compound to the silanol groups of the silica capillary. These siloxane linkages, which involve a Si–O–Si–C bond, are slowly hydrolyzed by the high-pH solution used in cIEF. After 5–10 uses, the coating is hydrolyzed away to such an extent that IEF is no longer possible. Therefore, a new type of coating process to eliminate this effect is desired.

This paper describes three types of capillary coatings that avoid siloxane chemistry, resulting in hydrolytically stable coatings: phenyl–silica, acrylamide-reacted vinyl–silica, and pure poly(tetrafluoroethylene), PTFE. Capillaries of these three types were compared using standard proteins and a biological mixture of proteins similar to what might be encountered in actual use. Of these, the acrylamide-coated capillary produced the highest-quality results.

MATERIALS AND METHODS

Coating of capillaries

Acrylamide–vinyl–silica capillaries. An 0.7-m length of 200 μm, 100 μm, or 75 μm I.D. silica capillary tubing was rinsed for 10 min with 1 *M* NaOH, then rinsed with water and dried for at least 2 h in an oven at 150°C with a flow of nitrogen under 5 p.s.i. through the capillary. During all oven treatments, the capillary was kept as straight as possible to prevent the formation of slight permanent bends in the capillary which caused breakage when the Beckman P/ACE autosampler was used. The PTFE septum in a bottle of $SiCl_4$ (Aldrich) was punctured with a 25-gauge needle and one end of the capillary was inserted through the hole. A second 25-gauge needle was inserted through the septum and nitrogen pressure (5 p.s.i.) was applied. Efflux of $SiCl_4$ vapor was verified by pointing the outlet end of the capillary onto a piece of pH paper. The end of the capillary inside the bottle was lowered under the surface and the capillary was filled with $SiCl_4$. The nitrogen pressure was released, the capillary was rapidly removed and its ends connected together by a small piece of silicone tubing (Manostat, 0.015 in. I.D. x 1/32 in. wall). The ends of the capillary were sealed with a small torch and the capillary was incubated overnight at 65°C in an oven. The next day one end was broken and rapidly inserted through a hole in the septum of a bottle of 1 *M* vinyl–MgBr in tetrahydrofuran. The bottle was pressurized with nitrogen as before, and the $SiCl_4$ was blown out. The capillary was flushed with nitrogen for at least 5 min, until the pH paper test indicated that all traces of $SiCl_4$ were removed. The end of the capillary was then submerged in the vinyl–MgBr solution and the solution was forced through the capillary for *ca.* 5 min. The ends of the capillary were sealed as before and the capillary was incubated for 1–2 h at 65°C. The capillary was then flushed with anhydrous THF and treated with $SiCl_4$ and vinyl-MgBr a second time using the same conditions and incubation times. The capillary was then rinsed with tetrahydrofuran, ethanol, water, 0.01 *M* H_3PO_4 and 0.01 *M* NaOH to remove any residual salts or organic compounds, and installed in a cartridge before coating with acrylamide. The final capillary length was 50–55 cm.

The washed capillary was then filled with a solution of 6% acrylamide, 0.4% N,N,N′,N′-tetramethylethylenediamine (TEMED), and 0.04% ammonium persulfate. When the acrylamide solution started to become viscous, the acrylamide was removed by applying pressure to the capillary and the coated capillary was rinsed with water for 10 min and incubated for 1 h at room temperature before use.

For comparison, some acrylamide-coated capillaries were also prepared by the method of Hjertén involving γ-methacryloxypropyltrimethoxysilane [8,14], except that excess silane reagent was removed by washing with ethanol before coating with acrylamide.

PTFE capillaries. A 0.5-m piece of PTFE tubing (0.304 mm I.D. × 0.76 mm O.D.) was flushed with hexane, chloroform, dimethylformamide, then ethanol for 20 min each in a bath of refluxing chloroform to remove any impurities. The tubing was straightened and inserted into a Beckman cartridge. In some cases, the PTFE was surface-dehydrofluorinated [15] by filling the tubing with 4 *M* NaOH containing 10% tetrabutylammonium phosphate solution (Alltech Low UV IPC-A) and incubating at room temperature overnight.

Phenyl-coated silica capillaries. A capillary was chlorinated with $SiCl_4$ as described above, and the chlorinated capillary was filled with phenyllithium (using the same procedure as used to fill the capillary with vinyl-MgBr) and reacted at 65°C for 1 h.

The $SiCl_4$ /phenyllithium treatment was repeated. The phenyllithium was removed by pressurizing the capillary with nitrogen and the capillary was rinsed sequentially with toluene, chloroform, ethanol, and water. Organolithium compounds react with Si–Cl bonds more vigorously than MgBr-containing Grignard reagents [16–18].

Capillary electrophoresis procedure. The coated capillary was installed in a cartridge and filled with a solution containing the protein sample, 2–5% Pharmalytes (pH 3–10), and in some samples, 1% Tween-20. The sample was focused at 10 or 30 kV in a Beckman P/ACE System 2050 with the anode in the inlet solution. The anolyte was 0.01 *M* H_3PO_4 and catholyte was 0.01 *M* NaOH. Absorbance was measured at 280 nm. For PTFE capillaries and 200 μm capillaries, the voltage was reduced to 4 and 5 kV, respectively.

RESULTS AND DISCUSSION

For analysis of protein mixtures from biological samples, isoelectric focusing is an ideal analytical method. Because the entire capillary can be filled with sample (as much as 0.01 ml in a large capillary), sample preconcentration, which results in aggregation and precipitation, is not necessary. In IEF, the proteins are concentrated automatically and can be easily filtered or centrifuged in these larger volumes. Another advantage is that capillary length and diameter are less of a factor in determining resolution, so shorter capillaries with attendant shorter elution times, or larger capillaries with larger sample capacities can be used. Finally, because lyophilization can be avoided, high salt concentrations are less of a problem. High salt concentrations in the sample can modify the appearance of the electropherogram [19,20].

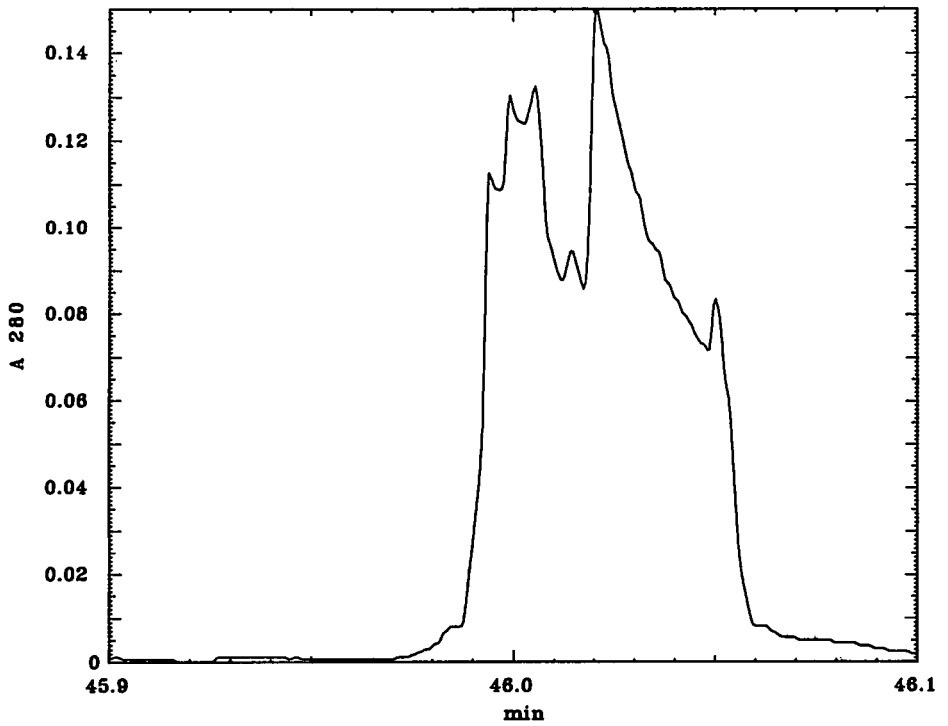

Fig. 1. Focusing of a mixture of bovine hemoglobin and bovine serum albumin in 2% ampholytes (Pharmalytes 3–10) in a 50 cm × 305 μm I.D. PTFE capillary focused for 45.0 min at 4 kV. The anolyte and catholyte contained 0.01 *M* H_3PO_4 in ethanol and 0.01 *M* NaOH in ethanol, respectively. The current decreased from 31 to 1.4 μA during focusing. After 45 min of focusing, the focused proteins were eluted using 0.5 p.s.i. pressure. Only a small degree of focusing is evident.

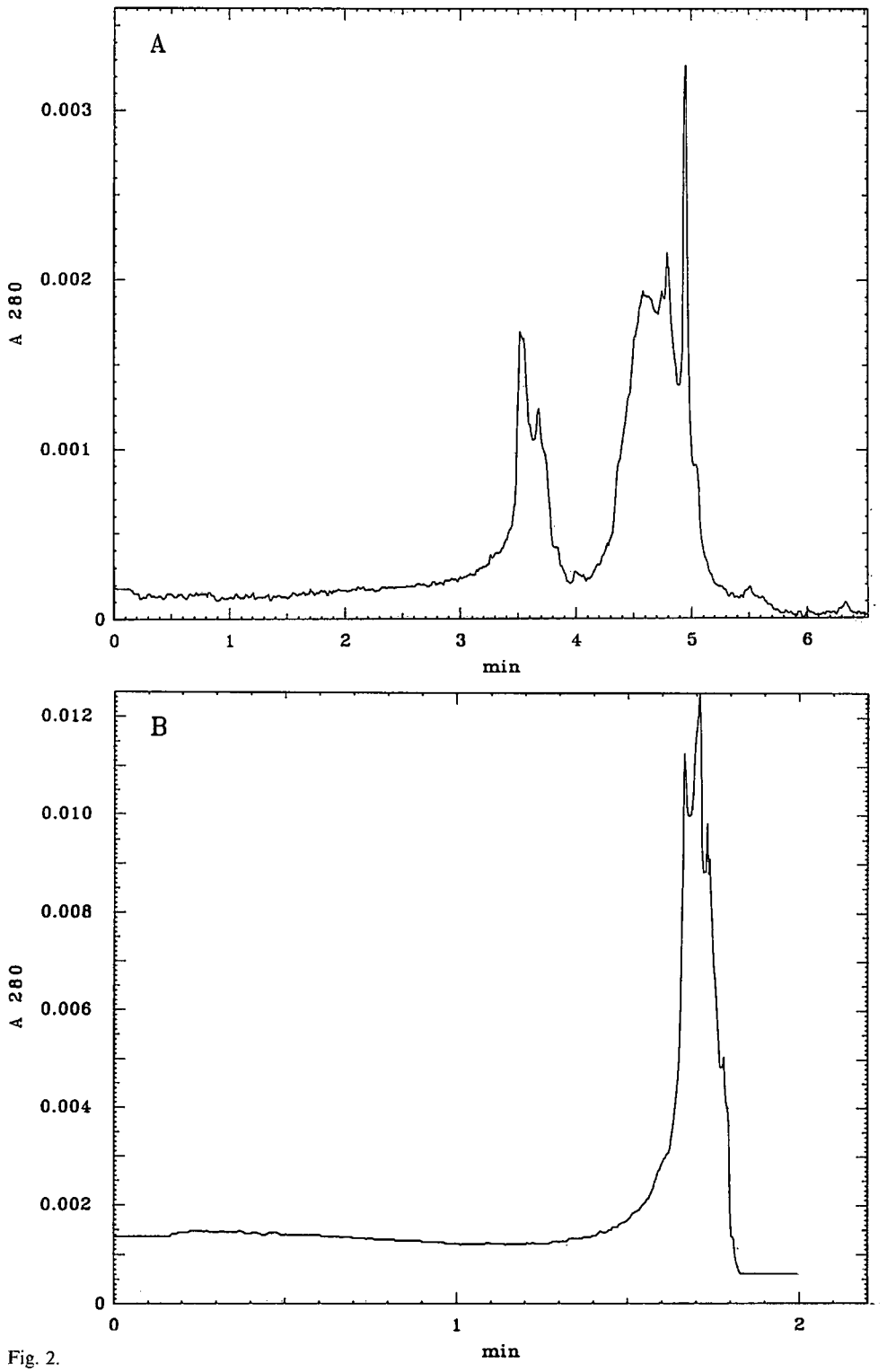
A
A 280
0.003
0.002
0.001
0
0
1
2
3
4
5
6
min
B
A 280
0.012
0.010
0.008
0.006
0.004
0.002
0
0
1
2
min

Fig. 2.

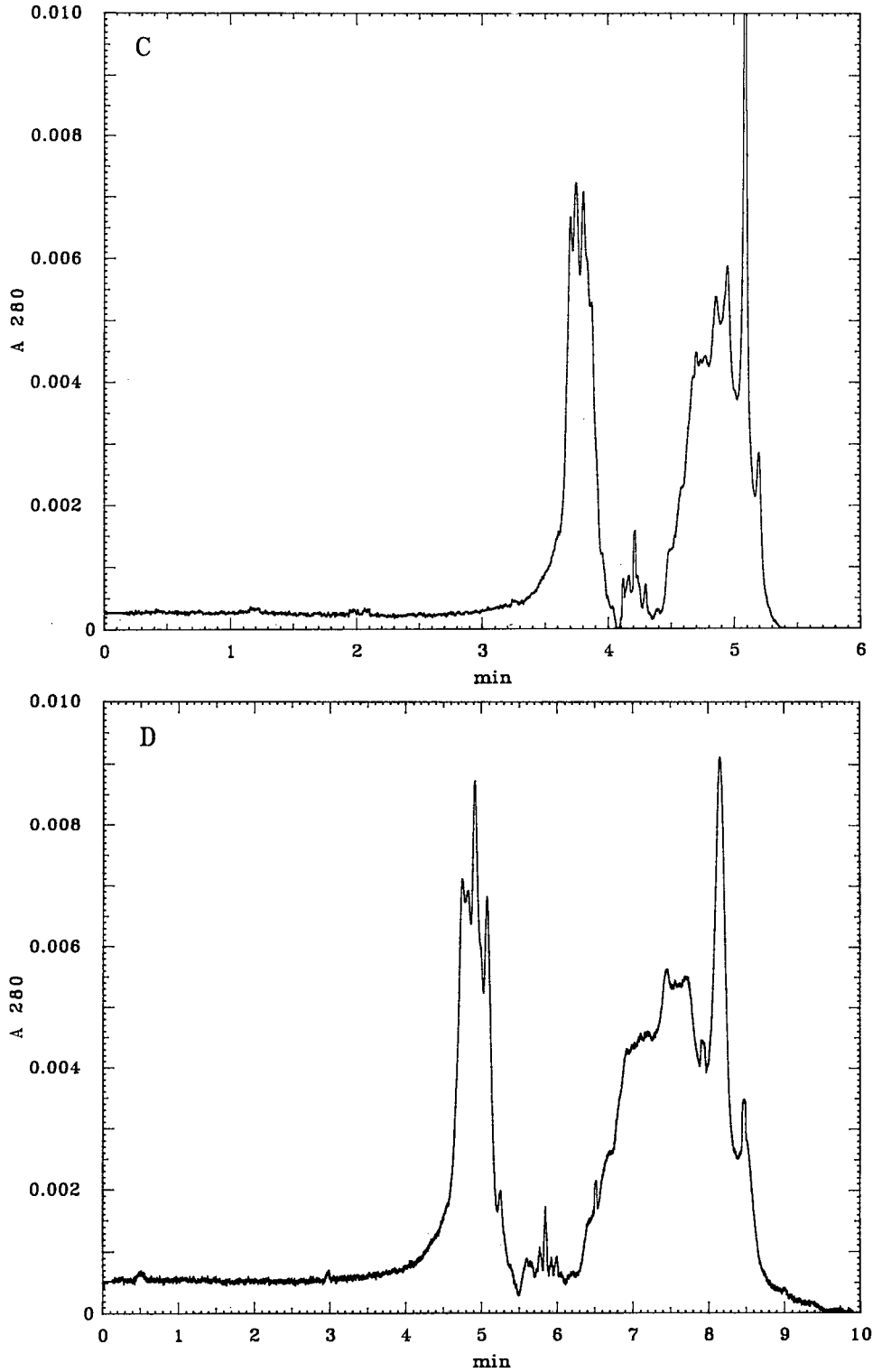

Fig. 2. (A) Focusing of a mixture of bovine hemoglobin and bovine serum albumin in 2% ampholytes (Pharmalytes 3-10) in a freshly prepared 50 cm × 100 μm I.D. capillary coated with acrylamide using the silanol method [8]. Focusing was carried out at 10 kV. During focusing, the current decreased from 8.2 to 4 μA in 6 min. The large peak at 4.95 min is albumin, and the small peak following albumin is an albumin contaminant. (B) Focusing of the protein mixture in the same capillary after 20 sample injections. (C) Focusing of the hemoglobin–serum albumin mixture in 2% ampholytes in a freshly prepared 50 cm × 100 μm I.D. capillary coated with acrylamide using the $SiCl_4$ method. Focusing was carried out at 10 kV. The current decreased from 8.0 to 3.7 μA in 6 min. (D) Focusing of the protein mixture in the same capillary after 30 sample injections.

Polymeric capillaries

Since electroosmotic flow is regarded as the predominant factor interfering with IEF, a variety of hydrophobic capillaries were tried, including PTFE, polyethylene (PE-10), and phenyl-coated silica. Both polyethylene and PTFE required low voltages (< 5 kV) in order to prevent thermally induced erratic increases in current. At higher voltages, heating also caused bubble formation, although this could be prevented by prior degassing of the sample. For PTFE capillaries, resolution and speed of focusing were improved by substuting 0.01 *M* H_3PO_4 and 0.02 *M* NaOH in 98% ethanol for aqueous electrode solutions. PTFE capillaries were sufficiently UV-transparent at 280 nm for direct use without modification. Both PTFE and surface-modified PTFE capillaries had unmeasurably low EOF, and a rapid decline in current occurred indicating that focusing of ampholytes was occurring. Because of the absence of EOF, the focused peaks did not elute spontaneously, but were eluted by pressure or replacement of anolyte with 0.02 *M* NaOH. Despite the lower EOF compared to acrylamide-coated capillaries of similar I.D., the focused proteins were incompletely resolved both with and without Tween-20 in the buffer (Fig. 1). No focusing was observed with phenyl-coated capillaries. These results with hydrophobic coatings suggest that the hydrophilicity of the surface coating is an important factor in IEF. However, these hydrophobic capillaries may be useful in separating other more hydrophilic substances, such as lipids.

Acrylamide-coated capillary

Acrylamide coated capillaries can be conveniently produced by silanization with γ-methacryloxypropyltrimethoxysilane followed by polymerization of acrylamide on the methacrylate moiety [8]. With acrylamide-coated capillaries, in contrast to polymeric capillaries, focusing occurred rapidly. In initial tests, the focusing was allowed to proceed for 3 min, after which the anolyte was replaced with 0.01 *M* NaOH to mobilize the focused proteins [21]. However, the mobilization procedure was found to be unnecessary, since these capillaries had sufficient EOF that the focused proteins eluted spontaneously even in the absence of mobilizing agent (Fig. 2A).

To test the efficiency of the coating procedure, the electroosmotic flow was measured in uncoated and acrylamide-coated capillaries. In uncoated capillaries filled with 20 m*M* sodium phosphate pH 7.0, the EOF was $4.63 \cdot 10^{-4}$ cm^2 V^{-1} s^{-1}. In the acrylamide-coated capillaries, EOF at pH 7 was reduced below measurable limits ($< 6.94 \cdot 10^{-6}$ cm^2 V^{-1} s^{-1}). However, the acrylamide-coated capillaries coated with the siloxane method exhibited measurable EOF after a few hours of exposure to high pH solution, presumably due to base hydrolysis of the Si–O–Si–C bonds. After a 4-h separation at pH 8.5, the EOF had risen to 1/3 that of an uncoated capillary.

This effect limited the usefulness for IEF of acrylamide-coated capillaries coated with the siloxane method. Fig. 2B shows a cIEF electropherogram of such a capillary after 20 IEF sample injections. Some separation is still evident, but all the peaks eluted by 2.0 min. Eventually, after more samples are analyzed, all peak resolution was lost. Thus, an improved coating technique was sought. An alternative reaction to link organic modifying groups to silica using the hydrolytically stable Si–C bond instead of a Si–O–Si–C bond has been suggested for creating stable stationary phases for liquid chromatography [22,23]. This method involves chlorinating the silica with $SOCl_2$. The chlorinated silicon then reacts avidly with Grignard reagents [17,18,23]. Previous workers showed that capillaries produced by reacting the chlorinated capillary with a Grignard reagent on which acrylamide could be polymerized exhibited reduced EOF [24]. However, these capillaries proved unsuitable for IEF (data not shown). The limiting step in creating this coating is chlorination of the surface silanols, while the Grignard reagent is believed to react instantaneously with the chlorinated silicon [17,23]. Therefore, a more agressive chlorination procedure was tried, using $SiCl_4$ [25]. At least two treatments with $SiCl_4$ were required to achieve measured EOF levels as low as those achievable with the silanol method. EOF can also be evaluated by comparing the current at equilibrium, *i.e.*, after the ampholytes have focused. Using this criterion, the $SiCl_4$ capillaries were also comparable to freshly coated capillaries prepared with the siloxane method (Fig. 2, legend).

Fig. 2C illustrates an electropherogram obtained with a $SiCl_4$ capillary. Acrylamide-coated capillaries coated using the $SiCl_4$ method produced results identical with acrylamide-coated capillaries pro-

duced using siloxane chemistry, but were considerably more stable. Fig. 2D shows an electropherogram of a mixture of standard proteins in the same capillary as in Fig. 2C after injection of 30 samples, some of which contained detergents, high salt, and high pH. Even after 30 runs, no deterioration of the $SiCl_4$ capillary was apparent. In fact, the proteins are retained longer, suggesting that additional residual EOF-inducing substances had been removed.

Fig. 3 shows an IEF pattern from *Hermissenda* tentacle supernatant in an 0.3-m acrylamide-coated capillary. Most of the proteins focused and eluted before the current had reached a plateau value. The entire electropherogram was produced within 3.0 min after sample was applied. Very sharp focusing was observed, with a peak width of *ca.* 0.5 s for the largest peak, while the later, more acidic proteins, were somewhat broader. At least 60 protein components are visible altogether.

Addition of non-ionic detergent (Tween-20) improved resolution for the *Hermissenda* samples, probably by reducing the interaction with uncoated silanols or by increasing the effective size of the proteins. However, for other samples, addition of detergent had little effect (data not shown).

The residence time of the proteins in the capillary could be increased by adding NaCl to the catholyte. However, this did not improve resolution or affect the relative elution order of the peaks (Fig. 4). Increasing the NaCl in the catholyte to 0.04 *M* prolonged the elution period to 10 min. Altering the H_3PO_4 and NaOH concentrations also had little effect on the separation (not shown). Because the proteins tended to elute spontaneously from the capillary, the retention times of the proteins were not a simple function of isoelectric point.

Fig. 5 shows an electropherogram of rabbit cerebral cortex supernatant. Because this sample contained a higher salt concentration than the sample

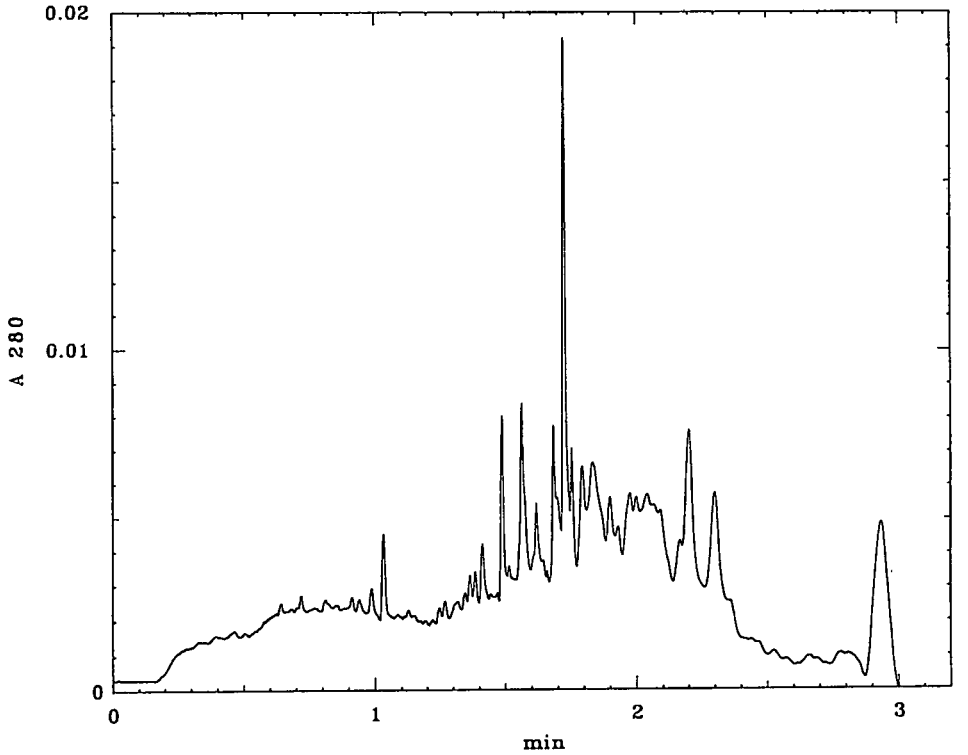

Fig. 3. Focusing of *Hermissenda* tentacle proteins in an acrylamide-coated capillary at 10 kV. The capillary was filled with *ca.* 50 μg/ml total cytoplasmic proteins containing 10% Pharmalytes 3-10 and 1% Tween-20 before focusing. The current decreased from 92 to 32 μA in 4.0 min.

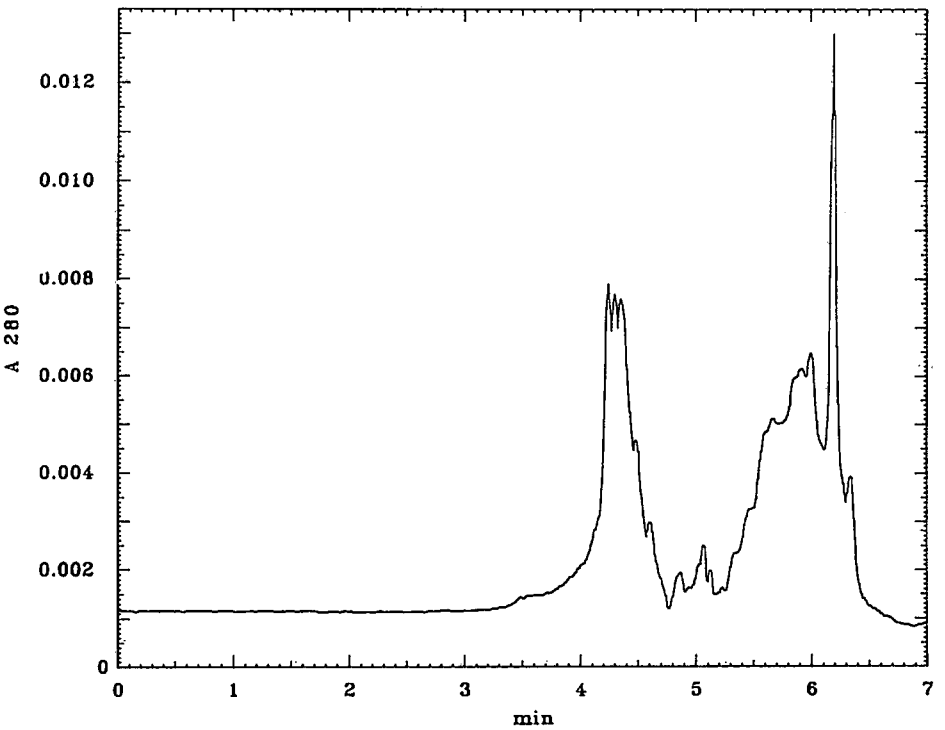

Fig. 4. Focusing of a mixture of bovine hemoglobin and bovine serum albumin in an acrylamide-coated capillary. Conditions were the same as in Fig. 2C except that 0.01 *M* NaCl was added to the catholyte solution. The elution pattern is similar to the pattern in Fig.2C except that the proteins are retained for a longer period.

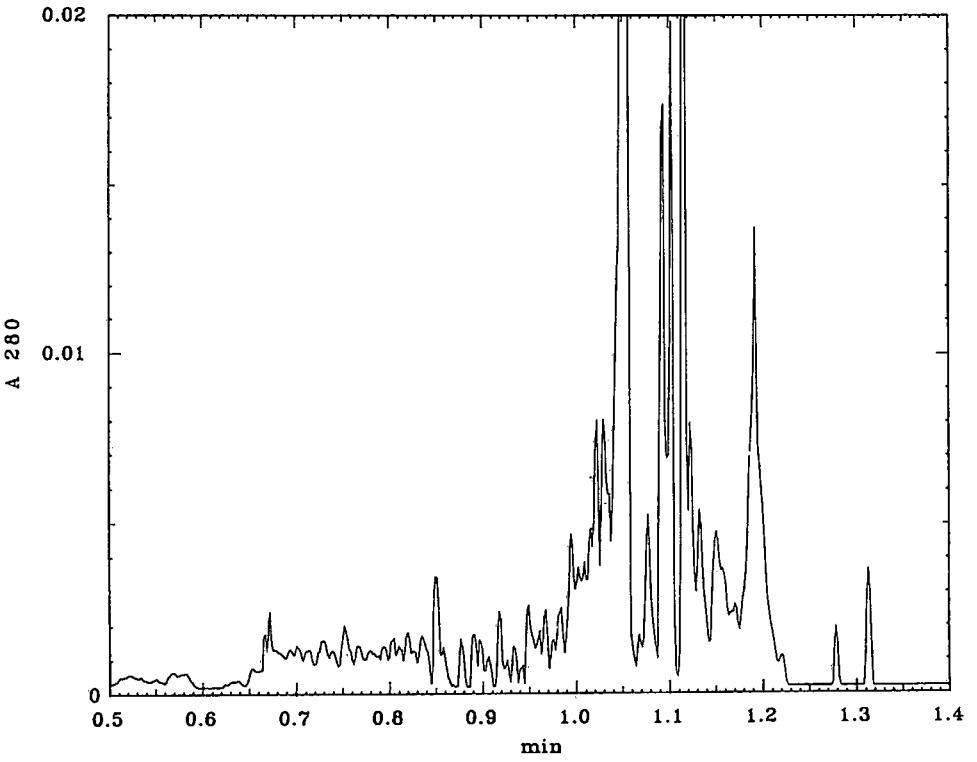

Fig. 5. Focusing of rabbit brain proteins in an acrylamide-coated capillary produced with the $SiCl_4$ method. A sample of rabbit cerebral cortex was homogenized in 10 volumes of water and centrifuged (10 000 *g* × 1 min). A 20-μl aliquot of the supernatant fraction was diluted to 100 μl, and 2 μl of ampholines were added before focusing at 10 kV. Most proteins eluted between 0.6 and 1.4 min.

in Fig. 3, the entire sample was eluted in under 1.5 min. Peaks were also extremely sharp, with minimum peak widths on the order of 0.15–0.25 s. Efficiency calculation was difficult, however, because at the maximum obtainable 10 Hz data acquisition rate, many of the peaks were only 1–2 data points wide. The decrease in absorbance to below baseline values at 1.25 min is caused by displacement of the ampholytes with buffer, and can be eliminated by addition of ampholytes to the anolyte and catholyte solutions.

The rapid elution of focused peaks in Fig. 5 indicates that focusing had occurred within the first $\approx$0.8 min. Since initially the capillary was uniformly filled with sample, this means that the earliest peaks represented proteins that must have travelled at up to 0.5 m/min. It is apparent that some EOF still remains in acrylamide-coated capillaries coated with both methods. This may be caused by a few remaining silanols at the high pH end of the capillary. EOF due to silanol ionization is known to be strongly pH dependent. To test whether focusing was complete, an IEF sample was tested with the proteins only filling the first 1/10 of the capillary nearest the anode or the cathode, with the remainder of the capillary filled with ampholytes alone. In both cases, resolution was greatly reduced.

Although the coated capillaries described here exhibited greater stability than other coatings at high pH, one would expect that after prolonged exposure, the Si–C bonds eventually would begin to hydrolyze. Polyacrylamide could also be hydrolyzed to acrylic acid by high pH, particularly at higher temperatures. Thus, the capillaries should be rinsed with water after use.

The above results demonstrate that cIEF carried out in the hydrolytically stable capillaries results in a rapid, highly reproducible, and high-resolution separation of complex protein mixtures.

REFERENCES

1 M. V. Novotny, K. A. Cobb and J. Liu, *Electrophoresis*, 11 (1990) 735.
2 S. A. Swedberg, *Anal. Biochem.*, 185 (1990) 51.
3 K. Cobb and M. Novotny *Anal. Chem.*, 61 (1989) 2226.
4 M. A. Firestone, J. Michaud, R. H. Carter and W. Thormann, *J. Chomatogr.*, 407 (1987) 363.
5 K. J. Ulfelder, E. E. Schwartz, J. M. Hall and F. J. Sunzeri, *Anal. Biochem.*, 200 (1992) 260.
6 A. Vinther and H. Søeberg, *J. Chromatogr.*, 559 (1991) 3.
7 F. Kilar and S. Hjertén, *Electrophoresis*, 10 (1989) 23.
8 S. Hjertén, *J. Chromatogr.*, 347 (1985) 191.
9 K. W. Yim, *J. Chromatogr.*, 559 (1991) 401.
10 M. Zhu, R. Rodriguez and R. Wehr, *J. Chromatogr.*, 559 (1991) 479.
11 S. Hjertén, K. Elenbring, F. Kilár, J.-L. Liao, A. J. C. Chen, C. J. Siebert and M.-D. Zhu, *J. Chromatogr.*, 403 (1987) 47.
12 J. R. Mazzeo and I. S. Krull, *Biotechniques*, 10 (1991) 638.
13 Y. Tanaka and W. Thormann, *Electrophoresis*, (1990) 11, 760.
14 S. Hjertén, *J. Chromatogr.*, 550 (1991) 811.
15 A. J. Dias and T. J. McCarthy, *Macromolecules*, 17 (1984) 2529.
16 E. A. V. Ebsworth, *Volatile Silicon Compounds*, Pergamon Press, New York, 1960, p.63.
17 C. Eaborn, *Organosilicon compounds*, Academic Press, New York, 1960.
18 R. K. Boeckman, D. M. Blum and B. Ganem, *Org. Synth.*, 58 (1978) 158.
19 W. Nashabeh and Z. el Rassi, *J. Chromatogr.*, 559 (1991) 367.
20 K. Salomon, D. S. Burgii and J. C. Helmer, *J. Chromatogr.*, 559 (1991) 69.
21 S. Hjerten and J.-L. Liao, *Protides Biol. Fluids*, 34 (1986) 727.
22 J. J. Pesek and S. A. Swedberg, *J. Chromatogr.*, 361 (1986) 83.
23 J. J. Pesek and S. Swedberg, *US Pat.*, 4 904 632 (1990).
24 K. A. Cobb, V. Dolnik and M. Novotny, *Anal. Chem.*, 62 (1990) 2478.
25 D. C. Locke, J. T. Schmermund and B. Banner, *Anal. Chem.*, 44 (1972) 90.

Journal of Chromatography, 623 (1992) 366–370
Elsevier Science Publishers B.V., Amsterdam

CHROM. 24 479

Short Communication

New approach for area determination of an overlapped pair of chromatographic peaks

W. Wei, N. S. Wu and X. H. Jiang

Department of Applied Chemistry, University of Science and Technology of China, Hefei, Anhui 230026 (China)

(First received May 4th, 1992; revised manuscript received June 30th, 1992)

ABSTRACT

Based on an exponentially modified Gaussian model, a new approach for the area determination of an overlapped pair of peaks was developed. Empirical equations for the accurate calculation of the area ratio are presented. Individual peak areas can be calculated from the area ratio and the total area of an overlapped pair. This method can be applied over a wide range provided that there is a clear and precise valley except for shoulder peaks. The relative error of the peak area determiantion is less than ±5%.

INTRODUCTION

The occurrence of unresolved or overlapped chromatographic peaks is a commonly encountered practical problem. The perpendicular-drop method is generally employed for the measurement of overlapped peaks. Foley [1] reported that the error due to a combination of peak tailing and differences in peak size can be exceed 200% for peak area measurement by this method. Jeansonne and Foley [2] reported a method with an accuracy of ±4% for the first peak area of an overlapped pair when the relative valley is less than 45%. Lin and Lu [3] reported a table of correction factors for the quantitative area determination of overlapped peaks. In previous papers [4,5] we reported two methods for the measurement of the areas of an overlapped pair of peaks. These methods were all based on the calculation of the first peak area of an overlapped pair, the second peak area being obtained by subtraction of the first peak area from the total area measured by an electronic integrator. In this paper, we report an approach for area determination based on the area ratio of an overlapped pair of peaks.

Correspondence to: Dr. N. S. Wu, Department of Applied Chemistry, University of Science and Technology of China, Hefei, Anhui 230026, China.

THEORY

The following exponentially modified Gaussian (EMG) peak-shape model is used:

$$h(t) = \left(\frac{A}{2\tau}\right)\exp\left(\frac{\sigma^2}{2\tau^2} - \frac{t - t_g}{\tau}\right)[1 + \mathrm{erf}(Z/\sqrt{2})] \quad (1)$$

where

$$Z = \frac{t - t_g}{\sigma} - \frac{\sigma}{\tau} \quad (2)$$

$$\mathrm{erf}(x) = \frac{2}{\sqrt{\pi}}\int_0^x e^{-y^2}\,dy \quad (3)$$

0021-9673/92/$05.00

t_g and σ are the retention time and standard deviation of the parent Gaussian peak, respectively, τ is the time constant of the exponential decay, $h(t)$ is the height at time t and the peak asymmetry is characterized by $S = \sigma/\tau$.

According to McWilliam and Bolton [6], assuming that the asymmetry and peak widths of two peaks are equal, the profile of an overlapped pair can be simulated by the following equation:

$$H(t) = h(t) + rh(t - d) \tag{4}$$

which represents an EMG function $h(t)$ followed after time d by another, $h(t - d)$, of equal width, where r is the area ratio of the second to the first peak ($r = A_2/A_1$, where A_1 and A_2 are the areas of the first and second of an overlapping pair of peaks) and $H(t)$ is the superposed height at time t.

From previous work [5] and ref. 2, the height of the first peak of an overlapped pair is less affected by the overlap (the increment of the height is usually less than 5%), as shown in Fig. 1. Therefore, it is reasonable to assume that the height of the first peak remains almost unchanged after overlap, *i.e.*, $h_1 \approx h_{10}$, where h_1 and h_{10} are the heights of the first peak after and before overlap, respectively.

The height of the second peak of an overlapped pair can be expressed as

$$h_2 = h_{20} + h_{12} \tag{5}$$

where h_{20} and h_2 are the heights of the second peak before and after overlap, respectively, and h_{12} is the increment of the second peak height resulting from the overlap with the first peak; h_{12} depends on the asymmetry of the first peak and the degree of overlap and, from eqn. 1, it can be expressed as

$$h_{12} = \left(\frac{A_1}{2\tau}\right)\exp\left(\frac{\sigma^2}{2\tau^2} - \frac{t_{r2} - t_g}{\tau}\right)[1 + \mathrm{erf}(Z_{12}/\sqrt{2})] \tag{6}$$

where

$$Z_{12} = \frac{t_{r2} - t_g}{\sigma} - \frac{\sigma}{\tau} \tag{7}$$

$$t_{r2} = t_{r1} + d \tag{8}$$

and t_{r1} and t_{r2} are the retention times of the first and the second peak, respectively, before overlap.

Dividing each term of eqn. 5 by h_1, we obtain

$$\frac{h_2}{h_1} = \frac{h_{20}}{h_1} + \frac{h_{12}}{h_1} \approx \frac{h_{20}}{h_{10}} + \frac{h_{12}}{h_1} \tag{9}$$

From eqns. 1, 6 and 9, the following form can be obtained:

$$\frac{h_2}{h_1} = \frac{h_{20}}{h_{10}} \approx \gamma - \exp\left(-\frac{d}{\tau}\right)\frac{1 + \mathrm{erf}(Z_{12}/\sqrt{2})}{1 + \mathrm{erf}(Z_{11}/\sqrt{2})} \tag{10}$$

where

$$Z_{11} = \frac{t_{r1} - t_g}{\sigma} - \frac{\sigma}{\tau} \tag{11}$$

and γ is the apparent height ratio of an overlapped pair of peaks.

The parameters in the last term of eqn. 10 are unknown in practice and eqn. 10 is inconvenient to use. In order to make eqn. 10 practicable, we arbitrarily substituted $\exp[-c\Delta t/W_{0.1(r)})$ for the last term in eqn. 10. Thus, eqn. 10 becomes

$$r \approx \gamma - \exp\left[-\frac{c\Delta t}{W_{0.1(r)}}\right] \tag{10a}$$

where $W_{0.1(r)}$ is the rear half-width at 10% height, Δt is the distance of an overlapped pair and c is a coefficient. The general expression can be obtained as follows. First, by using linear regression of the theoretical value of the last term in eqn. 10 and the calculated value of $\Delta t/W_{0.1(r)}$, the regression coefficient was taken as the initial value of c in eqn. 10a.

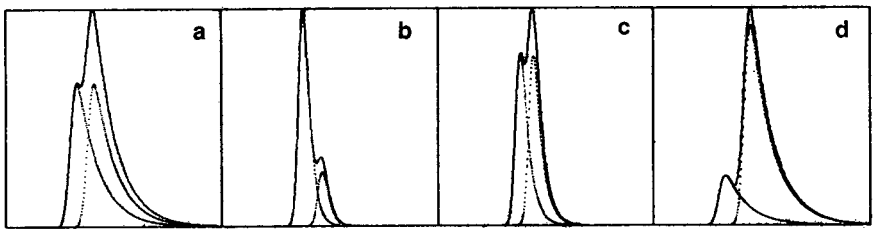

Fig. 1. Effect of the second peak of an overlapped pair on the height of the first peak. (a) $S = 0.2$, $r = 1{:}1$; (b) $S = 1$, $r = 1{:}5$; (c) $S = 1$, $r = 1{:}1$; (d) $S = 0.2$, $r = 5{:}1$.

Then, an iteration multiple regression program, *i.e.*, simplex algorithm, was used to adjust the residual sum of squares about the empirical regression equation (eqn. 20 or 21) to a minimum. Finally, eqns. 20 and 21 were obtained. The error resulting from the approximation we made can be reduced by this regression treatment.

The area of the first and second peak can be calculated by eqn. 12 or 13:

$$A_1 = \frac{A_t}{1 + r} \tag{12}$$

and

$$A_2 = \frac{r A_t}{1 + r} \tag{13}$$

where A_t is total area of overlapping peaks.

The expressions for the relative error of the first and second peak area ($\%RE_{A1}$, $\%RE_{A2}$) can be deduced as below. In general, the relative error ($\%RE$) is

$$\%RE = \frac{O - T}{T} \cdot 100 \tag{14}$$

where O and T are the calculated and real values, respectively. For the first peak area,

$$O = \frac{A_t}{1 + r_{cal}} \tag{15}$$

$$T = \frac{A_t}{1 + r} \tag{16}$$

where r and r_{cal} are the real area ratio and the area ratio calculated from eqn. 20 or 21, respectively.

Substituting eqns. 15 and 16 into eqn. 14, we obtain

$$\%RE_{A1} = \left(\frac{1 + r}{1 + r_{cal}} - 1\right) \cdot 100$$

$$= \frac{r - r_{cal}}{1 + r_{cal}} \cdot 100 \tag{17}$$

Similarly,

$$\%RE_{A2} = \frac{r_{cal} - r}{r(1 + r_{cal})} \cdot 100 \tag{18}$$

Obviously, the relative error of area ratio ($\%RE_r$) is

$$\%RE_r = \frac{r_{cal} - r}{r} \cdot 100 \tag{19}$$

EXPERIMENTAL

All calculations were run on an IBM-PC computer using a BASIC program. In this paper, the area ratio is restricted to 4:1 to 1:4, and the asymmetry (σ/τ) varied from 0.2 to 2, corresponding to $f_{0.1}$ from 1.003 to 4.147 (the definition of $f_{0.1}$ is shown below).

Gas chromatographic experiments were performed on a Model 102 G gas chromatograph (Shanghai Analytical Instrument Factory), connected with a Shimadzu C-R1B data processor. The column used was 2 m × 3 mm I.D. and contained 15% dinonyl phthalate as the stationary phase coated on 60–80-mesh white diatomite support (Shanghai Reagent Plant). The chromatograms were recorded at a chart speed of 120 mm/min. Overlapped peak pairs were generated according to the literature [2]. By consecutive injections of test solutions consisting of toluene–benzene or toluene–ethylbenzene at short time intervals, the overlapped profiles of two toluene peaks were obtained. Benzene and ethylbenzene were used as internal standards. From the princple of the internal standard method, the real r value of overlapped toluene peaks can be accurately determined.

High-performance liquid chromatographic experiments were performed on a Model 5060 instrument (Varian, Palo Alto, CA, USA) equipped with a UV–VIS detector. The mobile phase was 75% methanol–deionized water (75:25). The flow-rate was 0.8 ml/min and the UV detector was set at 275 nm. A 150 × 4.6 mm I.D. MCH-5 (ODS) column was used isothermally at 30°C. *p*-Chlorotoluene and *m*-chlorotoluene were taken as test materials. Under the conditions described above, *p*-chlorotoluene was eluted first. The chromatograms were recorded at a chart speed of 30 cm/min. Working solutions of *p*- and *m*-chlorotoluene of 0.1% and 0.2% in methanol, respectively, were used. The different mixing solutions were made by mixing different volumes of the two working solutions and diluting to 1 ml. The degree of overlap and the area ratio of an overlapped pair of peaks are dependent on the mixed solution. Dilute solutions of the two test compounds were prepared by taking the same volume of each working solution as that in the preparing mixed solution separately and diluting to 1 ml with methanol. The true area of either peak of

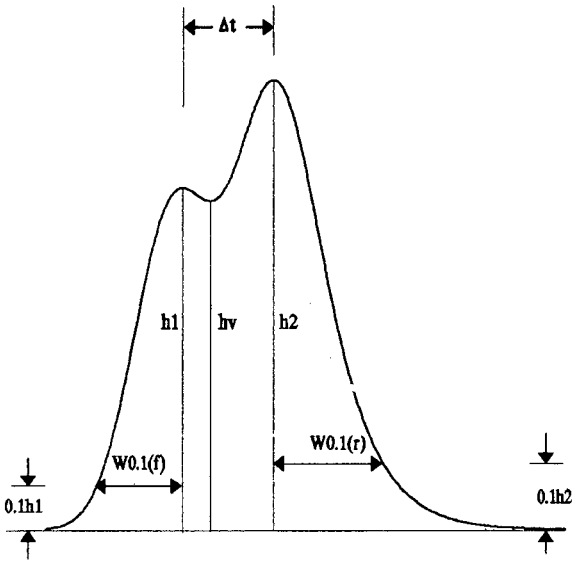

Fig. 2. Schematic diagram of parameters. $\gamma = h_2/h_1$; $f_{0.1} = W_{0.1(r)}/W_{0.1(f)}$.

TABLE I

THEORETICAL RELATIVE ERROR OF AREA RATIO CALCULATED FROM EQN. 20 OR 21

S	A_2:A_1					
	4:1		1:1		1:4	
	$\%V^a$	$\%RE_r$	$\%V^a$	$\%RE_r$	$\%V^a$	$\%RE_r$
0.2	99.77	−2.29	90.59	0.63	93.83	0.44
0.4	99.72	4.02	99.16	0.21	97.08	0.82
0.6	95.77	−2.82	97.26	0.01	98.12	−0.50
0.8	97.47	2.69	95.17	0.98	96.44	−0.96
1.0	93.08	2.03	94.50	−2.73	95.91	−1.50
1.2	92.69	4.65	99.04	3.24	98.70	−0.40
1.4	97.36	2.16	93.78	2.70	94.11	−0.38
1.6	97.13	0.22	97.84	−0.25	92.02	−0.48
1.8	99.86	0.60	96.61	−0.74	90.20	−0.41
2.0	99.33	−0.42	95.50	−1.13	98.30	−2.44

[a] $\%V = (h_v/h_{min}) \cdot 100$, where h_v and h_{min} are the height of the valley and the smallest height between two peaks of an overlapped pair, respectively; see also Fig. 1.

an overlapped pair can be determined by injecting each diluted solution three times and taking the mean. The overlapping chromatograms of phenanthrene and *n*-butylbenzene obtained in previous work [5] were also used.

The data needed were measured manually except that the total area and the area of the internal standard were provided by a data processor.

RESULTS AND DISCUSSION

The following two equations were obtained from 200 and 160 data sets calculated from eqn. 4, respectively:

$$r = 0.0052 + 1.0007\,\gamma - 1.1473 \exp\left[-\frac{2.62\,\Delta t}{W_{0.1(r)}}\right]$$

$$f_{0.1} = 1.399 - 4.147 \qquad (20)$$

$$r = -0.0152 + 1.0150\,\gamma - 0.3300 \exp\left[-\frac{2.45\,\Delta t}{W_{0.1(r)}}\right]$$

$$f_{0.1} = 1.003 - 1.445 \qquad (21)$$

where $f_{0.1} = W_{0.1(r)}/W_{0.1(f)}$ and $W_{0.1(r)}$ and $W_{0.1(f)}$ are the rear and front half-widths at 10% height, as shown in Fig. 2. The correlation coefficients of eqns. 20 and 21 are 0.9999 and 0.9998, respectively. The precisions of eqns. 20 and 21 are 2.13×10^{-2} and 2.68×10^{-2}, respectively.

Table I and II list the theoretical relative errors of the area ratio and the relative error of the area ratio for the experimental overlapped peak pair calculated from eqn. 20 or 21, respectively. Overall, the value of $\%RE_r$ listed in Table II is greater than that in Table I. This mainly results from the error in measurement. The greater is RE_r, the greater are RE_{A1} and RE_{A2}. The sign of RE_{A1} is opposite to that of RE_r and RE_{A2}, which can be explained as follows:

$$r = \frac{A_2}{A_1}$$

$$dr = -\frac{A_2}{(A_1)^2} \cdot dA_1 + \frac{1}{A_1} \cdot dA_2$$

$$\frac{\Delta r}{r} \approx -\frac{\Delta A_1}{A_1} + \frac{\Delta A_2}{A_2}$$

Therefore,

$$\%RE_r \approx -\%RE_{A1} + \%RE_{A2} \qquad (22)$$

TABLE II

RELATIVE ERRORS OF AREA RATIO OF THE EXPERIMENTAL OVERLAPPED PAIR CALCULATED FROM EQNS. 20 AND 21

Experimental conditions: see text unless stated otherwise.

$r = A_2:A_1$	$\%V$	$f_{0.1}$	$\%RE_{A1}$	$\%RE_{A2}$	$\%RE_r$	
0.3237:1	98.93	1.590	−0.24	0.73	0.97	GC
0.5938:1	93.69	1.898	1.64	−2.76	−4.33	GC
0.6384:1	89.36	1.919	−1.70	2.70	4.50	GC
0.6955:1	90.79	1.878	0.54	−0.78	−1.31	GC
1.1984:1	86.63	1.413	−1.66	1.39	3.10	GC
1.5434:1	91.14	1.362	2.79	−1.81	−4.47	GC
1.6958:1	93.70	1.380	0.54	−0.31	−0.85	GC
2.1000:1	74.67	1.420	0.82	−0.39	−1.21	GC
0.4241:1	93.95	1.940	0.33	−0.77	−1.10	LC
0.7234:1	97.31	1.964	2.21	−3.05	−5.15	LC
1.060 :1	76.96	1.634	−0.65	0.62	1.28	LC
1.6964:1	84.02	1.757	0.26	−0.15	−0.41	LC
1.852 :1	91.18	1.432	2.10	−1.13	−3.16	LC[a]
1.869 :1	81.94	1.376	−0.18	0.09	0.28	LC[a]
0.9346:1	84.58	1.279	0.68	−0.73	−1.40	LC[a]
2.804 :1	86.05	1.354	1.34	−0.48	−1.80	LC[a]
2.778 :1	88.85	1.337	3.84	−1.38	−5.03	LC[a]
0.4673:1	89.49	1.498	1.56	−3.34	−4.83	LC[a]
0.9259:1	77.93	1.486	−1.27	1.38	2.68	LC[a]

[a] Experimental conditions: see ref. 5.

This new approach for the determination of peak area based on area ratios is more accurate and simple than methods reported in the literature [2–5]. Eqns. 20 and 21 can be used for calculating the area ratio of two overlapping EMG peaks with an accuracy of ±5% provided that there is a clear and precise valley except for shoulder peaks. Further, it can be easily programmed. If a data acquisition system is used, the accuracy will be improved.

REFERENCES

1 J. P. Foley, *J. Chromatogr.*, 384 (1987) 301–303.
2 M. S. Jeansonne and J. P. Foley, *J. Chromatogr.*, 461 (1989) 149–163.
3 B. S. Lin and P. C. Lu, *J. High Resolut. Chromatogr. Chromatogr. Commun.*, 10 (1987) 449–454.
4 C. P. Cai and Y. Yang, *Chromatographia*, 30 (1990) 220–222.
5 N. S. Wu and G. H. Gu, *Chromatographia*, 32 (1991) 373–378.
6 I. G. McWilliam and H. C. Bolton, *Anal. Chem.*, 43 (1971) 883–890.

Journal of Chromatography, 623 (1992) 371–374
Elsevier Science Publishers B.V., Amsterdam

CHROM. 24 495

Short Communication

Use of chromatographic peak-heights ratios for quantitative analysis: application to the separation of enantiomers

Veronika R. Meyer

Institute of Organic Chemistry, University of Berne, Freiestrasse 3, CH-3012 Berne (Switzerland)

(First received May 4th, 1992; revised manuscript received July 8th, 1992)

ABSTRACT

In analytical chromatography, both peak heights and peak areas are proportional to the mass of compound injected. However, it is not possible to calculate the ratio of enantiomers from the respective peak heights without calibration. In isocratic or isothermal chromatography, the second peak of a pair is wider than the first and therefore its relative height is smaller; this effect is described here in mathematical form. With solvent gradients or temperature programming, peak-height ratios are influenced to a non-predictable extent and therefore calculations (without calibration) are not appropriate.

INTRODUCTION

It is well known that either peak areas or peak heights can be used for quantitative analysis by chromatography. Usually peak areas are used for this purpose, but peak heights can give more accurate results in the case of low signal-to-noise ratios, if the peaks of interest are very different in size or if the constancy of the mobile phase flow-rate cannot be guaranteed in studies where a concentration-dependent detector is used [1].

A special situation arises if enantiomeric ratios need to be determined by direct "chiral" chromatography (the formation of diastereomers before or after chromatographic separation is not discussed here). Then the detector properties of the two compounds are identical and peak areas can be used directly for quantification, *i.e.*, calibration is not needed (at least in principle, because the manner in which electronic integrators operate can be the reason for deviations form a "true" value [2]). In the author's experience this approach is in widespread use in laboratories which need to determine ratios of enantiomers. However, there are some laboratories which obtain "better" results if the peak-height ratio is used. This paper shows that such a procedure without calibration is not allowed in gas or liquid chromatography with isothermal, isocratic or programmed elution and with concentration-sensitive (*e.g.*, UV) or mass-sensitive (*e.g.*, flame ionization) detectors.

Correspondence to: Dr. V. R. Meyer, Institute of Organic Chemistry, University of Berne, Freiestrasse 3, CH-3012 Berne, Switzerland.

0021-9673/92/$05.00

PEAK-HEIGHT RATIO IN ISOCRATIC OR ISOTHERMAL CHROMATOGRAPHY

Calculations

In the following calculations it is assumed that the plate numbers for the two peaks 1 and 2 of a pair of enantiomers are identical, *i.e.*, $N_1 = N_2$. It is calculated from the retention time t_R and baseline peak width w:

$$N = 16\left(\frac{t_R}{w}\right)^2 \tag{1}$$

By solving for w and using the expression $t_R = k't_0 + t_0$, *i.e.*, replacing the retention time by the capacity factor k' and breakthrough time t_0, we obtain

$$w = \frac{4\,(k't_0 + t_0)}{N^{\frac{1}{2}}} \tag{2}$$

This equation is valid for both peaks, and therefore the ratio of the two peak widths is given by

$$\frac{w_1}{w_1} = \frac{k'_2 + 1}{k'_1 + 1} \tag{3}$$

To obtain an expression for peak-height ratios we can use the relationship between peak height h, peak area A and standard deviation σ, with $\sigma = w/4$ as is valid for peaks of Gaussian shape [3]:

$$h = \frac{A}{\sigma\sqrt{2\pi}} = 0.3989 \cdot \frac{A}{\sigma} = 1.596 \cdot \frac{A}{w} \tag{4}$$

Therefore, eqn. 3 becomes

$$\frac{h_1}{h_2} = \frac{A_1(k'_2 + 1)}{A_2(k'_1 + 1)} \tag{5}$$

or, if $A_1 = A_2$, as applies with a racemate,

$$\frac{h_1}{h_2} = \frac{k'_2 + 1}{k'_1 + 1} \tag{6}$$

Eqn. 5 shows why the ratio of peak heights is not proportional to the ratio of the peak areas. Therefore, an uncalibrated peak-height ratio must not be used for quantitative analysis.

Eqns. 5 and 6 are also valid for tailed peaks which can be described by the exponentially modified Gaussian function if their asymmetry, described as b/a (width of the trailing "half" of the peak to the width of the leading "half") at a given fraction of peak height, is equal; the area of this type of peak is described by equations of the type [4]

$$A = xhw_y\left(\frac{b}{a}\right)^z \tag{7}$$

where x is a constant factor, depending on y, y is the fraction of peak height where w, b and a are measured ($w = a + b$) and z is an exponent depending on y.

Cases where eqns. 5 and 6 are not valid

As shown above, the given relationship between peak-height ratio and capacity factor is valid if the plate numbers of the two peaks are identical and if they have the same degree, or absence of, asymmetry. Programmed elution is not allowed. Eqns. 5 and 6 are not valid in the following cases:

(1) If $N_1 \neq N_2$. This occurs if the retention mechanisms for the two compounds of the peak pair differ, as is often the case in enantioselective liquid chromatography.

(2) If the detector properties of the two peaks are not equal or if the detector is overloaded. Enantiomers have identical properties if the detector itself is non-chiral (an enzyme reactor is chiral) and if they are not derivatized to give diastereomers. If such derivatization is performed before or after the separation, the detector properties of the diastereomers need to be checked. They can be identical, but there is no guarantee. In the case of detector overload a large peak will give too small a signal.

(3) If a liquid chromatographic mobile phase is used which gives system peaks. Many additives to the liquid mobile phase can give rise to positive or negative, or even invisible, system (extra) peaks. In this event any peak area depends on the separation factor of (or distance between) the system and solute peaks. This effect was described by Schill and Crommen [5].

(4) In liquid chromatography if the composition of the mobile phase is not constant and in gas chromatography if the temperature is not constant. Both cases are an unwanted programmed elution. The effect on peak height is shown below.

All four effects lead to a non-predictable influence on peak heights, and calibration is more needed than ever.

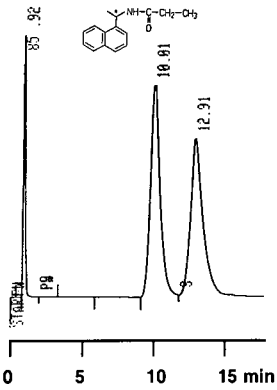

Fig. 1. Isocratic separation of racemic 1-(1-naphthylethyl)propionamide on R-DNBPG. Column, 125 mm × 2.1 mm I.D.; stationary phase, Nucleosil 5 NH_2 with ionically bound N-(3,5-dinitrobenzoyl)-D-phenylglycine; mobile phase, hexane–2-propanol (95:5); flow-rate, 0.5 ml/min; detection, UV (254 nm); integrator, Hewlett-Packard Model 3390 A. The first peak is toluene. Capacity factors: 10.8 for the *R* enantiomer, 14.2 for the *S* enantiomer.

Examples

Fig. 1 shows the liquid chromatographic separation of racemic 1-(1-naphthylethyl)propionamide on a Pirkle-type stationary phase. The peak-height ratio as obtained by the integrator (in the peak-height mode) is 1.35 and as calculated by eqn. 6 it is 1.29. The difference could be due to slightly different plate numbers of the two peaks.

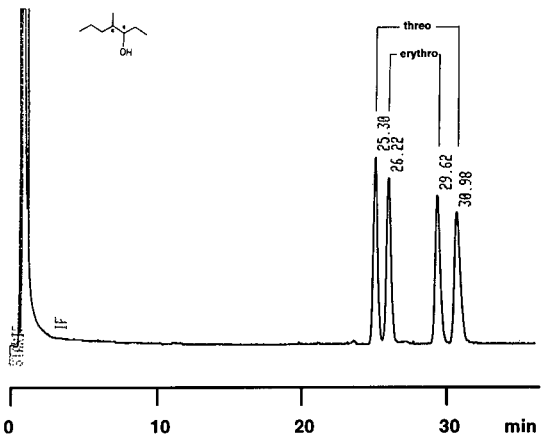

Fig. 2. Isothermal separation of racemic *erythro*- and *threo*-4-methyl-3-heptanol on perpropylated β-cyclodextrin. *Erythro* and *threo* isomers are present in slightly differing amounts, but the respective mixtures are racemic. Column, 10 m × 0.2 mm I.D.; stationary phase, 40% per-*n*-propyl-β-cyclodextrin in OV-1701; film thickness, 0.15 μm; mobile phase, helium, 42 kPa inlet pressure, t_0 was 0.58 min; temperature, 40°C.

Fig. 2 shows the gas chromatographic separation [6] of *erythro*- and *threo*-4-methyl-3-heptanol on perpropylated β-cyclodextrin [7]. The diastereomers are not present in equal amounts, but they are both racemates. The peak-height ratios are as follows: for the *erythro* enantiomers, by integrator 1.12, and by eqn. 6 1.13; and for the *threo* enantiomers, 1.41 and 1.22, respectively.

PEAK-HEIGHT RATIO IN PROGRAMMED CHROMATOGRAPHY

It was mentioned before and it is well known from experience that solvent gradients in liquid chromatography and temperature programmes in gas chromatography compress the peaks and thereby make

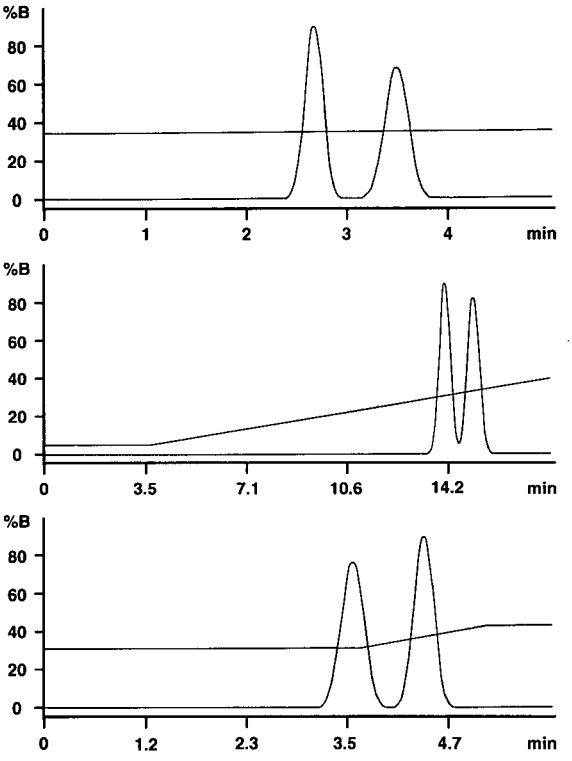

Fig. 3. Computer simulations of the separation of a hypothetical racemate. Software: DryLab G plus. Starting data: increase of the amount of strong solvent from 5% to 100% B in 15 min or 45 min, retention times 8.5 and 9 min or 14 and 15 min. The peak areas are equal in all instances (but the time axes are different), gradient profiles are overlaid. Top, isocratic separation, 35% B, peak-height ratio 1.30; middle, gradient from 5% to 40% B, peak-height ratio 1.10; bottom, gradient from 31% to 43% B, peak-height ratio 0.85.

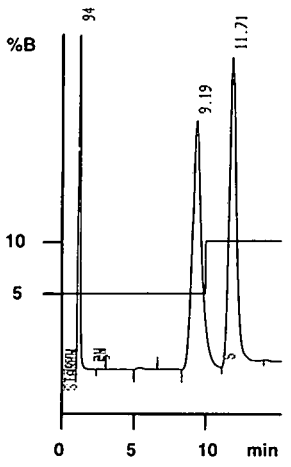

Fig. 4. Programmed separation of racemic 1-(1-naphthylethyl)-propionamide on R-DNBPG. Conditions as in Fig. 1 with the exception of a step gradient from 5 to 10% 2-propanol in hexane after 10 min.

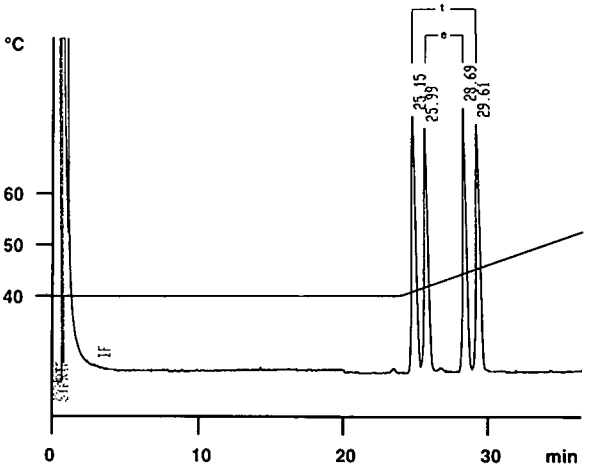

Fig. 5. Programmed separation of racemic *erythro-* and *threo*-4-methyl-3-heptanol on perpropylated β-cyclodextrin. Conditions as in Fig. 2 with the exception of a linear temperature programme of 1°C/min beginning at 24 min.

them narrower and higher. It is difficult to predict these effects from theory. Empirical predictions by using the data obtained by two gradient runs with differing pogramme times are possible [8] and the effects can be studied easily by applying appropriate software (*e.g.*, DryLab from LC Resources, Lafayette, CA, USA). Programmes are available for gas and liquid chromatographic separations and were developed for the computer-assisted optimization of difficult separations. Fig. 3 shows the influence of various gradients on the separation of a hypothetical racemate.

Figs. 4 and 5 show the same separations as in Figs. 1 and 2 but now with solvent and temperature gradients, respectively. Often the effects of (stepwise or continuous) programmed elution are so distinct that the later eluted peaks are higher than the earlier eluted peaks if their aras are equal. Although programmed chromatography could be used to "optimize" peak heights, this is nonsense, but these techniques are a powerful help in improving the resolution of complex sample mixtures. It is clear that with programmed elution peak heights give no quantitative information without calibration.

CONCLUSIONS

It is not possible to use peak-height ratios for quantitative analysis without calibration. In isocratic or isothermal chromatography the second-eluted peak is lower (in absolute or relative terms) than the first-eluted peak; an equation describing this effect has been given. In programmed chromatography the effect on peak heights is not predictable without assumptions or experiments.

ACKNOWLEDGEMENTS

The gas chromatographic separations were performed by Mr. A. Saxer. The DryLab G plus software was donated by Ciba-Geigy (Basle, Switzerland).

REFERENCES

1 V. R. Meyer, *Practical High-Performance Liquid Chromatography*, Wiley, Chichester, 1989, Ch. 20.4, p. 229.
2 N. Dyson, *Chromatographic Integration Methods*, Royal Society of Chemistry, London, 1990, Ch. 11, p. 41.
3 N. Dyson, *Chromatographic Integration Methods*, Royal Society of Chemistry, London, 1990, Ch. 5, p. 10.
4 J. P. Foley, *Anal. Chem.*, 59 (1987) 1984.
5 G. Schill and J. Crommen, *Trends Anal. Chem.*, 6 (1987) 111.
6 S. G. Claude, R. Tabacchi, A. Saxer and H. Arm, personal communication.
7 S. G. Claude, R. Tabacchi, A. Saxer and H. Arm, presented at the *Second International Symposium on Chiral Discrimination, Rome, May 1991.*
8 J. W. Dolan, L. R. Snyder and M. A. Quarry, *Chromatographia*, 24 (1987) 261.

Journal of Chromatography, 623 (1992) 375–380
Elsevier Science Publishers B.V., Amsterdam

CHROM. 24 556

Short Communication

High-performance liquid chromatographic analysis of chlorhexidine and *p*-chloroaniline using a specialty column and a photodiode-array detector

Walter K. Gavlick

Calgon Vestal Laboratories, P.O. Box 147, St. Louis, MO 63166-0147 (USA)

(First received May 19th, 1992; revised manuscript received August 5th, 1992)

ABSTRACT

A high-performance liquid chromatographic method has been developed for the separation of chlorhexidine and its known degradation product, *p*-chloroaniline. These amine-containing compounds can be separated without the addition of ion-pairing reagents and/or amine modifiers if the proper specialty column is selected. A photodiode-array detector was used to acquire spectral data and demonstrate the importance of the mobile phase pH when optimizing the response of *p*-chloroaniline.

INTRODUCTION

Chlorhexidine (CH) exhibits a high level of antibacterial activity and is often used as a skin disinfectant in various surgical handscrubs, patient preoperative skin preparation products, healthcare personnel handwashing products, and wound cleansing products [1]. *p*-Chloroaniline (PCA) is a known degradation product which must be assayed in any skin care product which contains chlorhexidine. An assay which can quantitate both compounds is essential for product stability studies.

Since CH and PCA each contain amine functionalities, previous high-performance liquid chromatography (HPLC) analyses have used ion-pairing reagents and/or amine modifiers to minimize peak tailing and enact a separation with conventional reversed-phase columns [2–9]. Recent advances in column technology have resulted in commercially available columns which minimize residual silanol interactions and are well suited for the analysis of basic type compounds. In this work, this type of column was used to separate CH and PCA without the addition of these types of mobile phase modifiers, and a photodiode-array detector was used to optimize the mobile phase pH in order to best detect PCA.

Correspondence to: Dr. W. K. Gavlick, Calgon Vestal Laboratories, P.O. Box 147, St. Louis, MO 63166-0147, USA.

EXPERIMENTAL

Apparatus

The HPLC system consisted of a Varian (Walnut Creek, CA, USA) 9095 autosampler with a 50-μl injection loop, a Varian 9010 gradient pump, and a Varian 9065 photodiode-array detector. The data were collected and analyzed with a Varian Star workstation.

0021-9673/92/$05.00

The HPLC columns used in this study were a Supelco (Bellefonte, PA, USA) Suplex pkb-100 (25 cm × 4.6 mm I.D., 5-μm packing) with a Suplex pkb-100 guard cartridge (2 cm × 4.6 mm I.D.) and holder and a Polymer Labs. (Amherst, MA, USA) PLRP-S (25 cm × 4.6 mm I.D., 5-μm, 100-Å packing) with a PLRP-S guard cartridge (5.0 mm × 3.0 mm I.D.) and holder.

Reagents

The mobile phase was prepared with HPLC-grade reagents only. Fisher (Pittsburgh, PA, USA) Optima water, Fisher Optima acetonitrile, Fisher Scientific glacial acetic acid, Fisher Scientific trifluoroacetic acid (TFA), and Fisher Scientific sodium acetate trihydrate were used. PCA (Fisher Scientific, 98% purity) and CH (99.9+% purity, Aldrich, Milwaukee, WI, USA) were used to prepare standards. Chlorhexidine digluconate (CHG) (20%, w/v, Sigma, St. Louis, MO, USA) was used in the preparation of the spiked-sample recovery studies. The CH-containing handwash product was prepared by the Calgon Vestal Laboratories Skin Care Product Development group (St. Louis, MO, USA).

Mobile phase preparation

Reservoir A contained HPLC-grade acetonitrile which had been degassed by vacuum filtration through a 0.45-μm nylon filter (Gelman Sciences, Ann Arbor, MI, USA). Reservoir B contained various acetate and TFA buffers. The acetate buffers were prepared by dissolving HPLC-grade sodium acetate trihydrate in HPLC-grade water to produce a 50 m*M* acetate solution. The pH was then adjusted to a final value through the addition of glacial acetic acid, and the solution was vacuum-filtered through a 0.45-μm nylon filter. The TFA buffer was prepared by adding TFA to HPLC-grade water to produce a 0.1% (v/v) TFA solution. When the TFA buffer was used, 0.1% TFA was also added to the acetonitrile.

Standard and sample preparation

PCA standards were prepared by dissolving an appropriate amount of PCA in 1.0 ml of acetonitrile and then diluting to a final weight with buffer. The CH standards were prepared by adding approximately 1.5 ml of buffer to an appropriate amount of CH followed by three drops of glacial acetic acid. The resultant solution was then briefly shaken to dissolve the CH before the sample was diluted to its final weight by the addition of buffer.

Placebo handwash product samples were spiked to a 1% CHG concentration and then diluted with buffer for analysis. Placebo handwash product samples were also spiked to a low-ppm PCA concentration and then diluted with buffer for analysis. All handwash product samples were syringe-filtered with a 0.45-μm Gelman Acrodisc LC13 PVDF filter after dilution before being analyzed by HPLC.

RESULTS AND DISCUSSION

Effect of pH on the CH/PCA separation using the PLRP-S column

The PLRP-S column consists of cross-linked polystyrene. The column was chosen for the analysis of amine-containing compounds such as CH and PCA because the absence of silanol groups would prevent the residual silanol interactions which are known to occur when silica-based columns are used to chromatograph amine-containing compounds [10]. The mobile phase buffer pH was changed in a series of analyses in order to determine the effect of pH on the separation of CH and PCA. The chromatograms in Fig. 1 demonstrate the improved separation and peak shape of each compound that was found as the mobile phase pH was lowered from 5.8 to 2. It was also noted that the elution order of the two compounds changed under the pH 2 conditions since PCA (pK_a 4.15 [11]) is ionized at this pH.

Effect of pH on the CH and PCA UV spectra

Just as the mobile phase pH had a dramatic effect on peak shape and resolution, it also affects the UV spectrum of the compounds. The photodiode-array detector was used to optimize mobile phase pH for detection of the compounds in terms of the best absorbance wavelengths. The UV spectrum of CH is similar at all of the different pH mobile phases that were examined. The UV spectrum of PCA at pH 2, however, is noticeably different from that at 5.8, and Fig. 2 demonstrates the pH effect on the spectra. It is important that the analysis is optimized with respect to PCA detection since it must be quantitated in the low ppm range. The low-pH mobile phase results in poor PCA absorbance at the

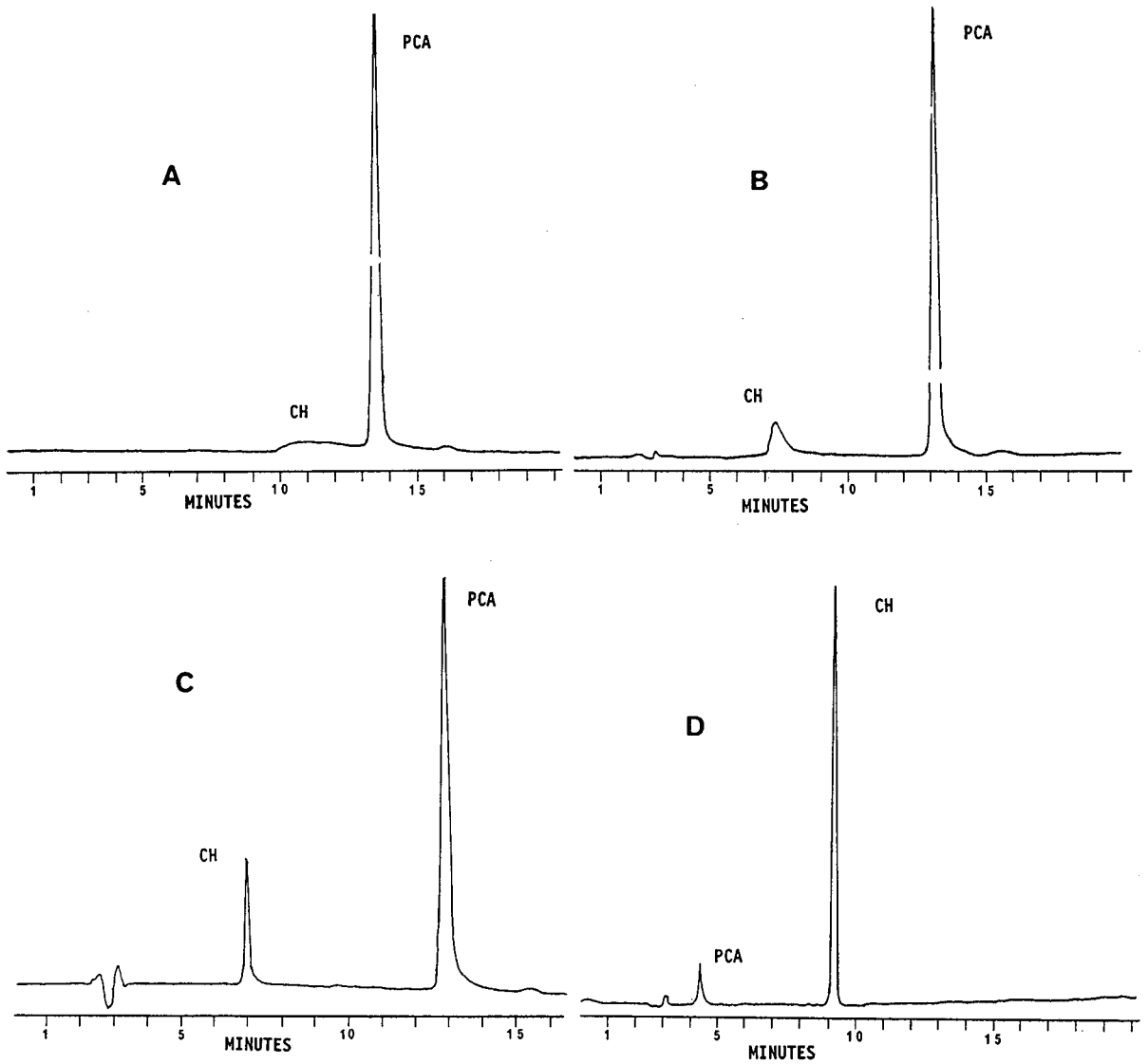

Fig. 1. Effect of the mobile phase pH on the CH/PCA separation. Column, PLRP-S, 25 cm × 4.6 mm I.D.; flow-rate, 1.0 ml/min; gradient elution, from 30 to 80% A in 15 min, hold at 80% A for 5 min; detection, 244 nm. (A) Mobile phase component A = acetonitrile, B = 50 m*M* acetate buffer, pH 5.8. (B) Mobile phase component A = acetonitrile, B = 50 m*M* acetate buffer, pH 4.8. (C) Mobile phase component A = acetonitrile, B = 50 m*M* acetate buffer, pH 3.8. (D) Mobile phase component A = 0.1% TFA in acetonitrile, B = 0.1% TFA buffer, pH 2.

higher UV wavelengths so the higher-pH mobile phase is needed to maximize the sensitivity of the assay for low levels of PCA.

The PLRP-S column produces the best chromatography when the pH 2 buffer is used in the mobile phase, but this does not produce the optimum UV spectrum for PCA. If the pH is raised to improve the spectral characteristics of PCA, then the chromatography suffers. In order to optimize both the chromatographic and spectral aspects of the analysis, another column which is often used for the analysis of basic compounds was investigated.

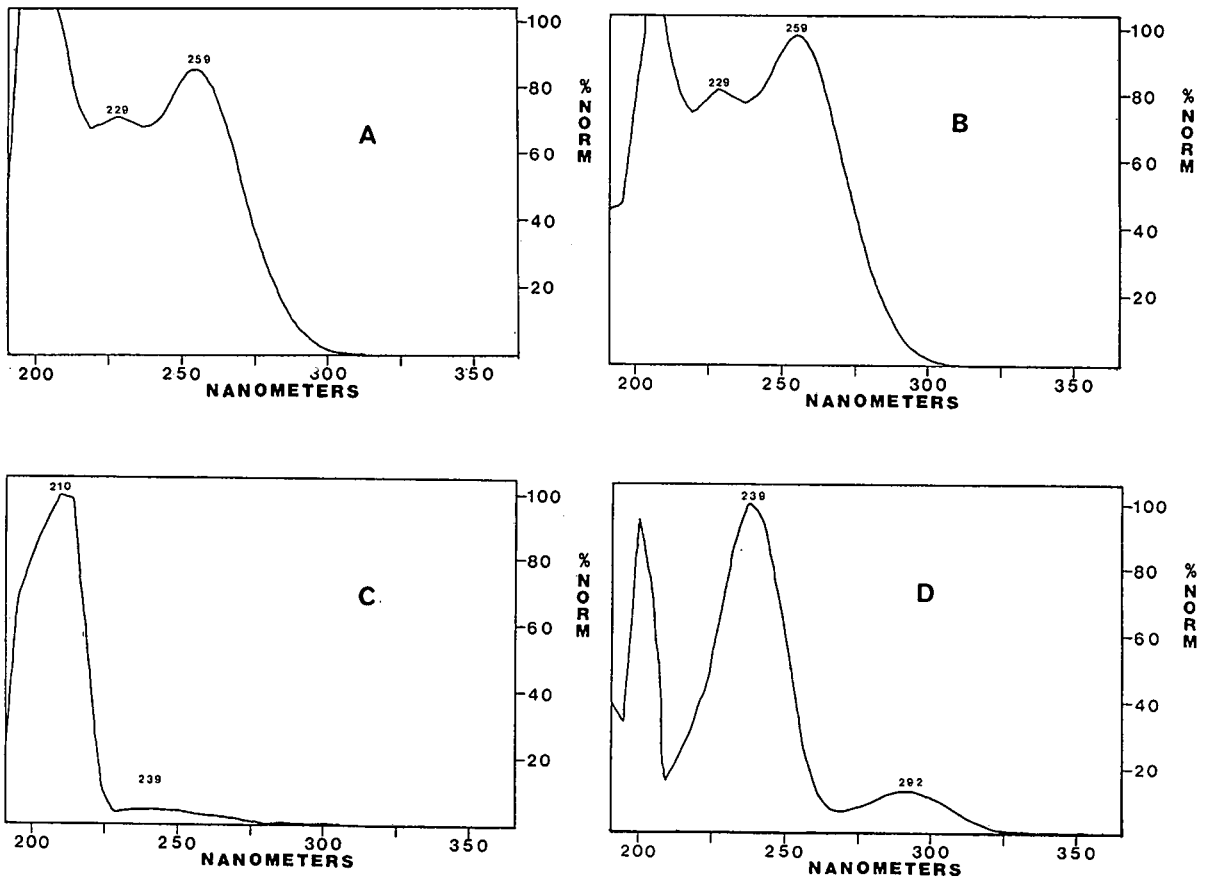

Fig. 2. Effect of the mobile phase pH on the CH and PCA photodiode array-generated UV spectra. (A) CH in pH 2, 0.1% TFA-containing mobile phase. (B) CH in pH 5.8, 50 m*M* acetate buffer-containing mobile phase. (C) PCA in pH 2, 0.1% TFA-containing mobile phase. (D) PCA in pH 5.8, 50 m*M* acetate buffer-containing mobile phase.

CH/PCA separation using the Suplex pkb-100 column

The Suplex pkb-100 is a silica based column which is used for the analysis of amine-containing (*i.e.* basic) compounds. The proprietary chemistry of the column allows for the analysis of such compounds without the addition of ion-pairing reagents and/or amine modifiers. A pH 5.8, 50 m*M* acetate buffer was used in the mobile phase to enact baseline resolution of CH and PCA with minimal tailing of the two peaks (Fig. 3). The pH 4.8 and 3.8 mobile phases also enacted a baseline separation of CH and PCA with minimal tailing of the two peaks, but were not considered to be the optimum mobile phase conditions since the spiked sample recovery studies of the handwash product yielded inconsistent results at these pH values relative to those obtained at pH 5.8. The pH 2 mobile phase separation was similar to that found with the PLRP-S column. The high mobile phase pH allows for optimum PCA sensitivity at a high (239 nm) UV wavelength. CH and PCA can thus be analyzed by HPLC without the addition of ion-pairing agents and/or amine modifiers to the mobile phase if the Suplex pkb-100 column is used. The column also allows for the optimum mobile phase pH to be used.

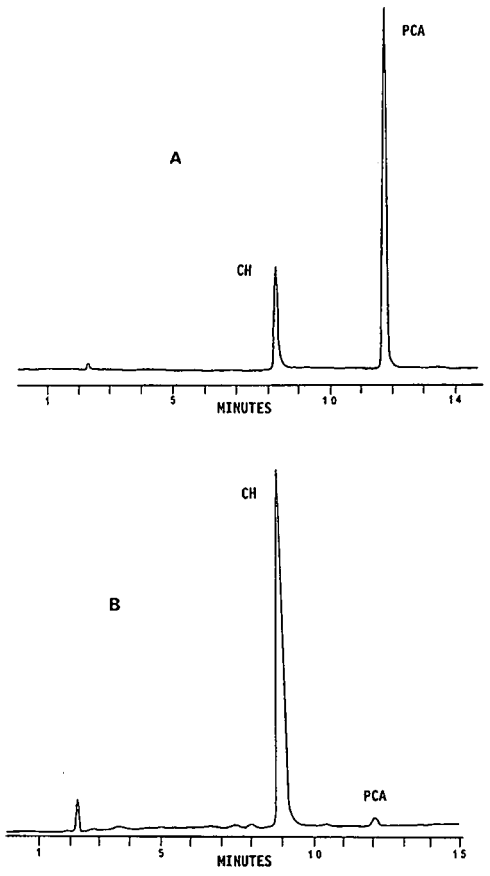

Fig. 3. Chromatograms of (A) CH and PCA standards and (B) CH and PCA separation in a dilute handwash product sample. Column, Suplex pkb-100, 25 cm × 4.6 mm I.D. ; flow-rate, 1.5 ml/min; gradient elution, from 20 to 55% A in 15 min; A: acetonitrile; B: 50 m*M* acetate buffer, pH 5.8; detection, 239 nm.

Calibration curve data

Calibration curve data were generated for CH and PCA standards. Two runs (analyses) of CH standards were performed but no detection limit was established since this is usually not an issue for CH analysis. The run 1 calibration curve consisted of standards ranging from 23.8 to 152 ppm CH, and the run 2 CH calibration curve consisted of standards ranging from 19.1 to 146 ppm CH with a linear response found over each standard concentration range.

Three PCA calibration curves were generated, and a limit of quantitation was established. The run 1 PCA calibration curve consisted of standards ranging from 1.58 to 177 ppm PCA, the run 2 standards ranged from 0.10 to 13 ppm PCA, and the run 3 standards ranged from 0.043 to 26.0 ppm PCA with a linear response found over each standard concentration range. The 0.043 ppm standard could be quantitated and lower amounts could be detected but not quantitated. Table I contains a summary of the CH and PCA calibration curve data.

Analysis of formulated handwash product

The HPLC assay was developed for CH and PCA analysis of a Calgon Vestal Laboratories (C.V.L) handwash product. In order to test the accuracy of the assay, spiked samples were prepared with respect to CHG and PCA. CHG is the CH salt form commonly used in this type of handwash product, and it was spiked into a placebo to yield an approximately 1% (w/w) sample. PCA was also spiked into a placebo to yield a low ppm range sample in an effort to duplicate a typical product sample. The spike recovery data generated from four separate spiked sample preparations for each compound were 103.5 ± 2.4% for CH and 96.2 ± 2.2% for PCA. The spiked sample recovery data indicate that the method provides accurate quantitation of both CH and PCA in the handwash product. Fig. 3 contains a chromatogram of a dilute handwash product sample. Photodiode array generated purity correlation data indicate that the CH and PCA peaks are homogeneous. These results are obtained by comparing spectra which are taken at different points across the chromatographic peak. When the spectra were compared, the best correlation value for the CH peak was 1.000000 and the worst was 0.999996. The best correlation value for the PCA peak was 0.999926 and the worst was 0.999643. The more similar the spectra, the closer the correlation value is to one and the greater the probability that the peak is a one component peak and no matrix components coelute.

In summary, an HPLC method has been developed in which a Suplex pkb-100 column is used to enact a separation of CH and PCA without the addition of ion-pairing reagents and/or amine modifiers to the mobile phase. The analysis is performed under pH conditions which optimize the PCA response. The method was demonstrated to be effective in the quantitation of CH and PCA in a handwash product.

TABLE I

CH AND PCA CALIBRATION CURVE DATA SUMMARY

Run	Number of standards	Correlation coefficient	Slope	*y*-Intercept
Chlorhexidine				
1	5	0.9997	6330	−31 594
2	6	0.9998	6258	−25 718
S.D.			51	4155
p-Chloroaniline				
1	5	1.000	11 916	3619
2	5	1.000	12 159	−582
3	6	1.000	11 948	−69
S.D.			132	2292

ACKNOWLEDGEMENT

A part of this work was presented at the *1992 Pittsburgh Conference.*

REFERENCES

1 G. W. Denton, in S. S. Block (Editor), *Disinfection, Sterilization, and Preservation*, Lea and Febiger, Philadelphia, London, 4th ed., 1991, Ch. 16, p. 274.
2 P. Wainwright and M. Cooke, *Analyst (London)*, 111 (1986) 1343.
3 M. Hoang, J. F. Moellmer and M. A. Khan, *J. Liq. Chromatogr.*, 13 (1990) 2677.
4 L. Gagliardi, A. Amato, A. Basili, G. Cavazzutti, E. Federici, F. Chimenti, M. G. Casanova, E. Gattavecchia and D. Tonelli, *J. Chromatogr.*, 348 (1985) 321.
5 M. Bauer, C. Degude and L. Mailhe, *J. Chromatogr.*, 315 (1984) 457.
6 A. Richard, M. Elbaz and G. Andermann, *J. Chromatogr.*, 298 (1984) 356.
7 B. Wyhowski De Bukanski and M. O. Masse, *Int. J. Cosmet. Sci.*, 6 (1984) 283.
8 R. L. Perez, *J. Chromatogr. Sci.*, 19 (1981) 570.
9 J. Bachner, G. Heinisch and H. Matous, *J. High Resolut. Chromatogr. Chromatogr. Commun.*, 4 (1981) 132.
10 J. W. Dolan, *LC · GC*, 7 (1989) 476.
11 R.C. Weast (Editor), *CRC Handbook of Chemistry and Physics*, CRC Press, Boca Raton, FL, 3rd ed., 1982, p. D-168.

Journal of Chromatography, 623 (1992) 381–385
Elsevier Science Publishers B.V., Amsterdam

CHROM. 24 528

Short Communication

Determination of phenylethylamines in hallucinogenic cactus species by high-performance liquid chromatography with photodiode-array detection

Hans-Jörg Helmlin, Daniel Bourquin and Rudolf Brenneisen

Institute of Pharmacy, University of Berne, Baltzerstrasse 5, CH-3012 Berne (Switzerland)

(Received May 26th, 1992)

ABSTRACT

A high-performance liquid chromatographic procedure with photodiode-array detection has been developed to create phytochemical profiles of phenylalkylamine-containing cactus species. The basic methanolic cactus extracts with methoxamine as internal standard were separated on a 3-μm ODS column with acetonitrile–water–phosphoric acid–hexylamine as the mobile phase. Peak assignation was performed by on-line UV detection (190–300 nm) and by gas chromatography–mass spectrometry of the isolated compounds. The quantitation of mescaline was done at 205 nm. The excellent sensitivity (the detection limit of mescaline was 500 pg, corresponding to 0.002% in cactus material) allowed the analysis of milligram amounts of cactus material taken from living plants. The mescaline content of the psychotropic Peyote cactus *Lophophora williamsii* (Lem. ex Salm-Dyck) Coult. ranged from 680 to 1010 mg per 100 g. The morphologically very similar *Lophophora diffusa* (Croizat) Bravo could be differentiated by the absence of mescaline and the dominant alkaloid pellotine.

INTRODUCTION

In the USA, Mexico and several countries in South America, different species of the Cactaceae family are known for their hallucinogenic properties. The most popular species are *Lophophora williamsii* (Lem. ex Salm-Dyck) Coult. and *L. diffusa* (Croizat) Bravo, both called Peyote and often confused because of their very similar morphology. *L. williamsii* grows on limestone soils of low hills and flatlands, mainly in the Chihuahua Desert of Central and Northern Mexico and in the adjacent parts of the United States, especially in the Rio Grande Valley. *L. diffusa* occurs only in a restricted area in the State of Queretaro, Mexico [1,2]. Today, Peyote is still used by several Indian tribes of northern Mexico. The use of Peyote has also spread to the United States and Canada, where members of the American Native Church still use the cactus in religious ceremonies. The main psychotropic principle of *L. williamsii* is the alkaloid mescaline, a phenylethylamine derivative. The internationally controlled mescaline can easily be synthesized by clandestine laboratories and appears from time to time on the illegal drug markets in the United States and in Europe. Minor alkaloids belong to the group of phenylethylamines (*e.g.* N-methylmescaline, hordenine) or tetrahydroisoquinolines (*e.g.* anhalamine,

Correspondence to: Dr. R. Brenneisen, Institute of Pharmacy, University of Berne, Baltzerstrasse 5, CH-3012 Berne, Switzerland.

0021-9673/92/$05.00

anhalonidine, anhalonine, isopellotine, pellotine). *L. diffusa* contains pellotine as the main alkaloid, with virtually no mescaline [2]. In Switzerland and other European countries *Lophophora* species are sold without legal restrictions in garden centres, flower shops and at flower markets.

Because these cactus species are morphologically very similar, and because of the potential for abuse, it was the aim of the present work to develop a selective, specific, accurate and sensitive analytical procedure using high-performance liquid chromatography with photodiode-array detection (HPLC–DAD) that would allow chemical differentiation of the two *Lophophora* species and rapid estimation of their psychotropic potency. Because wild Peyote has become endangered and is under international control [3], the sensitivity of the method should also allow the sampling of living cactus specimens without sacrificing the whole plant. To our knowledge this is the first HPLC–DAD procedure suitable for profiling *Lophophora* species. The efficiency of HPLC–DAD in the field of drug analysis, analytical toxicology, forensic chemistry and phytochemistry of psychotropic drugs has been shown previously [4–12]. Other methods for the determination of cactus alkaloids, such as normal phase HPLC [13], gas chromatography (GC) [14,15] and thin-layer chromatography (TLC) [2,15,16], use time-consuming extraction procedures or show poor resolution or low sensitivity.

EXPERIMENTAL

Instrumentation

The HPLC system consisted of a Hewlett-Packard (HP) 1090M liquid chromatograph (Hewlett-Packard, Waldbronn, Germany), a HP 1090L autosampler, a HP 1040M photodiode-array detector, a HP 79994A Chemstation (software version 1.05), a HP 7470A x/y plotter and a HP 2225A Thinkjet printer. The separation was performed isocratically at 25°C on a 150 × 4.6 mm I.D. column with a 20 × 4.0 mm I.D. precolumn, packed with 3-μm Spherisorb ODS-1 (Phase Separations), filled by Stagroma (Wallisellen, Switzerland). The mobile phase was acetonitrile–water (108:892) containing 5.0 ml (8.5 g) of orthophosphoric acid (85%) and 0.28 ml (0.22 g) of hexylamine per 1000 ml. The flow-rate was 1 ml/min. The eluent was filtered through a membrane filter (regenerated cellulose, 0.45 μm, Schleicher and Schuell) and degassed by sonication and during use with a constant flow of helium. Methanol was used for washing the column.

The absorption coefficients (ε) of mescaline (2–250 μg/ml mobile phase) were measured on a HP 8452A UV–VIS-diode-array spectrophotometer with a HP Vectra ES/12 PC (HP 89530 MS/DOS UV–VIS software).

The preparative work was done on a Waters HPLC system, consisting of an M 6000-A pump, a U6K injector, a 440 absorbance detector and a Shimadzu Chromatopac C-R1A data processor. Peak isolation was performed on a 250 × 10 mm I.D. column, packed with 5-μm Spherisorb ODS-1 using a slurry technique [17]. The mobile phase was acetonitrile–water (125:875), containing 5.0 ml (8.5 g) of orthophosphoric acid (85%) and 0.28 ml (0.22 g) of hexylamine per 1000 ml at a flow-rate of 4 ml/min. The detection wavelength was set at 254 nm.

The GC–MS system used for peak identification was a Hewlett-Packard HP 5990 gas chromatograph with a HP 5970 mass selective detector, a HP Chemstation (Pascal Rev. 3.1), a HP 2225A Thinkjet printer and a HP 7470A x/y plotter. A J&W DB-5 bonded-phase capillary column (20 m × 0.18 mm I.D. and 0.40-μm coating) was inserted directly into the ion source. The injector and transfer line temperatures were 250 and 260°C, respectively. The oven temperature was programmed from 70 to 250°C at 10°C/min. The scan range was m/z 33–400, and the scan-rate was set at 1.17 scans/s. Helium was used as carrier gas at a flow-rate of 0.7 ml/min (49 cm/s).

Chemicals and reagents

Hexylamine 99% (purum) was provided by Fluka (Buchs, Switzerland). Water used for HPLC was bidistilled. All other chemicals and solvents were of analytical or HPLC grade, purchased from Merck (Darmstadt, Germany). Mescaline hydrochloride was supplied by Laboratoires Plan (Geneva, Switzerland), and N-methylmescaline hydrochloride and methoxamine hydrochloride were provided by Sigma (St. Louis, MO, USA). Anhalamine, anhalonidine, anhalonine, isopellotine and pellotine were gifts from Hoffmann-LaRoche (Basle, Switzerland/Nutley, USA).

Cactus samples

The specimens of *Lophophora williamsii* (Lem. ex Salm-Dyck) Coult. and *L. diffusa* (Croizat) Bravo (Cactaceae) were bought at flower shops and shopping centres in Switzerland or obtained from private collections.

Methods

For the differentiation of living cactus specimens, cubic pieces with a fresh weight of *ca.* 0.8 g were lyophilized and stored in a desiccator under vacuum. After pulverization with a grinder, an accurately weighed amount of the powdered sample (*ca.* 10 mg) was washed with four 1-ml volumes of diethyl ether by sonication for 5 min and filtration through a 0.2-μm regenerated cellulose filter (Spartan 13/30, Schleicher and Schuell). The defatted sample was extracted with four 0.5-ml volumes of methanol–ammonia 33% (99:1), containing 150.0 mg/l methoxamine hydrochloride as the internal standard (I.S.) by sonication for 5 min and filtration through a 0.2-μm regenerated cellulose filter. Aliquots of 5 μl were injected into the HPLC–DAD system.

Mescaline was quantitated by measuring the peak areas of mescaline and the I.S. at 205 nm. The calibration graph was obtained by measuring five standard solutions in the concentration range 3.8–15.3 μg/ml mescaline with the addition of 25.6 μg/ml I.S. (aqueous solution, calculated as base).

The inter-day precision of the method was determined by analysing a dried and pulverized cactus specimen. The analyses were repeated three times on two different days at an interval of 1 week using the procedure described above.

The recovery of mescaline from cactus material was determined by analysing a dried and pulverized mescaline-free *L. diffusa* specimen spiked with a methanolic solution of 1 mg/ml mescaline, corresponding to 10 mg/g dried material. The solvent was evaporated before analysis. The analyses were repeated four times using the procedure described above.

Peaks were assigned by spiking cactus extracts with solutions of reference compounds. For the GC–MS confirmation of the correct peak identification, 100 mg of dried cactus material (*L. williamsii*) were extracted as described above; ten 100-μl volumes of this extract were injected in the semi-preparative HPLC system, and the main constituents were isolated by peak collection. The combined fractions were then reduced to about half volume under a stream of nitrogen, alkalized with ammonia 33% to pH 10–11, and extracted with four 5-ml volumes of chloroform. After evaporation under a stream of nitrogen, the residue was dissolved in 1 ml of methanol and 1 μl was injected splitless into the GC–MS system.

RESULTS AND DISCUSSION

With alkalized methanol (solvent/sample, 200:1, v/w) and sonication, mescaline is almost quantitatively extracted from the finely powdered and defatted cactus matrix. The efficiency of the extraction step has been demonstrated previously [11]. The recovery of mescaline was greater than 99%, showing that the loss of mescaline during the defatting process, which is necessary to remove interfering lipids and waxes, is negligible.

Among the reversed-phase materials tested, only the 3-μm spherical C_{18} phase with a minimum plate number of 120 000/m (calculated for the mescaline peak) showed the efficiency necessary to obtain the HPLC profiles of a complex cactus extract differentiating major and minor alkaloids (Figs. 1 and 2). It is well known that basic compounds may show a pronounced tailing effect on certain reversed-phase columns owing to interactions with the residual polar silanol groups of the stationary phase [18,19]. The addition of an amine modifier to the mobile phase as a masking agent for the silanol groups improves the peak shape and changes the capacity factor (k') of basic substances [20,21]. It has to be noted that the selectivity of the chromatographic system can be widely influenced by changing not only the ratio of acetonitrile to water but also the concentration of hexylamine. With the addition of orthophosphoric acid to the mobile phase, an acidic eluent with a pH of *ca.* 2 is obtained, so that the components of interest, such as mescaline and other basic phenylalkylamine derivatives, are protonated and eluted as associates with phosphate ions. The described chromatographic system, with slight modifications in the ratio of the four components, is routinely used in our laboratory for the analysis of a wide range of basic substances of toxicological and forensic interest. For example, cocaine and cocaine metabolites [9], ring-substituted ampheta-

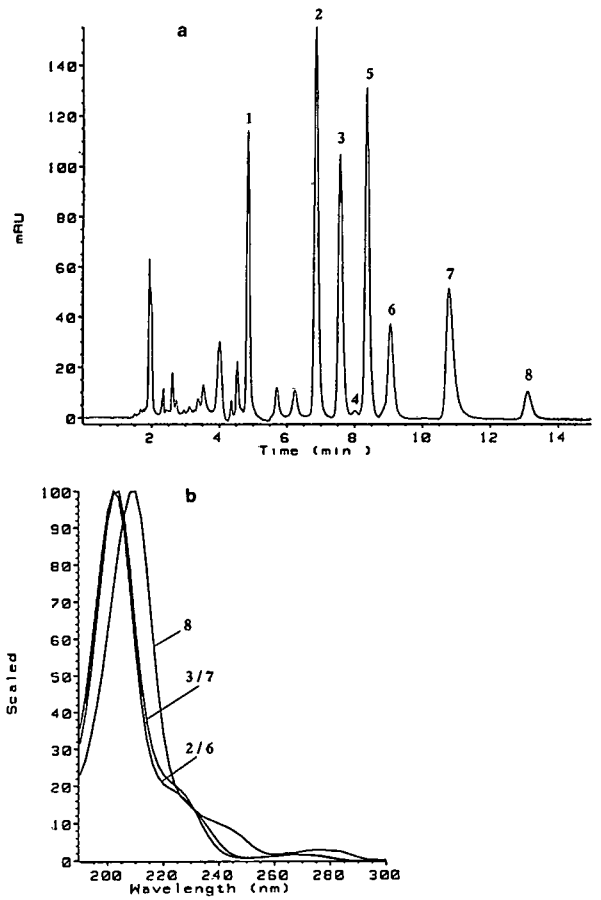

Fig. 1. (a) Chromatogram and (b) on-line UV spectra (DAD) of an extract of *L. williamsii* recorded at 205 nm. Peaks: 1 = anhalamine; 2 = mescaline; 3 = anhalonidine; 4 = isopellotine; 5 = methoxamine; 6 = N-methylmescaline; 7 = pellotine; 8 = anhalonine. Chromatographic conditions as described in Experimental.

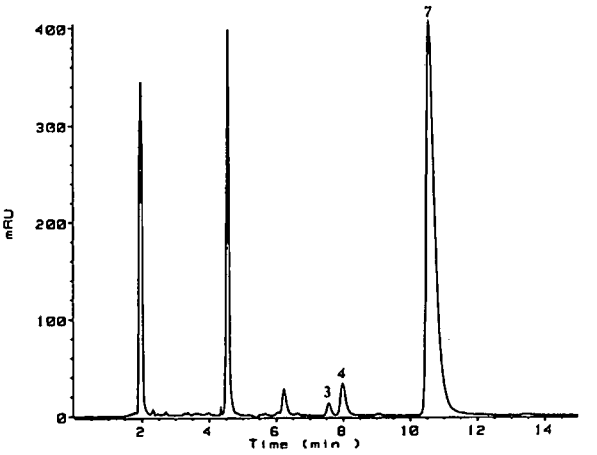

Fig. 2. Chromatogram of an extract of *L. diffusa*.

mines (*e.g.* methylenedioxymethylamphetamine, MDMA; methylenedioxyamphetamine, MDA) [11,22], cathinone [10], norpseudoephedrine [10] and methadone [8] can be analysed in different matrices, *e.g.* biological fluids and pharmaceutical formulations. Another advantage of this mobile phase is the low UV cut-off, which allows the detection of mescaline at its major UV absorption maximum (see Fig. 1: 205 nm, log ε 4.625) and thus to obtain a sixty times higher sensitivity compared to the maximum at 268 nm (log ε 2.833) mentioned in the literature [23]. The detection limit for mescaline at 205 nm and a signal-to-noise ratio of 5:1 was 500 pg, corresponding to 0.002% mescaline in cactus material. The excellent sensitivity makes it possible to analyse milligram amounts of the tissue of living cactus specimens, for example when studying the distribution of alkaloids or the influence of the vegetation period on the alkaloid pattern of one single plant. The linearity range for mescaline was 3.8–15.3 μg/ml with a correlation coefficient (r) of 0.999. The coefficient of variation of the inter-day precision was 3.3%.

Peak detection and identification of the alkaloids was performed by comparing retention times and UV spectra against those of standards, and by peak purity check (matching up-slope, apex and down-slope spectra) using a photodiode-array detector. Fig. 1a and b show the HPLC profile of an extract of *L. williamsii* and the on-line UV spectra of the main phenylethylamine and tetrahydroisoquinoline alkaloids, respectively. The UV spectra of mescaline and N-methylmescaline are identical and can be characterized by the major absorption maximum at 205 nm, a shoulder at 226 nm and a minor maximum at 270 nm. Pellotine and anhalonidine also have identical spectra, but can be differentiated from mescaline and N-methylmescaline by a slight bathochromic shift in the region of 190–230 nm. Anhalonine shows a major UV maximum at 208 nm. The peak assignation of mescaline, N-methylmescaline and pellotine was confirmed by isolation with preparative HPLC followed by GC–MS analy-

sis. The mass spectra were compared with those of reference compounds and showed the characteristic ions: for mescaline, *m/z* 211 (M^+), 182 (base peak), 181, 167, 151 and 148; for N-methylmescaline, *m/z* 225 (M^+), 182, 167, 151 and 44 (base peak); for pellotine, *m/z* 222 (M^+–15, base peak), 207, 206, 189, 178 and 161.

As demonstrated in Figs. 1a and 2, the typical HPLC profile of *L. williamsii* is generally more complex than that of *L. diffusa*. The alkaloid pattern of *L. williamsii* is dominated by mescaline, the psychotropic principle. The mescaline content of six specimens varied between 680 and 1010 mg per 100 g (calculated per dry weight). Other major alkaloids are the tetrahydroisoquinoline derivatives anhalamine and anhalonidine. Minor alkaloids are N-methylmescaline, isopellotine, pellotine and anhalonine. The very different alkaloid profile of *L. diffusa* is characterized by the dominant presence of pellotine and the absence of mescaline, anhalamine and anhalonine. The peak appearing at 4.5 min could not be identified. The UV spectrum indicates an alkaloid of the tetrahydroisoquinoline type

ACKNOWLEDGEMENTS

This work was supported by grants from the E. Steinegger Foundation for Medicinal Plant Research and the Swiss Federal Office of Public Health (Foundation of Narcotics Research). We thank Mr. J. Luthy, Institute of Botany, University of Berne, for cactus identification and for providing some of the cactus specimens. We also thank Hoffmann-La-Roche for the donation of reference compounds.

REFERENCES

1 N. H. Boke and E. F. Anderson, *Amer. J. Bot.*, 57 (1970) 569.
2 J. S. Todd, *J. Nat. Prod.*, 32 (1969) 395.
3 Convention on International Trade in Endangered Species of Wild Fauna and Flora (CITES), Washington, 1973.
4 R. Brenneisen and S. Geisshusler, *Pharm. Acta Helv.*, 60 (1985) 290.
5 R. Brenneisen and S. Borner, *Pharm. Acta Helv.*, 60 (1985) 302.
6 D. Bourquin and R. Brenneisen, *Anal. Chim. Acta*, 198 (1987) 183.
7 S. Borner and R. Brenneisen, *J. Chromatogr.*, 408 (1987) 402.
8 H. J. Helmlin, D. Bourquin, M. de Bernardini and R. Brenneisen, *Pharm. Acta Helv.*, 64 (1989) 178.
9 D. Bourquin and R. Brenneisen, *Proceedings of the 41th AAFS Meeting, Las Vegas*, American Academy of Forensic Sciences, Colorado Springs, 1989, p. 143.
10 R. Brenneisen, K. Mathys, S. Geisshüsler, H. U. Fisch, U. Koelbing and P. Kalix, *J. Liq. Chromatogr.*, 14 (1991) 271.
11 H. J. Helmlin and R. Brenneisen, *J. Chromatogr.*, 593 (1992) 87.
12 K. Mathys and R. Brenneisen, *J. Chromatogr.*, 593 (1992) 79.
13 J. Strömbom and J. G. Bruhn, *J. Chromatogr.*, 147 (1978) 513.
14 J. Lundström and S. Agurell, *J. Chromatogr.*, 36 (1968) 105.
15 H. Becker, *Pharm. uns. Zeit*, 14 (1985) 129.
16 J. Lundström and S. Agurell, *J. Chromatogr.*, 30 (1967) 271.
17 R. Brenneisen, *Pharm. Acta Helv.*, 59 (1984) 247.
18 D Chan Leach, M. A. Stadalius, J. S. Berus and L. R. Snyder, *LC-GC Int.*, 1 (1988) 22.
19 H. Engelhardt and M. Jungheim, *Chromatographia*, 29 (1990) 59.
20 R. Gill, S. P. Alexander and A. C. Moffat, *J. Chromatogr.*, 247 (1982) 39.
21 I. S. Lurie and S. M. Carr, *J. Liq. Chromatogr.*, 6 (1983) 1617.
22 H. J. Helmlin, L. Szajek, D. Bourquin and J. T. Clerc, *Proceedings of the 15th International Symposium on Column Liquid Chromatography (HPLC '91), Basel, 1991*, Poster 118/1, Abstract Book p. 76.
23 A. C. Moffat (Editor), *Clarke's Isolation and Identification of Drugs in Pharmaceuticals, Body Fluids, and Post-Mortem Material*, Pharmaceutical Press, London, 1986.

Journal of Chromatography, 623 (1992) 386–389
Elsevier Science Publishers B.V., Amsterdam

CHROM. 24 513

Short Communication

Determination of synephrine from Chinese medicinal drugs originating from *Citrus* species by ion-pair high-performance liquid chromatography

Kohko Hashimoto, Takaaki Yasuda and Keisuke Ohsawa

Tohoku College of Pharmacy, 4–1 Komatsushima 4 chome, Aobe-ku, Sendai, Miyagi 981 (Japan)

(First received April 15th, 1992; revised manuscript received July 17th, 1992)

ABSTRACT

A simple and precise method was established for the determnation of synephrine in Chinese crude drugs from *Citrus* plants using high-performance liquid chromatography with sodium dodecyl sulphate (SDS) as ion-pair reagent. Synephrine is known as a sympathomimetic drug contained in Chinese crude drugs from *Citrus* plants, namely Aurantii nobilis Pericarpium (Japanese name "Chinpi"), Aurantii fructus Immaturus ("Kijitsu"), "Kikoku" and "Seihi . The optimum conditions for extracting synephrine from these Chinese crude drugs was a 15-min reflux with water–acetonitrile–SDS–H_3PO_4 (65:35:0.5:0.1) as the mobile phase. Synephrine was eluted within 13 min without interference from co-existing components using an ODS column and SDS as an ion-pair reagent. The results revealed that synephrine was present at levels of 0.174–0.566% in the Chinese crude drugs, which were 1.3–2.2 times higher than those reported previously.

INTRODUCTION

Synephrine was developed originally as an orally applicable synthetic synpathomimetic drug and has been known to show actions such as vasoconstriction, raising blood pressure and bronchial muscle relaxation [1]. Since then, Stewart *et al.* [2] isolated synephrine as a hypertensive compound from the leaves and juice of tangerine. Subsequently, Kinoshita *et al.* [3] isolated it from Aurantii nobilis Pericarpium (Japanese name, "Chinpi"), Aurantii fructus Immaturus ("Kijitsu"), "Kikoku" and "Seihi" using bioassay for hot aqueous extracts of Chinese medicinal drugs with excised smooth muscle as a guideline and pointed out that synephrine is a common component found in Chinese Medicinal drugs originating from *Citrus* species. Quantitative analysis for synephrine revealed that the daily doses of 3–10 g of "Chinpi", "Kijitsu", "Kikoku" and "Seihi" contained 5–20 mg of synephrine, which would be a sufficient amount for exhibiting pharmacological effects. Further, Miyamoto and Furukawa [4] showed that "Chinpi" and synephrine had adrenergic β_2 activity. Hence the synephrine content is extremely important when considering pharmacological effects of these Chinese medicinal drugs and it is also assigned as one of standard components for quality evaluation [5].

Reports on the determination of synephrine include thin-layer chromatography densitometric

Correspondence to: Dr. Keisuke Ohsawa, Tohoku College of Pharmacy, 4–1 Komatsushima 4 chome, Aoba-ku, Sendai, Miyagi 981, Japan.

0021-9673/92/$05.00

analysis of hot aqueous extracts of Chinese crude drugs from *Citrus* species after treatment with an Amberlite column [3,6], high-performance liquid chromatography (HPLC) for 50% methanol extracts of "Kijitsu" after treatment with a cellulose ion-exchange column [5], HPLC with coulometric detection [7,8] and gas chromatography–negative-ion chemical ionization mass spectrometry [9]. However, these methods all employ complicated sample pretreatment and require long times.

In this study, we employed ion-pair HPLC and examined optimum conditions for extracting synephrine from "Chinpi". We also developed a simple, rapid and precise method for the determination of synephrine in Chinese crude drugs originating from *Citrus* species.

EXPERIMENTAL

Plant materials

"Chinpi" was derived from *Citrus unshiu* Markovich produced in Shikoku and "Kijitsu" from *C. natsudaidai* Hayata produced in China. "Kikoku" and "Seihi" were products from China but their original plants were unknown, as in a previous report [3]. We also conducted experiments on Aurantii Pericarpium ("Tohi"), derived from *C. aurantium* Linné var. *daidai* Makino, produced in China as "Tohi", which is an important crude drug although not a Chinese medicinal drug.

"Chinpi", "Kikoku", "Seihi" and "Tohi" were purchased from Matsuura Kanpo (Nagoya, Japan) and "Kijitsu" from Uchida Wakanyaku (Tokyo, Japan).

Apparatus and HPLC conditions

The HPLC system consisted of a CCPD pump, UV-8011 UV detector, CO-8010 column oven (Tosoh, Tokyo, Japan) and SIC Chromatocorder 12 integrator (System Instrument, Tokyo, Japan). A TSK gel ODS-120 T (particle diameter 5 μm) column (250 × 4.6 mm I.D.) (Tosoh) was used with a guard column (10 × 4.0 mm I.D.) (GL Sciences, Tokyo, Japan) packed with the same material. A Model M990 photodiode-array detector (Waters–Millipore, Milford, MA, USA) was used. Water–acetonitrile–sodium dodecyl sulphate–H_3PO_4 (65:45:0.5:0.1) adjusted to pH 2.6 was used as the mobile phase. The column temperature was maintained at 40°C and the flow-rate was 1.0 ml/min. The substances eluted were detected at a wavelength of 220 nm.

Reagents

DL-Synephrine [1-(4-hydroxyphenyl)-2-methylaminoethanol] (Sigma, St. Louis, MO, USA) was recrystallized from methanol. Sodium dodecyl sulphate (SDS) was purchased from Nacalai Tesque (Kyoto, Japan) and acetonitrile of special grade from Kanto Chemical (Tokyo, Japan).

Assay procedure

"Chinpi", "Kijitsu", "Kikoku", "Seihi" and "Tohi" were powdered and 500 mg of each drug were weighed accurately and subjected to a 15-min extraction by refluxing in 40 ml of the mobile phase on a water-bath. After cooling, the extract was centrifuged at 3000 *g* for 10 min and the supernatant was reserved while the residue was washed twice with 2 ml of the mobile phase. The supernatant together with the washings was made up to 50 ml with the mobile phase to serve as the test sample. After filtering this sample with a 0.45-μm membrane filter, a 10-μl volume was injected for HPLC. The amount present was calculated according to the calibration regression equation (see below).

Calibration

A calibration graph was prepared from peak areas obtained by injecting 10 μl of the compound for HPLC over the concentration range 20–50 μg/ml. The resulting calibration graph was linear. The regression equation was $y = 3.3160 \cdot 10^{-8}x + 2.61774 \cdot 10^{-3}$ ($r = 0.999$), where y is the concentration (mg/ml) and x is the peak area.

Solvent and time of extraction

Amounts of 500 mg of "Chinpi" were subjected to extraction with four solvents, namely methanol, methanol–water (50:50), water and the mobile phase, and the respective extracts were treated as described under *Assay procedure*. For methanol and methanol–water (50:50), each extract was made up to 50 ml, 10 ml were taken and concentrated under reduced pressure and a sample solution was prepared by addition of 10 ml of the mobile phase. Extraction was carried out for 15, 30, 45 and 60 min in order to compare synephrine contents quantitatively.

TABLE I

EFFECT OF EXTRACTION TIME AND EXTRACTION SOLVENT

Sample: "Chinpi".

Extraction time (min)	Synephrine content (%)			
	Mobile phase	Methanol	Methanol–water (50:50)	Water
15	0.408	0.350	0.363	0.345
30	0.398	0.365	0.376	0.354
45	0.388	0.373	0.370	0.352
60	0.382	0.375	0.363	0.356

RESULTS AND DISCUSSION

It was found that a 15-min extraction of "Chinpi" with the mobile phase showed the highest content of synephrine (Table I). The determination of synephrine in the various Chinese crude drugs was then carried out on the basis of the above extraction conditions.

Fig. 1 shows the chromatograms obtained. The peak for synephrine appeared at 13 min and there were no interfering peaks. For examination of a single synephrine peak in the respective chromatograms, we measured the three-dimensional chromatogram (contour chromatogram) using a photodiode-array detector. As shown in Fig. 2, synephrine in each Chinese crude drug exhibited maximum absorption at 222.5 and 274.5 nm, coinciding with those of the standard. No peaks due to impurities were present.

Table II gives the synephrine contents in the Chinese crude drugs as determined by the proposed method, together with values reported in the litera-

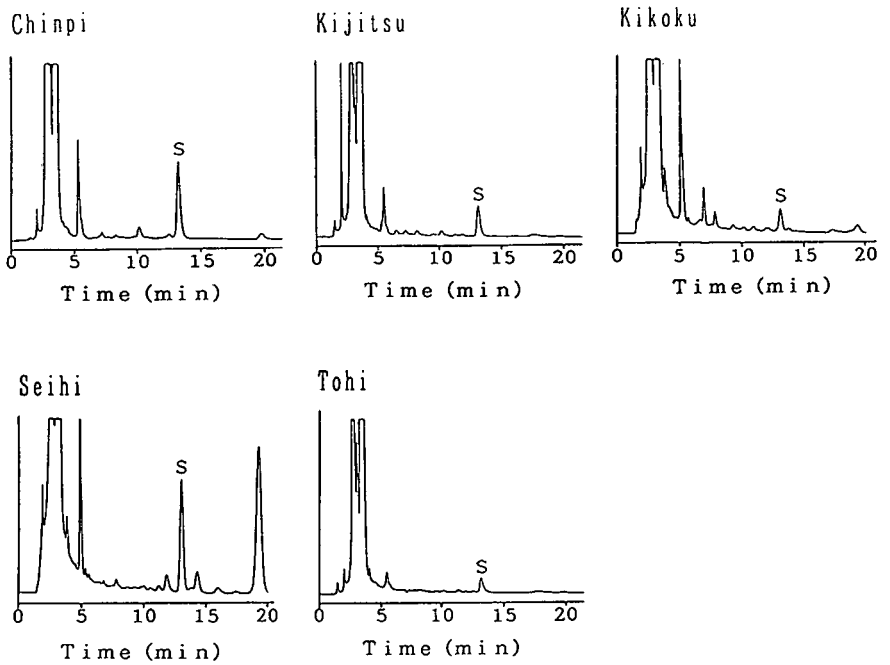

Fig. 1. Chromatograms of crude drugs. S = synephrine.

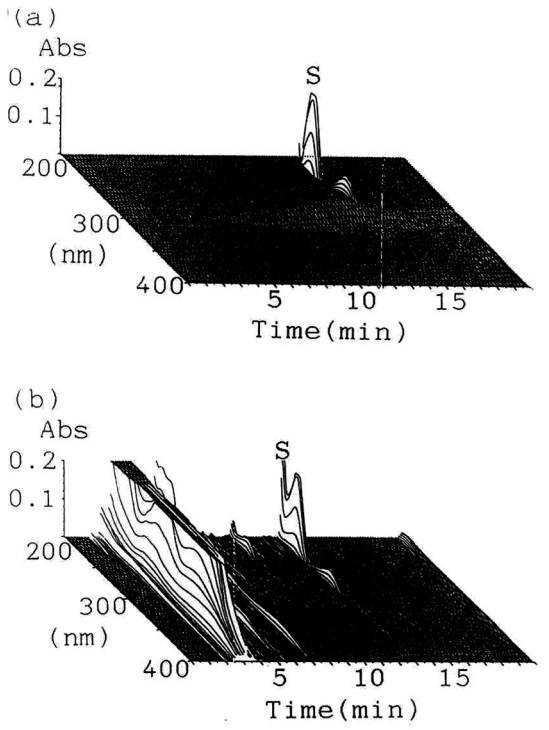

Fig. 2. Three-dimensional chromatograms: (a) standard synephrine; (b) "Chinpi". S = synephrine.

ture [3,5]. The highest content of synephrine was 0.566% in "Seihi", followed by 0.408% in "Chinpi", and the lowest value was 0.122% in "Tohi". The order of concentrations was the same as reported previously [3], but the individual concentrations were 1.3–2.5 times higher than those reported.

The daily consumption of synephrine calculated from the results of quantitative analysis amounted to 10–37 mg, the values at which pharmacological effects could be expected, as being pointed out by Kinoshita *et al.* [3], although the solvents used for extraction from Chinese crude drugs differed. The relative standard deviations were satisfactory (0.28–1.86%) and the method was very reliable. Further, the recovery rate of 93.0–107.0% after addition of a standard compound in a known amount was also satisfactory.

It is concluded that HPLC with SDS as the ion-pair reagent provides a simple, rapid and precise method for the determination of synephrine in Chinese medicinal drugs originating from *Citrus* species, giving higher quantitative values than those reported previously.

REFERENCES

1 U. Sankawa, *J. Trad. Sino-Jap. Med.*, 5 (1984) 52.
2 I. Stewart, W. F. Newhall and G. J. Edwards, *J. Biol. Chem.*, 239 (1964) 930.
3 T. Kinoshita, M. Sameshima and U. Sankawa, *Shoyakugaku Zasshi*, 33 (1979) 146.
4 K. Miyamoto and T. Furukawa, *J. Med. Pharm. Soc. Wakan-Yaku*, 5 (1988) 462.
5 K. Hosoda, M. Noguchi, T. Kanaya and M. Higuchi, *Yakugaku Zasshi*, 110 (1990) 82.
6 T. Namba, I. Araki, M. Mikage and M. Hattori, *Shoyakugaku Zasshi*, 39 (1985) 52.
7 Z. Hongjun, L. Yuanfeng and Z. Yuanyao, *Zhongcaoyao*, 14 (1983) 200.
8 R. G. H. Downer and R. I. Martin, *Life Sci.*, 41 (1987) 833.
9 N. Shafi, J. M. Midgley, D. G. Watson and G. A. Smail, *J. Chromatogr.*, 490 (1989) 9.

TABLE II

SYNEPHRINE CONTENTS IN CHINESE CRUDE DRUGS

Crude drug	Synephrine content (%)	R.S.D. (%)[a]	Recovery (%)	Literature synephrine contents (%)
"Chinpi"	0.408	0.28	97.7	0.22 [3]
"Kijitsu"	0.335	0.90	93.0	0.21 [3]
				0.18 [5]
"Kikoku"	0.174	1.15	107.0	0.13 [3]
"Seihi"	0.566	0.37	104.7	0.26 [3]
"Tohi"	0.112	1.86	103.3	0.045 [3]

[a] Relative standard deviation (n = 5).

Journal of Chromatography, 623 (1992) 390–394
Elsevier Science Publishers B.V., Amsterdam

CHROM. 24 561

Short Communication

Preparative separation and analysis of the enantiomers of [^{14}C]Zileuton, a 5-lipoxygenase inhibitor

Samuel B. Thomas and Bruce W. Surber

Drug Metabolism Department, Abbott Laboratories, 1 Abbott Park Road, Abbott Park, IL 60064-3500 (USA)

Mike Fitzgerald

CAPD Process Research, Abbott Laboratories, 1 Abbott Park Road, Abbott Park, IL 60064-3500 (USA)

(First received June 9th, 1992; revised manuscript received August 14th, 1992)

ABSTRACT

Preparative resolution and quantitative methodology for the optical purity determination of [^{14}C]Zileuton, N-[1-^{14}C]1-(benzo-[*b*]thien-2-yl)ethyl-N-hydroxyurea, [^{14}C]Abbott-64077, a 5-lipoxygenase inhibitor with potential clinical applications in the treatment of inflammatory diseases, is described. The method involves the use of a chiral stationary phase composed of amylose tris(3,5-dimethylphenylcarbamate) chemically bonded to 3-aminopropyl silica gel (ChiralPak AD) and a mobile phase consisting of *n*-hexane–ethanol (90:10). Optical and radiochemical purities of >99% were achieved for both.

INTRODUCTION

Zileuton (Abbott-64077, Fig. 1) is a 5-lipoxygenase inhibitor with potential clinical applications in the treatment of inflammatory diseases [1,2]. In order to carry out absorption, distribution, metabolism and elimination (ADME) studies with emphasis on the fate of each enantiomer, several milligrams of radiolabeled enantiomers of Zileuton of high optical purities were required. To achieve this goal, we sought a chromatographic method that would separate these enantiomers which can be scaled up to preparative scale without the need for derivatization. Zileuton was first separated on a Pirkle phenylglycine covalent column [3]. Later, using a second generation α_1-acid-glycoprotein (α_1-AGP) column, the analytical resolution was greatly improved [4]. These and other chiral stationary phases (CSP's) (for an excellent discussion of the CSPs mentioned here, see ref. 5) were investigated and the results of this investigation and the successful resolution of the labeled enantiomers are reported herein.

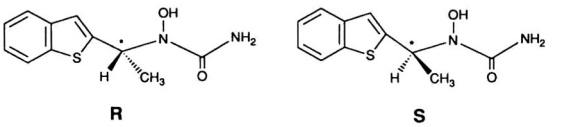

Fig. 1. [^{14}C]Zileuton: (left) [^{14}C]A-68967 (**1**,*R*), (right) [^{14}C]A-68968 (**2**,*S*). Asterisk denotes position of carbon-14 label.

Correspondence to: Dr. S. B. Thomas, Drug Metabolism Department, Abbott Laboratories, 1 Abbott Park, IL 60064-3500, USA.

0021-9673/92/$05.00

EXPERIMENTAL

Chemicals

n-Hexane (C_6H_{14}), methanol (CH_3OH), chloroform ($CHCl_3$), isopropanol (2-PrOH), ethanol (C_2H_5OH), *tert.*-butanol (*t*-BuOH), acetonitrile (CH_3CN), glacial acetic acid (HOAc), copper(II) acetate monohydrate [$Cu(OAc)_2$], triethylamine [$(C_2H_5)_3N$], ammonium acetate (NH_4OAc), potassium phosphate monobasic (KH_2PO_4), acetohydroxamic acid and perchloric acid were purchased from commercial vendors and used without purification. All solvents except the C_2H_5OH were HPLC grade and the chemicals were ACS reagent grade. The water used was from a Millipore Milli-Q water purification system. Scintillation cocktail (Flo-Scint III) was obtained from Radiomatic Instrument and Chemical Co., (Meriden, CT, USA). [^{14}C]Zileuton was synthesized in our laboratory. Zileuton, A-68967 and A-68968 "cold" reference materials were synthesized at Abbott Laboratories and used as received.

Analytical high-performance liquid chromatography

The chromatography mobile phase was delivered by a Perkin-Elmer Model 410 quaternary pump. Samples were injected using a Rheodyne Model 7125 syringe-loading sample injector with a 200-μl loop. Peaks were detected with an Applied Biosystems Model 785A UV programmable detector set at 235 nm connected in series with a Flo-One Beta Model 500 radioactivity detector (Radiomatic). Chromatograms were obtained by a Gateway 2000 computer (Gateway, N. Sioux, SD, USA) and a Panasonic Model KX-P1124i printer. A FlAtron CH-30 column heater was used for the high-temperature experiments. Analysis of the optical purity was performed using a ChiralPak AD (250 × 4.6 mm I.D.) column (Chiral Technologies, Drawer I Exton, PA, USA). The following columns were also investigated for enantiomeric resolution (Table I): β-Cyclodextrin (250 × 4.6 mm I.D.) (Advanced Separation Technologies, Whippany, NJ, USA), Pirkle's phenylglycine covalent (250 × 4.6 mm I.D.) (Regis, Morton Grove, IL, USA), Nucleosil Chiral-1 (250 × 4.6 mm I.D.) (Machery–Nagel, Germany), α_1-AGP (100 × 4.0 mm I.D.) (Chiral-AGP ChromTech AB, Norsborg, Sweden) and Merck cellulose triacetate (250 × 10 mm I.D.) (Merck, Darmstadt, Germany).

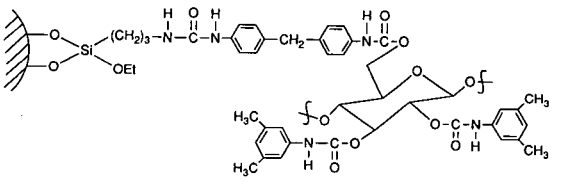

Fig. 2. Chiral stationary phase: cellulose tris(3,5-dimethylphenylcarbamate) bonded to silica gel (ChiralPak AD).

Radiochemical purity determination was performed using a Whatman Partisil 5 ODS 3 column (250 × 4.6 mm I.D.) (Whatman, Clifton, NJ, USA).

The mobile phase used for the optical purity determination consisted of *n*-hexane–ethanhol (90:10). The flow-rate was set at 1.0 ml/min. The mobile phase used for the radiochemical purity determination consisted of 70% NH_4OAc (0.1 *M*) containing 0.02% acetohydroxamic acid and 30% CH3CN with pH adjusted to 2.0 with perchloric acid. The flow-rate was set at 1.0 ml/min.

Preparative high-performance liquid chromatography

Separations were carried out using a Waters Delta Prep 3000, a Perkin-Elmer auto sampler Model ISS 200 and a Waters Model 484 variable-wavelength absorbance detector operated at 235 nm. The chromatograms were obtained using a Waters Model 745B integrator. The chiral semi-preparative HPLC column used was a ChiralPak AD (250 × 20 mm I.D.) (Chiral Technologies).The mobile phase consisted of *n*-hexane–ethanol (90:10). The flow-rate was set at 20.0 ml/min.

For sample preparation, a portion of [^{14}C]Zileuton (2.25 mCi, 0.119 mmol, 28.1 mg) was dissolved in a mixture of C_2H_5OH and C_6H_{14} and injected onto the column at about 7 mg per injection.

Isolation of pure enantiomers

Fractions containing purified **1** were pooled and the solvent was removed *in vacuo*. The residue (0.82 mCi, 75% yield) was dissolved in C_2H_5OH. Fractions containing **2** were pooled, concentrated, dissolved in mobile phase and further repurified from radiochemical impurities using a YMC-pack 5-μm silica (250 × 22 mm I.D.) (YMC, Morris Plains,

TABLE I

EFFECT OF CSP, MOBILE PHASE CONCENTRATION AND FLOW-RATE ON THE RESOLUTION AND ENANTIOSELECTIVITY OF [^{14}C]Zileuton

CSP	Mobile phase	Flow-rate (ml/min)	t_1[a] (min)	t_2[a] (min)	R_s[b]	α[c]
ChiralPak AD (250 × 4.6 mm I.D.)	C_6H_{14}–C_2H_5OH (90:10)	1.0	11.2	19.3	7.7	2.01
	C_6H_{14}-2-PrOH (90:10)	1.0	9.8	15.7	5.0	1.92
Cyclobond I β-Cyclodextrin (250 × 4.6 mm I.D.)	$(C_2H_5)_3N$ (1%), pH 7 with HOAc–CH_3OH (60:40)	1.0	22.7	24.5	1.2	1.09
		1.5	14.7	15.8	0.9	1.08
	$(C_2H_5)_3N$ (1%), pH 4 with HOAc–CH_3OH (60:40)	1.0	15.3	16.1	1.1	1.08
		0.7	22.0	23.7	1.3	1.08
		0.5	30.6	33.0	1.5	1.08
	CH_3OH-H_2O (45:55)	1.0	29.1	31.3	1.9	1.17
	CH_3OH-H_2O (40:60)	1.0	25.9	28.8	1.2	1.12
Cellulose triacetate (250 × 10 mm I.D)	C_2H_5OH-2-PrOH (50:50)	0.5	49.5	65.5	1.1	1.42
Pirkle covalent phenylglycine (250 × 4.6 mm I.D.)	C_6H_{14}–C_2H_5OH–t-BuOH (90:1.5:8.5)	2.0	43.7	47.0	0.7	1.08
α_1-AGP (100 × 4.6 mm I.D.)	KH_2PO_4 (0.01 *M*), pH 3–2-PrOH (97:3)	1.0	6.0	18.6	7.9	3.63
Nucleosil Chiral-1 (250 × 4.0 mm I.D.)	$Cu(OAc)_2$ (1 m*M*)–CH_3CN (95:5)	1.0	20.1	22.8	1.22	1.14
	$Cu(OAc)_2$ (1 m*M*), pH 4.0–CH_3CN (95:5)	1.0	13.8	13.8	0	1.0
	$Cu(OAc)_2$ (1 m*M*)–CH_3CN (98:2)	1.2	23.4	26.6	0.94	1.15
	$Cu(OAc)_2$ (1 m*M*), pH 5.5–CH_3CN (95:5)	1.0	20.5	23.8	1.15	1.14

[a] t_1 and t_2 refer to the retention times of [^{14}C]A68967 (**1**) and [^{14}C]A68968 (**2**), respectively.
[b] R_s is the resolution factor.
[c] α is the enantioselectivity factor.

NJ, USA) semi-preparative column. The mobile phase consisted of C_6H_{14}–2-PrOH–$(C_2H_5)_3N$ (85:15:0.5). The flow-rate was set at 35.0 ml/min. Fractions containing **2** were pooled and evaporated to dryness in vacuo. The residue (0.62 mCi, 55% yield) was dissolved in C_2H_5OH.

RESULTS AND DISCUSSION

Table I lists several different approaches to the LC separation of the enantiomers of Zileuton. While all of these CSPs resolve the enantiomers to some extent, three of these, Nucleosil Chiral-1 [6], Pirkle's phenylglycine covalent and Merck cellulose triacetate column [7], suffer from poor resolution and long retention times. The drawback to the successful separation that was achieved using an (α_1-AGP) column is that α_1-AGP column has a very low loading capacity (0.1 μg) which makes preparative work using this stationary phase very impractical. The initial resolution achieved on the β-cyclodextrin column [8] was suitable for our needs but we discov-

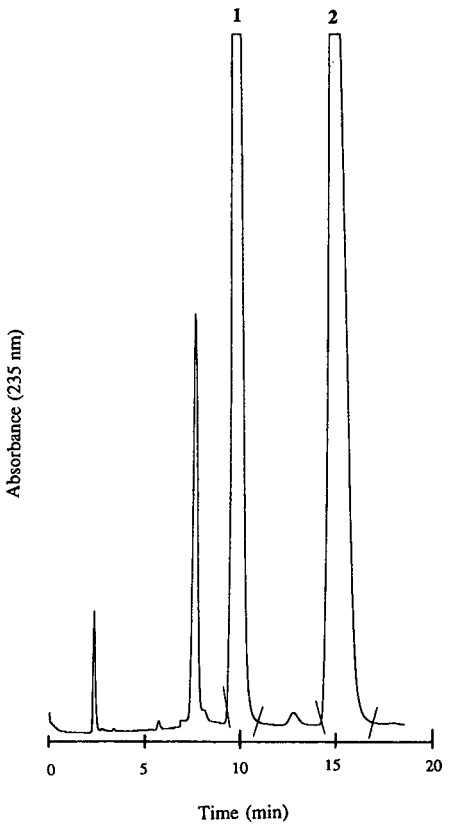

Fig. 3 Enantiomeric separation and resolution of [^{14}C]Zileuton on a Diacel ChiralPak AD, 250 × 20 mm I.D. column showing cutoff points for fraction collection during preparative runs. The mobile phase consisted of *n*-hexane–ethanol (90:10). Flow-rate was set at 20.0 ml/min.

ered over time that this CSP was inconsistent and unstable from one column to the other for the separation of Zileuton. Some batches achieved almost baseline separation while some batches did not. Also the retention time changed from one injection to another which led us to abandon the use of this column. Subsequently, we found that the ChiralPak AD gave good enantiomeric resolution with retention times under 25 min consistently from column to column. The CSP consists of tris(3,5-dimethylphenylcarbamate) cellulose chemically bonded to 3-aminopropyl silica gel via 4,4′-diphenylmethane diisocyanate (Fig. 2) [9,10]. Recently a preparative size column was purchased to resolve gram quantities of Zileuton and related compounds and it has displayed the same consistency and ruggedness shown in the smaller versions.

The chromatographic resolution of the optical isomers of [^{14}C]Zileuton using the semi-preparative ChiralPak AD column is shown in Fig. 3. The first of the two enantiomeric peaks was **1** identified by

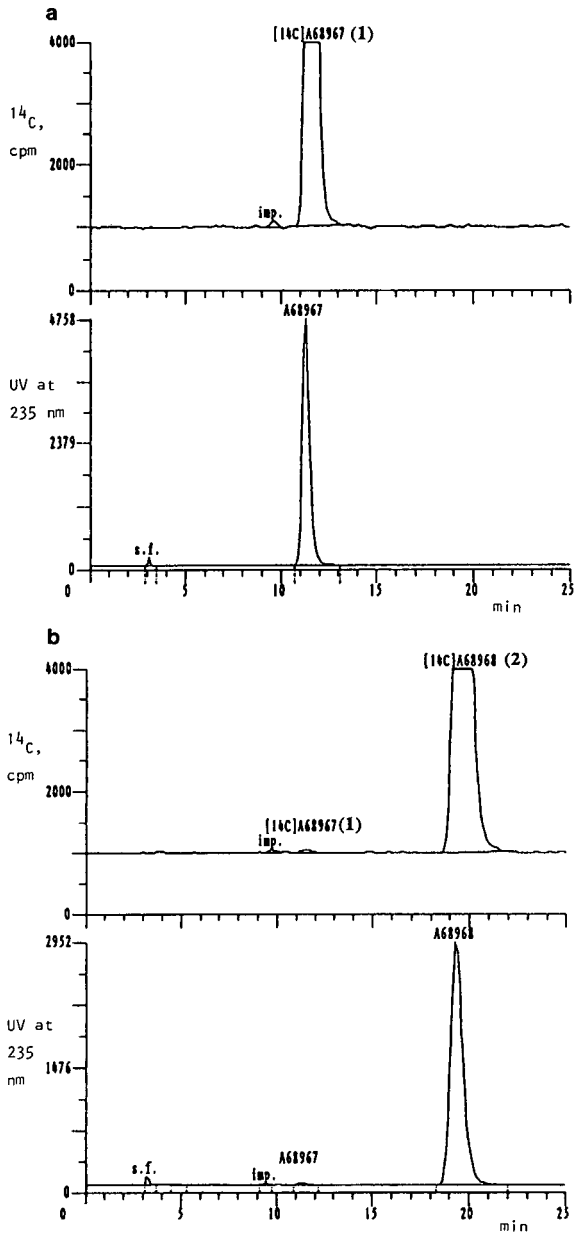

Fig. 4. Optical purity determination of (a) [^{14}C]A-68967 (**1**, >99%), (b) [^{14}C]A-68968 (**2**, >99%) on a ChiralPak AD, 250 × 4.6 mm I.D. column. The mobile phase consisted of *n*-hexane–ethanol (90:10). Flow-rate was set at 1.0 ml/min. s.f. = Solvent front; imp. = impurity.

comparison to authentic A-68967, followed by **2**, identified by comparison to authentic A-68968. The semi-preparative resolution of these enantiomers was uneventful owing to the excellent characteristics of this CSP and the volatility of the mobile phase. A yield of 75% for **1** and 55% for **2** is good considering that **2** had to be purified further from some radiochemical impurities not separated in the chiral chromatography.

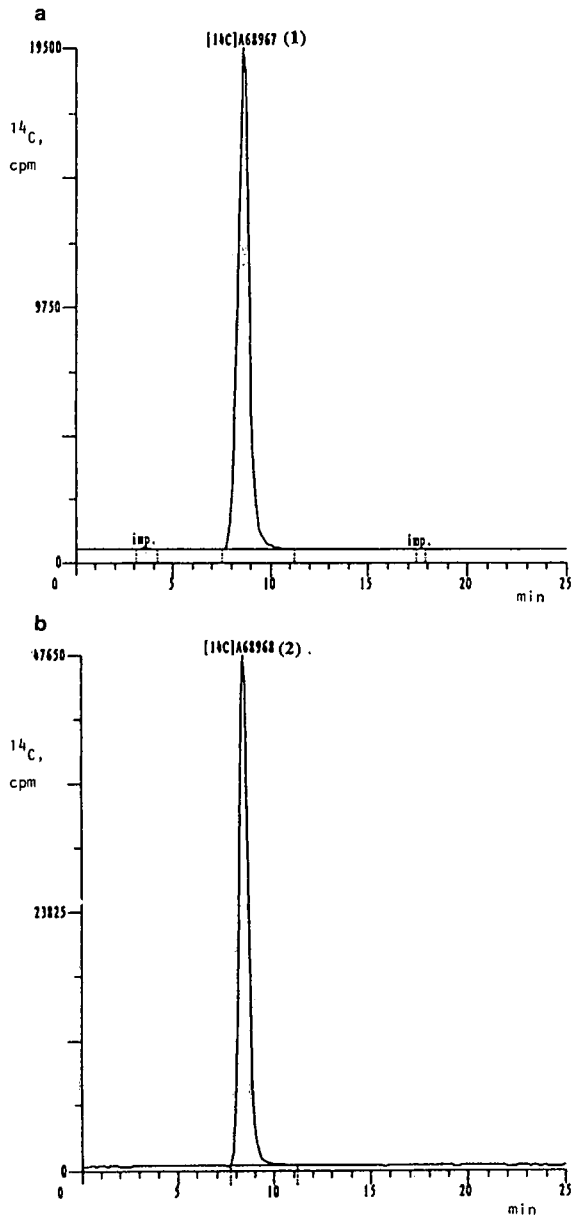

Fig. 5. Radiochemical purity determination of (a) [^{14}C]A-68967 (**1**, >99%), (b) [^{14}C]A-68968 (**2**, >99%) on a Whatman Partisil ODS 3, 5 μm, 250 × 4.6 mm I.D. column. The mobile phase consisted of ammonium acetate (0.1 *M*) containing 0.02% acetohydroxamic acid–acetonitrile (70:30), pH adjusted to 2.0 with perchloric acid. The flow-rate was set at 1.0 ml/min.

Optical purities of **1** and **2** were determined to be greater than 99% (Fig. 4a and b). The radiochemical purities of **1** and **2** were determined to be greater than 99% and the radioactive peaks corresponded to the UV peaks of A-68967 and A-68968, respectively, at 8.7 min (Fig. 5a and b). Assays of the effluents collected during the analyses of **1** and **2** showed that 101.6% and 98.8% of the radioactivity were recovered from the column, respectively.

In conclusion, the effectiveness of the cellulose tris(3,5-dimethylphenylcarbamate) CSP in the separation of the enantiomers of [^{14}C]Zileuton has been demonstrated. The preparative procedure described above allowed the resolution of mg quantities of the enantiomers of the labeled Zileuton of high optical purities.

ACKNOWLEDGMENT

The authors thank Ms. Karen Wegrzyn for assistance with the manuscript.

REFERENCES

1 G. W. Carter, P. R. Young, D. H. Albert, J. Bouska, R. Dyer, R. L. Bell, J. W. Summers and D. W. Brooks, *J. Pharmacol. Exp. Ther.*, 256 (1991) 929.
2 R. L. Bell, P. R. Young, D. H. Albert, C. Lanni, J. B. Summers, D. W. Brooks, P. Rubin and G. W. Carter, *Int. J. Immunopharm.*, 14 (1992) 505.
3 P. Rigas, *HPLC Separation of R- and S-Enantiomers of N-(1-benzo[b]thien-2-ylethyl)-N-hydroxyurea (A-64077); In-House Report*, Abbott Laboratories, Abbott Park, IL, July 1988.
4 G. S. Srivatsa, Abbott Laboratories, personal communication.
5 M. Zief and L. J. Crane (Editors), *Chromatographic Chiral Separations*, Marcel Dekker, New York, 1988.
6 S. B. Thomas and B. W. Surber, *J. Chromatogr.*, 586 (1991) 265.
7 I. W. Wainer, *Trends Anal. Chem.*, 6 (1987) 125.
8 T. J. Ward and D. W. Armstrong, *J. Liq. Chromatogr.*, 9 (1986) 407.
9 A. Ichida, T. Shibata, I. Okamoto, Y. Yuki, H. Namikashi and Y. Toga, *Chromatographia*, 19 (1984) 280.
10 Y. Okamoto, R. Aburatani, S. Miura and K. Hatada, *J. Liq. Chromatogr.*, 10 (1987) 1613.

Journal of Chromatography, 623 (1992) 395–398
Elsevier Science Publishers B.V., Amsterdam

CHROM. 24 541

Short Communication

Simultaneous, stability-indicating capillary gas chromatographic assay for benzocaine and the two principal benzyl esters of Balsam Peru formulated in a topical ointment

Thomas A. Biemer, Nuray Asral and Joseph A. Albanese

Consumer Products Division, Warner-Lambert Co., 170 Tabor Road, Morris Plains, NJ 07950 (USA)

(First received April 27th, 1992; revised manuscript received August 3rd, 1992)

ABSTRACT

A capillary gas chromatographic assay is presented for the determination of benzocaine and benzyl esters of Balsam Peru in a pharmaceutical preparation. The method is stability-indicating and allows for simultaneous assay of benzocaine in the presence of the non-polar Balsam esters.

INTRODUCTION

Balsam Peru, a viscous brown exude collected from trunks of the tree *Myroxylon pereirae*, has been variously used in the treatment of skin wounds and other dermatological ailments, and in the perfume and confectionery industries [1,2]. It is a complex mixture of aromatic esters and alcohols including benzyl and methyl benzoate and cinnamate, styracin, nerolidal, vanillin, and benzoic and cinnamic acids [3]. Balsam Peru levels in a sample can be conveniently monitored by quantitation of benzyl benzoate and benzyl cinnamate esters. These esters comprise the cinnamein content and include benzyl benzoate, benzyl cinnamate, cinnamyl cinnamate and peruviol, and are generally around 50% (w/w) of the balsam [1].

Literature reports have centered on packed-column gas chromatographic (GC) analysis of Balsam Peru [4,5]. There have been no reports published using wall-coated capillary GC columns. More recently, a paper described high-performance liquid chromatography (HPLC) of benzocaine and benzyl benzoate in a topical preparation [6]. Our efforts utilizing liquid chromatography to assay benzocaine in combination with Balsam Peru were unsuccessful due to the plethora of small peaks arising from the balsam that coelute with benzocaine. Resolution of benzocaine from these interfering peaks would have resulted in a lengthy analysis time for the non-polar benzyl esters and a corresponding loss of efficiency. GC has the advantage of separation by boiling points, and GC capillary analysis offers higher theoretical plate counts and efficien-

Correspondence to: T. A. Biemer, Consumer Products Division, Warner-Lambert Co., 170 Tabor Road, Morris Plains, NJ 07950, USA.

0021-9673/92/$05.00

cies. The high resolving power obtained with capillary columns is a distinct and powerful advantage over packed-column GC and HPLC in resolving components of complex mixtures.

This paper describes a capillary GC analysis of the benzyl esters of Balsam Peru and benzocaine (*p*-aminoethyl benzoate) in a topical ointment. The high resolving power of capillary GC offers wide application of the method to a variety of different sample matrices containing these compounds.

EXPERIMENTAL

Apparatus

The gas chromatograph was a Hewlett-Packard 5890 with a flame ionization detector and was equipped with a 7673A autosampler (Hewlett-Packard, Paramus, NJ, USA). The column was a Hewlett-Packard HP-1, 50 m × 0.2 mm I.D., with 0.5 μm film thickness of cross-linked methyl silicone. Peaks areas were collected and measured using Beckman CALS PeakPro software (Beckman Instruments, Allandale, NJ, USA).

Reagents

All the reagents used were ACS reagent grade. Benzocaine and benzyl benzoate were USP reference standards (United States Pharmacopeia, Rockville, MD, USA). Benzyl cinnamate and benzophenone were purchased from Aldrich (Milwaukee, WI, USA). The purity of benzyl cinnamate was established at 99.4% using three independent techniques as follows: reversed-phase HPLC with area normalization assay, differential scanning calorimetry and reversed-phase thin-layer chromatography. The USP materials were used at 100% purity.

Chromatographic conditions

The injector temperature was 280°C, and the detector was set at 250°C. The column temperature was programmed at 140°C for 10 min then ramped at 2°C/min to a final temperature of 240°C and held for 15 min. The injection volume was 2 μl. The injection port was equipped with a split–splitless glass sleeve obtained from Hewlett-Packard containing silanized glass wool. A split ratio of 20:1 was established at 0.03 min following injection. Flow through the capillary column was measured using an electronic flow meter and found to be 0.5 ml/min. The column head pressure was 28 p.s.i. The septum purge flow-rate was set to approximately 2 ml/min and the split vent flow-rate was determined to be *ca.* 10 ml/min. Helium, hydrogen and air used for the carrier and flame were all zero grade to ensure absence of spurious peaks and baseline noise.

Standard preparation

The benzophenone internal standard solution was prepared by dissolving 2.0 g in 200 ml of chloroform. A working standard was made by accurately weighing approximately 15 mg of benzyl cinnamate, 30 mg of benzyl benzoate and 100 mg of benzocaine into a 100-ml volumetric flask. Exactly 5 ml of internal standard were pipetted into the flask, then the standard was brought to volume using chloroform.

Sample preparation

Samples of ointment equivalent to approximately 15 mg of benzyl cinnamate, 30 mg of benzyl benzoate and 100 mg of benzocaine were accurately weighed into 250-ml Erlenmeyer flasks. About 95 ml of chloroform were added, then exactly 5 ml of internal standard solution were added by transfer pipet. The samples were shaken on a wrist shaker until thoroughly dispersed. Portions of the samples were filtered through 0.45-μm PTFE filters prior to injection into the gas chromatograph.

RESULTS AND DISCUSSION

Detector response linearity was ascertained by making duplicate injections of six different standard solutions prepared in the following concentration ranges: benzyl benzoate, 0.1840–0.4906 mg/ml; benzyl cinnamate, 0.0918–0.2449 mg/ml; and benzocaine, 0.5996–1.5990 mg/ml. The correlation coefficients for the three compounds were 0.9999, 0.9994 and 0.9997, respectively.

Reproducibility of the chromatographic system was assessed by injecting a standard preparation six times and measuring the peak area ratios. The mean peak-area ratios were 0.734, 0.240 and 1.1198 for benzyl benzoate, benzyl cinnamate, and benzocaine, with relative standard deviations of 0.1, 0.9 and 0.3%, respectively. Using the conditions described, the column developed approximately 18 500 theoretical plates/m. The capacity factors

(k') were 8.4, 9.5, 11.4 and 16.0 for benzocaine, benzophenone, benzyl benzoate, and benzyl cinnamate, respectively.

Recovery studies were conducted by spiking placebo ointment with benzyl benzoate, benzyl cinnamate and benzocaine at 80, 100 and 120% of the label claim for each analyte. The amounts of analyte added for each spiking level in the order benzyl benzoate, benzyl cinnamate and benzocaine, were as follows: 80% label claim, 4.8, 2.4 and 16 mg/g of placebo ointment; 100% label claim, 6, 3 and 20 mg/g; 120% label claim, 7.2, 3.6 and 24 mg/g. The average recovery for benzyl benzoate, benzyl cinnamate and benzocaine for the three spiking levels was 99.8, 100.1 and 99.7% with relative standard deviations of 0.4, 0.8 and 0.8%, respectively.

A typical sample chromatogram, depicted in Fig. 1, clearly shows the separation of the sample components from small excipient peaks. This is a stability-indicating method for the analytes and was demonstrated in the following manner: Aliquots of the analytes dissolved in methanol were treated with either 10 mmol of sodium hydroxide or 10 ml of 30% hydrogen peroxide. The solutions were then heated at 50°C for 1 h. Chromatograms of the stressed samples were compared to sample and standard chromatograms. None of the degradation products generated under these conditions interfered with the analysis of the analytes. Quantitation of the resulting chromatograms confirmed the loss of the peaks of interest.

The hydrolysis product of benzocaine is *p*-aminobenzoate. The benzyl esters undoubtedly cleave at the ester linkage. These resulting products would have lower boiling points and would be expected to elute much faster from this column. A typical alka-

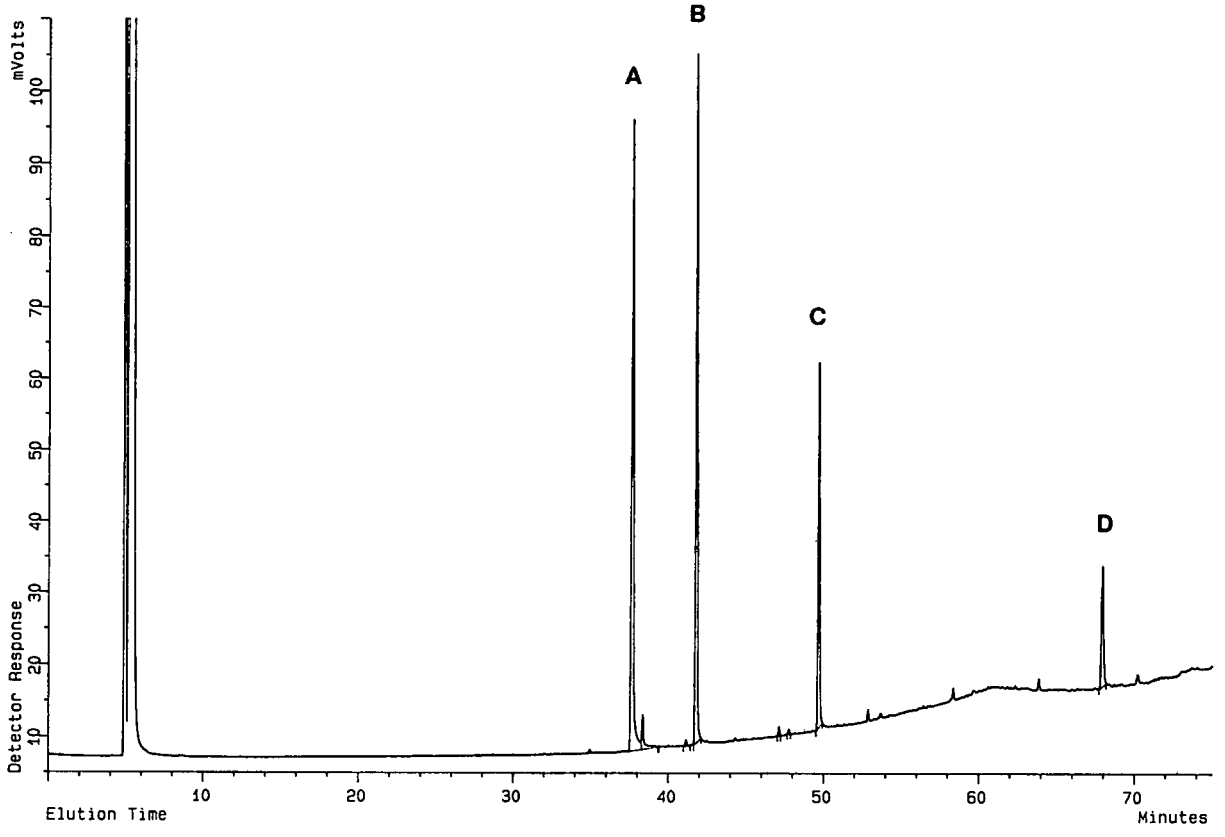

Fig. 1. Capillary gas chromatogram of an ointment sample preparation containing benzocaine and Balsam Peru. Peaks: A = benzocaine; B = benzophenone; C = benzyl benzoate; D = benzyl cinnamate.

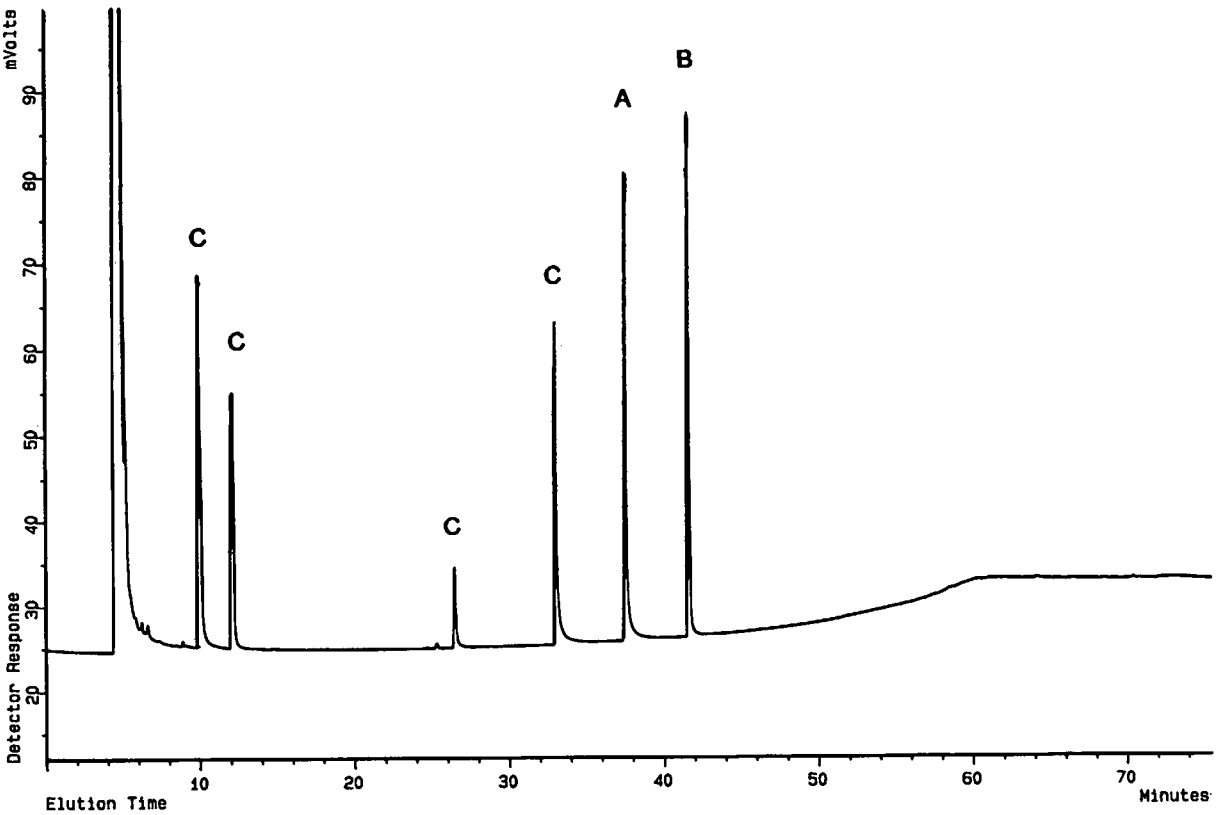

Fig. 2. Capillary gas chromatogram of an alkali-stressed standard solution showing loss of benzocaine, benzyl benzoate and benzyl cinnamate. Peaks: A = benzocaine; B = benzophenone; C = degradation product.

li-stressed standard solution is depicted in Fig. 2 which shows loss of the benzyl esters and the elution of degradation products early in the chromatogram. Quantitation of the remaining benzocaine peak confirmed the loss of this analyte.

While the lengthy run time of the analysis may appear unattractive for repetitive, routine sample quantitation, the complex nature of the Balsam Peru dictated the conditions to achieve separation of the analytes. Computer enlargement of the baseline showed numerous small peaks from an injected sample of Balsam Peru. The desired separation of the peaks of interest could be obtained only by choosing a system having high theoretical plate counts and efficiency. The column temperature was ramped slowly to achieve the desired resolution of the peaks of interest.

REFERENCES

1 S. Harvey, in A. Gennaro (Editor), *Remingtons Pharmaceutical Science*, Mack Publishing Co., Easton, PA, 18th ed., 1990, p. 765.
2 G. T. Walker, *Perfume Essent. Oil Rec.*, 59 (1968) 705–707.
3 H. Glash and H. Wagner, *Deutsch. Apoth. Ztg.*, 114 (1974) 45–49.
4 B. Mandrou, H. Mattras and S. Brun, *Trav. Soc. Pharm. Montpellier*, 38 (1978) 257–271.
5 A. Monard and A. Grenier, *5th Int. Symp. Chromatogr. Electrophoresis, Ann Arbor, 1968*, Humphrey Scientific Publishers, Ann Arbor, MI, 1969, pp. 529–536.
6 B. Gigante, A. Barros, A. Teixeira and M. J. Marcelo-Curto, *J. Chromatogr.*, 549 (1991) 217–220.

Journal of Chromatography, 623 (1992) 399–402
Elsevier Science Publishers B.V., Amsterdam

CHROM. 24 526

Short Communication

Fast and sensitive simultaneous staining method of Q-enzyme, α-amylase, R-enzyme, phosphorylase and soluble starch synthase separated by starch–polyacrylamide gel electrophoresis

Gerald Rammesmayer and Werner Praznik

Institut für Chemie, Universität für Bodenkultur, Gregor Mendelstrasse 33, A-1180 Vienna (Austria)

(First received June 4th, 1992; revised manuscript received July 23rd, 1992)

ABSTRACT

The present paper describes fast and sensitive techniques for simultaneous activity staining of Q-enzyme, α-amylase, R-enzyme, phosphorylase and soluble starch synthase on starch–polyacrylamide gel. Staining of Q-enzyme on starch–polyacrylamide gel electrophoresis (PAGE) leads to red bands on the blue background. The α-(1→6) transferred short-cahins cause a shift of λ_{max} of the iodine–starch complex to shorter wavelengths. R-enzyme is visible as a light-blue band, whereas the α-(1→4) hydrolytic activity of α-amylase causes a colourless band and can be clearly distinguished from Q-enzyme. White bands of phosphorylase and soluble starch synthase are visualized and the substrate specificity of phosphorylase is discussed, since the enzyme incorporates α-D-glucosyl residues in the growing α-(1→4) chain from ADP-glucose or its decomposition product as a substrate. The presented staining techniques permit the activity staining of the most important enzymes of the starch biosynthesis and offer simple methods of detection on starch–PAGE.

INTRODUCTION

Branching enzyme [Q-enzyme, (1→4)-α-D-glucan: (1→4)-α-D-glucan 6-glucosyltransferase, EC 2.4.1.18] was first detected in potato juice [1] and has been isolated during the years from various plants [2–13], animal tissue [14,15] and bacteria [16,17]) where starch is found as a storage polysaccharide. The action of Q-enzyme can be followed by the increasing number of (1→6) linkages, shown by the increased resistance towards β-amylolysis [18].

Correspondence to: Dr. G. Rammesmayer, Institut für Chemie, Universität für Bodenkultur, Gregor Mendelstrasse 33, A-1180 Vienna, Austria.

Many authors have suggested that the synthesis of starch or glycogen is based on by the cooperation of Q-enzyme and phosphorylase [(1→4) α-D-glucan-orthophosphate-glucosyltransferase, EC 2.4.1.1] [19–21] or starch synthase [(ADP-glucose: (1→4)-α-D-glucan 4-α-D-glucosyltransferase, EC 2.4.1.21] [22–25]. Usually the enzymic action *in vitro* is measured via inorganic phosphate, delivered from glucose 1-phosphate by phosphorylase or photometrically by the iodine staining method. This method, although rather unspecific and susceptible to interference in the presence of α-(1→4)-hydrolyzing enzymes, is unfortunately used for kinetic studies of Q-enzyme [26]. An activity staining method was performed by incubating the polyacrylamide gels

0021-9673/92/$05.00

after electrophoresis in an amylose solution [27] to observe the changes in λ_{max} of the iodine stain which is shifted to shorter wavelengths by the action of Q-enzyme. In a reaction based on the same principle phosphorylase is entrapped within the running gels [28] to synthesize glycogen within the gel as a substrate for subsequent activity staining of the branching enzyme. The described staining methods are suitable for multiple enzyme detection in crude or purified extracts. Activity detection of Q-enzyme, α-amylase, R-enzyme, phosphorylase and soluble starch synthase is shown on the same gel plate from starch–PAGE.

EXPERIMENTAL

Chemicals

Potato starch for electrophoresis (S-4501), glucose 1-phosphate, ADP-glucose and Coomassie Brilliant Blue R-250 (B-0149) were purchased from Sigma (Munich, Germany). All other chemicals were of analytical grade (Merck, Darmstadt, Germany). Pullulanase EN-200 (40 U/mg) was obtained from Hayashibara Biochemical Laboratories (Okayama, Japan).

Preparation of enzyme extract

Young potatoes were treated as described previously [29] and immediately blended with 10 ml of 1 *M* tris–citrate buffer (pH 7.5), containing 2.5 m*M* 1,4-dithio-DL-threitol.

Determination of protein content

After centrifugation protein determination with Lowry reagent was performed spectrophotometrically at 690 nm [30].

Starch polyacrylamide gel electrophoresis (starch–PAGE)

Gel electrophoresis was performed in a vertical slab gel apparatus. A separation gel with 15.0 % acrylamide, (pH 8.6), crosslinked 1:75 with N,N′-methylenebisacrylamide containing 1% starch was used. Starch synthase and phosphorylase (Fig. 2) were separated on 7.5 % acrylamide, (pH 8.6), crosslinked 1:75 with N,N′-methylenebisacrylamide containing 1% starch. 50 μl of the potato extract were sufficient for band detection. For detection of R-enzyme activity, which was negligible in the potato juice 5 μl of pullulanase were added. The electrophoresis buffer system consisted of tris–glycine (pH 8.9). The separation time was three h with a constant voltage of 300 V and a starting current of 120 mA. After electrophoresis the gels were rinsed in distilled water for 20 min.

Detection of Q-enzyme, R-enzyme and α-amylase activity

After electrophoretic separation the gel was soaked in 50 m*M* tris–citrate buffer (pH 7.0) containing 2 m*M* ascorbic acid for 4 h at 22°C. Afterwards the gel stripes were rinsed with distilled water and incubated in an iodine solution according to ref. 29 for 15 min. The zones of Q-enzyme activity appeared as sharp red bands on the blue stained background. R-enzyme activity could be seen as a light blue band, whereas α-amylase showed clear and transparent bands on the blue background. Staining of reference stripes with Coomassie Brilliant Blue R-250 [0.25% in methanol–glacial acid–water 5:1:5)] permits detection of the protein pattern matching to the activity stain.

Detection of soluble starch synthase activity (ADP-glucose)

Gel stripes incubated in a test tube containing 100 m*M* NaOH–glycine buffer, (pH 8.8) and 1 m*M* ADP-glucose were held at 37°C for 4 h.

Detection of phosphorylase

Phosphorylase activity became visible, when gel stripes were incubated in 50 m*M* tris–citrate buffer, (pH 6.2), containing 2.5 m*M* 1,4-dithio-*DL*-threitol, 10 m*M* glucose 1-phosphate and 5 m*M* EDTA in a test tube at 37°C for 1 h.

RESULTS AND DISCUSSION

The present work describes a simultaneous and sensitive technique for staining and detection of Q-enzyme, R-enzyme, soluble starch synthase, phosphorylase and α-amylase on starch–PAGE. In comparison with earlier works, the present one is more effective concerning Q-enzyme activity due to shorter reaction times and sharp stained bands on the gel. Our intention was to develop a simple and reliable method for activity staining which permits the detection of various enzymes of the starch me-

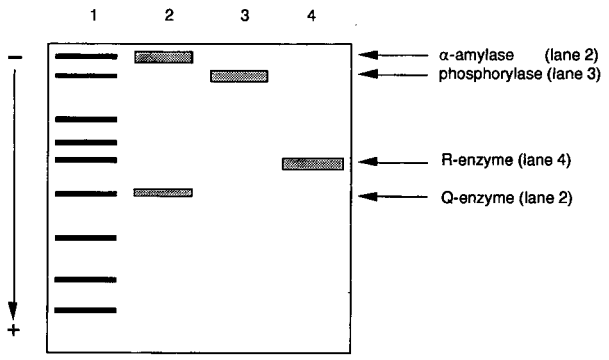

Fig. 1. Simultaneous staining of Q-enzyme, α-amylase, phosphorylase and R-enzyme activity on starch–PAGE. Aliquots (50 μl each) of crude potato juice were applied to the gel. After electrophoretic separation, the gels were incubated in the substrate solutions as described in the text. Lanes: 1 = Protein stain of the corresponding crude potato juice; 2 = simultaneous iodine stain of Q-enzyme and α-amylase; 3 = phosphorylase activity; 4 = iodine stain of R-enzyme activity.

tabolism on the same gel plate. In this manner it is possible to stain crude supernatants as well as purified enzyme extracts. In Fig. 1 the activity stains of Q-enzyme, α-amylase, phosphorylase and R-enzyme are shown. Lane 1 presents the Coomassie stain of the whole potato extract. Lane 2 shows the simultaneous iodine staining of Q-enzyme and α-amylase from a crude potato extract subjected to electrophoresis. Q-enzyme hydrolyses α-(1→4)-linkages with following chain transfer including the formation of α-(1→6)-linkages on suitable acceptor chains. The transferred short-chains give a sharp red band on the blue background basing on the shift of λ_{max} of the iodine–starch complex to shorter wavelengths and can be clearly distinguished from α-amylase activity which appears as clear and transparent bands on the gel. To avoid confusion between Q-enzyme and α-amylase activity from potatoes in starch gels of different acrylamide concentration, BSA can be used as a reference protein in the Coomassie stain (not shown). As we reported previously [29], Q-enzyme and BSA slightly differ in the relative mobilities in SDS-PAGE as well as in native PAGE using 15% acrylamide. Samples from either plant or animal tissue can be tested for enzyme activity in a short time. Q-enzyme activity could be detected even with the naked eye as a thin white band before iodine staining. This observation leads to the opinion that the transferred short-chains cause a band of higher starch density in the gel. To support evidence for this result the same stripe was stained again with iodine solution after three weeks rinsed in water to demonstrate that the red stained short-chains are all attached by newly synthesized α-(1→6) bonds to the starch in the gel. Secondly, by this observation we could confirm that branching enzyme is an enzymic entity. Decrease in reducing power in samples containing starch and the cut out Q-enzyme band could be observed by the modified Somogyi–Nelson method [31,32].

On addition of glucose 1-phosphate to the substrate phosphorylase activity (lane 3) becomes visible. A white band of elongated α-1,4-glucan chains synthesized by phosphorylase activity could be detected, when gel stripes are incubated in 50 m*M* tris–citrate buffer, (pH 6.6) containing 1 m*M* dithiothreitol, 20 m*M* glucose 1-phosphate and 5 m*M* EDTA at 37°C for 2 h. Using the same buffer system (pH 7.0) as described for Q-enzyme staining, a simultaneous staining of phosphorylase is possible although increasing reaction time is observed. The reaction time of the activity staining of synthesized α-(1→4)-bonds within one hour strongly varies with the amount of glucose 1-phosphate added in the substrate solution.

Lane 4 shows the activity stain of R-enzyme.The enzyme activity hydrolizes the α-(1→6) bonds and leads to light blue bands on the blue backgound of the iodine stained gel. The split off chains appear to be of a rather short length able to diffuse out of the gel.

The intention was to harmonize the pH value of the incubation medium corresponding to the different pH-optima of the enzymes in the stain. For this reason starch synthase activity which demands higher pH values could not be stained simultaneously with the other enzymes. Current studies show that Q-enzyme is inhibited at pH values from 8.5 to 9.0 [23]. Fig. 2, lane 1 shows the protein stain of crude potato extract subjected to starch-PAGE. Lane 2 presents the phosphorylase activity at pH 6.6 and in lane 3 the soluble starch synthase activity can be seen, presenting two white bands of synthesized α-(1→4) chains on the gel. One band corresponds to the phosphorylase activity (in lane 1). This observation has been confirmed by paired-ion reversed-phase high-performance liquid chromatography when gel stripes are cut out horizontal

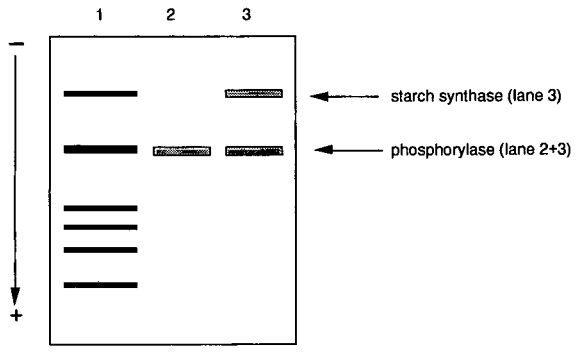

Fig. 2. 1 = Coomassie stain of a crude potato extract. 2 = Band of synthesized α-(1→4) chains in the gel stripe show the phosphorylase activity. Gel stripes were incubated in 50 m*M* tris–citrate buffer (pH 6.2), containing 2.5 m*M* 1,4-dithio-DL-threitol, 10 m*M* glucose 1-phosphate and 5 m*M* EDTA in a test tube at 37°C for 1 h. 3 = Primed soluble starch synthase activity and phosphorylase activity. The reaction was performed in a test tube containing 100 m*M* NaOH–glycine buffer (pH 8.8), and 1 m*M* ADP-glucose at 37°C (see Experimental).

and incubated with ADP-glucose in the presence of suitable primers (unpublished data).The results lead to the conclusion that phosphorylase can use ADP-glucose or decomposition products as a substrate. The above results imply that ADP-glucose could be metabolized to glucose 1-phosphate prior to incorporation into starch by phosphorylase. The question arises if the presence of ADP-glucose pyrophosphorylase (glucose 1-phosphate adenyltransferase, EC 2.7.7.27) in the extract could participate in this reaction. This enzyme is believed to play a key regulatory role in the gluconeogenesis which equally operates in amyloplasts and chloroplasts [33].Worth to be mentioned is the fact that this type of activity becomes visible on the gel with ADP-glucose as a glycosyl donor whether inorganic phosphate in the incubation medium is present or not.

The above results lead to the conclusion that in comparison with several other staining techniques the present system might be expected to give a more comprehensive and extensive activity staining of the discussed enzymes. The methods are appropriate to prove the activity staining of some important enzymes of the glucan metabolism. In this manner highly purified enzymes can be isolated in semipreparative scale from gels with a thickness of 3 mm as we use in our laboratory for enzymic synthesis of *de novo* products. Thus, the method may be helpful for the detection, purification and identification of enzyme activities in plant or animal tissues in the study of starch biosynthesis without the need of other time-consuming purification steps.

REFERENCES

1 W. N. Haworth, S. Peat and E. J. Bourne, *Nature (London)*, 154 (1944) 236.
2 H. L. Griffin and Y. V. Wu, *Biochemistry*, 7 (1968) 3063.
3 G. H. Vos-Scheperkeuter, J. G. De Wit, A. S. Ponstein, W. J. Feenstra and B. Witholt, *Plant Physiol.*, 90 (1989) 75.
4 H. L. Griffin and Y. V. Wu, *Biochemistry*, 10 (1971) 4330.
5 R. A. Pisigan and E. J. Del Rosario, *Phytochemistry*, 15 (1976) 71.
6 C. D. Boyer and M. B. Fisher, *Phytochemistry*, 23 (1984) 733.
7 D. J. Manners, *Carbohydr. Polym.*, 144 (1989) 87.
8 C. D. Boyer and J. Preiss, *Plant Physiol.*, 67 (1981) 114.
9 G. L. Matters and C. D. Boyer, *Phytochemistry*, 20 (1981) 1805.
10 J. L. Ozbun, J. S. Hawker and J. Preiss, *Biochem. J.*, 126 (1972) 953.
11 J. S. Hawker, J. L. Ozbun, H. Ozaki, E. Greenberg and J. Preiss, *Arch. Biochem. Biophys.*, 160 (1974) 530.
12 C. W. Chang, *Starch*, 36 (1984) 85.
13 J. L.Ozbun, S. J. Hawker, E. Greenberg, C. Lammel and J. Preiss, *Plant Physiol.*, 51 (1971) 1.
14 B. I. Brown and D. H. Brown, *Methods Enzymol.*, 8 (1966) 395.
15 J. Larner, *Methods Enzymol.*, 1 (1955) 222.
16 C. D. Boyer and J. Preiss, *Biochemistry*, 16 (1977) 3693.
17 K. Kawaguchi, J. Fox, E. Holmes, C. D. Boyer and J. Preiss, *Arch. Biochem. Biophys.*, 190 (1978) 385.
18 S. A. Barker, E. J. Bourne, I. A. Wilkinson and S. Peat, *J. Chem. Soc.*, (1950) 93.
19 C. Y. Tsai and O. E. Nelson, *Plant Physiol.*, 43 (1968) 103.
20 C. Y. Tsai and O. E. Nelson, *Genetics*, 61 (1969) 813.
21 N. P. Badenhuizen. in *Struktur und Bildung des Stärkekorns*, Paul Parey Verlag, Berlin, Hamburg, 1971, pp. 54–68.
22 A. S. Ponstein, K. Oosterhaven, W. J. Feenstra and B. Witholt, *Starch*, 43 (1991) 208.
23 A. S. Ponstein, G. H. Vos-Scheperkeuter, E. Jakobson, W. J. Feenstra and B. Witholt, *Plant. Physiol.*, (1990) 234.
24 J. S. Hawker, J. L. Ozbun and J. Preiss, *Phytochem.*, 11 (1972) 1287.
25 J. Fox, K. Kawaguchi, E. Greenberg and J. Preiss, *Biochem.*, 15 (1976) 849.
26 A. Blennow and G. Johansson, *Phytochemistry*, 30 (1991) 437.
27 A. Doi, *Biochim. Biophys. Acta*, 184 (1969) 477.
28 K. Satoh and K. Sato, *Anal. Biochem.*, 108 (1980) 16.
29 W. Praznik, G. Rammesmayer, T. Spies and A. Huber, *Carbohydr. Res.*, 227 (1991) 171.
30 O. H. Lowry, N. J. Rosenbrough, A. L. Farr and R.J. Randall, *J. Biol. Chem.*, 193 (1951) 265.
31 R. G. Spiro, *Methods Enzymol.*, 8 (1966) 3.
32 D. L. Morris, *Science (Washington, D.C.)*, 107 (1948) 254.
33 J. Preiss, *The biochemistry of plants*, Vol. 14, Academic, New York, 1988, p. 181.

Journal of Chromatography, 623 (1992) 403–407
Elsevier Science Publishers B.V., Amsterdam

CHROM. 24 571

Short Communication

High-resolution separation of polyunsaturated fatty acids by argentation thin-layer chromatography

Robert Wilson and John R. Sargent

Department of Biological and Molecular Sciences, School of Natural Sciences, University of Stirling, Stirling FK9 4LA, Scotland (UK)

(First received May 18th, 1992; revised manuscript received August 18th, 1992)

ABSTRACT

A simple procedure is described for separating methyl esters of polyunsaturated fatty acids (PUFAs) by argentation chromatography using silver nitrate-impregnated thin-layer chromatography plates. Esters are resolved into discrete classes containing 2, 3, 4, 5 and 6 double bonds and within each of these groupings esters are separated according to chain length. All commonly encountered (n − 6)PUFAs from C_{18} to C_{22} are resolved from each other, as are all commonly encountered (n − 3)PUFAs from C_{18} to C_{22}. The technique is particularly useful for metabolic studies of the chain elongation and further desaturation of PUFAs by separately incubating isolated cells with [1-^{14}C]18:2(n − 6) and [1-^{14}C]18:3(n − 3). R_F values for individual PUFAs are very reproducible and recoveries of individual [^{14}C]PUFAs for radioassay exceed 90%.

INTRODUCTION

Fatty acid methyl esters (FAMEs) can be efficiently separated and quantitated by gas chromatography (GC) [1] and high-performance liquid chromatography (HPLC) [2], and both GC and reversed-phase HPLC have been applied to study lipid metabolism using radio-labelled compounds [3–13]. Radio-labelled FAMEs separated by either packed column GC or reversed-phase HPLC can be either counted directly with commercial radiodetectors, or fractions collected for further analysis and/or liquid scintillation radioassay [3–13]. However, not all components may be well separated by packed column GC or HPLC and further analysis using other techniques is often required [3,4,7,8,12].

Argentation thin-layer chromatography (TLC) has been used to separate FAMEs according to their degree of unsaturation and to study the metabolism of polyunsaturated fatty acids (PUFAs) using radioisotopes [14–18]. However, not all PUFAs are well separated by existing silver nitrate techniques [14–21] and, in particular, separation of PUFA methyl esters with four or more double bond is difficult [18–21]. Furthermore, separation of FAMEs with the same degree of unsaturation but with different chain lengths is seldom possible [19]. We report here a simple method for separating PUFA methyl esters according to both degree of unsaturation and chain length. The application of the method in studies of chain elongation and further desaturation of C_{18} PUFAs is illustrated.

Correspondence to: Dr. Robert Wilson, Department of Biological and Molecular Sciences, School of Natural Sciences, University of Stirling, Stirling FK9 4LA, Scotland, UK.

0021-9673/92/$05.00

MATERIALS AND METHODS

Materials

Butylated hydroxytoluene (BHT) and standard FAMEs (at least 99% pure) were obtained from Sigma, Poole, UK. Silver nitrate was obtained from Johnson Matthey, Royston, UK. [1-^{14}C]18:2(n − 6) (54.7 mCi/mmol), [1-^{14}C]18:3(n − 3) (53.9 mCi/mmol) and radioactive ink were purchased from Amersham International, Aylesbury, UK. Ecoscint A scintillation fluid was supplied by National Diagnostics, Manville, NJ, USA. Konica A2 X-ray film was supplied by MAS Stirling, Crief, UK. Silica gel 60 TLC plates (Merck 5721, 20 cm × 20 cm × 0.25 mm) were purchased from BDH, Poole, UK. Aminopropyl columns were purchased from Jones Chromatography, Hengord, UK. 10% CP-Wax 51 coated on Chromosorb 100–120 mesh was obtained from Chrompack, Middelburg, Netherlands. All solvents were of HPLC grade and were purchased from Rathburn Chemicals, Walkerburn, UK.

Impregnation of silica gel plates with silver nitrate

Silica gel 60 TLC plates (20 cm × 20 cm × 0.25 mm) were sprayed uniformly with 20 ml acetonitrile containing 2 g silver nitrate until the plates were saturated. Spraying TLC plates gives a coating of silver nitrate as uniform as dipping [17,19]. The plates were air-dried in subdued light, heated at 110°C for 30 min to achieve activation [19] and used within 1 h.

Preparation of fatty acid methyl esters

FAMEs were prepared from mixtures of either (n − 3) or (n − 6) PUFAs by transmethylation in methanol containing 1% sulphuric acid for 16 h under nitrogen at 50°C [20]. The composition of the mixtures is given in the legend to Fig. 1. In other experiments, human skin fibroblasts cultured in 10 ml medium, were incubated with either 1 μM (0.05 μCi/ml) [1-^{14}C]18:2(n − 6) or 1 μM (0.05 μCi/ml) [1-^{14}C]18:3(n − 3) for 24 h to generate metabolic intermediates as described previously [4–6]. Total lipid was isolated from human skin fibroblasts [22] and FAMEs prepared as above [20]. FAMEs were purified on 500 mg aminopropyl (NH_2) columns (Bond-Elut) [23]. Using a syringe attached to the column by an adapter, 7 column volumes hexane–acetic acid (98:2, v/v) followed by 7 column volumes hexane were slowly pushed through the column. FAMEs were then applied to the column in hexane and eluted from the column using 7 column volumes hexane. The solvent was evaporated under a stream of nitrogen. FAMEs were redissolved in hexane containing 0.01% BHT at 50 mg/ml. Cholesterol and PUFA degradation products were retained on the column and are eluted using 7 column volumes hexane–acetic acid (98:2, v/v) followed by 7 column volumes hexane.

Separation of (n − 3) and (n − 6) mixtures by argentation TLC

FAME mixtures were applied to the impregnated TLC plates as a narrow band over 1 cm using a Hamilton micro-syringe at 0.5–1.0 mg/cm. Approximately 100 μg of each component were present in the mixtures using this loading. The plates were developed with toluene–acetonitrile (97:3, v/v) to 1 cm from the top in a standard TLC chamber lined with tissue to saturate the atmosphere with solvent. The plates were dried, lightly sprayed with 3% (w/v) copper acetate–8% (v/v) orthophosphoric acid in water and charred at 180°C for 20 min to visualise FAMEs.

Quantification of [^{14}C] FAMEs by argentation TLC

[^{14}C]FAMEs dissolved in hexane were applied to plates as a narrow band over 2–5 cm at 50 000 dpm/cm and plates developed using toluene–acetonitrile (97:3, v/v) to 1 cm from the top. The plates were marked with radioactive ink, including solvent front and origin, and subjected to autoradiography for 4 days using Konica A2 X-ray film. Areas of silica corresponding to radioactive FAMEs were located, scraped from the plates into vials and 5 ml Ecoscint A added. Radioactivity was determined using a Packard Tricarb 2000CA liquid scintillation analyser [6,17]. In other experiments FAMEs were located, scraped from the plates and eluted using 5 ml ice-cold chloroform–methanol (2:1) containing 0.01% BHT; 1.25 ml 0.88% KCl were added and the solutions mixed [23]. After separation, the chloroform layer was removed and the solvent removed under nitrogen. FAMEs were redissolved in hexane containing 0.01% BHT and washed with 20% NaCl to precipitate any remaining silver. The hexane layer was removed and an aliquot was radioassayed after adding 5 ml Ecoscint A and the remainder used for further analyses by GC or TLC.

Identification of [^{14}C] FAMEs by GC

[^{14}C] FAMEs eluted from thin-layer plates as above were added to authentic non-radioactive standards and subjected to GC on a Pye 104 gas chromatograph using a glass column (2 m × 4 mm I.D.) packed with 10% CP Wax 51 coated on Chromosorb (100–120 mesh) with nitrogen as carrier gas at a flow-rate of 30 ml/min and a programmed temperature from 220 to 250°C [6]. Separated components were identified by reference to standards and quantified using flame ionisation detection (FID) and a recording integrator [6]. The instrument was also equipped with a stream splitter situated before FID that allowed 90% of the column effluent to be collected outside the chromatograph. Fractions of column effluent corresponding to individual FAMEs were trapped on Gilson pipetteman safety filters wetted in Ecoscint A scintillation fluid [6]. Radioactivity on the filters was determined by liquid scintillation counting as described above. Location of radioactivity with authentic standards confirmed the identity of [^{14}C] FAMEs [6].

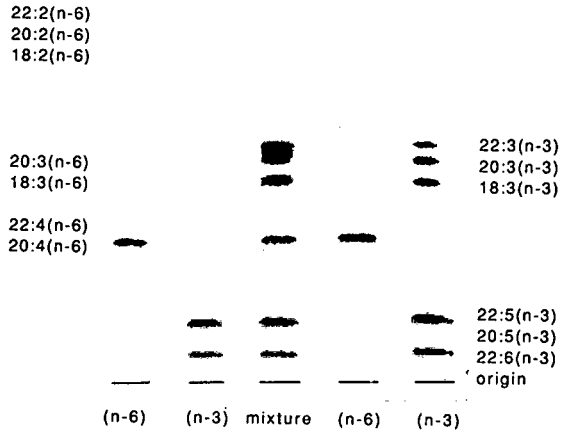

Fig. 1. Methyl esters prepared from the mixtures of (n − 6) and (n − 3) PUFAs were separated by argentation TLC as described in the Materials and Methods section. The separated esters were visualised by charring. Mixture compositions were, (n − 6) PUFAs: 18:2(n − 6), 20:2(n − 6), 22:2(n − 6), 18:3(n − 6), 20:3(n − 6), 20:4(n − 6) and 22:4(n − 6); (n − 3) PUFAs: 18:3(n − 3), 20:3(n − 3), 22:3(n − 3), 20:5(n − 3), 22:5(n − 3) and 22:6(n − 3). Mixture: (n − 6) PUFAs + (n − 3) PUFAs.

RESULTS

Representative lanes of TLC plates developed in toluene–acetonitrile (97:3, v/v) and charred are shown in Fig. 1. Separate mixtures of (n − 6) and (n − 3) FAMEs are resolved according to the degree of unsaturation with dienes being clearly separated from trienes that were in turn separated from tetraenes. Pentaenes and hexaenes were also well separated and in addition hexaenes had migrated clear of the origin. FAMEs were also resolved according to chain length with the same degree of unsaturation, this being most evident with PUFAs containing two or three double bonds. Thus, 18:2(n − 6), 20:2(n − 6) and 22:2(n − 6) were all resolved as were 18:3(n − 3), 20:3(n − 3) and 22:3(n − 3).

Although the R_F values for (n − 3) and (n − 6) PUFAs with identical degree of unsaturation and chain lengths are slightly different, they cannot be satisfactorily resolved when both are present in the same mixture (Fig. 1, see trienes). Thus, the mixture (n − 6) PUFAs + (n − 3) PUFAs is incompletely resolved. As shown in Fig. 2, however, this limitation can be simply overcome in metabolic studies by separate incubations with [1-^{14}C]18:2(n − 6) and [1-^{14}C]18:3(n − 3) and subsequent simultaneous analyses of the products from the two incubations. In the experiment shown the conversions of 18:2(n − 6) to 18:3(n − 6), 20:2(n − 6), 20:3(n − 6) and 20:4(n − 6), and of 18:3(n − 3) to 18:4(n − 3), 20:3(n − 3), 20:4(n − 3), 20:5(n − 3) and 22:5(n −

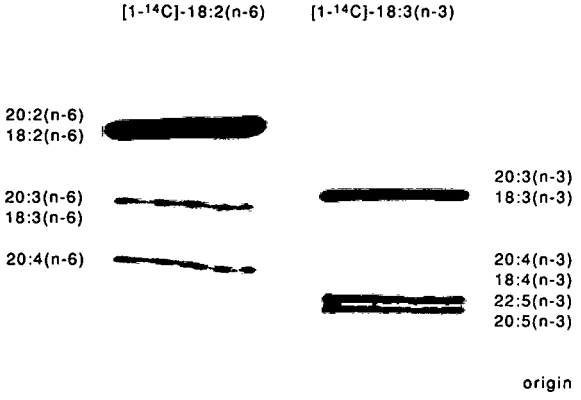

Fig. 2. FAMEs derived from the metabolism of [1-^{14}C]18:2(n − 6) and [1-^{14}C]18:3(n − 3) by cultured skin fibroblasts were separated by argenation TLC and visualised by autoradiography as described in the Materials and Methods section.

3) in cultured skin fibroblasts are clearly seen. Note that conversion to 22:6(n − 3) did not occur under the culture conditions employed.

A linear relationship exists between carbon number, degree of unsaturation and R_F values of individual methyl esters (Fig. 3), so that for each class of FAMEs containing 2, 3, 4 or 5 double bonds, an elution profile graph is created when R_F values are plotted against carbon number. As noted above, (n − 3) and (n − 6) PUFAs with identical degree of unsaturation and carbon number cannot be resolved and thus the graph for trienes and tetraenes in Fig. 3 represents both groups of PUFAs. 24:5 (n − 3) was identified from autoradiograms as a product of metabolism of [1-^{14}C]18:3(n − 3) in skin fibroblasts. This PUFA was characterised using a number of techniques, including catalytic hydrogenation, reversed-phase TLC and capillary GC.

The technique is highly reproducible with only 3–6% variation in R_F values being recorded over 5 separate analyses of the same mixture (data not shown). Recoveries of individual radioactive methyl esters, *e.g.* from experiments as in Fig. 2, were 90–92% as determined by elution of individual zones from the plates, radioassaying aliquots of the eluates, and re-chromatographing and radioassaying.

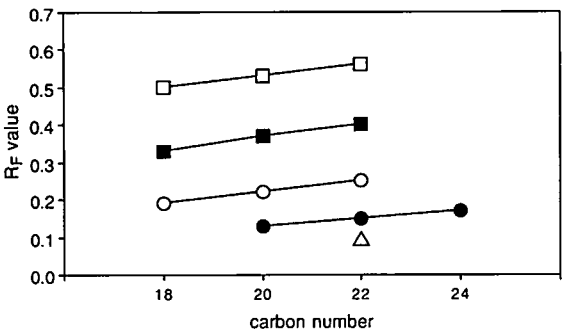

Fig. 3. R_F values were plotted against carbon number for dienes (□), trienes (■), tetraenes (○), pentaenes (●) and hexaenes (△). Methyl esters of (n − 3) PUFAs and (n − 6) PUFAs with identical degree of unsaturation and carbon numbers have slightly different R_F values but cannot be resolved. Thus the graphs for trienes and tetraenes represent both groups of PUFAs.

DISCUSSION

Development of plates with benzene–ethyl acetate (90:10, v/v) has been used previously to separate methyl esters of PUFAs with up to four double bonds with compounds of different chain lengths and the same degree of unsaturation being resolved [19]. However, complete separation of components with four or more double bonds has usually required multiple development. Separation of saturates, monoenes, dienes, trienes, tetraenes and pentaenes is achieved by a triple development technique in toluene–acetone (95:5, v/v) at −20°C [18], whereas pentaenes and hexaenes are also resolved when plates are developed twice in hexane–diethylether–acetic acid (94:4:2, v/v/v) [21]. Although these solvents resolved FAMEs into a number of classes, no separation according to chain length within a given class was noted [18,20,21].

We have examined several solvent systems for separating PUFA methyl esters and found toluene–acetonitrile (97:3, v/v) to be the most efficient. Increased resolution between pentaenes and hexaenes could be achieved using toluene–acetonitrile (95:5, v/v) but this led to poorer separation of some components in the mixture according to chain length. However, the use of this solvent may be advantageous in studies using longer-chain PUFAs. The present solvent system resolved FAMEs not only according to the degree of unsaturation but also due to chain length with the same degree of unsaturation. The technique is very reproducible and the relationship described in Fig. 3 is analogous to the homologous series of FAMEs in isothermal GC or isocratic HPLC [1,2]. In these techniques FAMEs can be identified by reference to equivalent chain length plots that can be created from retention time data and by reference to known standards [1,2]. Similarly, in the argentation TLC technique described in this paper, FAMEs can be identified from the elution profile graphs created from R_F data.

We applied this system to study the products of metabolism of [1-^{14}C]18:2(n − 6) and [1-^{14}C]18:3 (n − 3) in cultured skin fibroblasts. Other studies of PUFA metabolism using radio-labelled fatty acids have used GC or HPLC equipped with radiodetectors and computer data acquisition for analysis [3–5,10–13]. These techniques have various drawbacks, not least being the expense of the equipment

required and a need for high specific radioactivities in the analytes when flow detectors are used [1,2,20]. The technique here can be applied using low levels of radioactivity, it is inexpensive and it can be operated reliably and routinely by relatively non-skilled operators. It offers an excellent alternative and complementary method to GC or HPLC for studying the metabolism of PUFA using radiolabelled substrates.

ACKNOWLEDGEMENT

R. W. is a Croda Universal Ltd. Research Fellow.

REFERENCES

1 W. W. Christie, *Gas Chromatography and Lipids*, Oily Press, Ayr, 1989.
2 W. W. Christie, *HPLC and Lipids*, Pergamon Press, Oxford, 1987.
3 M. I. Aveldano, M. van Rollins and L.A. Horrocks, *J. Lipid Res.*, 24 (1983) 83.
4 R. R. Isseroff, V. A. Ziboh, R. S. Chapkin and D. T. Martinez, *J. Lipid Res.*, 28 (1987) 1342.
5 A. C. Voss and H. Sprecher, *Biochim. Biophys. Acta*, 958 (1988) 153.
6 R. E. Olsen, R. J. Henderson and B. J. McAndrew, *Fish Physiol. Biochem.*, 8 (1990) 261.
7 M. Maeda, O. Doi and Y. Akamatsu, *Biochim. Biophys. Acta*, 530 (1978) 153.
8 Y. Kawashima, K. Musoh and H. Kozuka, *J. Biol. Chem.*, 265 (1990) 9170.
9 L. Ulmann, J. P. Blond, C. Maniongui, J. P. Poisson, G. Durand, J. Bezard and G. Pascal, *Lipids*, 26 (1991) 127.
10 A. I. Leikin and R. R. Brenner, *Biochim. Biophys. Acta*, 876 (1986) 300.
11 A. I. Leikin and R. R. Brenner, *Lipids*, 24 (1989) 101.
12 S. Yoshida and M. Takeshita, *Arch. Biochem. Biophys.*, 254 (1987) 170.
13 G. Griffiths, A. K. Stobart and S. Stymne, *Biochem. J.*, 252 (1988) 641.
14 M. L. Garg, E. Sebokova, A. B. R. Thomson and M. T. Clandinin, *Biochem. J.*, 249 (1988) 351.
15 M. L. Garg, A. B. R. Thomson and M. T. Clandinin, *J. Lipid Res.*, 31 (1990) 271.
16 K. Punnonen, T. Puustinen and C.S. Jansen, *Lipids*, 22 (1987) 139.
17 D. R. Tocher and J. R. Sargent, *Lipids*, 25 (1990) 435.
18 S. Innis and D. E. Yuen, *Lipids*, 23 (1988) 546.
19 M. Inomata, F. Takaku, Y. Nagai and M. Saito, *Anal. Biochem.*, 125 (1982) 197.
20 W. W. Christie, *Lipid Analysis*, Pergamon Press, Oxford, 2nd ed., 1982.
21 P. A. Dudley and R. E. Anderson, *Lipids*, 10 (1975) 113.
22 J. Folch, M. Lees and G. H. Sloane-Stanley, *J. Biol. Chem.*, 226 (1957) 497.
23 K. C. van Horne, *Sorbent Extraction Technology*, Analytichem International, Harbour City, 1985.

Journal of Chromatography, 623 (1992) 408
Elsevier Science Publishers B.V., Amsterdam

CHROM. 24 498

Book Review

Gas Chromatographic Enantiomer Separation with Modified Cyclodextrins, by Wilfried A. König, Hüthig, Heidelberg, 1992, VIII + 168 pp., price DM 138, ISBN 3-7785-2026-1.

The importance of chiral separations has been pointed out in many reviews, books and international symposia dedicated to this subject. Chromatographic methods and various techniques based on modern electromigration processes have recently been developed for this purpose. High-performance liquid and gas chromatography, electrokinetic chromatography, capillary zone electrophoresis and isotachophoresis have been successfully employed. The investigations and results obtained document the growing knowledge in this area. In contrast to the book *Chiral Separations by Liquid Chromatography* (ACS Symposium Series) recently reviewed in this journal [*J. Chromatogr.*, 595 (1992) 375], the present book by König is highly specialized to capillary gas chromatography as a high-performance separation technique and cyclodextrin derivatives as the chiral selectors.

Before going into more detail it is worth pointing out that the book is mostly based on the experimental work and experience of the author and his co-workers.

Chapter 1 contains a brief introduction to the use of various kinds of chiral stationary phases in gas chromatography with special attention to the use of cyclodextrins and their derivatives. This is followed by subsections dealing with the preparation of different alkyl and alkylacyl derivatives of cyclodextrins, the characterization of these compounds and the preparation and testing of capillary columns coated with cyclodextrin derivatives. All this information is presented clearly and in a very condensed form (23 pages).

The main part (Chapter 2) is devoted to applications (112 pages). This chapter contains a many results obtained by König's research group, together with recent work done by other workers. It is subdivided into nineteen parts according to the types of organic molecules and the type of analysis in question. The applications involve, *e.g.*, enantiomer separation of alkanes and cycloalkanes, olefinic compounds, alcohols, diols and polyols, epoxides and ethers, spiroacetals, lactones, ketones and aldehydes and practical separations, *e.g.*, of the products of asymmetric synthesis, the analysis of alcohols as constituents of the insect communication system, alcohols as flavour compounds and constituents of essential oils and enantiomer separations of pharmaceuticals.

The last two short chapters, concerned with a possible mechanism of enantioselective host–guest interactions (3 pages) and NMR studies (4 pages), show some actual problems which have to be solved in order to clarify the fundamental processes in successful practical applications.

The book has 145 pages of text and contains 132 figures, most of them being chromatograms with baseline separations.

Now that some cyclodextrin capillary columns are commercially available (unfortunately still at a high price), there is no doubt that König has greatly contributed to the solution of many chiral separations and his book is a valuable contribution to this important field and will provide good a guide for various analytical laboratories.

Prague (Czechoslovakia)
E. Smolková-Keulemansová

Journal of Chromatography, 623 (1992) 409–410
Elsevier Science Publishers B.V., Amsterdam

CHROM. 24 499

Book Review

Affinity Membranes, Their Chemistry and Performance in Adsorptive Separation Processes, by Elias Klein, John Wiley & Sons, Inc., New York, Chichester, Brisbane, Toronto, Singapore, 1991, 152 pp., US$ 55.20, ISBN 0-471-52765-3.

Membrane-based purification systems and immobilized enzyme catalysis have several advantages over conventional particle-based methods. The high porosity and minimum mass transfer resistance in membranes allow a high volumetric throughput, resulting in extremely short process times. The membrane structure is such that the adsorbent molecule is situated on the inner surfaces of the membrane pores, in effect along the flow path of the soluble target protein, thereby minimizing the diffusional and accessibility problems associated with gel beads used in packed column operations. The end result is maximum utilization of the immobilized adsorbent molecule. The high mass transfer capabilities of the membrane facilitate maximum utilization of the fast adsorption kinetics of affinity chromatography.

The book under review provides the information that in 1986 Stimpson was the first investigator to point out the differences in kinetic response of bioaffinity membranes compared with bioaffinity chromatography columns. The rate at which ligate is transferred from the feed solution to the immobilized ligand is dependent on both the rate of transfer to the binding site (*i.e.*, diffusion) and the rate of complex formation. For chromatographic supports the available diffusion distances are between 25 μm (for hydrogels) and 2.5 μm (for silica particles). For membranes, whose pore diameters are 0.1–3.0 μm, the distances are much shorter. Hence the use of an affinity membrane provides not only the preferred shallow bed configuration recommended to reduce pressure drops (which compact the bed structure in resin beds), but also offers the additional advantage of much shorter diffusion paths. These two factors lead to extremely rapid processing, without an increased loss of product concentration into the filtrate.

Elias Klein, the founder and past president of the North American Membrane Society, wrote this book for polymer and/or membrane chemists interested in developing synthetic membranes for highly specific separations. The text is also written for biochemists or bioengineers who wish to learn more about the preparation and uses of synthetic membranes in biological separations. These might include membranes for (a) therapeutic devices to treat autoimmune diseases, (b) processes to recover products from gene-modified bacteria or mammalian cells or (c) membrane-bound enzyme reactors.

This is the first book to combine membrane technology and bioaffinity chromatographic techniques. The first third of the book is about the basis of bioaffinity chromatography. After an introductory chapter there is a chapter devoted to affinity adsorption. Chapter 3 describes solid supports, but under an incorrect titel "Substrates". Chapters 4, 5 and 6 deal with the binding chemistry, ligand types and the capacity of affinity matrices. It would have been useful to mention in the book that protein A is not only a ligand for the isolation of many immunoglobulins, but also that it can be used for the oriented preparation of a universal support medium for high-performance immunoaffinity chromatography which was described in 1985 by Phillips *et al.* [*J. Chromatogr.*, 327 (1985) 213–219]. In recent years many papers have appeared that deal with oriented immobilization using the biospecific complexes between protein A and immunoglobulins, biotin and avidin or streptavidin, antigens and antibodies, carbohydrate moieties and lectins, etc.

The next part of the book is about membrane formation, characterization, and uses of membranes in microfiltration. The last chapter discusses applications for affinity microfiltration membranes.

A number of variables will have an impact on the decision of whether to use affinity cross-flow filtration:

(a) Product instability. The reduced number of steps and the faster processing times of cross-filtration favour its use when product activity decays with time.

(b) Low-cost ligands. These reduce the cost of preparation of large-surface-area microfilters. When the latter can be prepared economically, all the difficulties of cross-flow filtration are simplified.

(c) Large cell sizes. The fluidization of the filter cake is simpler with larger particles. Consequently, higher fluxes and less fouling are encountered, permitting the use of small affinity cross-flow filters.

(d) Availability of hydrophilic microfilters. While this is a basic requirement for any affinity support, it is particularly useful for minimizing filter cake–membrane interactions. Reduced fouling increases product recovery and flux rates.

(e) High purification ratios of the affinity ligand. If the ligand–ligate pair interaction is highly specific, a single-step isolation of the product may be possible. This would reduce the product recovery for exogenous products to three steps: cross-flow affinity microfiltration, rinsing and product recovery from the elution buffer.

Products from mammalian cell cultures, such as monoclonal cell lines that secrete exogenous antibodies, must also be isolated from their growth medium. These complex mixtures contain intact cells, cell debris and other proteins. Suspension cultures rarely reach cell volume fractions as high as those found in normal blood, so the requirements for plasma recovery from whole blood should be suitable for the isolation of exogenous proteins from such cultures.

The author's correct assumption about the prospects for affinity membranes has been confirmed in a paper about the kinetic aspects of membrane-based immunoaffinity chromatography by M. Nachman [*J. Chromatogr.*, 597 (1992) 167–172]. With a view towards the efficient large-scale purification of recombinant proteins, Nachman studied factors influencing antigen–antibody adsorption kinetics in a model hollow-fibre membrane-based immunosorbent. Non-diffusion-controlled, homogeneous adsorption kinetics were approached in membranes. It was shown that adsorption kinetics, rather than mass transfer, first became limiting in membrane-based immunoaffinity chromatography. Nachman concluded that the kinetic aspects of membrane-based immunoaffinity chromatography render it a highly efficient system, well suited for the industrial-scale production of recombinantly produced biotherapeutics.

Prague (Czechoslovakia) Jaroslava Turková

Author Index

Hyphenated Techniques in Supercritical Fluid Chromatography and Extraction

edited by **K. Jinno,** Toyohashi University of Technology, Toyohashi, Japan

Journal of Chromatography Library Volume 53

This is the first book to focus on the latest developments in hyphenated techniques using supercritical fluids. The advantages of SFC in hyphenation with various detection modes, such as, FTIR, MS, MPD and ICP and others are clearly featured throughout the book. Special attention is paid to coupling of SFE with GC or SFC.

In this edited volume, chapters are written by leading experts in the field. The book will be of interest to professionals in academia, as well as to those researchers working in an industrial environment, such as analytical instrumentation, pharmaceuticals, agriculture, food, petrochemicals and environmental.

Contents:

1992 x + 334 pages
Price: US $ 157.00/ Dfl. 275.00
ISBN 0-444-88794-6

ORDER INFORMATION
For USA and Canada
ELSEVIER SCIENCE PUBLISHERS
Judy Weislogel
P.O. Box 945
Madison Square Station,
New York, NY 10160-0757
Tel: (212) 989 5800
Fax: (212) 633 3880

In all other countries
ELSEVIER SCIENCE PUBLISHERS
P.O. Box 211
1000 AE Amsterdam
The Netherlands
Tel: (+31-20) 5803 753
Fax: (+31-20) 5803 705

US$ prices are valid only for the USA & Canada and are subject to exchange fluctuations; in all other countries the Dutch guilder price (Dfl.), is definitive. Books are sent postfree if prepaid.

ELSEVIER
SCIENCE PUBLISHERS

711/414\141\0001-00

Announcement from the Publisher

ELSEVIER SCIENCE PUBLISHERS

prefers the submission of electronic manuscripts

Electronic manuscripts have the advantage that there is no need for the rekeying of text, thereby avoiding the possibility of introducing errors and resulting in reliable and fast delivery of proofs.

The preferred storage medium is a $5\frac{1}{4}$ or $3\frac{1}{2}$ inch disk in MS-DOS format, although other systems are welcome, e.g. Macintosh.

Your disk and (**exactly matching**) printed version (printout, hardcopy) should be submitted together to the accepting editor. In case of revision, the same procedure should be followed such that, on acceptance of the article, the file on disk and the printout are **identical**. Both will then be forwarded by the editor to Elsevier.

Please follow the general instructions on style/arrangement and, in particular, the reference style of this journal as given in 'Instructions to Authors'.

Please label the disk with your name, the software & hardware used and the name of the file to be processed.

Further information can be found under 'Instructions to Authors - Electronic manuscripts'.

Contact the Publisher for further information.

ELSEVIER SCIENCE PUBLISHERS B.V.
P.O. Box 330, 1000 AH Amsterdam
Netherlands
Fax: (+31-20) 5862-304

4/92

PUBLICATION SCHEDULE FOR 1993

Journal of Chromatography and *Journal of Chromatography, Biomedical Applications*

MONTH	O 1992	N 1992	D 1992
Journal of Chromatography	623/1 623/2 624	625/1 625/2	The publication schedule for further issues will be published later
Cumulative Indexes, Vols. 601–650			
Bibliography Section			
Biomedical Applications			

INFORMATION FOR AUTHORS

(Detailed *Instructions to Authors* were published in Vol. 609, pp. 437–443. A free reprint can be obtained by application to the publisher, Elsevier Science Publishers B.V., P.O. Box 330, 1000 AH Amsterdam, The Netherlands.)

Types of Contributions. The following types of papers are published in the *Journal of Chromatography* and the section on *Biomedical Applications:* Regular research papers (Full-length papers), Review articles, Short Communications and Discussions. Short Communications are usually descriptions of short investigations, or they can report minor technical improvements of previously published procedures; they reflect the same quality of research as Full-length papers, but should preferably not exceed five printed pages. Discussions (one or two pages) should explain, amplify, correct or otherwise comment substantively upon an article recently published in the journal. For Review articles, see inside front cover under Submission of Papers.

Submission. Every paper must be accompanied by a letter from the senior author, stating that he/she is submitting the paper for publication in the *Journal of Chromatography*.

Manuscripts. Manuscripts should be typed in **double spacing** on consecutively numbered pages of uniform size. The manuscript should be preceded by a sheet of manuscript paper carrying the title of the paper and the name and full postal address of the person to whom the proofs are to be sent. As a rule, papers should be divided into sections, headed by a caption (*e.g.*, Abstract, Introduction, Experimental, Results, Discussion, etc.). All illustrations, photographs, tables, etc., should be on separate sheets.

Abstract. All articles should have an abstract of 50–100 words which clearly and briefly indicates what is new, different and significant. No references should be given.

Introduction. Every paper must have a concise introduction mentioning what has been done before on the topic described, and stating clearly what is new in the paper now submitted.

Illustrations. The figures should be submitted in a form suitable for reproduction, drawn in Indian ink on drawing or tracing paper. Each illustration should have a legend, all the *legends* being typed (with double spacing) together on a *separate sheet.* If structures are given in the text, the original drawings should be supplied. Coloured illustrations are reproduced at the author's expense, the cost being determined by the number of pages and by the number of colours needed. The written permission of the author and publisher must be obtained for the use of any figure already published. Its source must be indicated in the legend.

References. References should be numbered in the order in which they are cited in the text, and listed in numerical sequence on a separate sheet at the end of the article. Please check a recent issue for the layout of the reference list. Abbreviations for the titles of journals should follow the system used by *Chemical Abstracts.* Articles not yet published should be given as "in press" (journal should be specified), "submitted for publication" (journal should be specified), "in preparation" or "personal communication".

Dispatch. Before sending the manuscript to the Editor please check that the envelope contains four copies of the paper complete with references, legends and figures. One of the sets of figures must be the originals suitable for direct reproduction. Please also ensure that permission to publish has been obtained from your institute.

Proofs. One set of proofs will be sent to the author to be carefully checked for printer's errors. Corrections must be restricted to instances in which the proof is at variance with the manuscript. "Extra corrections" will be inserted at the author's expense.

Reprints. Fifty reprints will be supplied free of charge. Additional reprints can be ordered by the authors. An order form containing price quotations will be sent to the authors together with the proofs of their article.

The most useful chiral separation column,

ULTRON ES-OVM, for enantiomeric drugs.

Substance	Rs	Substance	Rs	Substance	Rs
Acetylpheneturide	2.74	Disopyramid	2.04	Nisoldipine	2.36
Alimemazine	6.06	Eperisone	1.15	Nitrendipine	1.80
Alprenolol	1.09	Ethiazide	1.42	Oxazepan	2.65[2]
Arotinolol	1.95	Fenoprofen	0.80	Oxprenolol	1.38
Bay K 8644	5.92	Flurbiprofen	1.27	Pindolol	2.04
Benproperine	3.27	Glutethimide	1.36	2-Phenylpropionic acid	0.80
Benzoin	8.41	Glycopyrronium	1.73	Pranoprofen	0.63
Biperiden	3.17	Hexobarbital	1.70	Prenylamine	0.86
Bunitrolol	3.08	Homochlorcyclizine	3.04	Profenamine	3.31
Bupivacaine	1.26	Hydroxyzine	2.15	Promethazine	1.42
Chlormezanone	6.48	Ibuprofen	1.72	Propranolol	1.24
Chlorphenesin	2.23	Ketoprofen	1.37	Terfenadine	2.22
Chlorpheniramine	2.36	Lorazepam	2.55[2]	Thioridazine	0.72
Chlorprenaline	2.34	Meclizine	3.71	Tolperisone	1.50
Cloperastin	2.85	Mepenzolate	1.40	Trihexyphenidyl	5.16
Dimethindene	4.33	Mephobarbital	1.70	Trimipramine	3.69
1,2-Diphenylethylamine	1.74	Methylphenidate	1.13[1]	Verapamil	1.49

NOTE: 4.6×150mm column at room temp. except[1] 6.0×150mm at room temp. and[2] 6.0×150mm at 10°C

From trace analysis for metabolites

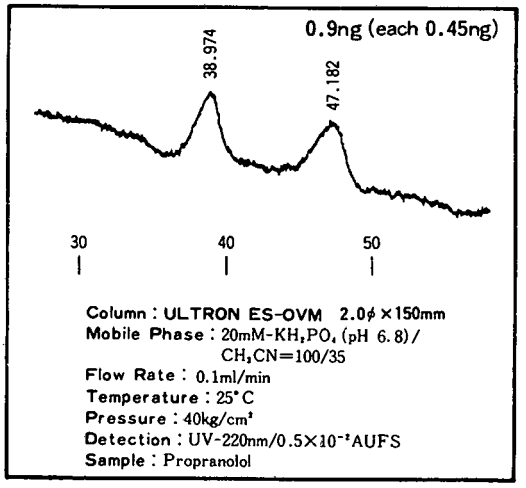

to preparative scale

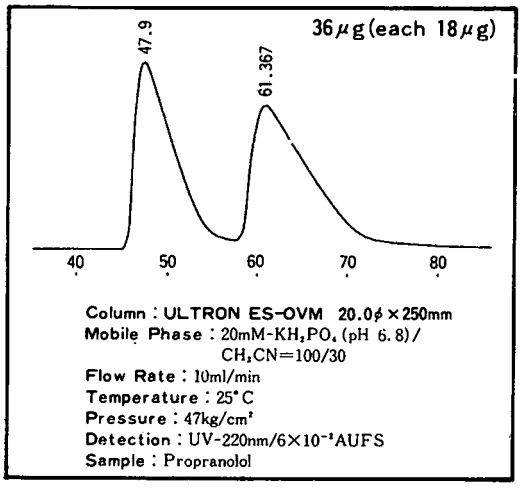

SHINWA CHEMICAL INDUSTRIES, LTD

50 Kagekatsu-cho, Fushimi-ku, Kyoto 612, JAPAN

Phone: 80-75-621-2360 Fax : 80-75-602-2660

Please contact in United States of America and Europe to :

Rockland Technologies, Inc. 538 First State Boulevard, Newport, DE 19804, U.S.A.

Phone : 302-633-5880, Fax : 302-633-5893

This product is licenced by Eisai Co., Ltd.

29 MA 95